QUANTIFYING PHOSPHORUS-BIOCHAR INTERACTIONS TO DETERMINE EFFECTIVENESS OF BIOCHAR AS A SUSTAINABLE SOIL IMPROVER

Kathryn Brian B.Sc. (Hons)

A thesis submitted to the University of Nottingham for the Degree of Doctor of Philosophy

Under the supervision of Dr Helen West and Professor Michèle Clarke

I would like to dedicate this work to my parents, Mark and Debbie Brian, who taught me hard work, patience and a little self-belief go a long way…I hope this thesis proves you right!

Acknowledgments

Firstly, I would like to thank the BBSRC for financially supporting this project. Further thanks to all my colleagues within the AES division, the relaxed yet supportive atmosphere has made the division a pleasure to be part of. In particular I would like to thank the like-minded Helen West, who wholly understood my abilities to abandon passports and purses in foreign countries and who encouraged me to pursue a project out of both our comfort zones. Thank you Helen for all of your support, both academically and pastorally, you have made working on this project fun, despite the academic challenges. I would also like to extend a huge thank you to Michèle Clarke, who has provided me with amazing global experiences, including the unforgettable trips up Sugarloaf Mountain, and without whom I would never have seen the famed Amazonian '*Terra Preta'* soils upon which this project is based.

Additional thanks to Scott Young and Saul Vazquez Reina for the light-hearted patience and guidance provided throughout my studies, without you the project would be lost! I would also like to extend gratitude to: Bill McNaughton, Andrew Rollinson, David Mee, Laura Holt and John Corrie for technical and analytical support and advice. A mammoth thank you to Emma Hooley for always making me laugh, letting me rant, keeping me positive and providing me with my daily Bourbon biscuit fix.

On a more personal note, I would like to thank:

My parents, Mark and Debbie Brian, and siblings, Richard Brian, James Munro-Brian and Mhairi Munro-Brian, without whose love, encouragement and ability to keep me laughing this would not have been possible. William Taylor for being understanding, ever-supportive and always knowing what to say, even if I don't always want to hear it. You seriously have the patience of a saint! Sofia Hirscher, Hannah Cooper, Heather Sanders, Alexander Fletcher, Stuart Bagley, Steven Grundy, Dorien VanHees, Daisy Dobrijevic, Samantha Dolan, Connie Clare and Olivia Cousins for always listening to my rambling and knowing when a Bodega distraction was absolutely necessary. Thanks for a fun four years with much more hilarity to come. Finally, thanks to my lifelong friends and personal cheerleaders, even though you don't really understand what I do: Nikki Gambles, Sarah Duckwith and Amy Brenndorfer.

Table of Contents

Table of Figures

Table of Tables

Glossary and List of Abbreviations

% AC	Percentage ash content of the chars
% MC	Percentage moisture content of a sample
% VC	Percentage volatile content of the chars
Ac	Acidic soil
AC	Acidic soil containing coffee char
AcHW	Acidic soil containing hardwood char produced using pyrolysis
ACS grade	An ACS grade chemical meets or exceeds the standards set by the American Chemical Society (ACS)
AGSW	Acidic soil containing softwood char produced using gasification
AHW	Artificially aged pyrolysed char from hardwood feedstock
AMR	Acid Molybdate Reagent
BET	Brunauer, Emmet and Teller nitrogen adsorption isotherm used to calculate the surface area of the chars characterised
Cal	Calcareous soil
CBD extract	Extractant containing sodium bicarbonate, sodium citrate and 0.07M sodium dithionite
CC	Calcareous soil containing coffee char
C_e	Solution concentration or equilibrium of P after shaking (mg L^{-1})
CGSW	Calcareous soil containing softwood char produced using gasification
CHW	Calcareous soil containing hardwood char produced using pyrolysis
DCP	Monetite
DCPD	Brushite
DOC	Dissolved organic carbon
$FA_{colloidal}$	Colloidal fulvic acid
Freundlich	Descriptive sorption isotherm model
GSW	High temperature gasifier char from mixed softwood feedstock
HA	Hydroxyapatite
$HA_{Particulate}$	Particulate humic acid
HW	Pyrolysed char from mixed hardwood feedstock
IBI	International Biochar Initiative
IC	Inorganic carbon (mg kg^{-1})
ICP-MS	Inductively coupled plasma mass spectrometry
Isotherm	A graph plotting P sorbed vs. solution concentration
K_a	Langmuir-Freundlich constant indicating binding strength
Kf	Freundlich distribution coefficient
K_l	Langmuir constant indicating binding strength
Langmuir	Descriptive sorption isotherm model
L-F	Langmuir-Freundlich descriptive sorption isotherm model
LGSW	Low temperature gasifier char from mixed softwood feedstock
LOI	Loss on ignition
MCP	Monocalcium phosphate
Milli-Q	'Ultrapure' water produced through successive filtration and purification using Millipore filterers (0.22µm) and deionisation techniques to reduce charge-carrying ions
n	Freundlich correction factor
NC	Neutral soil containing coffee char produced using pyrolysis
Neu	Neutral soil
NGSW	Neutral soil containing softwood char produced using gasification

NHW	Neutral soil containing hardwood char produced using pyrolysis
N_s	The maximum adsorption considering monolayer coverage according to the Langmuir isotherm.
OCP	Octacalcium phosphate
P_{added}	Concentration of P added to the char-P solutions (mg L^{-1})
P_{blank}	Measured absorbance of the blank
P_{char}	Measured absorbance of the soil-char samples
P_{native}	Used in isotherm models and indicates the P contributed to the system by biochar
P_{oslen}	Available phosphate in solution (mg kg^{-1})
P_{sol}	Concentration measured in the solution after incubation (mg L^{-1})
P_{sorbed}	P removed or adsorbed by biochar (mg kg^{-1})
RSD	Residual standard deviation
S.E.	Standard error
$Slope_{cal}$	Slope for the P absorbance calibration curve
TC	Total carbon (mg kg^{-1})
TOC	Total organic carbon (mg kg^{-1})
vol_{adsorb}	Volume of each sample used in colorimetry analysis (ml)
Vol_{sample}	Volume used throughout extraction (ml)
$weight_{char}$	Weight of char added to solution (g)
$weight_{desired}$	Weight of soils to be maintained to ensure a constant moisture content (g)
$weight_{dry}$	Weight of sample after drying (g)
$weight_{original}$	Weight of soil-char when experiment set up (g)
$Weight_s$	Weight of soil-char sample (g).
$weight_{sample}$	Cumulative sum of sample weight removed over time (g)
$weight_{wet}$	Weight of sample prior to drying (g)
WHAM VII	Windermere Humic Aqueous Model VII
WHW	Weather pyrolysed char from mixed hardwood feedstock
β -TCP	β-tricalcium phosphate

Abstract

The global population is increasing and will reach 9.7 billion by 2050, which, coupled with finite global phosphorus (P) reserves estimated to run out by 2030, places a clear strain on crop production systems. The essential nature of phosphorus for crop growth has led to the exploration of alternative phosphorus resources. Char, also known as biochar, is produced through carbonisation of waste materials in an oxygen-deficient environment and has potential as a soil fertiliser or improver (depending on feedstock used). Biochar can contribute P to soils and solutions in a process known as desorption and also removes P from soils and solutions by sorption. The interactions between chars and P vary from one char to another and alter according to soil type and texture due to different physicochemical properties of both chars and soils. Char/P interactions are important in determining phosphate availability to growing plants and understanding these dynamics before amending soils with char is therefore important. This project aimed to quantify char/P interactions across nine chars made from different feedstocks and/or production temperatures in order to understand which chars would be most suited to conserving or releasing P, both important processes in enhancing P sustainability. The approach was laboratory-based, focusing on batch P sorption experiments and speciation modelling within solutions in addition to soil-char incubation experiments. Char characterisation showed each of the nine chars used had unique chemical and physical properties which were influenced by production mechanism, feedstock and temperature. As a result of the varied physicochemical characteristics, each of the chars displayed different abilities to sorb P from solutions and the sorption behaviours were influenced by feedstock to a greater extent than by production regime. Upon further developing the sorption studies for three of the chars it was observed that adsorption, as oppose to solid-

phase precipitation, drove the P removal observed within solutions. The mechanism of adsorption remained unique to each char, where physical surface area likely drove sorption in gasified softwood chars (GSW) and anion exchange of P with oxygen-containing surface functional groups governed sorption in coffee and hardwood chars (HW). Addition of GSW, coffee and HW to acidic, neutral and calcareous soils showed the ability of biochar to influence soil P availability varied according to char and soil physicochemical characteristics. Each char behaved differently within each soil suggesting soil characteristics had a greater impact on P availability than char properties and highlighting how a ‘one-char-fits-all’ approach is not suitable when using char as a soil amendment and a potential source of P. Further studies in mapping char-soil-phosphorus interactions are necessary to understand which soils will benefit from char addition.

1 BIOCHAR AND SOIL FERTILITY: A REVIEW OF BIOCHAR PHOSPHORUS INTERACTIONS IN RELATION TO PRODUCTION AND FEEDSTOCK

The continual growth of the global population, with projections of more than 9 billion mouths to feed by 2050, places increased strain on crop production practices (UN, 2008; Baulcombe *et al.*, 2009; Godfray *et al.*, 2010; Cordell *et al.*, 2011). The foundation to increasing crop production is improved soil health and fertility (Hartemink, 2007). Finding suitable soil amendments to increase soil fertility and crop production is therefore of paramount importance to ensure the population can be fed (Nellemann, 2009).

Char, also referred to as biochar, is a carbonaceous material produced in oxygen deficient conditions (Sohi *et al.*, 2009; Manya, 2012) and has been suggested as a soil amendment to either directly or indirectly improve soil fertility. The presence of charred waste products in the extremely fertile '*Terra Preta'* soils found within the Amazon basin stimulated research into biochar as a soil improver (Glaser *et al.*, 2001; Glaser *et al.*, 2002). The potential of char to improve soil fertility is due to the variety of interactions observed influencing soil nutrient availability (Glaser *et al*., 2002; Lehmann *et al*., 2003; Chan *et al.*, 2007; Chan & Xu, 2009a). Before recommending biochar as an accessible and sustainable soil improver or fertiliser, the impact on essential plant nutrients such as phosphorus needs to be understood, as char has been associated with both reduced and increased phosphate availability (Rittmann *et al.*, 2011; Yao *et al.*, 2011a; Sarkhot *et al.*, 2013; Chintala *et al.*, 2014b; Wang *et al.*, 2015; Schneider & Haderlein, 2016). Understanding the potential of chars to modify phosphate availability within soils is worthwhile as the global phosphorus reserves used to create fertilisers are predicted to be depleted by 2030 (Cordell *et al.*, 2009; Cordell *et al.*, 2011); therefore improving P sustainability is crucial. The essential, yet finite, nature of phosphorus coupled with the growing population requiring increased crop production highlights the importance of exploring biochar-phosphate interactions.

The following review outlines the current state of knowledge regarding biochar and biochar/phosphate interactions.

1.1 BIOCHAR: WHAT AND WHY?

There is a wealth of literature available on the impacts of biochar amendment to soil with regard to carbon sequestration, water retention, pH, elemental availability and microbial abundance within soils (Figure 1.1) and char is often associated with increased crop yield (Lehmann *et al.*, 2006; Lehmann & Rondon, 2006; Lorenz & Lal, 2014; Sarma *et al.*, 2018), although not always (see Jeffery *et al.*, 2011 and references therein). The high and recalcitrant carbon content of chars has led to their positive association with climate change mitigation through increased carbon sequestration in soils (Lehmann, 2007; Sarma *et al.*, 2018). Each char, however, has a unique impact on soil depending on the feedstock and production mechanisms used because these alter the physicochemical characteristics of biochar (Cheng *et al.*, 2008a; Kookana *et al.*, 2011; Gul *et al.*, 2015). The effects of char on soil chemical, biological and physical properties are outlined in Figure 1.1.

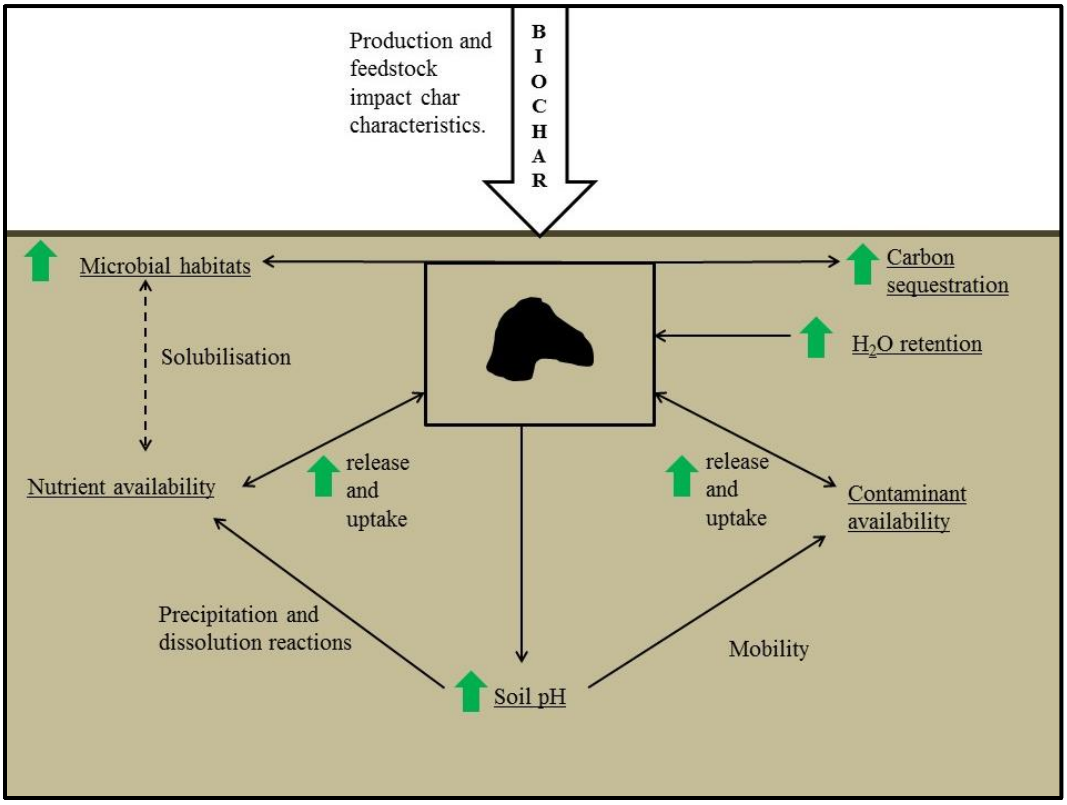

Figure 1.1 The potential impact of biochar within soils. Many biological, chemical and physical properties and interactions within soils can be influenced by biochar amendment, including: microbial habitats, nutrient availability, contaminant (organic or inorganic) availability, water retention, carbon sequestration, water holding capacity and soil pH (liming ability). The impact of char on soil varies according to char characteristics which are influenced by feedstock and production temperature. The release and uptake of elements refers to sorption/desorption interactions which are addressed at a later point within the review.

The role biochar holds within a soil is influenced, in part, by the physical characteristics of the char. The porous nature and high surface area associated with chars allows for removal of elements from soils and solutions, both contaminants and nutrients, which may improve soils if the former or limit nutrient availability if the latter (Lee *et al.*, 2013; Wang *et al.*, 2013). The pores on the char surface also provide habitats and protection for microbial communities (Pietikainen *et al.*, 2000; Gul *et al.*, 2015). Microbial populations are often positively correlated with enhanced nutrient availability due to their solubilising ability (Sarma *et al.*, 2018). For example, He *et al.* (2014) found P-solubilising microbial populations increased with char amendment, thereby enhancing phosphorus availability. The porosity and high surface area associated with char further acts to increase the water holding capacity of biochar amended soils which would benefit areas which suffer from drought (Atkinson *et al.*, 2010; Basso *et al.*, 2013).

The chemistry of chars also influences the role when added to soil as an amendment. The surface functionality, particle size, ash content and volatile matter content influence char pH, meaning each char has a unique pH despite most chars being alkali (Tryon, 1948; Brewer *et al.*, 2009; Novak *et al.*, 2009; Brewer *et al.*, 2011; Enders *et al.*, 2012; Zhao *et al.*, 2013; Pituello *et al.*, 2015; Marshall *et al.*, 2017; Noyce *et al.*, 2017). Increased soil pH is commonly associated with char amendment which is beneficial in infertile, acidic soils, particularly as alkaline environments are more favourable for nutrient solubilising bacteria (Tryon, 1948; Glaser *et al.*, 2001; Glaser *et al.*, 2002; Novak *et al.*, 2009; Mukherjee *et al.*, 2011; Biederman & Harpole, 2013; Wang *et al.*, 2013; Ch'ng *et al.*, 2014; Hong & Lu, 2018; Sarma *et al.*, 2018). Increased pH influences the mobility of elements within soils which can have both beneficial and detrimental effects. For instance, potentially toxic elements (i.e. heavy metals) are immobilised thereby improving plant growth (Buss *et al.*, 2012; Lucchini *et al.*, 2014; Tang *et al.*, 2013; Uchimiya *et al.*, 2010a), whilst formation of insoluble complexes such as calcium phosphate, potentially render beneficial nutrients unavailable (Lindsay, 1979; Yao *et al.*, 2011a, 2011b; Xu *et al.*, 2013; Wang *et al.*, 2015; Ngatia *et al.*, 2017). The negatively charged surface associated with chars causes repulsion of anionic compounds, including phosphate and nitrate, which increases nutrient availability within soils thereby increasing soil fertility (Murphy & Stevens, 2010; Sarma *et al.*, 2018; Xu *et al.*, 2014; Xue *et al.*, 2009; Yao *et al.*, 2011a; Zeng *et al.*, 2013; Zhang *et al.*, 2009). The available elements observed within chars also improve soil fertility potentially through desorption of essential nutrients to soils, however elemental contribution from chars can reduce fertility. For example, chars donating calcium to the environment could result in reduced phosphate availability through the formation of insoluble calcium phosphate precipitates (Lindsay, 1979; Ngatia *et al.*, 2017; Wang *et al.*, 2015; Xu *et al.*, 2013; Yao *et al.*, 2011a, 2011b). The chemistry of char, which varies as a result of production mechanism and feedstock, lends itself to the possibility of utilising different chars for different roles within soil. The next section aims to highlight the influence of biochar production, including temperature and feedstock, on char physicochemical properties and the impact these may have on a char's role within soil.

1.1.1 Biochar Production

There are a variety of cost-effective techniques to produce biochar through carbonisation processes, such as slow pyrolysis, fast/flash pyrolysis and gasification. Each production method has different influences on the physicochemical properties of char and therefore on the potential role of the char as a soil amendment (Manya, 2012; Mohan & Chander, 2006).

Biochar is often produced by carbonisation of waste products ranging from plant waste such as rice husk or corn cob, to animal wastes such as poultry manure (Hale *et al.*, 2013; Khan *et al.*, 2014; Kizito *et al.*, 2015; Novais *et al.*, 2018; Qian *et al.*, 2013; Uchimiya *et al.*, 2010a; Uchimiya *et al.*, 2010b.; Uchimiya *et al.*, 2012). The use of a wide range of waste products in char production makes it a sustainable avenue worth exploring as a soil amendment. Feedstock elemental content has an impact on total elemental concentrations of the char (Hong & Lu, 2018); for instance, manure-derived chars have higher total P concentrations than plant-based chars (Sun *et al.*, 2018b), although anion-induced release of P from plant-derived chars was reportedly higher than from manure-derived char (Ahmad *et al.*, 2014; Sun *et al.*, 2018b). Whilst increased elemental availability could benefit nutrient deficient soils, if potentially toxic elements were introduced into soil *via* biochar, this could be detrimental. Therefore, characterising chars produced from a variety of feedstocks at a range of production temperatures is required prior to soil addition to ensure a positive benefit is observed.

The surface area of char increases in line with production temperature (Tan *et al.*, 2018); a larger surface area is associated with increased elemental removal from soils which can be beneficial or detrimental, as discussed in section 1.2.1 (Lua *et al.*, 2004; Mukome *et al.*, 2013.; Peterson & Jackson, 2014). Furthermore, elemental concentrations alter with production temperature due to the presence or absence of nutrient-rich ash. Total P content, for example, increases in line with production temperature, suggesting chars produced at higher temperatures have a greater fertiliser potential (Cantrell *et al.*, 2012; Robinson *et al.*, 2018; Sun *et al.*, 2018b; Tan *et al.*, 2018). However, P solubility and therefore plant availability also needs to be acknowledged when considering char as a soil improver, as P may be present in insoluble compounds which are not phyto-available (Sun *et al.*, 2018b). Production temperature is negatively correlated with surface functionality, where functional groups are degraded as temperature increases (Fristak *et al.*, 2018; Novais *et al.*, 2018). The functional groups present on a char's surface influence the chemical interactions between char, soil and solutions. The reduction in functional groups and the bearing this has on the overall reactivity of char needs to be clearly mapped for different chars. Improved understanding of the relative impact of feedstock and production temperature on char characteristics would facilitate char production tailored to the required role within soil.

1.2 PHOSPHORUS INTERACTIONS WITH BIOCHAR

The need to sustainably manage soil P and the potential of biochar to contribute phosphorus to soils, has spurred research into the interactions of biochar with phosphorus, both in soils and solutions (Fristak *et al.*, 2018), particularly as some chars increase crop yield to the same extent as P fertilisers (Borno *et al.*, 2018). The contribution of P to soils from chars has also raised concerns about increased eutrophication (Sun *et al.*, 2018a), however some chars are also able to remove P from soils and solutions which may have environmental benefits. The ability of chars to remove P not only has benefits relating to eutrophication but suggest char may also act as a slow release fertiliser (Chen *et al.*, 2018b). Many of the interactions observed between char and phosphorus relate to sorption processes which need to be better understood to ensure a beneficial influence is observed on soils.

1.2.1 Sorption

Sorption is the movement of a compound from one phase to another, i.e. phosphorus moving from soil solution towards biochar (Crini & Badot, 2010) and may involve adsorption, absorption and precipitation; movement away from a substrate is known as desorption. Adsorption to a substrate is a surface phenomenon in which compounds interact with the exterior of the char often to form complexes, whereas absorption involves the association of compounds internally (Crini & Badot, 2010). Precipitation reactions occur externally of the char and involve the formation of solid-phase compounds. There are 4 main mechanisms of sorption: physi-sorption, precipitation, adsorption and absorption, each of which result in different levels of bonding. Phosphate sorption in chars tends to be associated with precipitation, adsorption or physi-sorption interactions which are distinct between chars due to variable char characteristics (Chintala *et al.*, 2014b; Lou *et al.*, 2016; Sparks, 1995; Wang *et al.*, 2015). The potential of char to influence phosphorus availability when added as an amendment is linked to the char P sorption capacity (Liu *et al.*, 2018), therefore exploring and quantifying the potential mechanisms of P sorption by chars is important in understanding the potential of char to act as a fertiliser.

1.2.1.1 *Sorption of Phosphorus by Chars*

Physical sorption to the biochar surface, also known as physi-sorption, relates to Van der Waals forces between chars and soils or solutions and has the potential to influence P availability (Mosa *et al.*, 2018). Chars demonstrating increased surface area and pore size are associated with higher P physi-sorption capacities (Kizito *et al.*, 2017a; Trazzi *et al.*, 2016; Xu *et al.*, 2018). At higher production temperatures, more compounds are volatilised increasing surface area and causing improved P sorption capacity of the char (Kasozi *et al.*, 2010). The impact of production temperature on char degradation and surface area (section 1.1.1) shows how the capacity of chars to sorb elements and ions physically varies according to production method. The negative surface associated with both chars and phosphate (Lou *et al.*, 2016; Yao *et al.*, 2011a; Zeng *et al.*, 2013) however, tends to cause phosphate repulsion from chars, meaning P sorption observed in chars tends to occur through specific adsorption or precipitation reactions as opposed to physical Van der Waals electrostatic interactions (Hale *et al.*, 2013; Liu *et al.*, 2018; Mukherjee *et al.*, 2011; Yin *et al.*, 2018).

Adsorption of P by chars occurs through the formation of surface complexes between phosphate and char surface compounds. The surface complexes formed can be either inner or outer sphere. Outer sphere reactions occur in the presence of water and are weaker than inner sphere. Inner sphere surface complexation involves ionic exchange or bonding and is the most common form of phosphorus adsorption associated with biochar (Chintala *et al.*, 2014b; Sarkhot *et al.*, 2013; Yao *et al.*, 2011a, 2011b). The surface functional groups present on chars govern the surface complexes able to form and chars with oxygen-containing functional groups have a high P sorption capacity (Ahmad *et al.*, 2014; Borno *et al.*, 2018; Chun *et al.*, 2004; Mukherjee *et al.*, 2011; Novais *et al.*, 2018; Sun *et al.*, 2018b; Yao *et al.*, 2011a, 2011b; Zornoza *et al.*, 2016). The chemical differences between functional groups, such as the presence of oxygen-containing and carbonate groups which influence P sorption, are influenced by production temperature and feedstock (Ahmad *et al.*, 2014; Borno *et al.*, 2018; Novais *et al.*, 2018; Sun *et al.*, 2018b), explaining the high P sorption observed in some chars (Chintala *et al.*, 2014b; Dari *et al.*, 2016; Jung *et al.*, 2015; Sarkhot *et al.*, 2013; Schneider & Haderlein, 2016; Takaya *et al.*, 2016; Wang *et al.*, 2015; Xu *et al.*, 2014), and the negligible levels observed in others (Parvage *et al.*, 2013; Wang *et al.*, 2015; Xu *et al.*, 2014; Yao *et al.*, 2011a; Yao *et al.*, 2012). Mapping the impact of production and feedstock on the functional groups present within chars is important in quantifying and understanding the ability of a char to sorb P.

Precipitation reactions result in the formation of solid phase compounds, effectively therefore, the sorption of ions from solutions. In the case of phosphorus, Ca, Mg, Al and Fe are the most common elements which precipitate P (Borno *et al.*, 2018; Chen *et al.*, 2018c; Hong & Lu, 2018; Sun *et al.*, 2018b; Wang *et al.*, 2018). Concentrations of Ca, Mg, Al and Fe vary between chars and in some chars elemental precipitation contributes the most dominant form of P sorption (Hong & Lu, 2018; Mosa *et al.*, 2018; Xu *et al.*, 2018) which further explains the varied sorption behaviour observed within the literature (Borno *et al.*, 2018). The system pH influences precipitation, which often occurs once maximal adsorption has been achieved (Lindsay, 1979). Ca and Mg precipitation of P is associated with alkaline systems, whereas Fe and Al-P precipitates tend to form in acidic systems (Lindsay, 1979; Liu *et al.*, 2018), therefore Ca-P and Mg-P precipitates are commonly associated with char, due to the alkaline nature of chars (Figure 1.1; Figure 1.2).

1.2.1.2 *Desorption of Phosphorus by Chars*

Desorption of P from chars had been observed, suggesting it may act as a fertilizer, directly contributing P to soils. For example, Hollister *et al.* (2013) found phosphate was unable to sorb onto chars produced from corn cobs over a range of production temperatures due to high initial P concentrations, meaning char contributed P. Addition of chars to soils can therefore result in higher P availability, where Liu *et al.* (2018) found biochar amendment rate was positively correlated with P availability when produced from rice straw due to high desorption capacities.

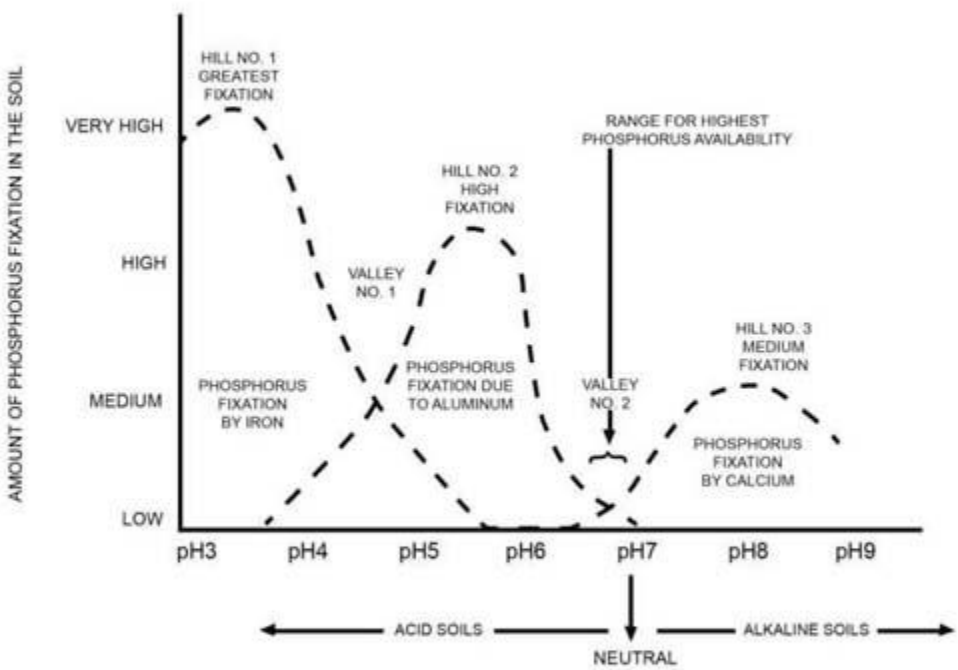

Figure 1.2. Phosphorus retention and fixation observed within soils over a pH range (Batjes, 2011).

The physical and chemical sorption processes highlight how the surface porosity (Sohi *et al.*, 2009), surface functionality and ion availability of char (Borno *et al.*, 2018; Cantrell *et al.*, 2012; Cheng *et al.*, 2008a; Glaser *et al.*, 2001) can physically and chemically stimulate sorption and desorption of P. The variable properties associated with char, as previously outlined, makes sorption behaviour and mechanisms unique to each char, which may result in potentially negative interactions with P-deficient soils where some chars may compete for phosphates (Joseph *et al.*, 2018). No one physicochemical property can be attributed to the variety of sorption patterns observed with different chars (Liu *et al.*, 2018), which explains the contradictory literature surrounding P adsorption and desorption and highlights the need to quantify and map the connection between production regime, feedstock, char characteristics and P sorption behaviours and mechanisms.

1.2.2 Designer Chars

The specificity of biochar production regimes, coupled with the ability of chars to sorb and desorb P, has led to experimental production of bespoke chars which could achieve a desirable trade-off between P desorption to increase phyto-available P, while managing P sorption to reduce eutrophication of watercourses (Joseph *et al.*, 2018).

Chars have been modified to increase P sorption by loading with Ca, Al, Fe and Mg which can benefit eutrophic waters and increase plant growth through indirect release of P (Chen *et al.*, 2018c; Hong & Lu, 2018; Novais *et al.*, 2018; Wang *et al.*, 2018; Xu *et al.*, 2018; Yin *et al.*, 2018). For example, modifying char by increasing Ca concentrations increases P sorption capacity through elevated Ca-P precipitation improving P saturated soils or solutions (Wang *et al.*, 2018). This was also noted for magnesium-loaded chars which demonstrated P sorption through precipitation and adsorption *via* surface complexation with Mg-O functional groups (Novais *et al.*, 2018; Xu *et al.*, 2018; Yao *et al.*, 2011a, 2011b). Although the production of designer biochars is an achievable end-goal, the influence of soil on biochar interactions with P needs to be further understood to ensure clear benefits are obtained.

1.2.3 The Complexity of Soils

Although quantifying a char's characteristics is paramount in understanding its influence on soil P availability, characterising soil properties is also essential in mapping P within char-amended systems, which is highlighted by the variation in sorption behaviour of chars in different soils (Borno *et al.*, 2018; Dari *et al.*, 2016; Laird *et al.*, 2010a; Parvage *et al.*, 2013; Xu *et al.*, 2014). Soils have many biological, chemical and physical parameters which will influence the ability of char to adsorb and desorb P and result in complex interactions between the char and soils.

Chemical properties of soils such as ion concentration, functionality and charge can influence the impact char has on soil. For example, co-existing anions in soil may act as competitors for P sorption to char, where P availability increases in line with the concentration of competing anions such as sulphate (Sun *et al.*, 2018b). Furthermore, in some alkaline soils, chars had minimal impact on P availability and therefore did not improve soil fertility or increase plant growth (Borno *et al.*, 2018). Calcareous soils, for example, are associated with an alkaline pH and high Ca concentrations, which facilitates P precipitation by Ca (Tunesi *et al.*, 1999; Von Wandruszka, 2006), meaning chars with higher Ca concentrations may have a detrimental influence on calcareous soils by further increasing Ca precipitation. Acidic soils, on the other hand, are more commonly associated with Al and Fe precipitation of P, or adsorption of P to Al, Fe and Mn oxides, which will also be influenced by elemental and surface groups on the char (Xu *et al.*, 2014). Char addition to acidic soils has been linked to increased P availability, although only to a limited extent because char stabilises Al, Fe and Mn oxides which are more prevalent in acidic soils, thereby increasing P sorption sites (Chen *et al.*, 2018b). Quantifying the initial elemental and ionic concentrations, as well as pH, of soils is therefore important in understanding the impact char will have on P sorption and therefore availability.

The physical and biological properties associated with soils will also alter with char amendment and influence P availability. The microbial population increases with char addition as discussed in Section 1.1 (Figure 1.1). P-solubilising bacteria release available P from insoluble forms and this will influence P availability in soils; char will likely adsorb or precipitate the available P that is not utilised by the plants or microorganisms, but this will ultimately be re-solubilised by the appropriate microbiota (Lehmann *et al.*, 2011; Omil *et al.*, 2013; Zhai *et al.*, 2015). The organic matter content of soil will also influence sorption. Soils with a high organic matter content, which is increased by char addition, demonstrate increased P sorption to Al and Fe oxides; therefore P availability in the soil will be much lower than if a char was introduced to a soil with lower organic matter content (Liu *et al.*, 2018). Physical soil properties, such as soil texture and pore size, influence the number of sorption sites within soils. Studies linking the chemical, physical and biological parameters of soil-char combinations to P sorption and availability need to be developed to ensure chars have a beneficial impact on soil P availability.

1.3 CONCLUSIONS AND PROJECT AIMS

The current literature highlights the unique nature of the physicochemical properties of different chars and has begun to explore how production temperature and feedstock influence char characteristics and impact in soil. The varied characteristics result in disparities in P sorptive abilities of chars within soils and solutions. The different sorption behaviours of chars mean their role within soils varies, where some release P and others remove it. Both sorption and direct desorption can be of benefit if added to the correct soil. Soils lacking in P, for example, would benefit from direct desorption and soils at risk of P leaching due to saturation would benefit from a char's sorptive abilities. The production of designer biochars to either contribute or sorb P, as discussed in Section 1.2.4, is a contemporary and valuable avenue of research. However, improved understanding of a char's properties and the mechanisms driving P sorption behaviour coupled with soil characteristics, needs to be further developed to enable precise char production techniques tailored to specific soil requirements.

1.3.1 Project Aims and Outline

Given the disparities within the literature outlined, the project aimed to determine the potential of a range of chars to modify P availability using laboratory-scale experiments to address the interlinked influence of production, feedstock, char properties and soil properties on P sorption and availability as outlined in Figure 1.3. **The individual chapter aims used to address the overall direction of the project are detailed below:**

- **Chapter 2** aimed to determine the chemical and physical characteristics of nine different chars and relate the characteristics of each char to production mechanism and feedstock.

- **Chapter 3** aimed to quantify the ability of the nine chars characterised in Chapter 2 to sorb or desorb P from solutions containing a range of P concentrations and establish if precipitation of P was the key driver of the P sorption observed.
- **Chapter 4** aimed to rationalise the sorption behaviours of three of the chars presented in Chapter 3 over a specific and focussed range of P concentrations and establish the mechanisms.
- **Chapter 5** aimed to explore the chemistry of P within soils by quantifying the P availability in three soils with and without biochar amendment using a variety of P extraction techniques and highlighting the potential sorption mechanisms influencing P availability within soils.

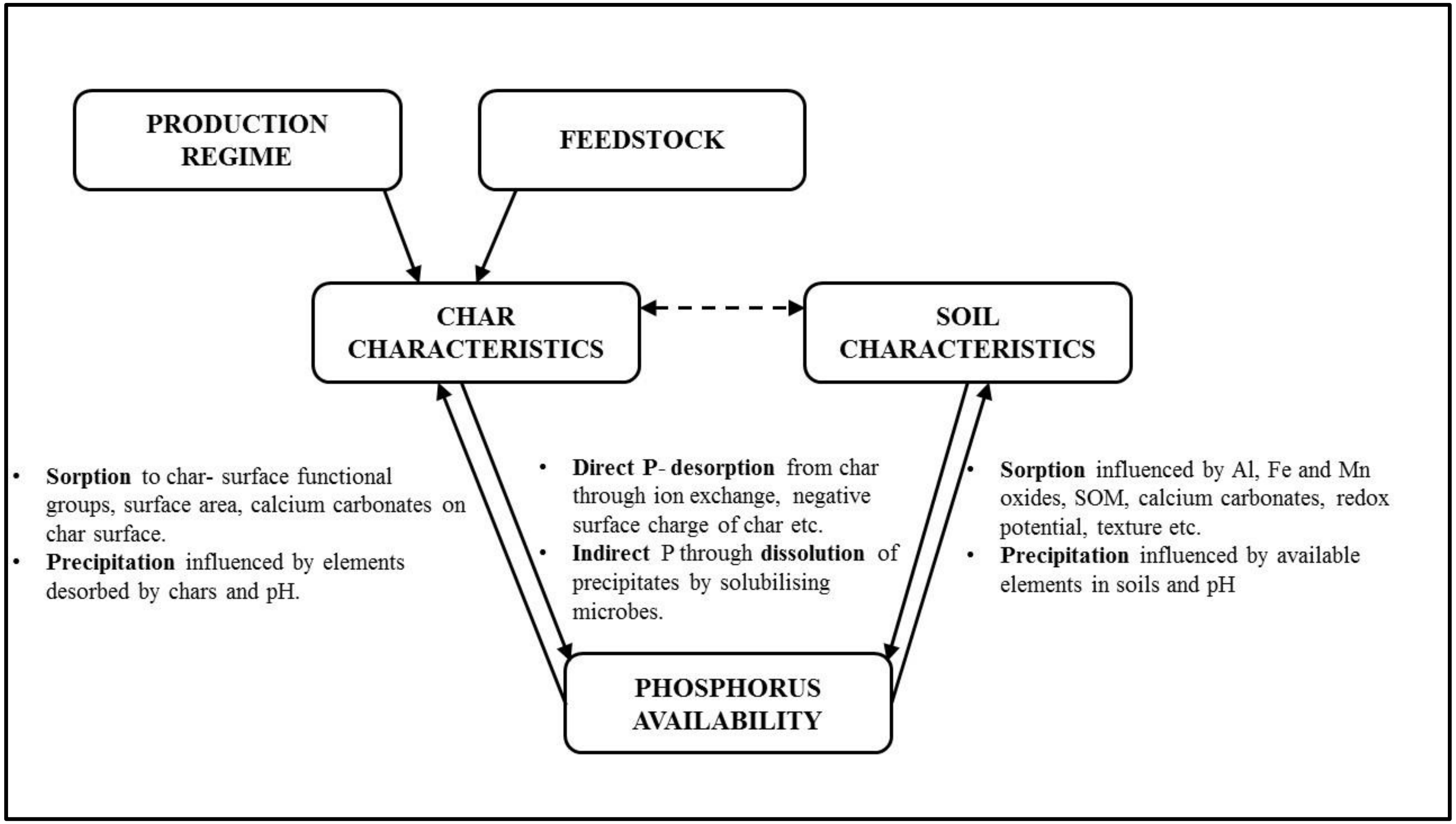

Figure 1.3. Production regime and feedstock influence char characteristics which in turn impact P availability within solution. When char is used as a soil amendment, the soil characteristics also contribute to P solubility showing the complexity of the soil-char system in relation to P availability. The general chemical interactions explored throughout the project are added including: adsorption and desorption and precipitation and dissolution, however there are many more contributing reactions relating to phosphorus within soils.

2 CHARACTERISATION OF NINE BIOCHARS PRODUCED USING DIFFERENT FEEDSTOCKS AND PRODUCTION METHODS

2.1 INTRODUCTION

Biochar has been linked to many processes within soils when added as an amendment (Chapter 1; Section 1.1). The ability of char to influence soil processes is due to the variation in physical and chemical properties of each char, which in turn results from the wide range of feedstocks used (Liu *et al.*, 2018; Novais *et al.*, 2018; Wang *et al.*, 2018) and production methods employed to produce char, e.g. slow pyrolysis, fast/flash pyrolysis or gasification (Mohan *et al.*, 2006). The production regime influences many physiochemical properties of the biochar, such as pH, ash content, surface area and elemental concentration and availability, all of which govern the role biochar holds in soils (Manya, 2012.) For example, chars produced at higher temperatures are associated with increased surface area, through feedstock degradation (Lua *et al.*, 2004; Mukome *et al.*, 2013; Peterson & Jackson, 2014; Tan *et al.*, 2018), which enables char to adsorb elements from the soil. Improved sorptive properties could allow use of char as a remediation technique for soils contaminated with heavy metals; however, sorption in nutrient deficient soils could exacerbate any fertility problems already being faced. Understanding how production affects the chemistry of chars, such as the presence of functional groups and their charge, may help in understanding why sorption differs between chars and ensure beneficial impacts on soil fertility are observed.

The original feedstock influences the final char properties as it impacts the chemical changes that occur during pyrolysis (Ahmad *et al.*, 2014; Cantrell *et al.*, 2012; Hong & Lu, 2018). The variation in char properties as a result of production conditions and feedstock needs to be understood in order to ensure soil amendment is beneficial and will facilitate the discussion of biochar-phosphorus interactions explored in later experimental Chapters.

The specific objective of the work presented in this Chapter were to:

1. Quantify the chemical and physical characteristics of nine different biochars.
2. Relate the characteristics of each char to production mechanism and feedstock.
3. Use the data as a foundation for understanding the char-P interactions explored in later Chapters.

2.2 MATERIALS AND METHODS

2.2.1 Biochar Preparation

Biochars used throughout the characterisation studies were produced from different feedstocks using a variety of production methods (Table 2.1). Two of the chars were produced during gasification of chipped *Pinus* spp. (here referred to as 'softwood') using a 10 kW 'Power Pallet' gasifier (GEK All Power Labs, USA).

Further chars were produced through slow pyrolysis of mixed species hardwood (commercially produced in the UK), bamboo (made in a small-scale Indian gasifier), açaí seeds, coffee grounds and cacao husks (all pyrolysed under controlled laboratory conditions). The pyrolysed hardwood char underwent two additional weathering treatments (in soil and chemically); therefore, nine chars were characterised overall.

During gasification, temperature is not a finely controlled variable, due to the exothermic nature of the process, however temperature was monitored during production. High temperature gasification (GSW char) was achieved at reduction zone temperatures between 916°C and 770°C, whereas low temperature gasification (LGSW char) occurred between 862°C and 731°C. Temperature was measured *via* thermocouples situated inside the gasifier at each end of the reduction zone and in contact with the feedstock. Both gasification processes ran for 6 hours at 4 kW (see Rollinson, 2016 for details relating to the downdraft Power Pallet gasifier, University of Nottingham). Bamboo char was also produced by gasification in a downdraft gasifier, but at the Indian Institute of Technology, Guwahati, Assam. Exact conditions are unknown, but the production temperature was between 700-900°C.

A variety of slow pyrolysis techniques were employed to produce the remaining chars. Pyrolysed hardwood (HW) chars were sourced from BioRegional Homegrown® in which *Fraxinus excelsior*, *Fagus sylvatica* and *Quercus robur* were pyrolysed at 450°C for 48 hours (Jones *et al.*, 2011). Açai char and cacao char were produced from waste açai seeds and cacao husks, respectively sourced from Belém in the state of Pará, Brazil. Coffee char was produced from waste *Coffea arabica* grounds sourced from the 'C Store' café, Sutton Bonington Campus, University of Nottingham, using ground Aspretto Triple Certified Coffee Beans. Açai, coffee and cacao char were made by slow pyrolysis in a muffle furnace (Carbolite, AAF 1100 furnace) at 450°C for 10 hours for açai and coffee and 450°C for 8 hours for cacao.

Table 2.1. The abbreviations, feedstock and production regimes for the nine chars characterised.

Açai	Açaí - pyrolysed at 450°C, 10 hours
AHW	Artificially aged HW char (Section 1.2.11)
Bamboo	Bamboo stem - likely gasified at 700-900°C
Cacao	Cacao husk - pyrolysed at 450°C, 8 hours
Coffee	Coffee grounds - pyrolysed at 450°C, 10 hours
GSW	High temperature softwood (916- 770°C)- gasified for 6 hours
LGSW	Low temperature softwood (862- 731°C)- gasified for 6 hours
HW	Hardwood - pyrolysed at 450°C, 48 hours
WHW	Weathered, aged HW (Section 1.2.11)

2.2.1.1 *Artificial Ageing and Weathering of Pyrolysed Hardwood (HW) Char*

Artificial ageing of pyrolysed hardwood (HW) char was achieved through thermal and chemical oxidation using methods similar to those of Cross and Sohi (2013). HW char was oven dried (GenLab Oven) for 36 hours at 105°C. A 1g sample was then weighed into a Digitube with 7 ml hydrogen peroxide (0.01 M) and heated at 80°C for 48 hours on a heating block, during which samples were agitated 2-3 times a day. Once the solution within the samples had evaporated, the samples were then oven dried at 105°C overnight.

'Natural' weathering of the HW char was achieved through long-term incubation in a heavy metal contaminated soil collected from a dedicated sewage sludge disposal farm in Nottinghamshire. The moisture content of the soil was calculated using Eq. 2.1 after oven drying 50 g of soil for 18 hours at 105°C (GenLab Oven):

$$\text{MC}\ (\%) = \left(\frac{\text{weight}_{\text{wet}} - \text{weight}_{\text{dry}}}{\text{weight}_{\text{wet}}}\right) \times 100$$

Eq. 2.1

Where, % MC equates to the moisture content, $\text{weight}_{\text{wet}}$ refers to the weight of the sample prior to drying (g) and $\text{weight}_{\text{dry}}$ is the sample weight after oven drying (g).

HW char was ground and sieved to 4.0- 4.75 mm, after which 25 g of char was added to 500g of soil sieved to <2 mm and deionised water was added to create and maintain a 20% moisture content. Treatments were placed in an unheated shed for two years and moisture was maintained by weight. The char was characterised before and after weathering treatment.

2.2.2 Proximate analysis

Standards for the chemical analysis of wood charcoal (ASTM D1762) suggests char particle sizes of 0.15-0.85 mm are best suited to proximate analysis as excessive grinding results in moisture loss due to heat generation. Particle sizes between 0.5-0.7 mm were therefore used to analyse moisture, ash and volatile content of all chars. Percentage moisture of all chars was calculated using Eq. 2.1 after oven drying at 105°C for 24 hours. The volatile matter of all chars was calculated using Eq. 2.2 after placement in a muffle furnace (Carbolite, AAF 1100 furnace) at 950°C for 10 minutes.

$$\mathrm{VC}\ (\%) = \left(\frac{\mathrm{weight_{dry}} - \mathrm{weight_{remaining}}}{\mathrm{weight_{dry}}}\right) \times 100$$

Eq. 2.2

Where VC% equates to the percentage volatile content of the chars, weight $_{dry}$ is the dry weight prior to placing in the muffle furnace but after oven drying (g) and $\mathrm{weight_{remaining}}$ is the weight of samples after igniting in the muffle furnace. The percentage ash of all chars was found using Eq. 2.3 after igniting char in a muffle furnace (Carbolite, AAF 1100 furnace) for 6 hours at 750°C.

$$\mathrm{AC}\ (\%) = \left(\frac{\mathrm{weight_{ash}}}{\mathrm{weight_{dry}}}\right) \times 100$$

Eq. 2.3

Where AC% refers to the ash content of the chars, $\mathrm{weight_{ash}}$ refers to the remaining residue after ash analysis and $\mathrm{weight_{dry}}$ refers to the weight after oven drying.

Biochar pH and EC were measured according to the International Biochar Initiative standards (IBI, 2012) by making up a ratio of 1g char to 20 ml deionised water in triplicate in centrifuge tubes. Samples were placed on an end-over-end shaker for 90 minutes after which pH (HANNA instruments, pH 209, pH meter) and EC (HANNA, HI9835 Microprocessor Conductivity/TDS meter) were measured, allowing 5 minutes for measurement stabilisation per sample.

2.2.3 Ultimate and Elemental Analysis

2.2.3.1 *Acid Digestion*

The total elemental compositions of all chars were determined by ICP-MS analysis after nitric acid (HNO_3) plus hydrogen peroxide (H_2O_2) digestion. A 0.2 g sample of char was weighed into Digitubes with 8 ml of HNO_3, allowing 5 replicates for each sample and left overnight. Prior to heating samples to 95°C for 2 hours on a block digester, 2 ml of H_2O_2 were added and watch glass lids placed on top of the tubes. Following digestion, the samples were made up to 50 ml with Milli-Q water and transferred into polypropylene universal tubes using a 0.22 µm syringe filter (BD Discardit II Luer Slip Syringe; Millex Syringe Driven Filter Unit, 33 mm, PES membrane). A 2 ml subsample of each filtered solution was diluted with 8 ml Milli-Q water to prepare for ICP-MS analysis.

The digestion techniques used produced a dark coloured, tarry substance, therefore further concentrations of hydrogen peroxide were added to see if greater oxidation could be facilitated. A 0.2 g sample of each char was again weighed into Digitubes with 8 ml of HNO_3, allowing for 3 replicates for each sample and watch glasses placed on top as before and left overnight. H_2O_2 was then added at increasing concentrations of 2 ml, 4 ml, 6 ml, 8 ml and 10 ml and heated for 2 hours at 95°C to oxidise the carbon within the chars. The digestates were then syringe filtered (0.22 µm) and a 1:10 dilution using Milli-Q water was added to ICP-MS tubes. Additional H_2O_2 did not affect the results so the original digestion technique was maintained throughout.

2.2.3.2 *Water and Ammonium Nitrate Extractions*

Exchangeable and water available elements within the biochar were evaluated using ammonium nitrate (NH_4NO_3) and water extractions, respectively. A 1g sample of each char was weighed into centrifuge tubes with 9 ml of either NH_4NO_3 (1 M solution) or with Milli-Q H_2O in triplicate. The char-suspensions were placed on an end-over-end shaker for 2 hours and then centrifuged (Thermo Scientific Heraeus Megafuge 40) at 2500 rpm for 10 minutes. The samples were then syringe filtered (0.22µm) into Universal tubes and a 1:10 dilution of the filtered extracts was added to ICP-MS tubes.

2.2.3.3 *C-H-N and Organic Carbon*

C-H-N analysis was conducted by weighing 15 mg of each char and 2-3 mg of a standard (sulphanilamide) in triplicate before analysis on a C-H-N elemental analyser (ThermoFisher, Flash 2000, Organic Elemental Analyser). Oxygen contents were calculated by mass difference, using Eq. 2.4.

$$(O_2\% = 100 - (C\% + N\% + H\% + ash\ \%)$$

Eq. 2.4

Where O% is the percentage oxygen, C% is the percentage carbon, N% is the percentage nitrogen, H% is the percentage hydrogen and ash% is the ash content previously calculated.

Extractable TOC (total organic carbon) content of the chars was determined using a Shimadzu, TOC-V CPH TOC Analyser. A 20 ml sample of 0.01 M $Ca(NO_3)_2$ was added to 2 g of each powered char treatment and samples were placed on an end-over-end shaker for 2 hours followed by centrifugation at 2500 rpm (Thermo Scientific Heraeus Megafuge 40) for 10 minutes and then syringe filtering (0.22µm) into Universal tubes. A 1:10 dilution of the syringe filtered samples was performed prior to analysis.

2.2.4 BET Surface Area

The specific surface area and pore size for the nine chars was determined using the BET (Brunauer, Emmet and Teller) equation to produce nitrogen adsorption isotherms at 77 K in liquid nitrogen (Quantachrome Autosorb-1 Surface Area and Pore Analyser facility).

2.2.5 Statistical Analysis

To establish whether the observed differences for each biochar characteristic were significant, a one-way analysis of variance followed by a Tukey's post-hoc multiple comparison test ($p<0.05$) was conducted using GenStat (16^{th} Edition, VSN International).

2.3 RESULTS

2.3.1 Proximate Analysis

Moisture ($p<0.001$), volatile matter ($p<0.001$), ash content ($p<0.001$), pH ($p<0.001$) and EC ($p<0.001$) all significantly differed between the chars (Table 2.2). Moisture content was low in the high and low temperature gasified softwood chars (GSW and LGSW) and in the pyrolysed hardwood char (HW) and higher in the remaining chars (Table 2.2). Açaí and the artificially and naturally weathered pyrolysed hardwood chars (AHW and WHW respectively) had the highest volatile content and the low temperature gasified softwood (LGSW) the lowest volatile content. The key observation is that pyrolysed chars had a higher volatile content than the gasified softwood chars, but gasified bamboo char had a volatile content which was similar to that of the pyrolysed materials (Table 2.2). Ash content was highest in the softwood gasified chars ($p<0.001$; Table 2.2), with the exception of bamboo which showed the second lowest ash content. Both gasified softwood (GSW and LGSW) and cacao had the most basic pH at >11 and weathered pyrolysed hardwood (WHW) had the lowest pH of around 6. The remaining chars were all around pH 7 (Table 2.2). Low temperature gasified softwood char (LGSW) had the highest EC followed by the high temperature gasified softwood (GSW) char. The naturally aged pyrolysed (WHW) and the unweathered pyrolysed hardwood (HW) chars, açaí and bamboo chars had the lowest EC values (Table 2.2).

Table 2.2. Proximate analysis of the nine chars characterised showing moisture content, volatile matter, ash, pH and electrical conductivity. Cacao char stocks were low, so EC measurements were not performed. Volatile matter ($p<0.001$), ash content ($p<0.001$), moisture content ($p<0.001$), pH ($p<0.001$) and EC ($p<0.001$) were significantly different between chars. Chars similarly superscripted within columns are not significantly different (Tukey's multiple comparison test). Data are means ± SE.

Char	Moisture (%)	Volatiles (%)	Ash (%)	pH	EC
Açai	9.32 ± 1.59^{a}	105 ± 1.20^{a}	0.83^{e}	7.06 ± 0.06^{c}	732 ± 119^{e}
AHW	5.24 ± 0.21^{a}	100 ± 0.08^{ab}	0.00^{e}	7.16 ± 0.02^{c}	2590 ± 288^{c}
Bamboo	6.15 ± 0.17^{a}	96.2 ± 0.19^{c}	5.71 ± 0.28^{d}	7.07 ± 0.03^{c}	101 ± 2.37^{e}
Cacao	8.58 ± 0.76^{a}	84.8 ± 0.79^{d}	15.3 ± 0.79^{c}	$11.\ 2 \pm 0.13^{a}$	ND
Coffee	4.79 ± 0.29^{a}	96.2 ± 0.66^{bc}	3.73 ± 0.65^{e}	7.66 ± 0.33^{bc}	1540 ± 103^{d}
GSW	0.01^{b}	27.7 ± 0.99^{e}	71.1 ± 1.11^{b}	11.8 ± 0.02^{a}	6760.01 ± 169^{b}
LGSW	0.01^{b}	17.7 ± 0.65^{f}	80.8 ± 0.63^{a}	11.8 ± 0.01^{a}	8803.34 ± 135^{a}
HW	0.01^{b}	95.2 ± 0.21^{c}	4.27 ± 0.25^{d}	8.32 ± 0.03^{b}	418.33 ± 40.0^{e}
WHW	7.22 ± 0.32^{a}	101.7 ± 0.64^{a}	0.01^{e}	6.09 ± 0.05^{d}	80.03 ± 7.17^{e}

N=- not derived (due to technical issues).

2.3.2 Ultimate analysis

The carbon ($p<0.001$), hydrogen ($p<0.001$), oxygen ($p <0.001$) and nitrogen ($p<0.001$) concentrations differed across the char types (Figure 2.1a-d). The total carbon content ranged from 27-75% and pyrolysed chars had higher C concentrations than the gasified chars (Figure 2.1a). Whilst there was some significant variability in hydrogen and oxygen concentrations between the chars, the most notable observation was that the two gasified softwood chars (GSW and LGSW) contained the lowest amounts of each (Figure 2.1b-c). Coffee and açaí contained relatively high nitrogen concentrations compared to the other chars (Figure 2.1d).

The total $Ca(NO_3)_2$ extractable carbon (TC), extractable inorganic carbon (IC) and extractable organic carbon (TOC) all significantly ($p<0.001$) differed between chars (Figure 2.2a-c). Total extractable carbon was highest in gasified softwood chars with the lower temperature production method resulting in a higher concentration of total extractable C than that measured in char produced at the higher temperature. This is reflected by the inorganic rather than the organic C. Interestingly, the extractable organic C derived from artificially aged pyrolysed hardwood char was significantly higher than for all other chars and significantly higher than for the unweathered and naturally weathered equivalent char type (Figure 2.2c).

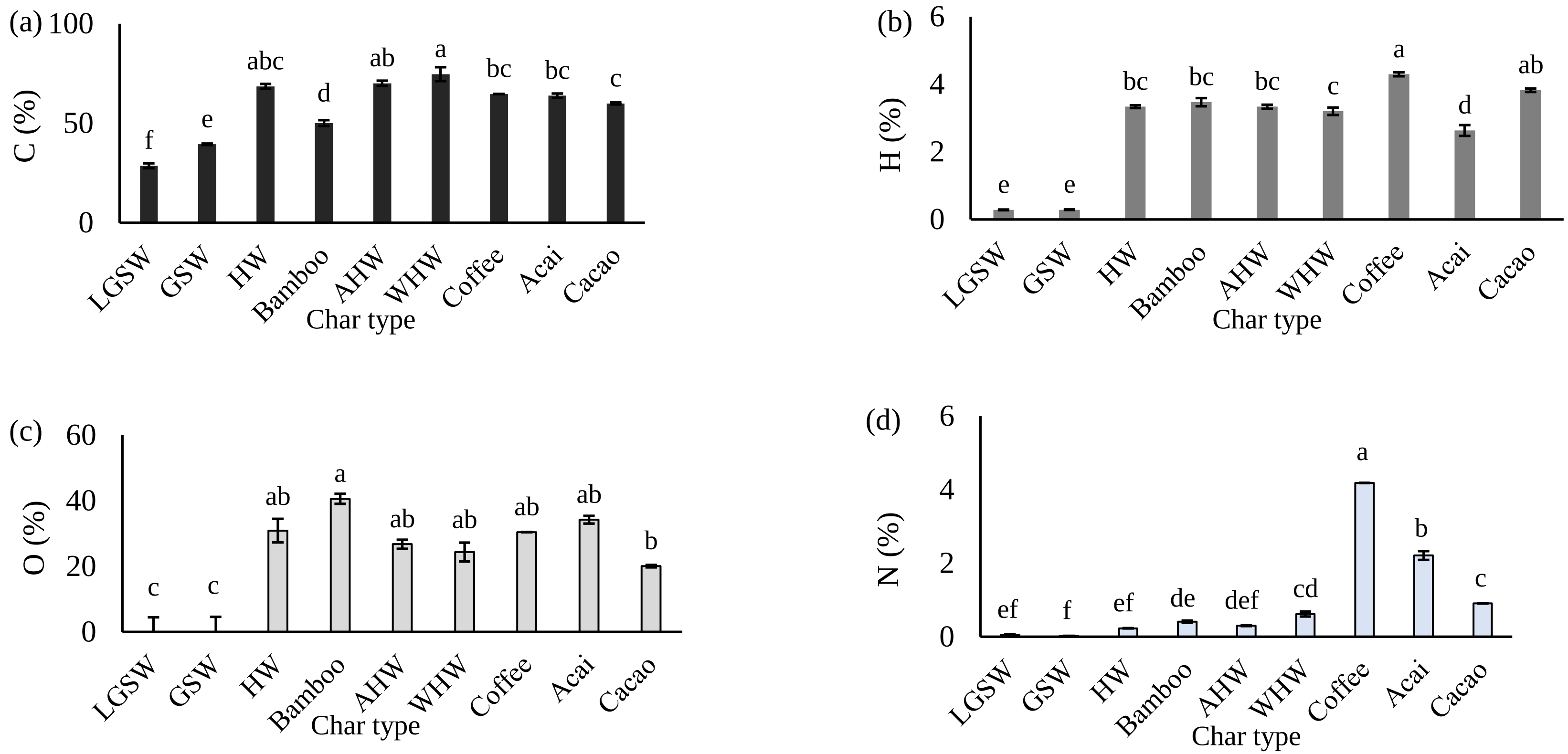

Figure 2.1. The percentage (a) carbon, (b) hydrogen, (c) oxygen and (d) nitrogen present in the chars tested. Data are means ± S.E. Chars similarly superscripted are not significantly different (Tukey's multiple comparison test). One-way ANOVA: Char effect for all elements, $p<0.001$. See Table 2.1 for abbreviations relating to char types.

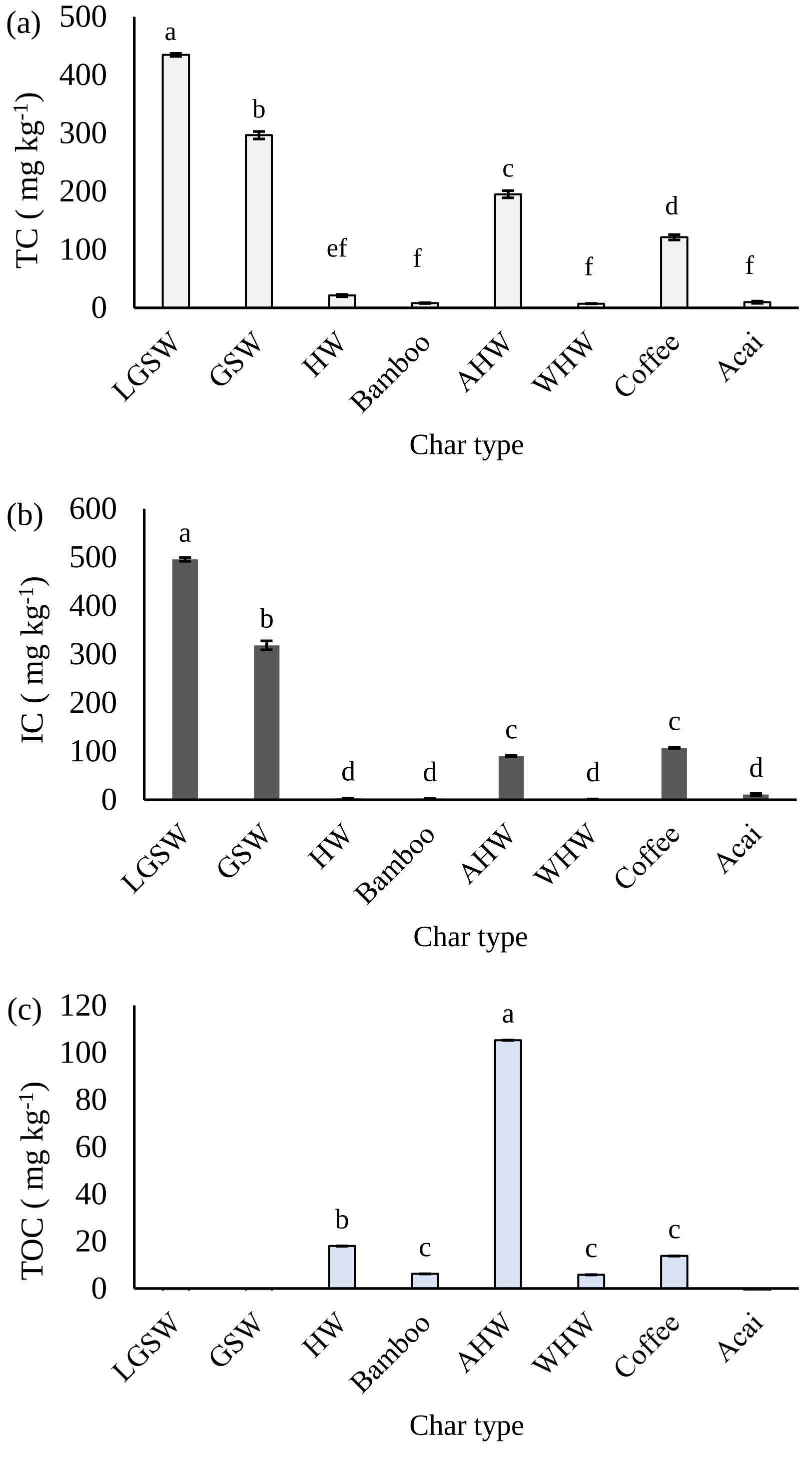

Figure 2.2. The (a) total extractable C (TC), (b) extractable inorganic C (IC) and (c) extractable organic C (TOC) concentration (mg kg^{-1}) for LGSW, GSW, HW, bamboo, AHW, WHW, coffee and açaí chars. Data are means ± S.E. Chars similarly superscripted are not significantly different (Tukey's test). One-way ANOVA: Char effect for all elements, $p<0.001$. See Table 2.1 for abbreviations relating to char types.

2.3.3 Elemental Analysis

2.3.3.1 *Total Elemental Concentrations*

Total elemental concentrations varied from one char to another (one-way ANOVA, $p<0.001$ for all total elements shown; Table 2.3). In general, the three gasified chars (GSW, LGSW and bamboo) contain the highest concentrations of total elements, relative to the pyrolysed chars (Table 2.3).

2.3.3.2 *Ammonium Nitrate Extractable Elements*

There was more variation between the different chars with regard to ammonium nitrate extractable elements than there was for the total elemental concentrations (Table 2.4). The two gasified softwood chars yielded the least exchangeable P and açaí, cacao and coffee chars the most, although only açaí was significantly different from the others.

Cacao char had the highest concentration of exchangeable K and the pyrolysed hardwood the lowest; the gasified softwood char had the highest concentrations of exchangeable Ca and Mg.

2.3.3.3 *Water Extractable Elements*

The water extractable concentrations reflect the immediate potential elemental release into soil solution and therefore bioavailability. The gasified softwood and pyrolysed hardwood chars yielded the least P into water, with the açaí and cacao chars releasing the highest concentrations of available P (Table 2.5). The highest concentrations of water-soluble K, Mg, Fe and Zn originated from the cacao char.

Table 2.3. Examples of total elemental concentrations of the nine chars characterised. Data are means ± S.E. Chars similarly superscripted are not significantly different (Tukey's test). One-way ANOVA: Char effect for all elements, $p<0.001$. See Table 2.1 for abbreviations relating to char types. Note the macro- and micro-elements have different units.

Char	P (mg kg^{-1})	K (mg kg^{-1})	Ca (mg kg^{-1})	Mg (mg kg^{-1})	Fe (µg kg^{-1})	Al (µg kg^{-1})	Mn (µg kg^{-1})	Zn (µg kg^{-1})	Sr (µg kg^{-1})	Ba (µg kg^{-1})
Açai	701 ± 66.6^{d}	2570 ± 231^{e}	307 ±20.5^{d}	299 ±21.2^{cd}	5680 ± 215^{c}	261 ±10.1^{d}	83500 ±7400de	4600 ±204^{d}	827 ±89.7^{c}	424 ±16.2^{c}
AHW	94.3 ± 1.09^{e}	532 ± 17.2^{e}	1130 ±25.1^{d}	95.8 ±2.77^{d}	5270 ± 293^{c}	3250 ±82.3^{d}	105000 ±3270de	9920 ±295^{d}	3020 ±84.1^{c}	5300 ±102^{c}
Bamboo	1730 ± 7.66^{c}	9060 ± 93.6^{d}	1580 ±26.2^{d}	699 ±4.03^{bc}	337000 ± 17300^{c}	358000 ±2810^{c}	535000 ±9000^{c}	39400 ±556^{c}	5600 ±92.4^{c}	36700 ±908^{c}
Cacao	277 ± 39.6^{e}	17700 ±2260^{c}	1960 ±247^{d}	1500 ±188^{b}	9190 ± 1280^{c}	2890 ±345^{d}	41800 ±5130^{e}	16400 ±1870^{d}	12200 ±1470^{c}	15500 ±1540^{c}
Coffee	670 ± 13.9^{d}	3130 ± 75.2^{e}	691 ±16.9^{d}	934 ±22.4^{b}	18200 ± 513^{c}	2310 ±74.9^{d}	20500 ±486^{e}	4250 ±139^{d}	3410 ±82.7^{c}	3330 ±77.2^{c}
GSW	6370 ± 85.4^{a}	35200 ± 243^{a}	109000 ±388^{a}	15800 ±45.6^{a}	54900000 ± 957000^{b}	3650000 ±30800^{a}	13000000 ±30800^{a}	307000 ±9210^{a}	501000 ±2310^{a}	2230000 ±13600^{a}
LGSW	2850 ±30.3^{b}	28500 ± 602^{b}	72200 ±1490^{b}	9840 ±176^{a}	76500000 ±1980000^{a}	2810000 ±48100^{b}	6390000 ±149990^{b}	181000 ±4790^{b}	385000 ±7960^{b}	1630000 ±17600^{b}
HW	252 ± 3.51^{e}	2320 ±17.4^{e}	4920 ±45.5^{c}	328 ±0.90^{cd}	92900 ± 28200^{c}	8060 ±517^{d}	366000 ±2510^{cd}	44800 ±185^{c}	10500 ±74.4^{c}	17800 ±195^{c}
WHW	119 ± 5.50^{e}	308 ± 49.7^{e}	724 ±90.7^{d}	114 ±7.71^{d}	13800 ±1280^{c}	8710 ±776^{d}	65500 ±7220de	12100 ±2610^{d}	1920 ±93.1^{c}	4060 ±121^{c}

Table 2.4. Examples of ammonium nitrate extractable elements associated with the nine chars characterised. Data are means ± S.E. Chars similarly superscripted are not significantly different (Tukey's test). One-way ANOVA: Char effect for all elements, $p<0.001$, except for Al which was not significantly different ($p=0.083$) despite the large range in concentrations observed. See Table 2.1 for abbreviations relating to char types. Note the macro- and micro-elements have different units.

Char	Extraction	P ($mg\ kg^{-1}$)	K ($mg\ kg^{-1}$)	Ca ($mg\ kg^{-1}$)	Mg ($mg\ kg^{-1}$)	Fe ($\mu g\ kg^{-1}$)	Al ($\mu g\ kg^{-1}$)	Mn ($\mu g\ kg^{-1}$)	Zn ($\mu g\ kg^{-1}$)	Sr ($\mu g\ kg^{-1}$)	Ba ($\mu g\ kg^{-1}$)
Açai	NH_4NO_3	968 $\pm150^{a}$	10500 $\pm1360^{c}$	682 $\pm144^{cd}$	493 $\pm90.4^{d}$	3930 $\pm596^{a}$	301 $\pm112^{a}$	75000 $\pm11000^{a}$	524 $\pm66.3^{c}$	2430 $\pm494^{d}$	671 $\pm126^{c}$
AHW	NH_4NO_3	43.8 $\pm2.96^{b}$	904 $\pm141^{d}$	1710 $\pm200^{c}$	45.7 $\pm4.31^{d}$	39.4 $\pm15.1^{c}$	121 $\pm18.7^{a}$	53800 $\pm5650^{ab}$	1500 $\pm47.3^{c}$	3260 $\pm344^{d}$	4480 $\pm458^{c}$
Bamboo	NH_4NO_3	85.0 $\pm19.3^{b}$	1860 $\pm1280^{d}$	11.0 $\pm0.08^{d}$	95.3 $\pm28.9^{d}$	51.0 $\pm13.2^{c}$	1180 $\pm953^{a}$	383 $\pm1.76^{d}$	366 $\pm230^{c}$	1560 $\pm1260^{d}$	1270 $\pm891^{c}$
Cacao	NH_4NO_3	290 12.0^{b}	114000 $\pm2360^{a}$	685 $\pm11.2^{cd}$	3290 $\pm89.4^{a}$	2050 $\pm100^{b}$	343 $\pm5.86^{a}$	7590 $\pm165^{d}$	3600 $\pm123^{b}$	11300 $\pm36.8^{c}$	14000 $\pm203^{c}$
Coffee	NH_4NO_3	270 $\pm22.8^{b}$	6800 $\pm498^{cd}$	246 $\pm20.1^{d}$	313 $\pm27.1^{d}$	774 $\pm93.4^{bc}$	472 $\pm87.7^{a}$	1450 $\pm106^{d}$	140.5 $\pm53.1^{c}$	1220 $\pm104^{d}$	916 $\pm72.0^{c}$
GSW	NH_4NO_3	2.48 $\pm0.13^{b}$	47900 $\pm1850^{b}$	26000 $\pm553^{a}$	2470 $\pm174^{b}$	259 $\pm10.1^{c}$	0.00^{a}	64000 $\pm3790^{ab}$	21500 $\pm931^{a}$	104000 $\pm2690^{a}$	258000 $\pm7310^{a}$
LGSW	NH_4NO_3	4.92 $\pm0.16^{b}$	5200 $\pm1420^{b}$	12200 $\pm199^{b}$	1180 $\pm57.5^{c}$	13.3 $\pm5.64^{c}$	0.00^{a}	16100 $\pm281^{cd}$	3680 $\pm215^{b}$	75700 $\pm934^{b}$	110000 $\pm983^{b}$
HW	NH_4NO_3	36.6 $\pm1.54^{b}$	1060 $\pm10.7^{d}$	1890 $\pm6.64^{c}$	54.7 $\pm0.86^{d}$	0.00^{c}	0.00^{a}	39000 $\pm439^{bc}$	58.7 $\pm32.8^{c}$	3450 $\pm1.51^{d}$	4100 $\pm80.9^{c}$
WHW	NH_4NO_3	32.7 $\pm1.36^{b}$	32.7 $\pm1.36^{d}$	648 $\pm20.1^{cd}$	104 $\pm1.41^{d}$	701 $\pm103^{c}$	1770 $\pm260^{a}$	8620 $\pm207^{d}$	5670 $\pm184^{b}$	1070 $\pm29.1^{d}$	2950 $\pm149^{c}$

Table 2.5. Examples of water extractable elements associated with the nine chars characterised. Data are means ± S.E. Chars similarly superscripted are not significantly different (Tukey's test). One-way ANOVA: Char effect for all elements, $p<0.001$. See Table 2.1 for abbreviations relating to char type. Note the macro- and micro-elements have different units.

Char	**Extraction**	**P (mg kg^{-1})**	**K (mg kg^{-1})**	**Ca (mg kg^{-1})**	**Mg (mg kg^{-1})**	**Fe (µg kg^{-1})**	**Al (µg kg^{-1})**	**Mn (µg kg^{-1})**	**Zn (µg kg^{-1})**	**Sr (µg kg^{-1})**	**Ba (µg kg^{-1})**
Açai	H_2O	845 ±113^{a}	6390. ±1480^{bc}	158 ±39.6^{b}	269 ±53.0^{b}	1510 ±233^{b}	154 ±19.0^{c}	25400 ±1900^{a}	127 ±42.7^{c}	549 ±137^{b}	34.1 ±4.88^{d}
AHW	H_2O	20.5 ±0.42^{b}	401 ±24.3^{bc}	290 ±6.98^{a}	26.0 ±1.15^{b}	33.0 ±9.23^{cd}	143 ±7.35^{c}	11100 ±252^{b}	189 ±4.58^{c}	782 ±26.9^{b}	680 ±24.5^{b}
Bamboo	H_2O	110 ±1.07^{b}	119 ±72.8^{c}	11.1 ±0.14^{c}	60.5 ±0.86^{b}	71.0 ±5.12^{cd}	7.66 ±3.44^{c}	382 ±0.38^{c}	84.4 ±0.78^{c}	15.5 ±0.24^{d}	154 ±22.0^{d}
Cacao	H_2O	792 ±45.7^{a}	76300 ±5900^{a}	304 ±17.1^{a}	1630 ±163^{a}	4670 ±306^{a}	340 ±20.4^{c}	13400 ±1200^{b}	6390 ±379^{a}	2250 ±145^{a}	2410 ±153^{a}
Coffee	H_2O	198 ±4.37^{b}	1850 ±18.6^{bc}	11.0 ±0.64^{c}	34.9 ±1.02^{b}	272 ±7.25^{cd}	302 ±7.91^{c}	222 ±3.99^{c}	122 ±12.4^{c}	33.3 ±0.86^{cd}	15.1 ±0.93^{d}
GSW	H_2O	20.3 ±0.64^{b}	39600 ±967^{abc}	98.5 ±4.66^{bc}	0.49 ±0.28^{b}	631 ±22.8^{cd}	494000 ±11500^{b}	331 ±13.9^{c}	238 ±12.4^{c}	437 ±4.68^{bc}	500 ±9.91^{bc}
LGSW	H_2O	24.2 ±0.47^{b}	43400 ±454^{ab}	101 ±1.96^{bc}	0.10 ±0.01^{b}	783 ±36.2^{bc}	822000 ±6780^{a}	232 ±7.85^{c}	0.00^{c}	487 ±7.95^{b}	270 ±8.53^{cd}
HW	H_2O	3.15 ±0.37^{b}	470 ±29.6^{bc}	144 ±8.38^{b}	15.5 ±0.99^{b}	0.00^{d}	305 ±72.7^{c}	3690 ±186^{c}	0.00^{c}	432 ±27.4^{bc}	162 ±21.1^{d}
WHW	H_2O	13.4 ±0.23^{b}	153 ±2.67^{c}	271 ±4.41^{a}	83.9 ±1.67^{b}	214 ±1.32^{cd}	299 ±3.68^{c}	2860 ±43.3^{c}	1050 ±38.1^{b}	447 ±8.19^{bc}	308 ±3.56^{cd}

2.3.4 BET Surface Area

The BET surface area measurements from the adsorption isotherms showed each char had a different surface area (Table 2.6). The high temperature gasified softwood char (GSW) had the highest surface area, followed by açaí char and then the low temperature gasified softwood char (LGSW). The pyrolysed hardwood char (unweathered and artificially and naturally weathered) had the lowest surface area of all the chars tested (Table 2.6).

Table 2.6. Summary of production conditions and surface area of the nine chars tested. Surface area was determined from BET (Brunauer, Emmet and Teller) nitrogen adsorption isotherms.

Char	Production Temperature (°C)	Production Time (hours)	BET Surface Area (m^2 g^{-1})
Açaí	450	10	234
AHW	450	48	0.04
Cacao	450	8	2.39
Coffee	450	10	ND
GSW	916- 770	6	453
LGSW	862- 731	6	154
HW	450	48	0.10
WHW	450	48	0.11
Bamboo	~700-900	Unknown	ND

ND = not derived (due to technical issues)

2.4 DISCUSSION

Biochar characteristics alter a char's ability to act as a fertiliser within soils due to the impact on nutrient interactions and availability (Wang *et al.*, 2013). Feedstock characteristics, production temperature and production methods are all linked to variable biochar properties (Azargohar *et al.*, 2014; Bird *et al.*, 2011; Enders *et al.*, 2012; Hong & Lu, 2018; Novak *et al.*, 2009; Wang *et al.*, 2013; Zhao *et al.*, 2013), therefore quantifying the influence of feedstock and production regime on char characteristics is essential in understanding the potential interactions with nutrients in soils.

2.4.1 Chemical Characterisation

2.4.1.1 *Proximate Analysis*

2.4.1.1.1 Volatile Matter Content

Volatile matter content varies between chars according to production temperature, mechanism and feedstock (Brewer *et al.*, 2011; Cantrell *et al.*, 2012; Keiluweit *et al.*, 2010; Lee *et al.*, 2010; Zhao *et al.*, 2013). Char production temperature is negatively correlated with volatile content, as observed with the chars presented here, with the exception of bamboo char (Table 2.2), as higher production temperatures often facilitate the loss of volatile compounds (Cantrell *et al.*, 2012; Downie *et al.*, 2009; Enders *et al.*, 2012; Keiluweit *et al.*, 2010; Knicker, 2007; Novak *et al.*, 2009). Brewer *et al.* (2011) demonstrated that gasification reduced the presence of volatile compounds when compared to fast pyrolysis, suggesting production method caused the lower volatile content of the gasified chars tested here (Table 2.2). However, gasification temperatures are often higher (700-900°C) than pyrolysis temperatures (300-600°C), making it difficult to distinguish between the role of production temperature and method *per se* (Mohan *et al.*, 2006).

Char feedstock can influence the volatile content of chars to a greater extent than production temperature and mechanism (Brewer *et al.*, 2011; Chen *et al.*, 2011; Keiluweit *et al.*, 2010). The bamboo char produced through gasification at IIT in India contained a high proportion of volatiles compared to both the high- and low-temperature UK-produced gasified softwood char, suggesting feedstock as opposed to production mechanism influence volatile content (Table 2.2). Bamboo is known to contain high concentrations of terpenes and Huang *et al.* (2016) demonstrated enhanced volatility of these with increasing temperature and time of heating bamboo. The duration of the gasification process is unknown for the bamboo used here, but residual terpenes (or other volatile compounds) were present in the char. However, the softwood used during the UK gasification process was pine, a feedstock that also has high concentrations of volatiles. Nevertheless, using a model, Fjellerup *et al.* (2005) demonstrated that volatile compounds in pine stabilise during gasification at 400^{o}C, although experimental data suggest the temperature at which volatiles stabilise is 600^{o}C; they stabilise at a 73% (model prediction) or at a 77% (experimental) loss, thus leaving 23-27% within the char. Without comparative analysis of the feedstock, it is difficult to determine why there are differences between the bamboo and pine (softwood) chars.

The pyrolysed chars, such as açaí, hardwood char (weathered and unweathered), cacao and coffee chars, varied in volatile content, despite the uniform production temperature, further showing the influence of feedstock (Table 2.2), although it should be noted that production times were different.

The ageing processes to which the naturally and artificially weathered pyrolysed softwood chars were subjected, appeared to influence volatile content (Table 2.2). The decreased stability associated with aged chars (Cross & Sohi, 2013) may cause weakening of bonds thereby increasing volatilisation, which may explain the higher concentration of volatiles observed in the artificially weathered char and potentially the naturally weathered char, compared to the unweathered pyrolysed softwood char (Table 2.2).

Understanding the volatile content of chars is important when considering char as a soil amendment as a higher volatile content stimulates microbial growth. Increased microbial growth can both reduce and increase plant growth through microbial assimilation and immobilisation respectively of phyto-essential N and P and enhance growth by solubilising nutrients (Deenik *et al.*, 2009; Deenik *et al.*, 2010; Sarma *et al.*, 2018).

2.4.1.1.2 Ash Content

Ash content in chars increases in line with production temperature (Cantrell *et al.*, 2012; Chen *et al.*, 2011; Enders *et al.*, 2012; Hossain *et al.*, 2011; Novak *et al.*, 2009; Pituello *et al.*, 2015; Wang *et al.*, 2013), which may explain the higher ash content of the low- and high-temperature gasified softwoods compared to that of the pyrolysed chars (Table 2.2). The reason for this is that at higher production temperatures, more ash forms because mineral constituents in effect, become more concentrated (Cao & Harris, 2010). Furthermore ash and carbon contents are often negatively correlated due to combustion of carbon at high temperatures (Cantrell *et al.*, 2012.; Cao & Harris, 2010; Chen *et al.*, 2011; Hossain *et al.*, 2011; Qian *et al.*, 2015); this was observed for the two gasified softwood chars (Table 2.2; Figure 2.1) which contained the lowest measured %C and highest ash content of all the chars. However, it should be acknowledged that % elemental C is a different measure from 'fixed C' which would be determined by thermogravimetric analysis. Nevertheless, the data here suggest that production temperature alone is not the only driver of ash content. This is exemplified by considering the ash content of the pyrolysed chars which were produced at the same temperature

(Table 2.2); for instance, cacao char produced more ash than did açaí char. The original feedstock was not analysed here, but according to the literature, cocoa husks contain 15.7% lignin, 35.4% cellulose and 37.0% hemicelluloses (Daud *et al*., 2013), whilst açaí seeds contain 7.7% lignin, 34.4% cellulose and 12.3% hemicellulose (M.M.C. Ferreira, 2010, DIBANET presentation, Rio de Janeiro). Since all the chars studied originated from lignocellulosic biomass, the ratio of lignin, cellulose and hemicellulose, in addition to other chemical constituents, determine not only the thermal behaviour of the feedstock, but the chemistry of the resulting char and the ash produced (Garcia-Maraver *et al*., 2013). Engineers interested in optimising combustion in order to develop sustainable fuel products could modify the pyrolysis processes and conditions to suit the particular biomass. However, the intention here was to compare a range of feedstocks across a standardised pyrolysis regime in addition to comparing two gasified products. The low ash content of the gasified bamboo char compared to the gasified softwood char suggests feedstock stability as well as the lignin/cellulose ratio is as important as production temperature and method (Enders *et al.*, 2012; Novak *et al.*, 2009; Wang *et al.*, 2013; Zhao *et al.*, 2013).

The weathering and chemical oxidation processes that the pyrolysed hardwood char was subjected to lowered the ash content from ~4% in the unweathered char to negligible amounts in the treated char, most likely because ash was washed from the char. The presence of ash within chars can block sorption sites and therefore modify char/nutrient interactions. Chars with lower ash contents, such as açaí, may therefore sorb elements more efficiently, potentially reducing contamination and improving soil fertility.

2.4.1.2 *pH Values*

Biochars produced at elevated temperatures often have an alkali pH, primarily due to the higher ash content which retains basic elements such as K, Ca and Mg (Brewer *et al.*, 2009; Brewer *et al.*, 2011; Cantrell *et al.*, 2012; Enders *et al.*, 2012; Mukherjee *et al.*, 2011; Novak *et al.*, 2009; Pituello *et al.*, 2015; Wang *et al.*, 2013; Yuan *et al.*, 2011; Zhao *et al.*, 2013). The high pH value and ash content of the gasified softwood chars observed here (Table 2.2) corroborate this. Furthermore, acidic functional groups such as carboxyl groups are degraded at high production temperatures resulting in decreased surface acidity and increased pH (Enders *et al.*, 2012; Hollister *et al.*, 2013; Nguyen & Lehmann, 2009; Novais *et al.*, 2018; Wang *et al.*, 2013).

Feedstock also influences biochar surface acidic groups which are often associated with crop-derived chars as opposed to wood-based chars (Wang *et al.*, 2013). Cacao char had a higher pH than pyrolysed hardwood char in spite of the same production temperature being used for both; although not measured, acidic groups may have been the cause. The presence of acidic groups will vary between feedstocks. Higher Ca and Mg contents, which are linked to original feedstock, are also associated with high pH chars (Novak *et al.*, 2009); this may also explain the basic pH of cacao as Mg and Ca were readily available (Table 2.2; Table 2.5). The pH of chars decreases through ageing (Sorrenti *et al.*, 2016), as observed for the chemically and naturally weathered pyrolysed hardwood char compared to the unweathered variant (Table 2.2). Both weathering and artificial ageing increases oxidation of chars facilitating production of acidic carboxyl groups on the char resulting in a reduced pH (Sorrenti *et al.*, 2016). The lower pH of the weathered chars relative to that of the unweathered char suggests the liming benefits associated with char amendment to acidic soils may be short-lived. Developing an understanding of long-term chemical interactions is therefore required to ensure beneficial results are observed.

2.4.1.3 *Electrical Conductivity*

EC is a measure of salinity therefore is an important measurement to understand the impact of char on salt content in soils (Azargohar *et al.*, 2014; Cantrell *et al.*, 2012). EC often varies from one char to another (Shenbagavalli & Mahimairaja, 2012) and high production temperatures are associated with lower EC values (Azargohar *et al.*, 2014) as seen here with the gasified softwood char, although not with the gasified bamboo char (Table 2.2). The elemental contents of ash are also associated with high EC measurements explaining the influence of production temperature (Azargohar *et al.*, 2014), which complements the data obtained for EC and ash contents for the gasified softwood chars (Table 2.2; Table 2.3). Artificially weathered char and coffee char were both exposed to oxidation; weathered char during artificial ageing of the char and coffee beans, during the roasting process prior to making char. The prior treatment of artificially weathered and coffee chars likely increased the disintegration of salts from the char surface, increasing EC measurement (USDA, 2015).

2.4.1.4 *Ultimate Analysis*

2.4.1.4.1 Carbon Content

The heating required to produce chars causes a reduction in oxygen and hydrogen while increasing the carbon content (Lee *et al.*, 2010; Lee *et al.*, 2013; Novak *et al.*, 2009). An elevated presence of carbon therefore is generally associated with higher production temperatures (Angin *et al.*, 2013; Azargohar *et al.*, 2014; Enders *et al.*, 2012; Lee *et al.*, 2013; Zhao *et al.*, 2013) as the rate of aliphatic cleavage increases, thereby freeing up the aromatic carbon backbone of the char (Azargohar *et al.*, 2014; Cheng *et al.*, 2008a; Keiluweit *et al.*, 2010) and this explains the high C associated with the high-temperature gasified softwood char (Figure 2.1a). However, carbon concentrations within the pyrolysed chars were higher than those in the gasified chars, and C content of the three gasified chars differed (Figure 2.1a) indicating feedstock influences carbon contents, which is supported by Brewer *et al.* (2011). Wood based chars usually have higher C contents compared to crop derived chars (Wang *et al.*, 2013); however coffee, açaí, cacao and pyrolysed hardwood chars all show similar amounts of C which is unlikely if feedstock was influencing (Figure 2.1a). The apparent lack of effect of production temperature or feedstock on C content suggests production mechanism was important (Zhao *et al.*, 2013), with gasification reducing C the most. The lower total carbon content of gasified compared to pyrolysed chars may be linked to the density at which feedstocks are packed during production (Peterson & Jackson, 2014). Gasification requires a low density and loosely packed feedstock whereas the pyrolysed chars were more tightly packed. The reduced feedstock density of gasification methods allows increased combustion causing loss of carbon (Peterson & Jackson, 2014).

The lability of organic carbon (TOC data) appeared to be related to production method with negligible soluble TOC measured from the gasified softwood chars and the chemical weathering treatment of the pyrolysed hardwood char which enhanced release of organic C into solution (Figure 2.2c). Inorganic carbon (IC) is often most prevalent within chars and increases at higher production temperatures (Lee *et al.*, 2013), again, due to the freeing up of the aromatic backbone (Figure 2.2b; Figure 2.1a) and the data here support that assertion since higher concentrations of IC were released into solution by the gasified softwood chars than by the pyrolysed chars. The high prevalence of carbon, particularly inorganic carbon, means that when used as a soil amendment the char enables soil to act as a carbon sink (Lee *et al.*, 2013); therefore understanding the feedstock and production methods to enable production of 'carbon-efficient' char will have clear environmental benefits.

Some of the chars presented demonstrate a higher inorganic carbon measurement than total carbon which may be due to the associated high pH (Figure 2.2a &b). The mechanism for measuring TC, IC and TOC involves acidification and oxidation of the samples (Findlay *et al.*, 2010). The high pH the gasified softwood chars would reduce the degree of acidification, potentially resulting in overestimation of inorganic carbon (Table 2.2). One aliquot of the sample undergoes oxidation and is compared to an unoxidised second aliquot to allow calculation of DOC (Findlay *et al.*, 2010). The exposure of the chemically weathered pyrolysed hardwood char to oxidation during the artificial ageing treatment post-char manufacture may explain the increased DOC, which may be an overestimation. Alternatively it may be the result of a Type 1 error, although the small S.E. suggests consistency across the replicates and the aging process may be a speeded up reflection of the long-term effect of weathering on this char.

2.4.1.4.2 Hydrogen Content

Dehydration reactions reduce hydrogen content and occur more often at higher temperatures (Angin *et al.*, 2013; Zhao *et al.*, 2013). Dehydration reactions are associated with char production temperatures above 350°C when cellulosic components are broken down (Angin *et al.*, 2013; Zhao *et al.*, 2013) and therefore likely occur in all the chars explored here (Table 2.1). Reduced hydrogen occurs through the breakdown of -OH functional groups as temperatures increase resulting in the loss of O and H bound to C (Antal & Grønli, 2003; Lee *et al.*, 2013; Novak *et al.*, 2009) explaining the lower H and O in the gasified softwood chars (Figure 2.1b &c). Elevated dehydration reactions at increased temperatures also explain the increased moisture content of pyrolysed chars in comparison to gasified, with the exception of the pyrolysed hardwood and bamboo chars (Table 2.2) (Ahmad *et al.*, 2014; Keiluweit *et al.*, 2010.).

The production mechanism also influences hydrogen content. The requirement of gasification to produce a gas rich in carbon monoxide (Mohan *et al.*, 2006) and hydrogen (Keiluweit *et al.*, 2010) may reduce the carbon and hydrogen concentrations of chars, however in the gasified bamboo C and O remain high (Figure 2.1a, b &c). This may be a reflection of the process, which may have been less controlled than the gasification carried out at Nottingham. Although production temperature is likely to be the main influencer relating to H % within chars, due to the bearing it has on dehydration reactions, the variation within the pyrolysed and the high content in gasified bamboo suggests feedstock stability in part plays a role (Figure 2.1b).

2.4.1.4.3 Nitrogen Content

The decomposition of char observed at higher temperatures (Cheng *et al.*, 2008a; Hossain *et al.*, 2011; Wang *et al.*, 2013) will lower nitrogen contents in the gasified chars through the breakdown and volatilisation of nitrogen containing functional groups. Pituello *et al.* (2015) found nitrogen decreased at temperatures greater than 550°C and postulated the reduction was due to the cracking of nitrile-N and heterocyclic-N compounds at higher temperatures, which supports the low N concentrations in the gasified softwood chars here (Figure 2.1d).

The conversion of N compounds during char production and therefore maintenance of N within char has also been linked to feedstock (Enders *et al.*, 2012; Suliman *et al.*, 2016), which supports the data here as coffee, açai and cacao chars had higher nitrogen contents than the wood chars produced at the same temperature (Figure 2.1d). The higher nitrogen content of crop-derived chars when compared to wood chars may be due to the lower N enrichment of woods (Wang *et al.*, 2013) as crop feedstocks will have been encouraged to take up N as it is an essential nutrient for crop growth. It should be noted that coffee and açaí chars originated from the seed of the plant (and cacao, the husk) rather than the main stem (e.g. the wood chars); therefore the original feedstock would have been relatively N-rich.

The lack of difference between unweathered and chemically weathered pyrolysed hardwood char with regard to percentage C, N, H and O (Figure 2.1a-d) further suggests production mechanism and feedstock influence the final make-up of the char which remains fairly stable when exposed to chemical oxidation.

2.4.1.5 *Inorganic Elemental Analysis*

The elemental contents of the chars presented here were selected for analysis because of their importance with regard to soil fertility, either directly or because they interact with phosphorus, e.g. Ca, K, P, Mg and Fe (Azargohar *et al.*, 2014). The elemental concentrations often relate to the ash contents, suggesting elements should be highest in the gasified softwood char and lowest in the açaí and pyrolysed hardwood wood chars (Azargohar *et al.*, 2014), but this was not observed. Alkali elements such as Mg, K and Ca are often the most abundant minerals within chars, likely causing the basic pH observed in all chars, and therefore will improve the micronutrient availability of amended soils (Azargohar *et al.*, 2014).

2.4.1.5.1 Phosphorus and Associated Elements

The use of char as a soil amendment coupled with the requirement of phosphorus within plants highlights the importance of understanding char-phosphorus interactions (Azargohar *et al.*, 2014). Pituello *et al*. (2015) found that total P concentrations decreased with increasing production temperature, which was not observed in this study as the high temperature gasified softwood char had a significantly higher total P concentration than the low temperature equivalent (Table 2.3) and both these gasified chars contained more

P than the pyrolysed chars. However, high temperature chars can contain more concentrated total P because P is not lost through volatilisation until 700°C (DeLuca *et al.*, 2015; Novak *et al.*, 2009; Robinson *et al.*, 2018; Sun *et al.*, 2018b; Tan *et al.*, 2018), which could explain the high total P for the gasified chars. Although production temperature achieved within the reduction zone was higher than 700°C (Table 2.1), lignin breaks down slowly after 450^{o}C is exceeded (Gani & Naruse, 2007) potentially 'trapping' P within the matrix. Furthermore, according to Prieur *et al*. (2017), P enhances the thermal stability of lignin, particularly at high temperatures. This is borne out by the lack of water- or NH_4NO_3-extractable P from the gasified softwood chars relative to the other chars tested despite the differences in total P concentrations. Feedstock stability influences available P (Enders *et al.*, 2012; Gaskin *et al.*, 2008; Hossain *et al.*, 2011; Peng *et al.*, 2011; Sun *et al.*, 2018b; Wang *et al.*, 2013) and *vice versa*. Also, P speciation will be different depending on feedstock and this will affect availability (DeLuca *et al.*, 2015).

The high P availability observed with cacao and açaí chars (Table 2.5) would improve the fertility of soils which are P deficient (Sohi *et al.*, 2009). However if desorption of P is too great, saturation would be observed resulting in P precipitation into a solid phase or loss of P into the terrestrial environment potentially resulting in eutrophication of water courses (DeLuca *et al.*, 2015). Precipitation of available P is enhanced by the presence of Ca, Mg, Fe and Al meaning unavailable forms of P are formed, thus illustrating why an understanding of the char chemistry is essential in determining its likely affect as a fertiliser or soil improver (DeLuca *et al.*, 2015; Eberhardt *et al.*, 2006; Stutter, 2015; Yao *et al.*, 2011a, 2011b; Zeng *et al.*, 2013).

Total Ca, Mg and Fe all increase in line with elevated production temperature (Cheah *et al.*, 2014; Ding *et al.*, 2014; Hollister *et al.*, 2013; Srinivasan & Sarmah, 2015), and the data here are generally in agreement with this (apart from the gasified bamboo char); however elemental availability appears to alter according to char feedstock.

Production mechanism influences elemental concentration within chars (Ahmad *et al.*, 2014; Cantrell *et al.*, 2012). During certain gasification processes, the char produced mixes with a fine dust called olivine which decomposes any tar created during the process (Rapagna *et al.*, 2000). Olivine is a mineral containing magnesium and iron oxides (Rapagna *et al.*, 2000) resulting in a biochar ash with high concentrations of Mg and Fe, as observed for total Mg and Fe in the gasified softwood chars here (Table 2.3). However, bamboo char has low total Mg and Fe concentrations in spite of gasification, suggesting production mechanism in not the primary influencer (Table 2.3).

Hollister *et al.* (2013) attributed increased concentrations of available Ca to elevated production temperature, where corn biochar produced at 550°C leached up to 105% higher Ca amounts than char produced at 350°C, however only one feedstock was compared. The increased ash contents of chars produced at higher temperatures are known to influence a char's elemental availability. For example, Brewer *et al*. (2009) found Al concentration to increase in line with production temperature due to increased ash presence, which complements the ash and Al data for gasified chars (Table 2.3; Table 2.4; Table 2.5) although there is a difference between the presence of ash within the char and that formed through combustion in a muffle furnace. Production temperature has been linked to increased ash contents, however feedstock is often attributed to the variation in elements within the ash, highlighting that not all elements increase in line with ash content, but relate to initial feedstock (Brewer *et al.*, 2009; Enders *et al.*, 2012). Quantifying the amount and availability of elements within the char and associated ash and the potential impact on soil biological and chemical characteristics is required before recommending char as a soil amendment.

2.4.1.5.2 Other Essential Elements

Potassium availability often increases in line with pyrolysis temperature due to degradation of bonds at elevated temperatures (Hossain *et al.*, 2011; Peng *et al.*, 2011; Pituello *et al.*, 2015) and this trend was observed in the gasified softwood chars which had high concentrations of available K (Table 2.5). The lower K availability from bamboo compared to cacao char, despite the higher production temperature again suggests that feedstock may have a greater influence over K availability (Table 2.5). Crop derived chars have been associated with higher K concentrations than manure based chars showing feedstock may be causing the differences observed (Zhao *et al.*, 2013).

Higher ash contents are linked to elevated Zn concentrations (Qian *et al.*, 2015) as seen by the total and NH_4NO_3 extractable Zn in gasified softwood chars (Table 2.3; Table 2.4). Zn availability is also affected by external influences such as soil characteristics which is demonstrated by the increased total and available concentrations in the naturally weathered pyrolysed hardwood char compared to the unweathered char. Natural weathering was carried out in metal contaminated soil and the available Zn and Fe profiles of this char (Table 2.5) reflect adsorption from the soil solution during weathering (Ahmad *et al.*, 2014). Zn is considered a potentially toxic metal if present in high concentrations, therefore chars that adsorb of Zn have potential uses in soil remediation. Similarly, Zn and Fe can be limiting in some soils and ‘loaded’ char could be used as a means of fortifying these soils. The high concentrations of Zn available from cacao char (Table 2.5) could have the potential to be detrimental to soils, however the maximum H_2O available Zn observed, 6390 µg kg^{-1} (6.39 mg kg^{-1}), suggests little risk of soil toxicity if any of the chars were to be used as an amendment (Azargohar *et al.*, 2014).

Overall the different available elemental concentrations demonstrated by the chars appear to be influenced by feedstock, whereas total levels increase in line with production temperature, which is in agreement with the literature (e.g. Hong & Lu, 2018; Zhao *et al.*, 2013). Production temperature and ageing treatment of chars have an elemental influence due to the impact on the production of ash and weakening of bonds, respectively (Atkinson *et al.*, 2010). Feedstock has been heavily linked to char final elemental composition (Hong & Lu, 2018; Mohanty *et al.*, 2013; Pituello *et al.*, 2015; Suliman *et al.*, 2016) and been implicated as a strong predictor for ash and C/N contents of char as opposed to pyrolysis temperature (Mukome *et al.*, 2013). The analysis of the feedstock both before and after char production is therefore necessary to interpret whether production temperature or feedstock is influencing final elemental concentrations within chars.

Improving the understanding how both production and feedstock influence the chemical nature of chars is essential in creating bespoke biochars for soils. Once added to soils chars appear to be stable, evidenced by the maintained carbon content within the chemically and naturally aged pyrolysed hardwood chars (Figure 2.1a), however stability after ageing has been found to vary according to feedstock (Cross & Sohi, 2013). This highlights the importance of quantifying interactions and the influence of environmental factors on char on determining elemental availability. Chars with higher proportions of alkaline elements have been proposed as successful soil amendments (Azargohar *et al.*, 2014), therefore the high availability of K, Ca and Mg desorbed from cacao char suggests this would act as a good soil amendment (Table 2.5). The ability of chars to be considered a ‘good’ amendment, however varies depending on the requirements and characteristics of the soil.

2.4.2 Physical Characterisation

2.4.2.1 *BET Surface Area*

Although both feedstock and production temperature are linked to BET surface area (Wang *et al.*, 2013), temperature is considered the more important factor as temperature influences the fundamental physical changes during production (Downie *et al.*, 2009; Lee *et al.*, 2010; Lee *et al.*, 2013; Tan *et al.*, 2018). At temperatures above 350°C, cellulose within lignocellulosic materials decomposes thereby increasing surface area because 'gaps' are formed within the lignin framework (Zhao *et al.*, 2013). As production temperatures further increase, surface pores become larger and more abundant through the breakdown of walls between pores, creating a greater distance between aromatic C, which further increases surface area (Chia *et al.*, 2015; Downie *et al.*, 2009; Lee *et al.*, 2013; Novak *et al.*, 2009). Sustained heating to temperatures above 750°C, however, has been linked to reduced surface area as lignin within the char begins to breakdown (Chia *et al.*, 2015). Surface area variation also often relates to the rate of heating (Brown *et al.*, 2006). Lower production temperatures are linked to reduced char surface area due to the lack of de-volatilisation and degradation reactions required for surface pore creation (Lee *et al.*, 2013).

The oxidative burn-off associated with gasification systems, which is less common in pyrolysis, is linked to increased surface area (Zabaniotou *et al.*, 2008) supporting the higher surface area measured in both the gasified softwoods chars (Table 2.6). However, char surface pores can get blocked when a char has a high ash content (Novak *et al.*, 2009), explaining the lower surface area of the lower temperature gasified char relative to the high temperature gasified softwood char (Table 2.6), despite high production temperatures and oxidative burn off.

Surface area is also influenced by char feedstock (Novak *et al.*, 2009). During biochar production, cracking of the feedstock can occur in which the surface of a material degrades at a quicker rate than the interior altering surface area (Downie *et al.*, 2009). Cracking often occurs at temperatures below 450°C, meaning all the chars characterised here are exposed (Table 2.1) (Brown *et al.*, 2006). The amount of cracking during production varies as a result of both feedstock used and heating (Downie *et al.*, 2009; Ronsse *et al.*, 2013) suggesting the high surface area of açaí may be due to the feedstock being more susceptible to cracking during heating.

Surface area and pore size relate to a chars ability to adsorb elements within soils, which influences many of the beneficial processes associated with biochar amendment such as nutrient cycling, water retention and microbial activity (Lee *et al.*, 2013; Wang *et al.*, 2013). Chars both directly and indirectly influence nutrient availability within soils through desorption of nutrients and the support of nutrient-solubilising bacteria, respectively (Rillig & Thies, 2012; Wang *et al.*, 2013). Larger surface areas, therefore increase the ability of chars to fix and desorb nutrients within soils which would have beneficial impacts on soil fertility (Lee *et al.*, 2013), meaning higher production temperature chars with increased surface area will provide a positive soil amendment.

2.5 CONCLUSIONS AND FUTURE WORK

The conclusions from this Chapter in relation to the experimental aims are:

1. Physical and chemical characteristics are unique to each char, however all chars have an alkali pH which is beneficial to acidic soils.
2. Both feedstock and production mechanism influence a char's final physical and chemical characteristics and production temperature influences a greater proportion of the char characteristics tested here.

a. Feedstock had most impact on char volatile and N% content.
b. Production temperature influenced char pH, EC, H%, O%, ash, total elemental concentrations of K, Ca, Mg, Fe, Al, and BET surface area.
c. The feedstock stability and production temperature both contributed to C%, TC, labile elements and ash where initial feedstock concentrations and stability influenced the ability of production temperature to degrade bonds and increase availability.

The surface area investigated here used N_2 to determine BET surface area as detailed in the International Biochar Initiative (IBI, 2012) and European Biochar Certification (EBC, 2012) standards. The use of N_2 however has been criticised when conducted on chars due to the low pressure and diffusional problems associated with the process (Lozano-Castelló *et al.*, 2004). Developing characterisation studies using CO_2 adsorption followed by BET analysis and SEM imaging has been suggested to gain a more accurate surface area measurement and would provide a clearer insight into the influence char may have within soils.

The basic nature of chars also impacts the methods used to analyse TOC, IC and TC (Findlay *et al.*, 2010). Improved methods considering the requirement of acidification and oxidation of chars for analysis would explain the whereabouts of carbon within the char, thereby increasing the understanding of char as a potential climate change mitigation technique.

The varied nature of char characteristics developed throughout this Chapter shows, while some chars could improve soil properties, other chars could exacerbate soil problems. The relationship between char properties and the impact on soil improvement and increased fertility is not clearly understood (Chan & Xu, 2009b). Using the characterisation studies here, to conduct and interpret experiments exploring char interactions with essential nutrients, such as P, in solution and within soils will aid in elucidating desirable char properties for improved soil fertility. Further research and experimentation could therefore provide an insight into the potential of creating bespoke chars tailored to the requirement of a particular soil.

3 EXPLORING PHOSPHORUS ADSORPTION-DESORPTION INTERACTIONS IN NINE DIFFERENT BIOCHARS

3.1 INTRODUCTION

Biochar has been suggested as a soil amendment due to its positive impact on soil fertility through increased nutrient availability (Glaser *et al.*, 2001; Glaser *et al.*, 2002; Lehmann & Rondon, 2006). Phosphorus is an essential plant nutrient, therefore enhancing the availability of phosphorus in soils is advantageous (Rittmann *et al.*, 2011; Takaya *et al.*, 2016; Wang *et al.*, 2015). Chars influence soil P availability through phosphorus-biochar sorption interactions (Dari *et al.*, 2016; Laird *et al.*, 2010a; Parvage *et al.*, 2013; Xu *et al.*, 2014; Yao *et al.*, 2012). Understanding the influence biochar may have on P availability is essential in ensuring soil fertility is not compromised should char be added as an amendment.

There are several geochemical processes which can influence P availability, including: physical adsorption, chemical adsorption and precipitation which are influenced by the environment surrounding P, including the presence of biochar (Chintala *et al.*, 2014b; Hong & Lu, 2018; Lou *et al.*, 2016; Mosa *et al.*, 2018; Sparks, 1995; Xu *et al.*, 2018). Physical sorption is positively correlated with char surface area and pore size (Kizito *et al.*, 2017a; Trazzi *et al.*, 2016), whilst chemical sorption of P to biochar is more variable and can occur through adsorption and precipitation.

Chemical adsorption is a surface phenomenon and often involves surface complexation of P with biochar surface ions (Sparks, 1995). Adsorption through surface complexation has been evidenced within chars and can be inner sphere or outer sphere (Chintala *et al.*, 2014b; Hale *et al.*, 2013; Mukherjee *et al.*, 2011; Yao *et al.*, 2011a; Zhang *et al.*, 2016). Inner sphere complexation involves stronger bonding such as ionic or covalent bonding to surfaces, potentially via a surface ligand or functional group. Outer sphere complexation tends to involve weaker, non-specific surface bonds such as electrostatic bonding meaning its more rapid and reversible (Sparks, 1995; Sposito, 2008).

Sorption of P by precipitation involves the formation of a solid phase and often occurs after saturation of biochar reactive sites through surface complexation has occurred (Sparks, 1995). Should free Ca, Mg, Fe or Al ions be desorbed from char into solution, then precipitation of P may be observed (Hong & Lu, 2018; Lindsay, 1979; Mosa *et al.*, 2018; Ngatia *et al.*, 2017; Wang *et al.*, 2015; Xu *et al.*, 2013; Xu *et al.*, 2018; Yao *et al.*, 2011a, 2011b).

Feedstock and production regime strongly influence char chemical and physical characteristics, as evidenced in Chapter 2, meaning each char will have a unique sorption interaction with phosphorus (Borno *et al.*, 2018). In some cases chars contribute P, yet in other instances char can sorb P from solution systems (Chintala *et al.*, 2014b; Sarkhot *et al.*, 2013; Schneider & Haderlein, 2016; Wang *et al.*, 2015; Yao *et al.*, 2011a). Developing an understanding of the range of biochar-P sorption interactions and potential mechanisms within solutions, will provide a clear understanding of a char's chemical behaviour when subjected to a more complex soil environment.

The specific objectives of this chapter were to:

1. Quantify the ability of the nine chars characterised in Chapter 2 to sorb P from solutions containing a range of P concentrations.
2. Establish if precipitation of P occurs and if it does, quantify the role of Ca, Mg, Al and Fe.

The approach was to conduct laboratory-scale batch sorption experiments to quantify the P sorption capacity of the nine chars at a range of incubation times and P concentrations.

3.2 MATERIALS AND METHODS

3.2.1 Biochar Preparation

The biochars used throughout the range finding experiments were prepared as per Chapter 2 (Section 2.2.1).

3.2.2 Phosphorus Solution Preparation

A stock solution of 1000 mg L^{-1} of phosphorus (P) was made up by adding 8.787 g of KH_2PO_4 (potassium dihydrogen orthophosphate, ACS grade, Fisher Scientific, Loughborough, UK) to Milli-Q water in a 2 L volumetric flask. Experimental solutions were made by removing 50, 25, 5, 2.5, 0.5 and 0.05 mL from the stock solution (1000 mg L^{-1}) and making up to 500 ml to give final working P solutions of 100, 50, 10, 5, 1 and 0.1 mg L^{-1} respectively, which were stored in the refrigerator (4°C) and used within 2 days.

3.2.3 Batch Sorption Experiments

Earlier pilot studies were conducted to determine the optimum char to solution ratio to use for the sorption studies described here.

P sorption studies were conducted on all 9 chars. A 0.1 g sample of powdered (<500 µm) biochar was weighed into a 50 ml centrifuge tube with 30 ml of one of the working P solutions; i.e. 100, 50, 10, 5, 1, 0.1 or 0 mg L^{-1} P. This was repeated for each P solution and char type in triplicate. The pH readings (HANNA instruments, pH 209, pH meter) of each biochar-P solution were taken before and after placement on an end-over-end shaker. A complete set of triplicate char-P solutions was shaken at room temperature (20^{o}C) for one of 6 times: 120, 96, 72, 48, 24 or 1 hour(s), after which samples were centrifuged (Thermo Scientific Heraeus Megafuge 40) at 2500 rpm for 10 minutes before filtering 10ml to 0.22µm (BD Discardit II Luer Slip Syringe; Millex Syringe Driven Filter Unit, 33 mm, PES membrane) into ICP tubes containing 0.4 ml of 50% nitric acid (Fisher Scientific, trace analysis grade). Elemental analysis of solutions was undertaken by ICP-

MS (iCAP-Q, Thermo Scientific, UK). The P concentration within each solution enabled calculation of the P removed (P_{sorbed}) by biochar using Equation 3.1:

$$P_{sorbed} = (P_{added} - C_e) \times (\frac{Volume}{weight_{char}}) \qquad \text{Eq 3.1}$$

Where P_{added} is the concentration of P added to the char-P solutions (mg L^{-1}), C_e is the concentration measured in the solution after incubation (mg L^{-1}), volume is the amount of solution in the sample (ml), $weight_{char}$ is the weight of char added to solution (g) and P_{sorbed} is the amount of P adsorbed from the solution (mg kg^{-1} of char).

3.2.4 Isotherm Modelling

The P removal data were input into modified Freundlich, Langmuir and Langmuir-Freundlich (L-F) isotherm models to describe the data. Freundlich, Langmuir and L-F isotherm parameters, with added consideration of 'native P' desorbed by the chars at 0 mgL^{-1}, were determined using the Solver add-in in Excel to minimise RSD (relative standard deviation). Equations 3.2- 3.4 were used for the modified Freundlich, Langmuir and L-F isotherms respectively, each considering the char's native P contents.

$$P_{sorbed} = (K_f \text{ x } C_e^{n}) - P_{native} \qquad \text{Eq 3.2}$$

$$P_{sorbed} = \left(\frac{(K_l \text{ x } N_s \text{ x } C_e)}{1 + K_l \text{ x } C_e}\right) - P_{native} \qquad \text{Eq 3.3}$$

$$P_{sorbed} = \left(\frac{(N_s \text{ x } (K_a \text{ x } C_e)^n}{(1 + (K_a \text{ x } C_e)^n}\right) - P_{native} \qquad \text{Eq 3.4}$$

Where P_{sorbed} and C_e were defined earlier; K_f and n are constants determined from the Freundlich isotherm, where K_f is the Freundlich distribution coefficient, providing an indication of phosphorus solution-char equilibrium, and n acts as a correction factor. K_l and N_s are constants determined from the Langmuir isotherms. K_l relates to binding strength of phosphorus to char and N_s shows the maximum adsorption considering monolayer coverage of char, in which a single layer of phosphorus is absorbed at the char surface. N_s, K_a and n are constants determined from the L-F isotherm, where N_s and n were defined earlier and K_a relates to binding strength. P_{native} refers to the P contributed to the system by char and accounts for the negative y-intercept observed by the isotherms in the chars.

3.2.5 Speciation Modelling

The geochemical speciation model WHAM VII (Windermere Humic Aqueous Model VII) was used to better understand the P solubility and elemental speciation within the char-P solutions. Speciation was conducted on the ICP-MS data from the batch sorption studies. Default WHAM VII parameter settings and input files were used for modelling. The model simulations were used to predict the speciation of P, Mg, Fe, Al and Ca using the following input parameters: (i) pH of the char-P solution, (ii) the P, Mg, Ca (mg L^{-1}), Fe and Al (µg L^{-1}) concentrations measured by ICP-MS, (iii) atmospheric partial pressure of CO_2 (set to 400 ppm), (iv) temperature (20°C). Output from WHAM VII included the total element concentration (mol L^{-1}) and the activity of different elemental species within char-P solutions (mol L^{-1}).

3.2.5.1 *Ca and Mg Phosphate Solubility*

The alkaline nature of chars support Ca-P and Mg-P complex formation over Al-P and Fe-P, as discussed in Chapter 1. In order to explore complex formation and P speciation, data output from WHAM VII was used to produce phosphate stability diagrams. Double function parameters consisting of phosphate potential (log $H_2PO^-_4$ – pH) vs lime (log Ca^{2+} +2pH) and magnesium (log Mg^{2+} +2pH) potential were used to draw stability diagrams comparing the solubility of known Ca and Mg phosphate solid phases with the P, Ca and Mg data gained from WHAM VII analysis. It was assumed that $H_2PO^-_4$ concentration was influenced by lime (calcium ion availability), magnesium and hydrogen ion (pH) potential and that the solubility of phosphate in chars is controlled by the solid phase of Mg and Ca minerals. The stability diagrams produced are based on published solubility products (K_{sp}) (Table 3.1) (Lindsay, 1979).

3.2.6 Statistical Analysis

A one-way analysis of variance (ANOVA) followed by a post-hoc Tukey multiple comparison test using GenStat (17th Edition; VSN International Ltd.) compared the P adsorption and elemental concentration for each individual char type over time and according to P added to explore significance. The different P sorption of chars were compared, irrespective of time and P added using a one-way ANOVA followed by a post-hoc Tukey multiple comparison test.

Table 3.1. Calcium and magnesium phosphate minerals, reaction equations and K_{sp} used to draw phosphate solubility diagrams (Lindsay, 1979).

.

Mineral Formed	Reaction Equation	Log_{10} K_{sp}
$Ca(H_2PO^-_4)_2.H_2O$ (MCP)	$Ca(H_2PO_4)_2.H_2O + 2H^+ \longleftrightarrow Ca^{2+} + 2H_2PO^-_4 + 2H^+ + H_2O$ $(Ca^{2+})(H^+)^2(H_2PO^-_4)^2 / (H^+)^2 = 10^{-1.15}$ $-1.15 = 2(\log H_2PO^-_4 - pH) + (\log Ca^{2+} + 2pH)$ $-0.575 = (\log H_2PO^-_4 - pH) + 0.5(\log Ca^{2+} + 2pH)$ $\log (H_2PO^-_4 - pH) = -0.575 - 0.5(\log Ca^{2+} + 2pH)$	-1.15
$CaHPO_4.H_2O$ Brushite (DCPD)	$CaHPO_4.H_2O + 2H^+ \longleftrightarrow Ca^{2+} + H_2PO^-_4 + H^+ + H_2O$ $(Ca^{2+})(H^+)(H_2PO^-_4) / (H^+)^2 = 10^{0.63}$ $Log(Ca^{2+}) - pH + log(H_2PO_4^-) + 2pH = 0.63$ $\log (H_2PO_4^-) - pH = 0.63 - (\log Ca^{2+} + 2pH)$	0.63
$CaHPO_4$ Monetite (DCP)	$CaHPO_4 + 2H^+ \longleftrightarrow Ca^{2+} + H_2PO^-_4 + H^+$ $(Ca^{+2})(H^+)(H_2PO^-_4) / (H^+)^2 = 10^{0.3}$ $log(Ca^{2+}) - pH + log(H_2PO^-_4) + 2pH = 0.3$ $\log (H_2PO_4^-) - pH = 0.3 - (\log Ca^{2+} + 2 pH)$	0.3
$Ca_3(PO_4)_2$ β-tricalcium phosphate (β-TCP)	$Ca_3(PO_4)_2 + 6H^+ \longleftrightarrow 3Ca^{2+} + 2H_2PO^-_4 + 2H^+$ $(Ca^{2+})^3(H^+)^2(H_2PO^-_4)^2 / (H^+)^6 = 10^{10.18}$ $3 \log(Ca^{2+}) - 2pH + 2log(H_2PO^-_4) + 6pH = 10.18$ $10.18 = 3(logCa^{2+} + 2pH) + 2(\log H_2PO^-_4 - pH)$ $5.09 = 1.5(\log Ca^{2+} + 2pH) + (\log H_2PO^-_4 - pH)$ $\log (H_2PO_4^-) - pH = 5.09 - 1.5(\log Ca^{2+} + 2pH)$	10.18

$Ca_5(PO_4)_3OH$ Hydroxyapatite (HA)	$Ca_5(PO_4)_3OH + 10H^+ \longleftrightarrow 5Ca^{2+} + 3H_2PO^-_4 + 3H^+ + H_2O$ $(Ca^{2+})^5 (H^+)^3 (H_2PO^-_4)^3 / (H^+)^{10} = 10^{14.16}$ $5\log(Ca^{2+}) – 3pH + 3\log(H_2PO^-_4) + 10pH = 14.16$ $14.16 = 5(\log Ca^{2+} +2 pH) + 3(\log H_2PO^-_4 - pH)$ $\log (H_2PO^-_4) - pH = 4.82 - 1.66(\log Ca^{2+} + 2pH)$	14.16
$Ca_4H(PO_4)_3.2.5H_2O$ Octacalcium phosphate (OCP)	$Ca_4H(PO_4)_3.2.5H_2O + 8H^+ \longleftrightarrow 4 Ca^{2+} + 3H_2PO^-_4 + 3H^+ +2.5H_2O$ $(Ca^{2+})^4 (H^+)^3 (H_2PO^-_4)^3 / (H^+)^8 = 10^{11.76}$ $4\log(Ca^{2+}) – 3pH + 3\log(H_2PO^-_4) + 8pH = 11.76$ $11.76 = 4(\log Ca^{2+} +2pH)+ 3(\log H_2PO^-_4 -pH))$ $\log (H_2PO_4^-) - pH = 3.92 - 1.33 (\log Ca^{2+} + 2pH)$	11.76
$MgHPO_4.H_2O$ (Newberyite)	$MgHPO_4.3H_2O + 2H^+ \longleftrightarrow Mg^{2+} + H_2PO^-_4 + H^+ + 3H_2O$ $(Mg^{2+}) (H_2PO_4^-) (H^+)/ (H^+)^2 = 10^{1.38}$ $\log(Mg^{2+}) + \log(H_2PO_4^-) - pH + 2pH = 1.38$ $\log (H_2PO_4^-) - pH = 1.38- (\log Mg^{2+} + 2pH)$	1.38
$Mg_3(PO_4)_2$	$Mg_3(PO_4)_2 + 6H^+ \longleftrightarrow 3Mg^{2+} + 2H_2PO^-_4 + 2H^+$ $(Mg^{2+})^3 (H^+)^2 (H_2PO_4^-)^2 / (H^+)^6 = 10^{24.11}$ $3\log(Mg^{2+}) – 2pH + 2\log(H_2PO_4^-) + 6pH = 24.11$ $12.05 =1.5(\log Mg^{2+} + 2pH) + (\log H_2PO_4^- - pH)$ $\log H_2PO_4^- - pH = 12.05 -1.5(\log Mg^{2+} + 2pH)$	24.11
$Mg_3(PO_4)_2.8H_2O$ (Bobierrite)	$Mg_3(PO_4)_2.8H_2O + 6H^+ \longleftrightarrow 3Mg^{2+} + 2H_2PO^-_4 + 8H_2O + 2H^+$ $(Mg^{2+})^3 (H^+)^2 (H_2PO^-_4)^2 / (H^+)^6 = 10^{14.10}$ $3\log(Mg^{2+}) – 2pH + 2\log(H_2PO_4^-) + 6pH = 14.10$ $\log H_2PO_4^- - pH = 7.05- 1.5 (\log Mg^{2+} + 2pH)$	14.1
$Mg_3 (PO_4)_2. 22H_2O$	$Mg_3(PO_4)_2. 22H_2O + 6H^+ \longleftrightarrow 3Mg^{2+} + 2H_2PO^-_4 + 22H_2O +2H^+$ $(Mg^{2+})^3 (H^+)^2 (H_2PO_4^-)^2 / (H^+)^6 = 10^{16.01}$ $3\log(Mg^{2+}) – 2pH + 2\log(H_2PO_4^-) + 6pH = 16.01$ $\log H_2PO_4^- - pH = 8.01- 1.5 (\log Mg^{2+} + 2pH)$	16.01

3.3 RESULTS

3.3.1 Batch Sorption

Each char demonstrated a different P sorption profile ($p<0.001$). All chars demonstrated an initial desorption step in solutions with low P concentrations of 0.1- 1 mg L^{-1} before displaying different behaviours (Figure 3.1; 3.2 & 3.3a- f). To clearly present and discuss the P adsorption-desorption results, the nine chars were classified into three separate groups according to sorption behaviour. Group one includes GSW, LGSW, cacao and WPy; group two includes APy, HW and açai and group three includes bamboo and coffee chars.

Members of group one, showed a clear increase in sorption at P concentrations above 1 mg L^{-1} which stabilised at concentrations higher than 50 mg L^{-1} P, at which point maximum sorption is likely achieved (Figure 3.1a-f). LGSW ($p=0.004$) and GSW ($p<0.001$) showed increased sorption over time, regardless of P added to the system (Figure 3.1a - f). Sorption was the highest in GSW and LGSW chars followed by cacao and WHW (Figure 3.1a-f).

Table 3.2. The grouping of the nine chars according to sorption profile.

Group	Char	Production
One	GSW	Gasified softwood (916- 770°C) for 6 hours
	LGSW	Gasified softwood (862- 731°C) for 6 hours
	Cacao	Coco husk pyrolysed at 450°C, 8 hours
	WHW	Weathered, aged HW char (Section 1.2.11)
Two	AHW	Artificially aged HW char (Section 1.2.11)
	HW	Hardwood pyrolysed at 450°C, 48 hours
	Açai	Açai pyrolysed at 450°C, 10 hours
Three	Bamboo	Bamboo Stem gasified at ~700-900°C
	Coffee	Coffee grounds pyrolysed at 450°C, 10 hours

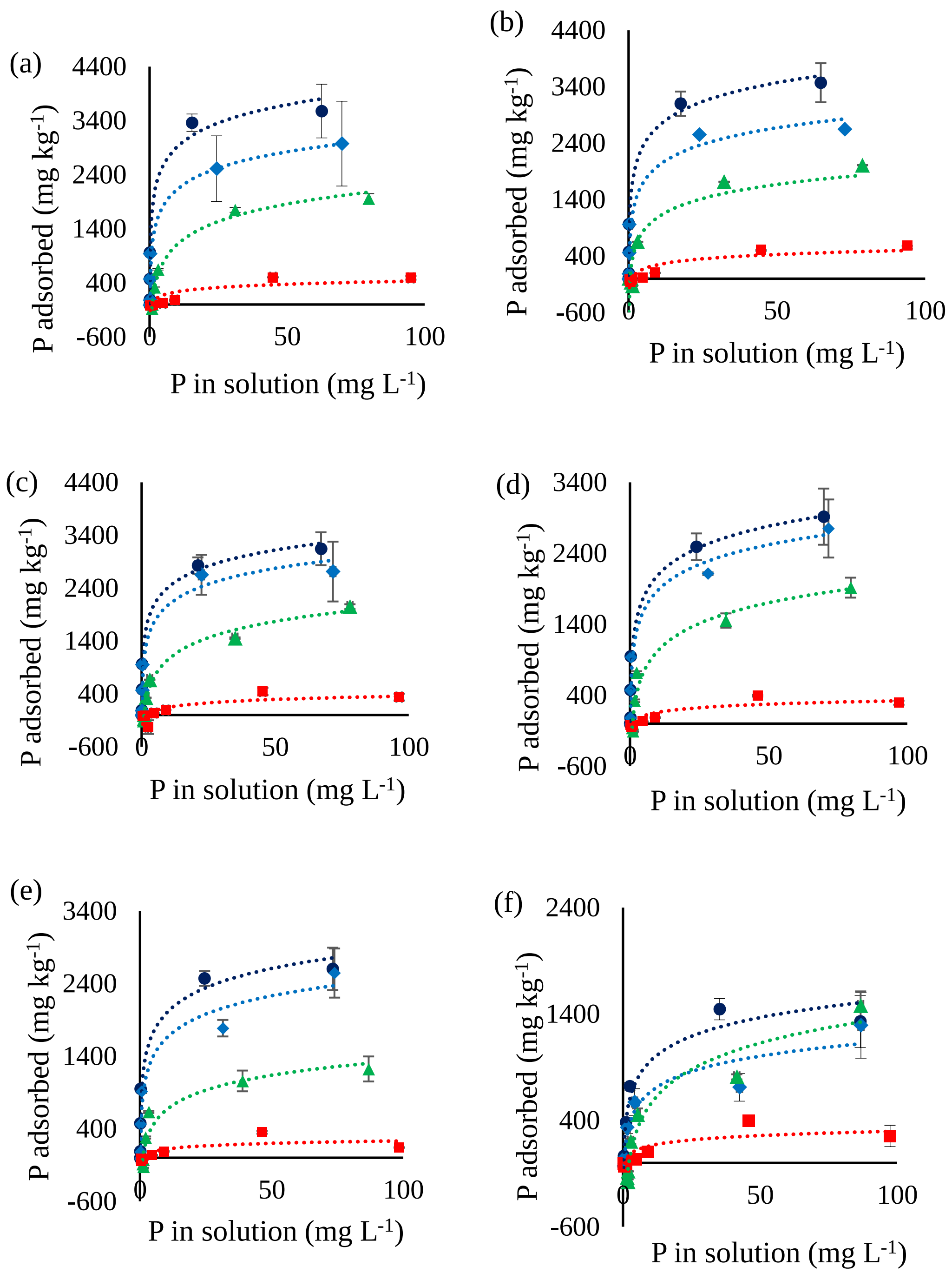

Figure 3.1. Phosphorus sorption patterns of biochars in group 1 at (a) 120, (b) 96, (c) 72, (d) 48, (e) 24 and (f) 1 hour (s). GSW (navy circles), LGSW (blue diamonds), cacao (green triangles) and WHW (red squares). Logarithmic trend lines have been added to highlight trends. Data are means ± SE. Char type ($p<0.001$) and P added ($p<0.001$) influence sorption irrespective of time. GSW ($p< 0.001$) and LGSW ($p= 0.004$) are influenced by time as a single factor.

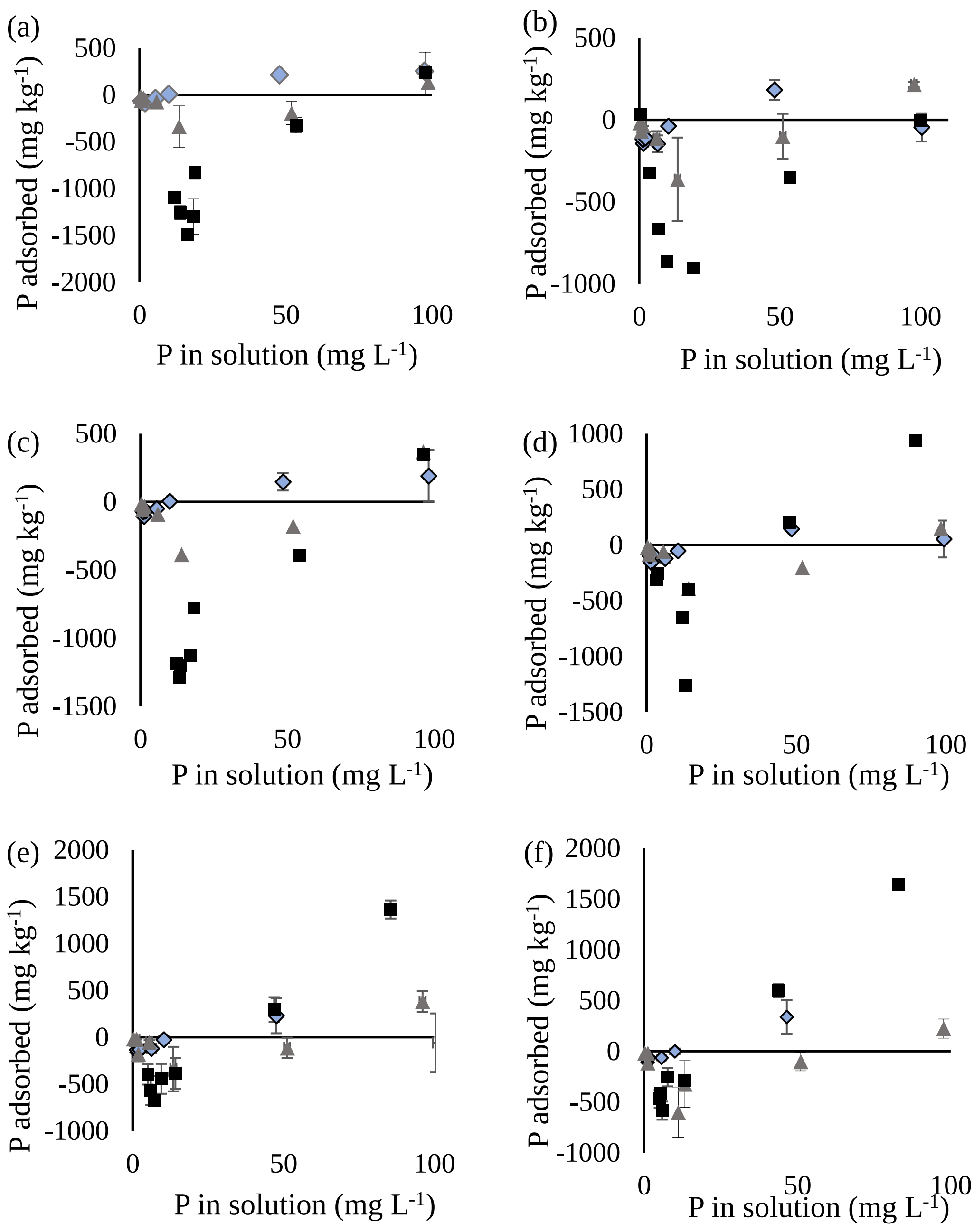

Figure 3.2. Phosphorus sorption patterns of biochars in group 2 at (a) 120, (b) 96, (c) 72, (d) 48, (e) 24 and (f) 1 hour (s). Açai (black squares), HW (grey triangles), and AHW (blue diamonds). Data are means ± SE. Char type ($p<0.001$) and P added ($p<0.001$) influence sorption irrespective of time. GSW ($p< 0.001$) and LGSW ($p= 0.004$). Açai ($p= 0.009$) sorption of P is influenced by time.

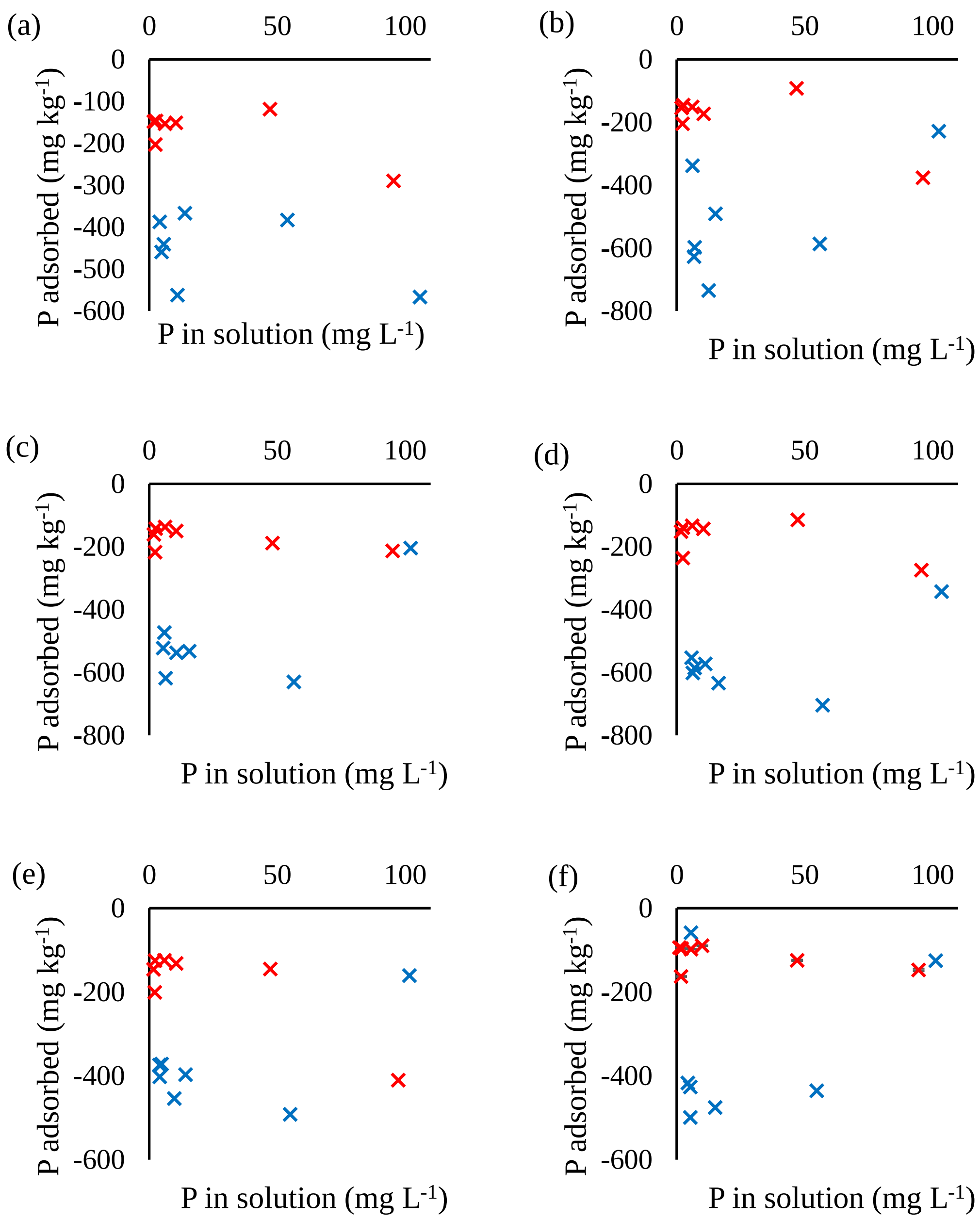

Figure 3.3 Phosphorus sorption patterns of biochars in group 3 at (a) 120, (b) 96, (c) 72, (d) 48, (e) 24 and (f) 1 hour (s). Coffee (blue crosses) and bamboo (red crosses), show desorption at all time points, regardless of P added. Data are means ± SE. Neither coffee ($p= 0.236$) nor bamboo ($p= 0.418$) desorption were influenced by time.

Within group two, clear adsorption/ desorption differences are seen. For the chars in group two, any P sorption observed occurs above 50 mg L^{-1} P, after rapid desorption of P (Figure 3.2 a-f). P adsorption onto açai char was greater after one hour than after 120 hours ($p=0.009$) (Figure 3.2a & f) whereas P sorption in HW ($p= 0.829$) and AHW ($p = 0.229$) chars does not change over time.

Group three chars showed stable desorption of P (Figure 3.3 a-f), which does not alter, regardless of P concentration within the system. Desorption was higher in coffee chars than in bamboo at all time points (Figure 3.3 a-f).

The pooled means across solution P additions and time, show members of group 3 desorb less P than açai char. The overall desorption in açai is due to the large release of P at low P concentrations, which is not outweighed by any adsorption observed at higher P concentrations. GSW and LGSW chars demonstrated the highest adsorption ($p<0.001$; Figure 3.4).

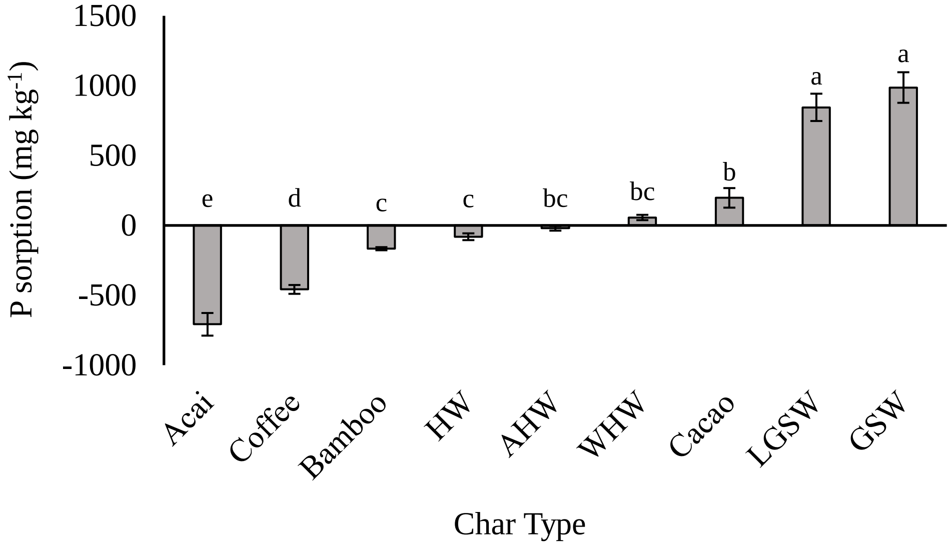

Figure 3.4. Mean (± SE) P ad- or de-sorption pooled across the solution P additions and incubation time. All chars, other than LGSW and GSW, showed a different average P sorption from each other ($p<0.001$). Chars similarly superscripted are not significantly different. Minus integers indicate higher overall desorption of P from char. The data showed the overall effect of each char on P availability and therefore the role it likely has on P contribution or removal from solutions.

3.3.2 Isotherm Models

Langmuir, Freundlich and L-F isotherms fit the data obtained for chars designated to group one (Figure 3.5a-d). The maximum adsorption (N_s) and distribution coefficient (K_f) constants for group one chars gained from Langmuir, L-F and Freundlich models increased in the same order as P adsorbed by chars, meaning the isotherm parameters complement the data for group one (Table 3.3). All models plateau as P concentration in solution reached 50 mg L^{-1} for chars in group one and AHW (Figure 3.5a- d &f) as distribution coefficient and maximum adsorption were achieved.

The Freundlich isotherm best describes the LGSW char data, whereas the Langmuir isotherm suits the data obtained for cacao and GSW chars (Figure 3.5a- c), supported by the RSD values (Table 3.3). AHW and WHW sorption data fits the L-F model most clearly (Figure 3.5d & f; Table 3.3). Data for açai char fits Langmuir and Freundlich models at 1 and 24 hour(s), however a plateau is not achieved on the isotherm presented (Figure 3.5e; Table 3.3). Isotherm constants, such as N_s and K_f, for Açai char after 1 hour are the second highest after GSW char (Table 3.3). Data for chars belonging to group three do not fit any isotherm models and when input the data ‘flat line’.

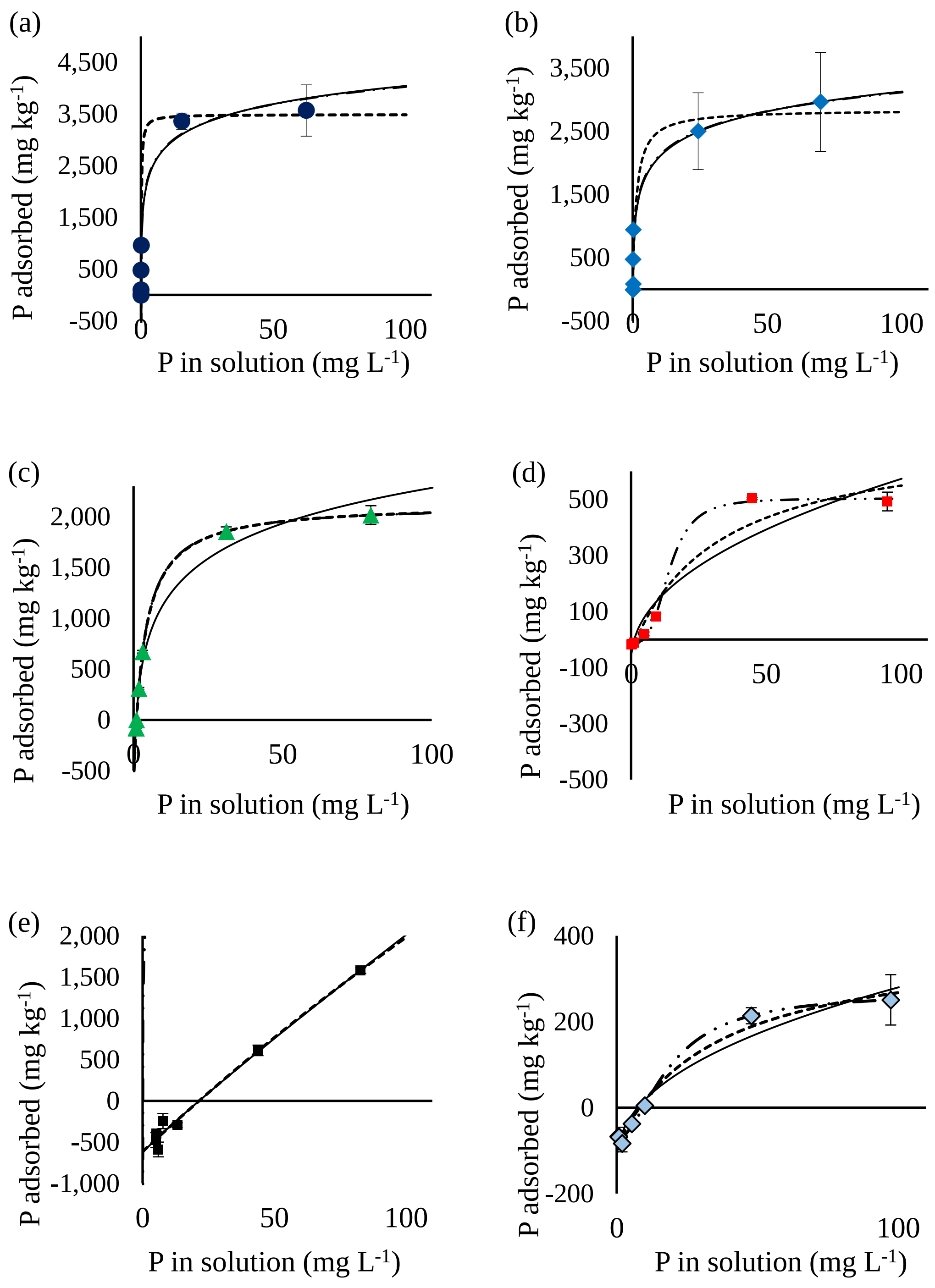

Figure 3.5. Phosphorus sorption patterns of different biochars with Langmuir, Freundlich and L-F models fitted to the data obtained across the concentration range tested. (a) GSW char at 120 hrs, (b) LGSW char at 120 hrs, (c) cacao char at 120 hrs, (d) WHW char at 120 hrs (e) Açai at 1 hour and (f) AHW at 120 hours with isotherms fitted to the data. Solid lines depict the Freundlich model, --- represents the Langmuir model and -··- represents the L-F model. Data are means ± SE.

Table 3.3. Langmuir, Freundlich and L-F sorption isotherm constants for GSW, LGSW, WHW, cacao and AHW chars at 120 hrs and açai char at 1 hr fitting Langmuir, Freundlich and L-F isotherm models found through batch sorption experiments. Model output is derived from inputting mean P adsorbed values for each time point.

Char Type	Langmuir			Freundlich			Langmuir- Freundlich			
	N_s	K_l	RSD	K_f	n	RSD	N_s	K_a	N	RSD
GSW	4440	8.14	189	42700	0.01	294	70000	0.00	0.03	324
LGSW	2840	0.74	387	27700	0.02	371	61400	0.00	0.03	414
WHW	423	0.03	55.0	83.9	0.35	77.0	326	0.09	5.94	13.0
Cacao	1950	0.18	19.0	22300	0.02	116	33100	0.00	0.10	21.0
AHW	484	0.03	19.0	55.2	0.44	30.0	341	0.05	1.83	9.00
Açai	3500	0.01	101	27400	0.01	101	33100	0.00	0.10	4500

3.3.3 Speciation Modelling and Stability Diagrams

Stability diagrams for possible Ca-P complexes forming within the biochar systems showed lime ($p<0.001$) and P potential ($p<0.001$) were unique to each char. Systems containing AHW, coffee, and bamboo chars were under-saturated with regards to solution P concentrations meaning Ca-P precipitates were not able to form, irrespective of P added (Figure 3.6a &b). The solubility of Ca-P complexes in the presence of açai, Py, HT, LGSW and cacao chars altered depending on the P concentration added (Figure 3.6b; $p< 0.001$). Açai char appears at upper-saturation limits when no P was added to the system with respect to HA, whereas for HW char, solubility appears to be variable at both of the P concentrations presented (Figure 3.6a &b). The solutions containing cacao, GSW and LGSW chars show enhanced saturation with increasing P addition which is most notable for cacao char (Figure 3.6b). The data for cacao, LGSW and GSW chars suggest increased solubility of Ca-P complexes when 100 mg L^{-1} was added, with cacao data sitting close to brushite (DCPD).

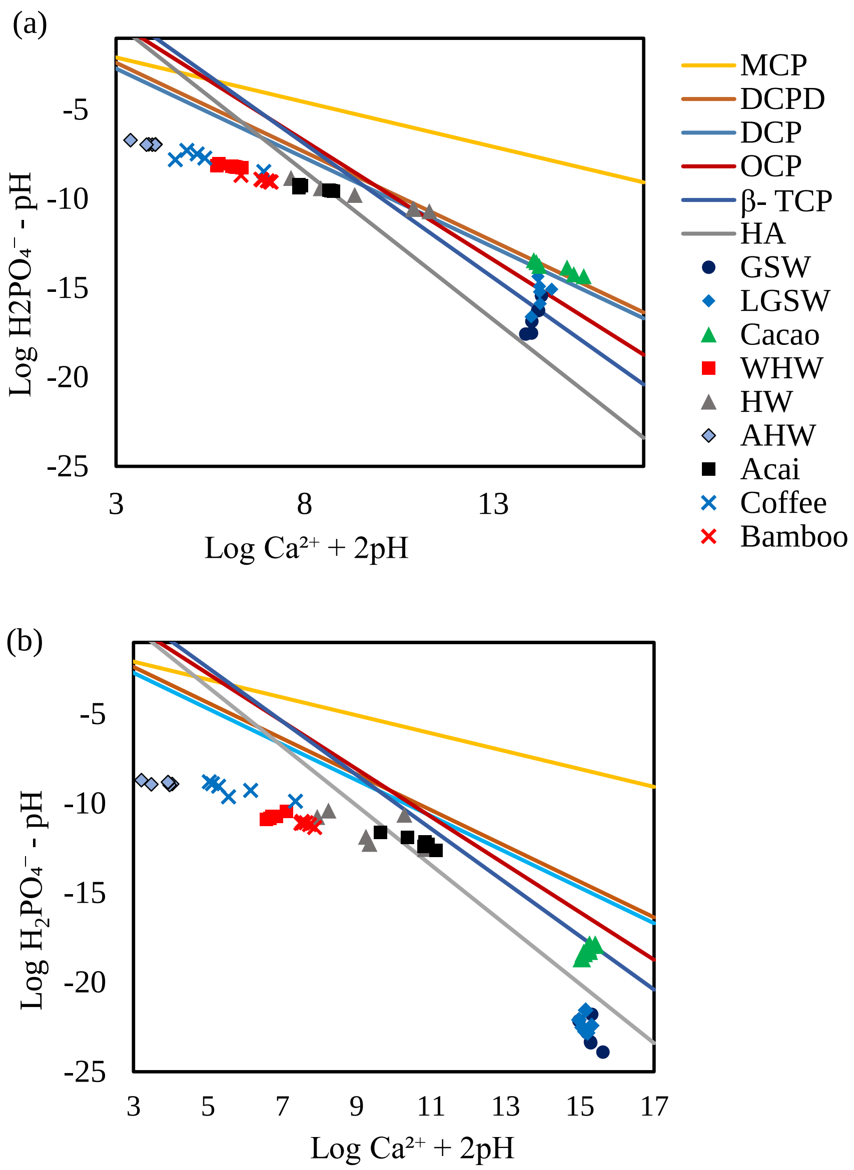

Figure 3.6. Calcium phosphate complex stability diagrams when (a) 100 mg L^{-1} and (b) 0 mg L^{-1} of phosphorus was added. The calcium phosphate double function plots showed the solubility of Ca-P complexes in studied chars in relation to the crystalline calcium phosphates monocalcium phosphate (MCP), brushite (DCPD), dicalcium phosphate (DCP), octacalcium phosphate (OCP), β-tricalcium phosphate (TCP) and hydroxyapatite (HA) represented by solid lines. Equilibrium lines for the mineral phases were calculated based on the K_{sp} values reported by Lindsay (1979). Lime and phosphate potentials were calculated from the mean H_2PO_4 and Ca^{2+} activities (M) for each char at each time point derived from WHAM VII modelling. The points at which the lines overlap indicate coexistence of the solid phase (Lindsay, 1979). Data are means and SE is omitted for clarity Char type influenced lime and P potential ($p < 0.001$). Ca-P solubility associated with açai, HW, GSW, LGSW and cacao chars was influenced by P solution concentration ($p < 0.001$). Solubility did not change over time ($p = 0.627$).

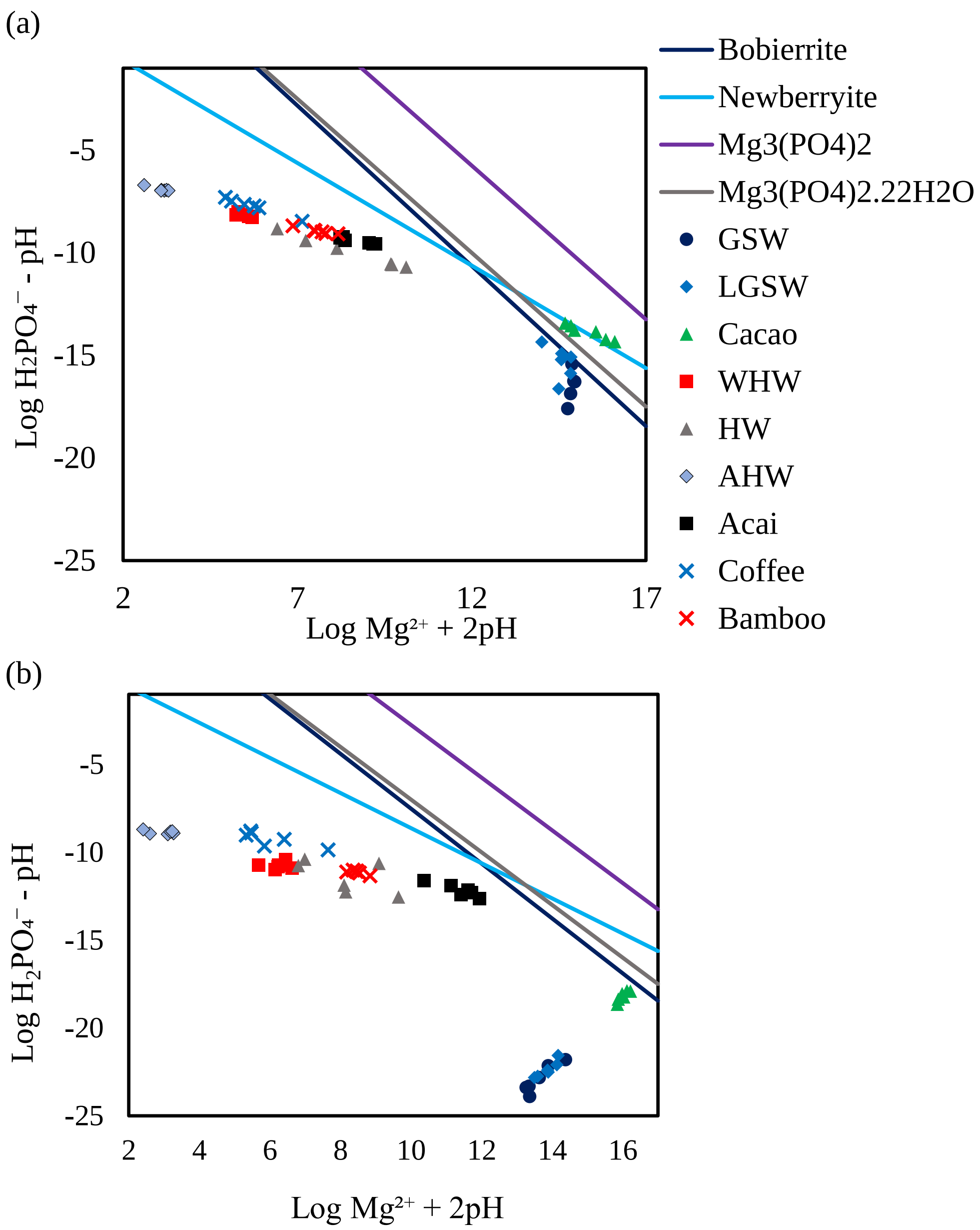

Figure 3.7. Magnesium phosphate complex stability diagrams when (a) 100 mg L^{-1} and (b) 0 mg L^{-1} of phosphorus was added. The magnesium phosphate double function plots show the solubility of Mg-P complexes in studied chars in relation to the crystalline magnesium phosphates bobierrite, newberyite, $Mg_3(PO_4)_2$ and $Mg_3(PO_4)2.22H_2O$, represented by solid lines. Equilibrium lines for the mineral phases were calculated based on the K_{sp} values reported by Lindsay (1979). Magnesium and phosphate potentials were calculated from the mean H_2PO_4 and Mg^{2+} activities (M) for each char at each time point derived from WHAM VII modelling. The points at which the lines overlap indicate the coexistence of the solid phase (Lindsay, 1979). Data are means and SE is omitted for clarity. P potential and Mg potential are influenced by P added ($p<0.001$). Solubility did not change over time ($p= 0.307$).

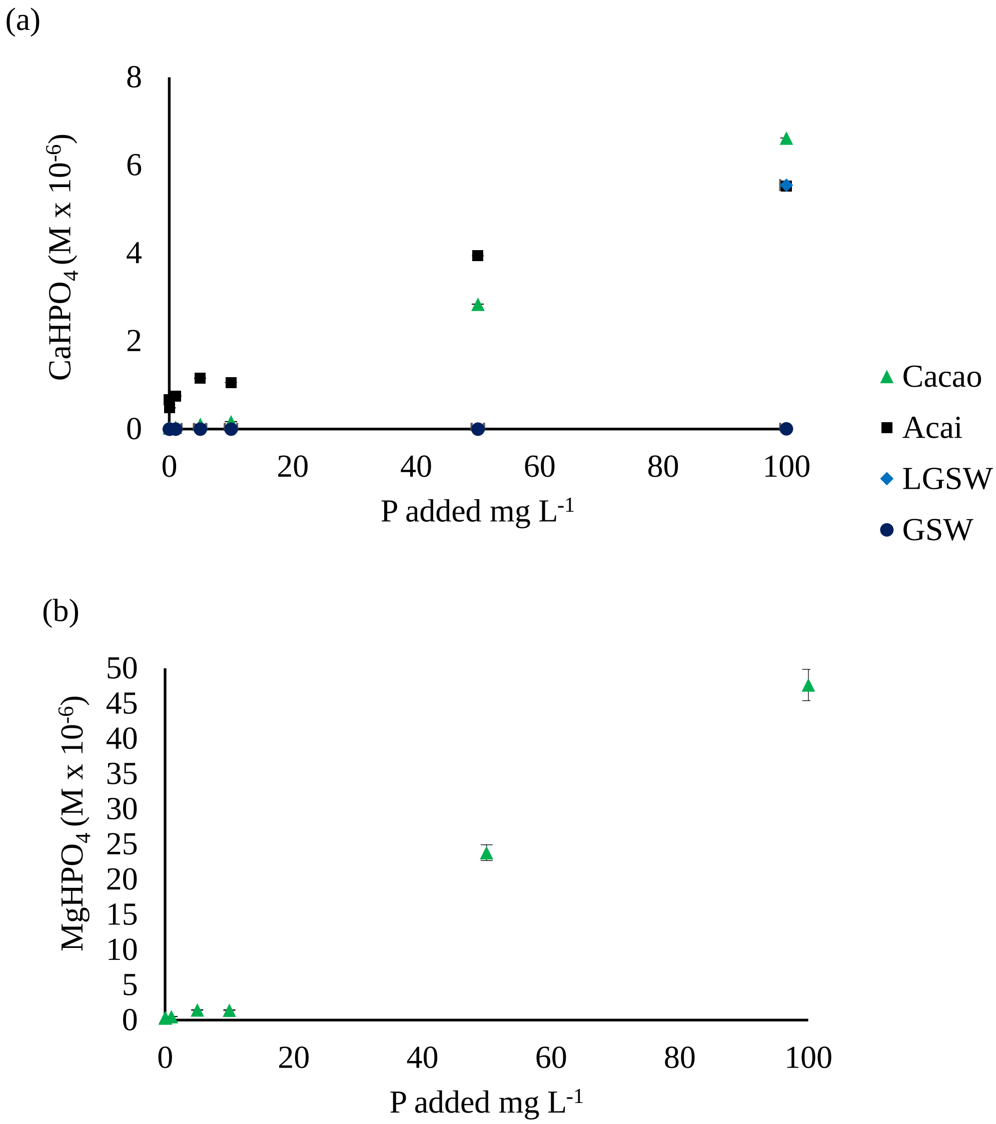

Figure 3.8. (a) Calcium phosphate precipitates in systems containing cacao, GSW, LGSW and açai char (b). Magnesium phosphate precipitates in cacao char at 120 hours according to P added to system. Data are means ± SE. A positive correlation between P added and $CaPO_4$ activity was observed for cacao ($p<0.001$), açai ($p<0.001$), and LGSW char ($p<0.001$) is observed, whereas $CaPO_4$ in GSW char was not influenced by P added ($p=0.321$). MgPO4 was also influenced by P added in systems containing cacao ($p<0.001$), açai ($p= 0.001$) and LGSW ($p<0.001$) and p addition in GSW systems influenced MgPO4 effect ($p=0.031$).

(a)

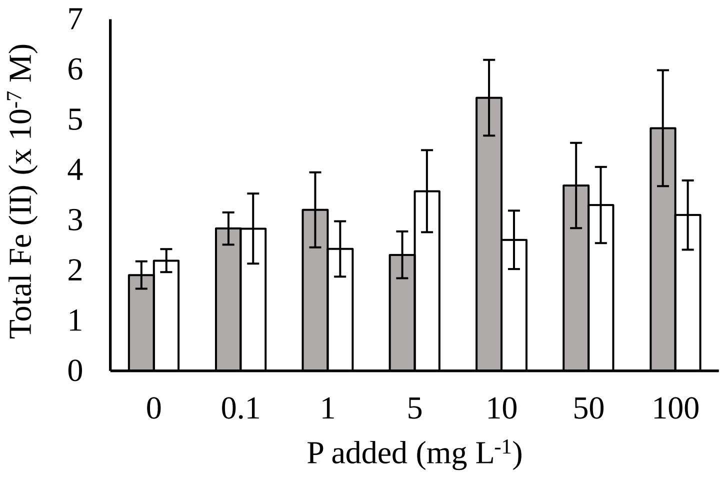

(b)

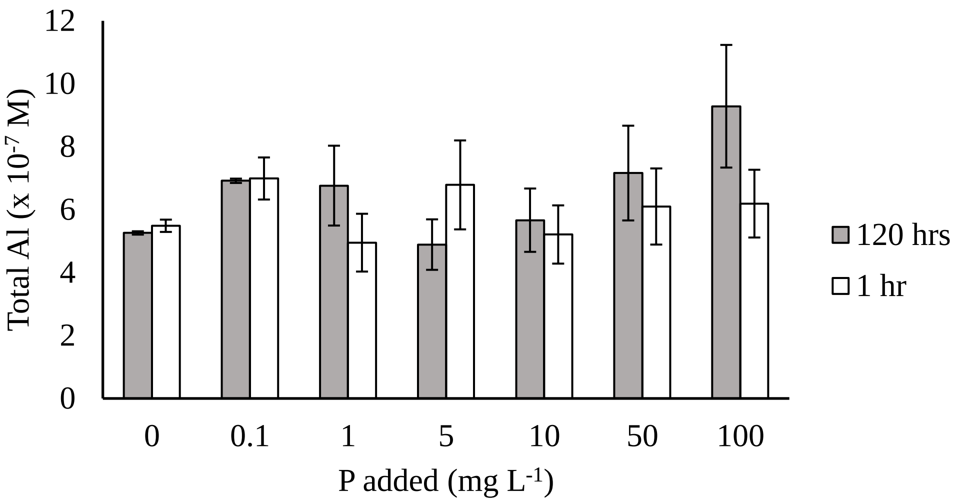

Figure 3.9. Total (a) Fe (II) (p=0.502) (b) Al (p=0.268), concentrations (M) for AHW char did not significantly change between 120 and 1 hour(s) of incubation when different P concentrations were added. Data are means ± S.E.

Although P potential and Mg potential are influenced by P added ($p<0.001$) all systems, barring cacao char, remained under-saturated with Mg-P, regardless of P concentration added (Figure 3.7a &b). When 100 mg L^{-1} P was introduced, cacao systems became saturated and sat close to the newberyite solubility line (Figure 3.7a). GSW and LGSW also seem to increase in saturation and sit close to the bobierrite line, however still reside below. The clustering of data points for both Mg-P ($p= 0.307$) and Ca-P ($p= 0.627$) shows solubility does not change over time (Figure 3.6a& b & Figure 3.7a &b).

The formation of $CaPO_4$ was explored in cacao, açai, LGSW and GSW chars due to the potential saturation observed (Figure 3.6a). $CaPO_4$ complexes increased in line with P addition in systems containing cacao, açai and LGSW chars ($p<0.001$; Figure 3.8a). $MgPO_4$ was explored in cacao due to the observation of potential saturation (Figure 3.7a). In systems containing cacao, $MgPO_4$ positively correlated with P added (Figure 3.8b; $p<0.001$).

The lower pH associated with AHW char (see Chapter 2) and during batch sorption experiments, could suggest Al and Fe precipitation; however, neither Al ($p= 0.269$) nor Fe ($p=0.502$) concentrations changed with P added (Figure 3.9 a & b).

3.4 DISCUSSION

3.4.1 Phosphate Sorption Patterns

The variation in P sorption behaviour observed with the different chars tested here (Figure 3.1; Figure 3.2; Figure 3.3 a- f) may explain inconsistencies within the literature regarding different elemental interactions and therefore availabilities when char is added to soil. Many chars demonstrate a capacity to strongly sorb P (Chintala *et al.*, 2014b; Dari *et al.*, 2016; Jung *et al.*, 2015; Sarkhot *et al.*, 2013; Schneider & Haderlein, 2016; Takaya *et al.*, 2016; Wang *et al.*, 2015; Xu *et al.*, 2014), while increased P availability in biochar amended soils and solutions through desorption of P has also been observed (Liu *et al.*, 2018; Parvage *et al.*, 2013; Wang *et al.*, 2015; Xu *et al.*, 2014; Yao *et al.*, 2011a; Yao *et al.*, 2012). The heterogeneity of char characteristics through varying production regimes and feedstock have been linked with the different P availability (Morales *et al.*, 2013; Ngatia *et al.*, 2017).

3.4.1.1 *Production Temperature and P Sorption*

P sorption appears to increase in line with production temperature (Figure 3.1; Figure 3.2; Figure 3.3 a-f), potentially due to an increase of surface area at higher temperatures through volatilisation and degradation of feedstocks (Hale *et al.*, 2013; Mukome *et al.*, 2013; Ngatia *et al.*, 2017; Peterson & Jackson, 2014; Tan *et al.*, 2018; Trazzi *et al.*, 2016). Chars with larger surface areas and pore volumes often have higher P sorption capacities through physi-sorption (Kizito *et al.*, 2017a; Mosa *et al.*, 2018; Trazzi *et al.*, 2016), supporting the P sorption (Figure 3.1; Figure 3.2; Figure 3.3 a-f) and surface area data presented in chapter 2 where GSW holds the highest BET surface area and LGSW the third highest. However, Morales *et al.* (2013) found chars produced at higher temperatures had reduced P sorption, highlighting the role of chemisorption, which may explain the disparity between the low BET surface area of cacao (2.39 m^2g^{-1}) and WHW chars (0.11m^2g^{-1}) (Chapter 2) and the high P sorption (Figure 3.1a-f). Furthermore, the higher sorption seen in GSW and LGSW chars (Figure 3.1a-f) may relate to the production mechanism of gasification, as oppose to production temperature. Producing chars using either pyrolysis at higher temperatures or gasification at lower temperatures would aid in quantifying the influence of production temperature on P sorption.

Production temperatures are also linked to char hydrophobicity which influence nutrient interactions and sorption (Zornoza *et al.*, 2016). Hydrophobic properties of chars are lessened at higher production temperatures (Gray *et al.*, 2014; Zornoza *et al.*, 2016) through degradation of hydrophobic functional groups (Kinney *et al.*, 2012). Reduced hydrophobicity would allow increased interactions between the P in solution and the char surface, potentially explaining the high sorption of P in the high temperature LGSW and GSW and reduced P sorption in the lower temperature coffee char (Figure 3.1; Figure 3.3 a-f). Cacao char, however, was produced at a relatively low temperature and demonstrates a high P sorption (Figure 3.1a-f), suggesting more than production temperature needs to be considered when discussing sorption.

3.4.1.2 *Feedstock and P Sorption*

The similar P sorption profiles observed here for the LGSW and GSW chars, suggests feedstock is a key factor in determining adsorption/desorption dynamics (Figure 3.1 a-f), because both chars were derived from the same feedstock but production temperature was different for each. In contrast, coffee and cacao chars were both produced by pyrolysis at 450^{o}C (Chapter 2, Section 2.2.1), yet cacao adsorbed P from solution whilst coffee only exhibited desorption (Figure 3.1; Figure 3.3 a-f). This suggests feedstock has a strong influence over P sorption behaviour and corroborates the much of the literature (Kizito *et al.*, 2017a; Kizito *et al.*, 2017b; Morales *et al.*, 2013; Ngatia *et al.*, 2017).

3.4.1.3 *P Sorption and pH*

GSW, LGSW and cacao chars all have pH values above 11 and show high P sorption capacities (Chapter 2; Figure 3.1 a-f). P sorption at pH readings above 10 has been attributed to competitive ligand exchange mechanisms between anions such as phosphate and hydroxyl groups (Biswas *et al.*, 2007; Trazzi *et al.*, 2016). Although high pH and competitive ligand exchange mechanisms may explain the P absorption profiles for HT, LGSW and cacao chars, other chars showing sorption (e.g. WPy) have lower pH values. The link between pH and P sorption may also be due to increased Ca and Mg availability resulting in P precipitation (Liu *et al.*, 2018; Ngatia *et al.*, 2017; Sparks, 1995) which is supported by the high availability of Ca and Mg in cacao. However, neither GSW or LGSW chars, have high Ca and Mg availability relative to other chars (Chapter 2) yet the highest concentrations of P were removed from solutions when gasified chars were present (Figure 3.1 a-f).

More commonly, increased P sorption is associated with lower solution pH (Takaya *et al.*, 2016). Lower pH favours an increase in surface protonation which, as a result, provides more positive surface sites to attract negatively charged phosphate (Sposito, 2008; Xue *et al.*, 2009; Zhang *et al.*, 2009). The pH values of groups two (HW, AHW, açai) and three (bamboo, coffee) chars do not seem to influence sorption as they all demonstrated neutral pH values during characterisation (Chapter 2), however demonstrate varied P sorption/desorption within solutions, suggesting the difference in P sorption observed is controlled by alternative factors.

3.4.1.4 *P Sorption and P Concentration and Availability*

P solution concentration positively correlates with P sorption (Kizito *et al.*, 2017a; Lou *et al.*, 2016; Sarkhot *et al.*, 2013; Schneider & Haderlein, 2016; Trazzi *et al.*, 2016) which is apparent here with the chars designated to group one, possibly due to the creation of a concentration gradient from P solution to P at the char surface, until 50 mg L^{-1} where sorption slows due to the saturation of surface reactive sites (Figure 3.1 a-f) (Kizito *et al.*, 2017a). According to Ngatia *et al.* (2017), biochar P availability is negatively correlated with P sorption. The high initial water available concentrations of coffee, bamboo and acai could therefore explain the desorption exhibited by coffee and bamboo and the rapid initial desorption exhibited by açai (Figure 3.3 a- f) char as P is readily released (Chapter 2). Furthermore, GSW and LGSW display low water available P (chapter 2) and maintain high P sorption (Figure 3.1a-f), suggesting available P concentrations do influence sorption/desorption interactions in chars as found by Ngatia *et al.* (2017). Alternatively, many biochars have been found to hold a negative surface charge causing repulsion of negative phosphate ions, resulting in desorption, which may also explain the results obtained for the chars in group three and açai and the initial desorption demonstrated by nine all chars (Figure 3.2; Figure 3.3 a-f) (Yao *et al.*, 2011a; Zeng *et al.*, 2013).

The differences observed between the chars studied here show feedstock and production parameters should be considered when generating chars with the aim of influencing P sorption. Each group of chars can potentially contribute to improving soil P status in different ways, highlighted by the mean adsorption-desorption reactions of the chars irrespective of the P concentration added (Figure 3.4). Knowledge of the adsorption-desorption behaviour for each char in solution may assist in understanding potential interactions when char is applied to soil and ultimately enable 'designer' chars to be used in specific situations. For instance, the P sorption ability of chars classed in group one may benefit soils with excessive P concentrations and reduce P run-off and therefore eutrophication (Laird *et al.*, 2010a; Takaya *et al.*, 2016; Wang *et al.*, 2015; Yao *et al.*, 2011a, 2011b). In contrast, desorption of P by chars in group three and by açai char would contribute P to deficient soils (Lehmann *et al.*, 2003; Liu *et al.*, 2018; Tryon, 1948; Xu *et al.*, 2014).

3.4.2 Sorption Isotherm Models

Langmuir, Freundlich and L-F isotherm models are commonly used in sorption studies to describe expected trends within data. The output values from the models provide insight into sorbent affinity through binding strength (K_l), maximum adsorption (N_s) and distribution coefficient (K_f) relating to sorption interactions (Wasewar *et al.*, 2008).

The Freundlich isotherm model works on the assumption of sorption to a heterogeneous surface, potentially explaining why the Freundlich models better fit the LGSW char, due to the mixed feedstock (Figure 3.5 b; Table 3.3) (Kilpimaa *et al.*, 2014; Wasewar *et al.*, 2008). The Langmuir model assumes sorption to a uniform surface and explains the cacao char sorption data (Figure 3.5c; Table 3.3), potentially because it was produced from a single feedstock (Gao *et al.*, 2013; Kilpimaa *et al.*, 2014; Trazzi *et al.*, 2016; Wasewar *et al.*, 2008). The better fit of the Langmuir model to GSW data (Table 3.3) rather than to the Freundlich model (as for the LGSW char), suggests feedstock does not influence the isotherm fit as GSW and LGSW were produced from the same mixed feedstock. The combined L-F assumes both isotherm behaviours and shows P sorption by WHW and AHW chars (Figure 3.5d &f; Table 3.3) is predictable (Jeppu & Clement, 2012). The high sorption observed with açai char (Table 3.3) and linear relationships (Figure 3.5e) predicted by Langmuir and Freundlich models could indicate non-specific and rapid sorption, explaining why açai data obtained after short periods of incubation fits the models (Sparks, 1995). Isotherm models fail to describe P desorption interactions as desorption is often independent of solution P concentration, as seen for chars within group three (Sarkhot *et al.*, 2013).

The low binding strength (N_s) associated with all chars, excluding the GSW Langmuir output (Table 3.3), could suggest weaker sorption mechanisms, such as outer-sphere surface complexation. However, development of the discussion on P sorption in the nine chars using the stability diagrams produced (Figure 3.6; Figure 3.7), as seen later within this experimental chapter, will provide a more definitive conclusion regarding sorption mechanisms and is necessary due to the descriptive nature of sorption isotherm models.

3.4.3 Speciation and Sorption Mechanisms

The heterogeneous nature of chars opens up a variety of potential physical and chemical sorption mechanisms making biochar P sorption mechanisms complex to decipher (Lou *et al.*, 2016). Sorption, as observed in char belonging to group one, could be influenced by both adsorption and precipitation, as discussed in section 1.4.1 (Sparks, 1995).

3.4.3.1 *Stability Diagrams and Precipitation*

Stability diagrams allow determination of the solubility of P minerals within the system by comparison with known solid phases (Sparks, 1995). Understanding solubility and system saturation can provide an insight into potential precipitation of P by other elements. The data points observed below the known solid phase solubility lines, seen for chars designated to group three, AHW and WHW chars for Ca-P (Figure 3.6a &b), and all but cacao chars for Mg-P (Figure 3.7a &b), indicate under-saturation (Lindsay, 1979) of the system.

According to Tunesi *et al.* (1999), the precipitation of P minerals only occurs at super-saturation of a system, where data points lie above the solubility lines presented (Figure 3.6&b and 3.7 a &b) (Tunesi *et al.*, 1999). Continued P sorption at super-saturation therefore indicates surface precipitation of P because P solution concentration is in excess, causing the formation of a solid phase (Sparks, 1995). The proximity of the chars in group one, except for WPy, and of açai at 0 mg L^{-1} P to Ca-P solid phases (Figure 3.6b) and cacao to newberyite for Mg-P (Figure 3.7a&b), indicates saturation where maximum adsorption has been achieved. The saturation observed in Açai at 0 mg L^{-1} may be due to the high water available P concentrations from açai, as presented in chapter 2. The plateau in sorption observed at P concentrations above 50 mg L^{-1} for HT, LGSW and cacao chars (Figure 3.1 a-f) suggests the maximum sorption limit of chars has been reached as active binding sites are filled. The stability diagrams (Figure 3.6a; Figure 3.7a) indicate slower precipitation reactions may be occurring at higher P concentrations explaining the levelling off in sorption observed for GSW, LGSW and cacao chars for Ca-P, and cacao for Mg-P (Figure 3.1 a-f). The increase in Ca-P in systems containing LGSW, açai and cacao chars and in Mg-P in cacao char (Figure 3.8a) further suggests precipitation occurs in these char systems. However, the increase in CaPO4 and MnPO4 activity in the char systems (Figure 3.8a) is trivial and cannot account for the high level of P sorption seen (Figure 3.1 a-f) suggesting adsorption is the primary driver.

Al and Fe can precipitate P out of systems with low pH values (Ngatia *et al.*, 2017; Trazzi *et al.*, 2016). AHW char P systems hold an acidic pH of 5 which neutralises to a pH of 7 throughout incubation meaning Al and Fe precipitation may be observed. Precipitation of P into AlP or FeP would result in decreased measureable Al and Fe concentrations with increasing P concentrations, which is not the case for the AHW char (Figure 3.9a &b) suggesting removal of P is through adsorption or precipitation by elements not discussed here.

Overall elemental and speciation results indicate adsorption, not precipitation, is likely to be the predominant driver of P sorption as most char systems were under-saturated. Adsorption of P in some chars has been attributed to divalent ligand bridging which forms inner sphere complexes (Chintala *et al.*, 2014b; Hale *et al.*, 2013; Sparks, 1995). The low binding strength (N_s) produced by the sorption isotherm models supports adsorption as the main driver of sorption, as precipitation would lock P into the system resulting in a high N_s value.

P adsorption to char is driven by many mechanisms and therefore can be influenced by many characteristics (Chintala *et al.*, 2013; Ngatia *et al.*, 2017; Sparks, 1995). The surface characteristics of char, such as functional groups and surface charge influence such adsorption mechanisms (Chintala *et al.*, 2014b; Ngatia *et al.*, 2017; Sparks, 1995) which in turn are influenced by char production regimes (Lou *et al.*, 2016; Mukherjee *et al.*, 2011; Trazzi *et al.*, 2016). Understanding how functional groups and surface charge change between the groups of chars presented here may explain the vast differences in P sorption observed (Figure 3.1; Figure 3.2; Figure 3.3 a- f) and allow a definitive understanding of the mechanisms driving adsorption.

3.5 CONCLUSIONS AND FUTURE WORK

The general conclusions drawn from this Chapter in relation to the research aims are:

1. The P sorption ability of the nine chars over a range of P concentrations was extremely varied and unique to each char due to distinct chemical and physical characteristics of the chars. The data presented here suggests feedstock has a greater influence on P sorption behaviour than production temperature and time of incubation.
2. The unique nature of chars means the P sorption mechanism varies from one char to another. The data presented here suggests adsorption, not precipitation, is the main mechanism for P sorption, however precipitation likely begins once reactive sites are filled. A clear mechanism e.g. inner surface complexation through ligand bonding cannot be established from the work here.

In order to reach more definitive conclusions about P adsorption behaviours and mechanisms in chars, more detailed experiments and improved chemical understanding of the chars is required. Batch sorption experiments encompassing a greater number of P concentrations over a lower range may provide further insight into sorption behaviours. Sorption ability is also linked to the hydrophobicity of chars (Gray *et al.*, 2014; Kinney *et al.*, 2012; Zornoza *et al.*, 2016). Introducing a ‘wetting period’ to sorption experiments would account for hydrophobicity. Furthermore, the negative surface charge associated with char (Yao *et al.*, 2011a; Zeng *et al.*, 2013) will influence P sorption. Understanding surface functional groups and consequently charge and hydrophobicity through FTIR would allow better understanding of the sorption behaviours exhibited.

Finally, sorption may occur through precipitation with elements other than those discussed here. Gaining speciation data for further elements using WHAM VII when conducting speciation modelling would be valuable in confirming precipitation is not the explanation for the P sorption observed. These points will be addressed in the following chapter.

4 DEVELOPING AND UNDERSTANDING THE MECHANISMS DRIVING PHOSPHORUS ADSORPTION-DESORPTION INTERACTIONS IN THREE DIFFERENT BIOCHARS

4.1 INTRODUCTION

Every char shows a unique P sorption behaviour due to the diversity of char characteristics which are influenced by production regime and feedstock, as shown in Chapter 3 (Morales *et al.*, 2013; Ngatia *et al.*, 2017; Borno *et al.*, 2018). A char's characteristics impact the mechanism of P sorption influencing the dynamics of sorption (Chintala *et al.*, 2014b; Lou *et al.*, 2016; Wang *et al.*, 2015). P sorption can be driven by many mechanisms including: elemental precipitation, surface complexation and physi-sorption (Chintala *et al.*, 2014b; Lou *et al.*, 2016; Mosa *et al.*, 2018; Sparks, 1995).

P sorption by chars has been attributed to the precipitation of P by Ca, Mg, Al and Fe (Hong & Lu, 2018; Kizito *et al.*, 2017a; Lindsay, 1979; Lou *et al.*, 2016; Mosa *et al.*, 2018; Sarkhot *et al.*, 2013; Wang *et al.*, 2015; Xu *et al.*, 2013; Xu *et al.*, 2018). Precipitation by Ca and Mg was not observed in Chapter 3, suggesting adsorption was likely the main driver of P sorption in the chars assessed. Further elements to Ca and Mg, however may have been acting to precipitate P (Lindsay, 1979). Additional elements, including Sr, Mn, Ba and Al, are therefore considered within this Chapter. The presence of MnP precipitates within soils (Lindsay, 1979), coupled with the suggestion of biochar as a soil amendment, means MnP precipitation is worth exploring. Sr and Ba were added due to the interesting results for the gasified softwood chars (GSW and LGSW) shown in Chapter 3, where elemental concentrations decreased as P added increased.

A variety of adsorption mechanisms have been linked to P sorption within char (Chintala *et al.*, 2014b; Lou *et al.*, 2016; Sarkhot *et al.*, 2013; Wang *et al.*, 2015; Yao *et al.*, 2011a, 2011b). Adsorption to chars acts through physi-sorption and surface complexation. Physi-sorption is primarily regulated by chars surface area and surface charge (Trazzi *et al.*, 2016), whereas surface complexation involves interactions between ions and the chars surface ligands and functional groups (Sparks, 1995).

Surface functional groups have been shown to play a significant role in P adsorption processes within chars (Borno *et al.*, 2018; Chintala *et al.*, 2014b; Novais *et al.*, 2018; Sarkhot *et al.*, 2013; Sun *et al.*, 2018b; Yao *et al.*, 2011a, 2011b; Zhang *et al.*, 2016). The huge variety of functional groups in chars, influenced by production regime and feedstock (Ahmad *et al.*, 2014; Borno *et al.*, 2018; Chun *et al.*, 2004; Fristak *et al.*, 2018; Mukherjee *et al.*, 2011; Novais *et al.*, 2018; Sun *et al.*, 2018b; Zornoza *et al.*, 2016) alter the chars reactivity and ability to form surface complexes, both inner and outer sphere. P sorption in chars has been heavily linked to inner sphere complexation through ligand exchange mechanisms with available groups on a char's surface (Chintala *et al.*, 2014b; Sarkhot *et al.*, 2013; Yao *et al.*, 2011a, 2011b).

FTIR (Fourier-Transform Infrared Spectroscopy) explores the degree of IR light adsorption to structures to produce an adsorption spectrum, which can be interpreted to identify the surface functional groups (Singh *et al.*, 2017). The use of FTIR on GSW, HW and coffee char may provide a more specific mechanism for the distinct P sorption (Chapter 3) behaviours and explain why each group of chars behaves differently.

In this Chapter, the char sorption behaviours and mechanisms detailed in Chapter 3 were further quantified and developed.

This experimental chapter therefore aims to:

1. Rationalise the sorption behaviours of the three groups of chars presented in Chapter 3 over a specific and focussed range of P concentrations.
2. Establish the mechanisms causing sorption in GSW, HW and coffee chars through:

a. Examination of potential phosphate precipitation within the GSW, HW and coffee chars.
b. Assessment of adsorption mechanisms within GSW, HW and coffee chars by employing FTIR methods.

Research aims were achieved through laboratory-scale batch sorption studies on chars from each group exhibiting different sorption behaviours observed in Chapter 3. Adsorption appears to be the main mechanism of sorption (Chapter 3) and is known to occur, prior to precipitation, at low P concentrations (Sparks, 1995; Tunesi *et al.*, 1999), therefore the focus here was on low and specific P concentrations. The hydrophobic nature of chars may reduce sorption through minimising the interaction of solution with chars and the hydrophilic P anion (Ahmad *et al.*, 2014; Chun *et al.*, 2004; Kinney *et al.*, 2012; Zornoza *et al.*, 2016). To address and overcome any potential hydrophobic effects on P sorption, this Chapter includes the addition of a weeklong 'wetting' period.

4.2 MATERIALS AND METHODS

4.2.1 Biochar preparation

GSW, HW and coffee chars used throughout batch sorption experiments were produced as detailed in Chapter 2.

4.2.2 Batch Sorption Experiments

Prior to ICP-MS analysis, 0.1 g of powdered (<0.5mm) char was weighed, in triplicate, into a 50 ml centrifuge tube (Fisher Scientific) with 22 ml Milli-Q water and placed on an end-over shaker for a 170 hours (1 week). After the 'wetting period', the required volume of 1000 mg L^{-1} P batch solution (Chapter 3) and Milli-Q water was pipetted into each sample to achieve final solution concentrations of 25, 20, 16, 12, 8, 4, 2, 1, 0.1 and 0 mg L^{-1} P.

The pH readings were taken before and after placement on an end over end shaker for 96, 24 and 1 hour(s). At each time point, samples were centrifuged at 2500 rpm for 10 minutes and a 2 ml subsample of each solution was syringe filtered (0.22 µm; BD Discardit II Luer Slip Syringe; Millex Syringe Driven Filter Unit, 33mm, PES membrane) into acidified ICP tubes containing 3 ml of 50% nitric acid (Fisher Scientific, Trace analysis grade). P sorption was determined as per Chapter 3 (equation 3.1).

4.2.3 Isotherm Modelling

Modified Freundlich, Langmuir and L-F isotherm descriptive models were fitted to the data from the batch sorption experiments as described in chapter 3 (equations 3.2, 3.3 and 3.4).

4.2.4 Speciation Modelling

Speciation modelling using WHAM VII (Windermere Humic Aqueous Model VII) was conducted on the ICP-MS data from batch sorption studies, as in Chapter 3. The model was run using a modified solute database with additional phosphorus complexes, including strontium phosphate and further calcium phosphates. The model simulations were used to predict the speciation of P, Mg, Fe, Sr, Ba, Al, Mn and Ca using the following input parameters: (i) pH of the char-P solution, (ii) the P, Mg, Ca (mg L^{-1}), Mn, Fe, Sr, Ba and Al (µg L^{-1}) concentrations measured by ICP-MS (iii) atmospheric partial pressure of CO_2 (set to 400 ppm), (iv) temperature (20°C). The output from WHAM VII was as discussed in Chapter 3.

4.2.4.1 *Phosphate Solubility*

Data output from WHAM VII was used to produce phosphate stability diagrams with double function parameters of P potential vs lime, Mg, Mn (Log Mn^{2+}+ 2pH), Sr (Log Sr^{2+}+ 2pH), and Al (Log Al^{3+}+ 3pH) potential as in chapter 3 based on published solubility products (Table 3.1; Table 4.1) (Lindsay, 1926).

Table 4.1. Aluminium, manganese and strontium phosphate mineral reaction equations and Ksp used to draw phosphate solubility diagrams (Lindsay, 1979).

Mineral Formed	Reaction Equation	Log K_{sp}
$AlPO_4$ Berlinite	$AlPO_4 + 3H^+ \leftrightarrow Al^{3+} + H_2PO_4^- + H^+$ $(Al^{3+}) (H_2PO_4^-) (H^+)/ (H^+)^3 = 10^{0.5}$ $\log(Al^{3+}) + \log(H_2PO_4^-) – pH + 3pH = 0.5$ $\log H_2PO_4^- - pH = 0.5 - (\log Al^{3+} + 3pH)$	0.5
$AlPO_4$. $2H_2O$ Variscite	$AlPO_4.2H_2O + 3H^+ \leftrightarrow Al^{3+} + H_2PO_4^- + H^+ + 2H_2O$ $(Al^{3+}) (H_2PO_4^-) (H^+)/ (H^+)^3 = 10^{-2.5}$ $\log(Al^{3+}) + \log(H_2PO_4^-) – pH + 3pH = -2.5$ $\log H_2PO_4^- - pH = -2.5 - (\log Al^{3+} + 3pH)$	-2.5
$MnHPO_4$	$MnHPO_4 + 2H^+ \leftrightarrow Mn^{2+} + H_2PO^-_4 + H^+$ $(Mn^{2+}) (H_2PO^-_4) (H^+) / (H^+)^2 = 10^{-5.74}$ $\log(Mn^{2+}) + \log(H_2PO_4^-) – pH + 2pH = -5.74$ $\log H_2PO^-_4 - pH = -5.74 - (\log Mn^{2+} + 2pH)$	-5.74
$Mn_3(PO_4)_2$	$Mn_3(PO_4)_2 + 8H^+ \leftrightarrow 3Mn^{2+} + 2H_2PO_4^- + 4H^+$ $(Mn^{2+})^3 (H_2PO^-_4)^2 (H^+)^4 / (H^+)^8 = 10^{11.78}$ $11.78 = 3\log(Mn^{2+}) + 2\log(H_2PO^-_4) – 4pH + 8pH$ $11.78 = 3(\log Mn^{2+} + 2pH) + 2(\log H_2PO_4^- - pH)$ $\log (H_2PO_4^-) - pH = 5.89 - 1.5(\log Mn^{2+} + 2 pH)$	11.78
$SrHPO_4$	$SrHPO_4 + 2H^+ \leftrightarrow Sr^{2+} + H_2PO_4^- + H^+$ $(Sr^{2+}) (H_2PO_4^-) (H^+)/ (H^+)^2 = 10^{2.22}$ $\log(Sr^{2+}) + \log(H_2PO_4^-) – pH + 2pH = 2.22$ $\log H_2PO_4^- - pH = 2.22 - (\log Sr^{2+} + 2pH)$	2.22
$Sr_3(PO_4)_2$	$Sr_3(PO_4)_2 + 8H^+ \leftrightarrow 3 Sr^{2+} + 2H_2PO^-_4 + 4H^+$ $(Sr^{2+})^3 (H_2PO^-_4)^2 (H^+)^4 / (H^+)^8 = 10^{11.64}$ $11.64 = 3\log(Sr^{2+}) + 2\log(H_2PO^-_4) – 4pH + 8pH$ $11.64 = 3(\log Sr^{2+} + 2pH) + 2(\log H_2PO_4^- - pH)$ $\log H_2PO_4^- - pH = 5.82 - 1.5(\log Sr^{2+} + 2 pH)$	11.78

4.2.5 FTIR Spectral Analysis

FTIR spectral analysis was conducted on original and ‘wetted’ HW, GSW and coffee chars to see how functionality changed during the wetting period. The ‘wetted’ char was created by adding 0.1 g char to 22 ml Milli-Q water and placing on an end-over-end shaker for 170 hours (1 week). The char was then dried at 50°C for 48 hours. FTIR spectra for ball-milled wetted and original samples were found using a Bruker Tensor 27 ATR-FTIR (Attenuated Total Reflection FTIR) Spectrometer and OPUS analytical software. The spectral resolution was set at 4 cm^{-1} and spectral range at 4000-500 cm^{-1}, where 128 scans were taken for each sample. A spectrum obtained from a background sample was subtracted from the spectrum of each sample to eliminate the effect of ambient moisture and CO_2. Normalisation of the spectra by the mean was conducted by dividing the overall mean by the data standard deviation. Interpretation of individual bands and peaks of the spectra was conducted on Spectragryph 1.2.

4.2.6 Statistical Analysis

A general ANOVA followed by a post-hoc Tukey's multiple comparison test using GenStat (17^{th} Edition) compared the P adsorption, elemental concentration, lime, P, Mg, Sr, Mn and Al potential within each char type using incubation time and P added as the main factors.

4.3 RESULTS

4.3.1 Batch Sorption

All three chars showed P sorption, after an initial desorption step (Figure 4.1 a-f). The sorption observed in each system was higher than previously observed in Chapter 3, with the exception of the GSW char which showed a similar increase in sorption (Figure

4.1a-f). Coffee and HW both showed sorption, which was not observed in Chapter 3, where only desorption was seen at the given P concentrations.

In contrast to the data presented in Chapter 3, char type here did not influence P sorption trends ($p=0.093$). P sorption significantly increased with solution P ($p<0.001$) but was not affected by time ($p=0.827$) (Figure 4.1a-f). Sorption was not observed until a solution concentration of 5 mg L^{-1} P for coffee char but was seen at much lower concentrations for the HW and GSW chars. The slope for sorption from solutions with increasing P concentration was lower in GSW and HW char systems. Systems containing coffee char, however showed a sustained increase in sorption (Figure 4.1e &f). None of the systems reached a steady state of P sorption where equilibrium is established.

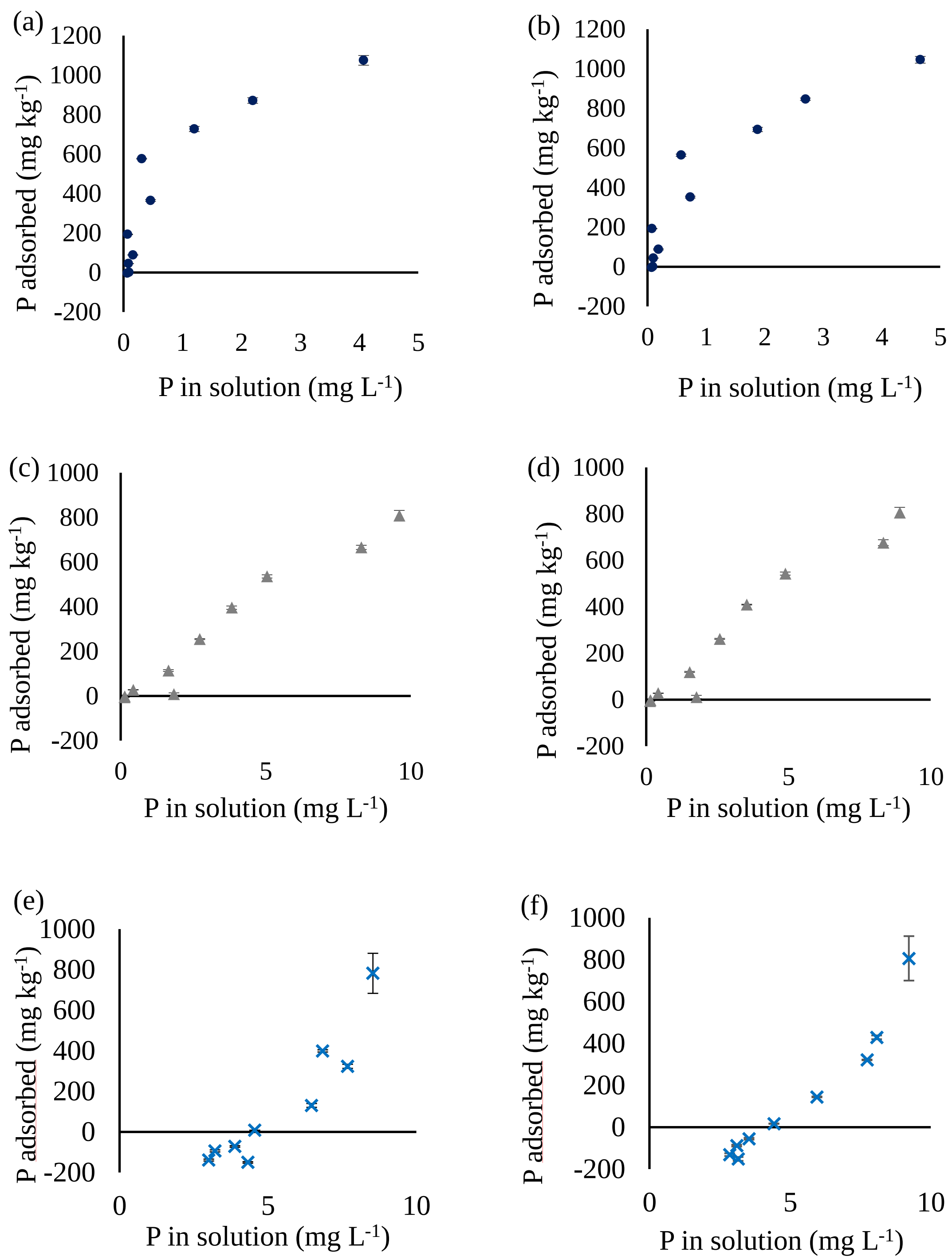

Figure 4.1. Phosphorus sorption patterns of GSW (navy circles) HW (grey triangles) and coffee (blue crosses) chars at 96 (a, c & e) and 24 (b, d & f) hour(s). Data are means ± S.E. Char type ($p=0.093$) did not influence P sorption. P added ($p<0.001$) has a positive correlation with sorption in chars irrespective of time ($p=0.827$).

4.3.2 Isotherm Models

The sorption observed in all three chars can be described by modified Langmuir, Freundlich and L-F sorption isotherm models as discussed in Chapter 3 (Figure 4.2a- c). All isotherm models complement the sorption data produced for GSW at all time points (Figure 4.2a), producing low RSD values (Table 4.2). Different isotherms complement the HW char sorption data depending on time point, shown by the variability in RSD values between models (Table 4.2). All models complement the sorption data produced for coffee char at all time points (Figure 4.2c), however Freundlich and L-F best described the continued sorption seen shown by low RSD values (Table 4.2). Coffee char isotherm models showed a linear increase, whereas GSW and HW showed a reduced slope (Figure 4.2a-c). Binding strength (K_l and K_a) are low for all isotherms produced, with the exception of Freundlich models for GSW at 1hr (Table 4.2).

4.3.3 Speciation Modelling

The pH of a system can influence precipitation (Liu *et al.*, 2018), therefore understanding pH aids in clarifying which elements to explore. Char type affected solution pH ($p<0.001$); broadly, the GSW char resulted in an alkaline pH, the HW char a near neutral pH and the coffee char an acidic pH (Figure 4.3).

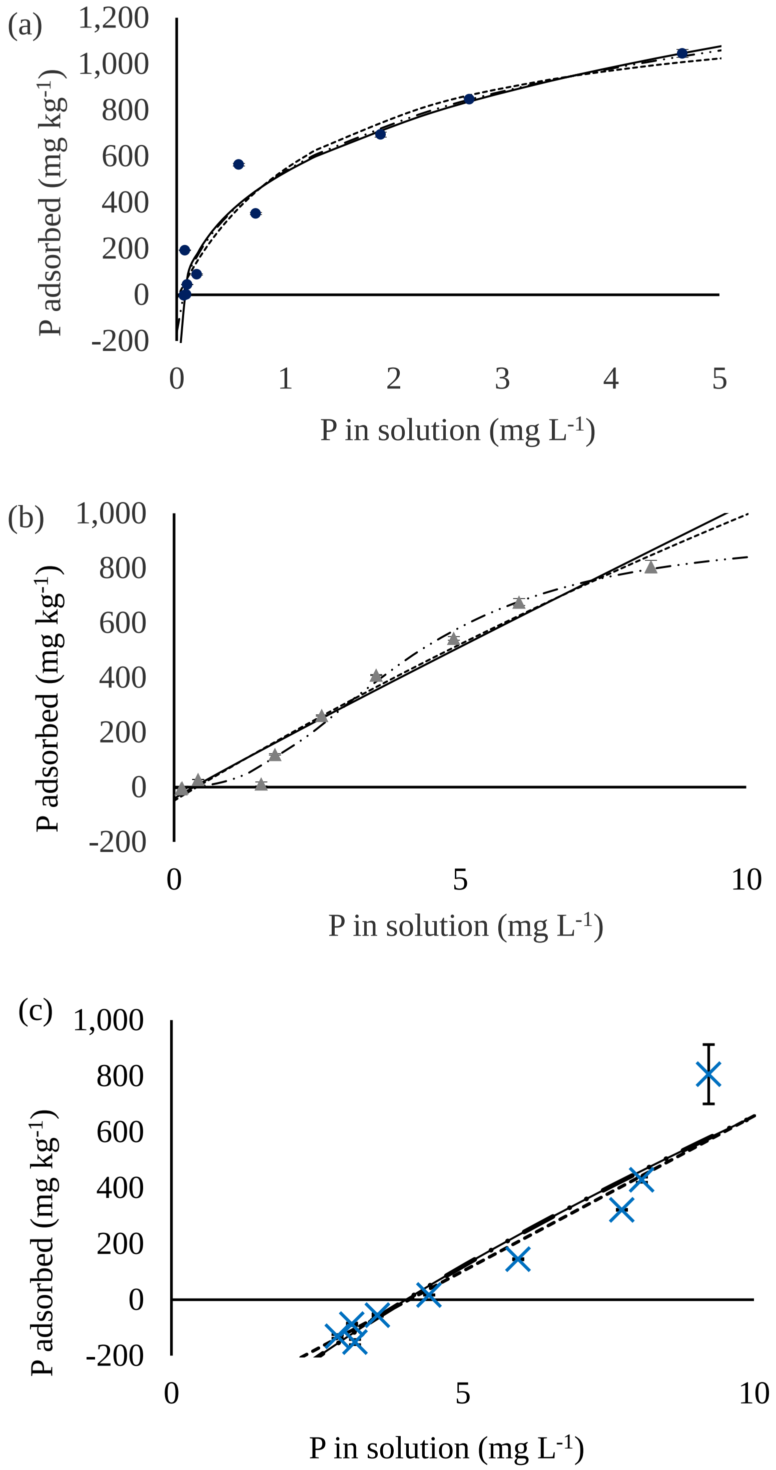

Figure 4.2. Phosphorus sorption patterns of (a) GSW char (navy circles), (b) HW char (grey triangles) and (c) coffee char (blue crosses) biochars at 24 hours with Langmuir, Freundlich and L-F models fitted to the data. All chars fit sorption isotherms. Solid lines depict the Freundlich model, --- represents the Langmuir model and -¨- represents the L-F model. Data are means and error bars represent S.E.

Table 4.2. Sorption isotherm constants for GSW, HW and coffee chars fitting modified Langmuir, Freundlich and L-F isotherm models at various time points found through batch sorption experiments. Model output is derived from inputting mean P adsorbed values for each time point

CHAR TYPE	TIME (HRS)	LANGMUIR			FREUNDLICH			LANGMUIR- FREUNDLICH			
		N_s	K_l	RSD	K_f	n	RSD	N_s	K_a	n	RSD
GSW	1	6360	52.6	101	4830	0.01	120	3500	0.28	0.04	92
	24	1320	0.74	75.0	935	0.29	73.0	2500	0.18	0.56	76
	96	1270	1.62	88.0	2550	0.11	86.0	2200	0.85	0.51	89
HW	1	241000	0.00	45.0	56.6	1.33	40.0	635	0.31	3.39	55
	24	6080	0.02	49.0	118	0.97	50.0	927	0.25	2.51	32
	96	29300	0.00	2.00	1.05	0.99	25.0	986	0.22	2.45	30
COFFEE	1	3490000	0.00	110	12.3	1.81	81.0	1040	0.13	5.26	67
	24	1600000	0.00	109	48.2	1.27	108	156000	0.00	1.28	112
	96	6670	0.02	105	211	0.78	106	1150	0.13	3.79	104

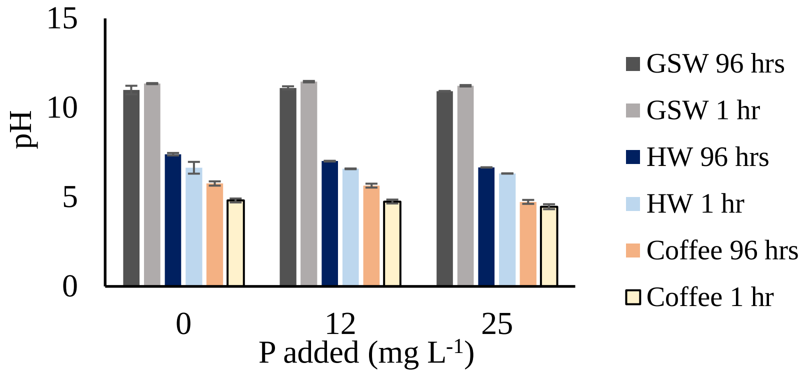

Figure 4.3. The pH of chars at 96 and 1 hr(s) when 0, 12 and 25 mg L^{-1} P was added. Data are means ± S.E. Char type as a single factor affected pH irrespective of time ($p<0.001$). pH in GSW char ($p=0.727$) did not change over time, whereas pH in HW and coffee chars did change over time ($p<0.001$ for both chars, time as a single factor). pH was not affected by P added ($p=1.00$).

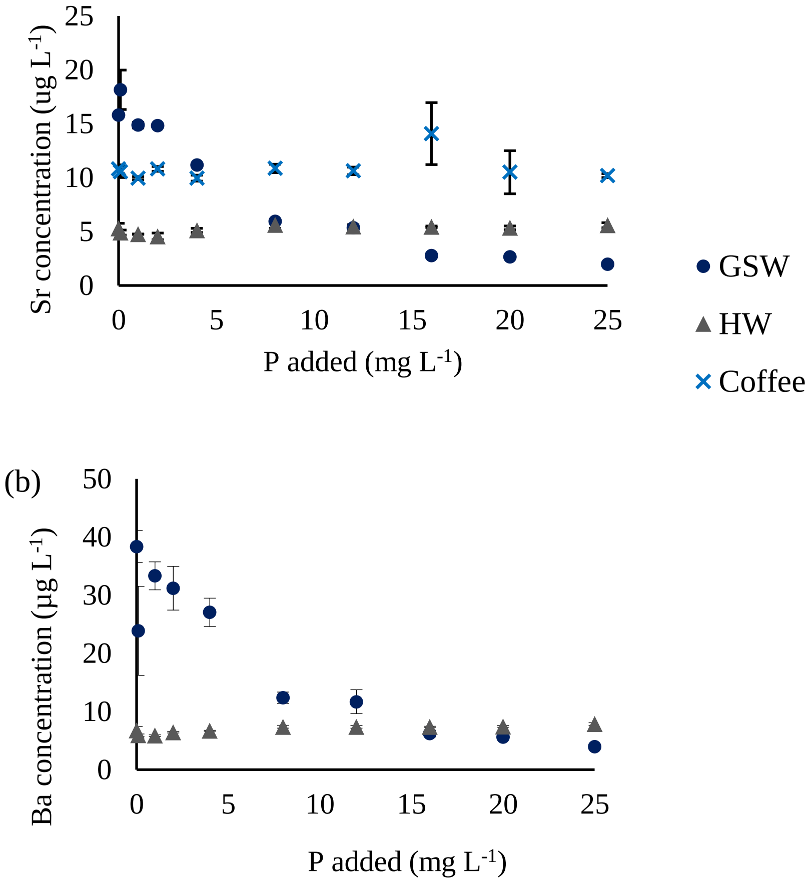

Figure 4.4. Total (a) Sr in systems containing GSW, HW and coffee chars and (b) Ba in systems containing GSW and HW at 96 hours with increasing P concentration. Data are means ± S.E. Coffee char not included for Ba as 0 µgL^{-1} of Ba was measured in all samples. Sr ($p=0.001$) and Ba ($p=0.001$) are affected by P concentration.

4.3.3.1 *Alkali Earth Metal Solubility*

The speciation and solubility of alkali earth metals in each char system was investigated. Sr and Ba showed a negative correlation with increased P concentration in systems containing GSW char (Figure 4.4) therefore, Sr solubility and stability was also explored. BaP speciation and stability diagrams were not produced due to lack of published solubility data. The remaining alkali earth metals, Be and Ra, were not considered as concentrations remained at 0 mgL^{-1} for all samples or the element was not measured by ICP-MS, respectively.

Stability diagrams for potential CaP complexes forming within the biochar systems showed all chars have a different lime ($p<0.001$) and P potential ($p<0.001$). Systems containing coffee or GSW were under-saturated with CaP regardless of P added (Figure 4.5). HW char systems were under-saturated with CaP, despite some data points sitting close to HA (Figure 4.5) as overlapping S.E.s showed systems remained under-saturated.

All chars have a different Sr ($p<0.001$), Mg ($p<0.001$) and P potential ($p<0.001$) shown in the MgP and SrP (Figure 4.6a &b) stability diagrams. Systems containing all three chars were under-saturated with both MgP and SrP, regardless of P added (Figure 4.6a &b).

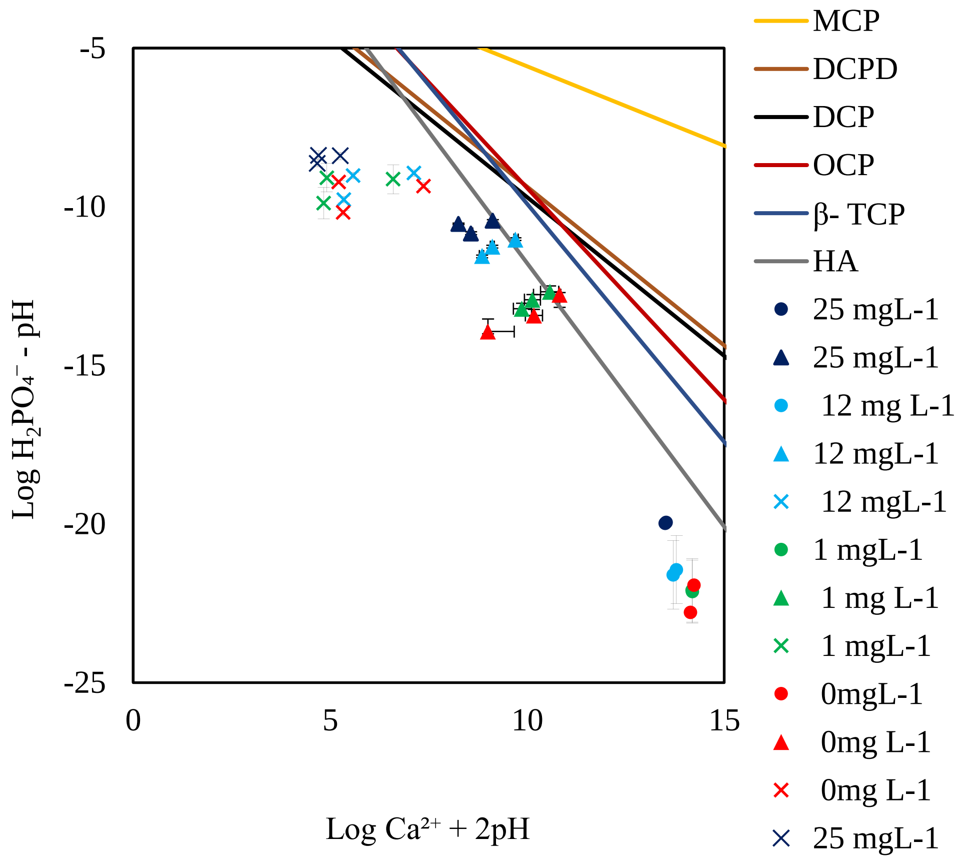

Figure 4.5. Stability diagrams for calcium phosphate complexes when 25, 12, 1 and 0 mgL^{-1} was added at all time points. Circles indicate GSW, triangles HW and crosses coffee char. Data are means. Error bars represent SE and are only shown in cases where saturation is observed for clarity. The Ca phosphate double function plots show the solubility of CaP complexes in chars in relation to the crystalline CaP: monocalcium phosphate (MCP), brushite (DCPD), dicalcium phosphate (DCP), octacalcium phosphate (OCP), β-tricalcium phosphate (TCP) and hydroxyapatite (HA) represented by solid lines. Equilibrium lines for the mineral phases were calculated based on the log K_{sp} values reported by (Lindsay, 1979). The points at which the lines overlap indicate coexistence of the solid phase. Char type influences lime ($p<0.001$) and P potential ($p< 0.001$).

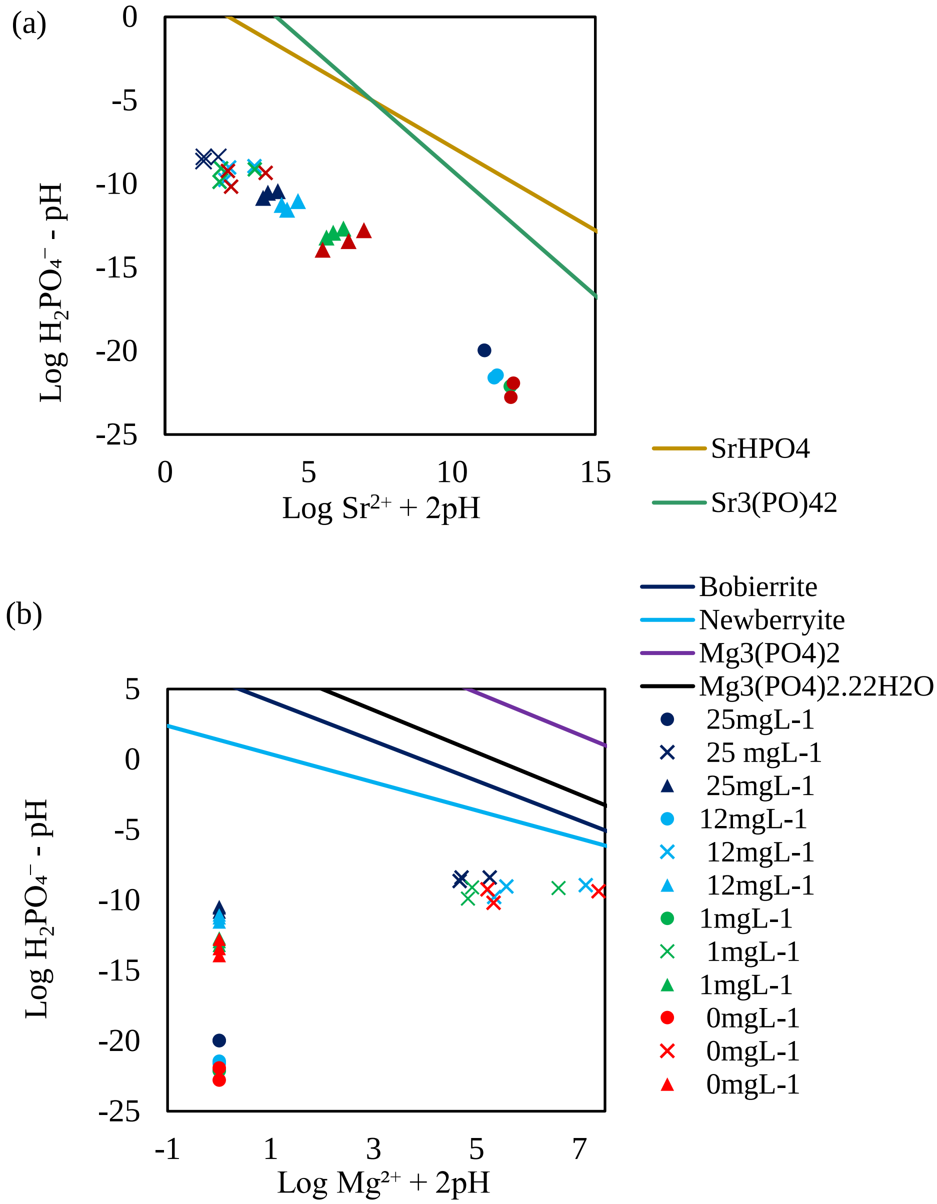

Figure 4.6. Stability diagrams for (a) strontium and (b) magnesium phosphate complexes when 25, 12, 1 and 0 mgL^{-1} P was added (data for at all time points combined). Circles indicate GSW, triangles HW and crosses coffee char. Data are means; error bars are excluded for clarity. The Sr phosphate double function plots show the solubility of SrP complexes in chars in relation to the crystalline Sr phosphates $Sr_3(PO_4)_2$ and $SrHPO_4$ and the MgP plots in relation to: Bobierrite, newberyite, $Mg_3(PO_4)_2$ and $Mg_3(PO_4)2.22H_2O$ represented by solid lines. Equilibrium lines for the mineral phases were calculated based on the log K_{sp} values reported by (Reddy *et al.*, 1989) for SrP and (Lindsay, 1979) for MgP. The points at which the lines overlap indicate coexistence of the solid phase. Char type influences Sr ($p<0.001$), Mg ($p<0.001$) and P potential ($p< 0.001$).

4.3.3.2 *FeP solubility*

The alkaline pH of HW and GSW (Figure 4.3) suggest precipitation by Fe was not a driving factor as precipitation is influenced by pH. Fe was undetectable in all coffee char solutions meaning Fe was not driving the sorption of P in those.

4.3.3.3 *Al and MnP solubility*

The lower pH of the coffee systems (Figure 4.3) suggests Al may be forming AlP precipitates. Stability diagrams for possible AlP complexes forming within the biochar systems showed all chars have a different Al and P potential ($p<0.001$). Systems containing GSW char were under-saturated, regardless of P added (Figure 4.7a). HW char systems were under-saturated with Al-P, despite some data points sitting close to variscite (Figure 4.7a), as overlapping S.E.s demonstrate the systems were under-saturated. Some systems for coffee sit above the variscite line suggesting potential saturation.

Systems containing GSW char were under-saturated with MnP, regardless of P added (Figure 4.7b). Coffee and HW systems lay in between the two MnP solid phases presented (Figure 4.7b), with the exception of the 25 mg L^{-1} P samples, where data lay above the MnP solid phases (Figure 4.7b). The activity of $MnPO_4$ complexes is positively correlated with P added in systems containing HW char ($p<0.001$), but not in systems containing coffee char ($p=0.095$) (Figure 4.8).

The Al ($p<0.001$), Mn ($p<0.001$), Ca ($p<0.001$) and Sr ($p<0.001$) potentials in all systems were influenced by time. P concentrations did not affect Al ($p=1.00$), Mg ($p=1.00$), Mn ($p= 0.965$), Ca ($p= 0.987$) and Sr ($p=0.928$) potential in any char system.

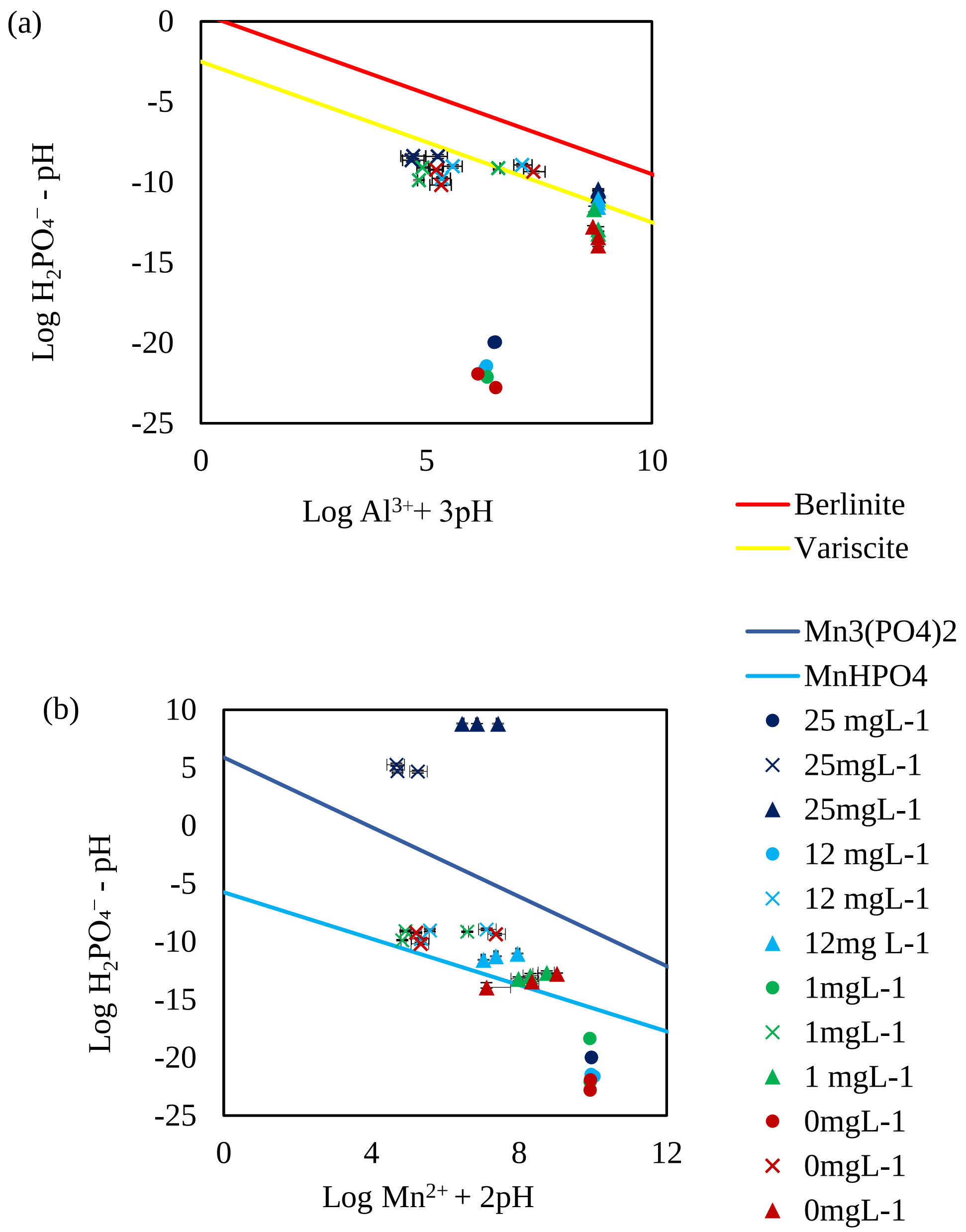

Figure 4.7. Stability diagrams for (a) aluminium phosphate and (b) manganese phosphate complexes when 25, 12, 1 and 0 mgL^{-1} was added (data for all time points combined). Circles indicate GSW, triangles HW and crosses coffee char. Data are means. Error bars represent S.E.s and are only shown in cases where saturation was observed for clarity. The Al and Mn phosphate double function plots show the solubility of AlP and MnP complexes in chars in relation to the crystalline Al phosphates Berlinite and Variscite and the Mn phosphates, $Mn_3(PO_4)_2$ and $MnHPO_4$, are represented by solid lines – see legend key for colour coding. Equilibrium lines for the mineral phases were calculated based on the log K_{sp} values reported by (Lindsay, 1979). The points at which the lines overlap indicate coexistence of the solid phase. Char type influences Al ($p<0.001$) Mn ($p<0.001$) and P potential ($p< 0.001$).

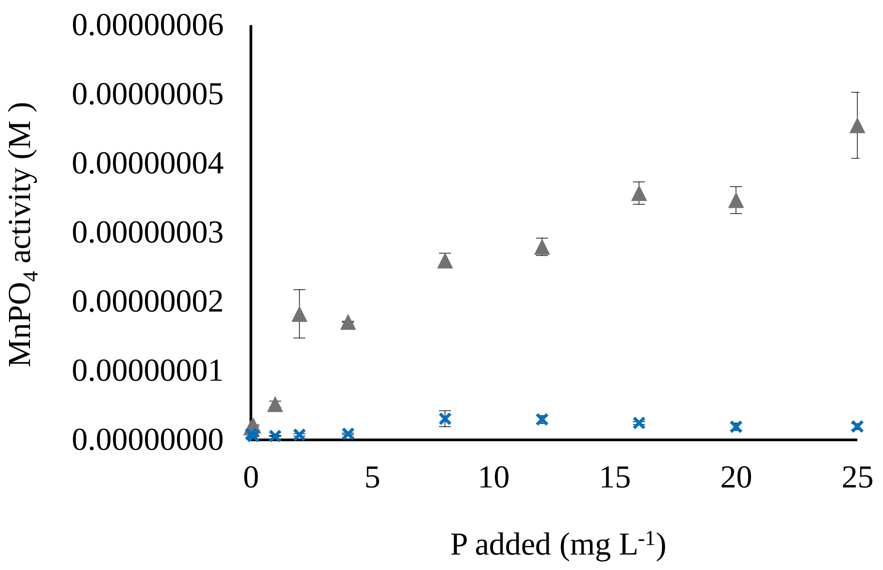

Figure 4.8. Manganese phosphate precipitates in HW char (grey triangles) and coffee char (blue crosses) systems according to P concentration. Data are means ± S.E. A positive correlation between P concentration and $MnPO_4$ activity was seen in HW char ($p<0.001$). $MnPO_4$ in coffee char was not influenced by P concentration ($p=0.095$). GSW char data are not presented here as the MnP stability diagram (Figure 4.7) suggests that no $MnPO_4$ precipitates form in systems containing GSW char.

4.3.4 FTIR Spectral Analysis

The spectra obtained for the GSW char show different adsorption bands from those for the HW and coffee chars, which both show similar spectral trends (Figure 4.9a &b). HW chars had the greatest number of spectral peaks, followed by coffee and GSW chars (Figure 4.9a). HW and coffee had peaks above 3000 nm unlike the GSW (Figure 4.9a) which indicates hydroxyl and potentially aromatic hydrocarbons were present within HW and coffee but not in GSW (Table 4.3). All three chars showed clear adsorption bands at 870, 1370-90, 1990 and 2350 nm (Figure 4.9a), which indicated the presence of β-glucosidic linkage, phenolic groups, C≡ C stretching and C=N bonds, respectively (Table 4.3). Coffee and HW showed similar peaks with both having clear bands at 615, 747, 1570, 2120 and 2280 nm (Figure 4.9a) suggesting the presence of aromatic hydrocarbons, C-N-C bending and aliphatic hydrocarbons (Table 4.3). Both coffee and HW chars showed clear peaks after 2350 nm where multiple small bands were observed and are concentrated between at 2350 nm and 3650-3900 nm (Figure 4.9a), which likely indicated hydroxyl and aliphatic C-H groups (Table 4.3).

The spectra for the original and wetted chars were not clearly different and HW presented the highest amount of adsorption bands followed closely by coffee and GSW within the wetted chars (Figure 4.9a&b). All three wetted chars presented more adsorption bands than the original unwetted chars. Additional adsorption bands between 520-530 nm were observed in all three suggesting increased aromatic hydrocarbons and 1020-1030 in coffee and GSW chars (Figure 4.9b), which indicated the presence of siloxane groups but have also been attributed to P-O stretching in phosphate-containing functional groups and C-O stretching of cellulose (Table 4.3). Coffee and GSW chars presented more bands at higher wavelengths after the wetting period, with coffee having further peaks between 3700-3900nm and GSW at 3650nm (Figure 4.9b), showing an increase in hydroxyl groups (Table 4.3). Wetted coffee char did not show peaks at 618 and 747 nm as observed in the original char, but additional or more frequent peaks at 1030, 2100-2300 and 3700-3900nm were observed (Figure 4.9b), showing C-O stretching of cellulose and lignin, carbonyl and hydroxyl groups increased, respectively (Table 4.3). Wetted GSW char presented additional peaks at 710, 1600 and 3600 nm (Figure 4.9b), showing increased aromatic, phenolic and hydroxyl groups, respectively (Figure 4.9b). The additional peaks at 1180, 1510, 2050, 2840, 3030, 3200-3900 nm (Figure 4.9b) seen in wetted HW shows carbonyl, aliphatic and hydroxyl groups (Table 4.3).

(a)

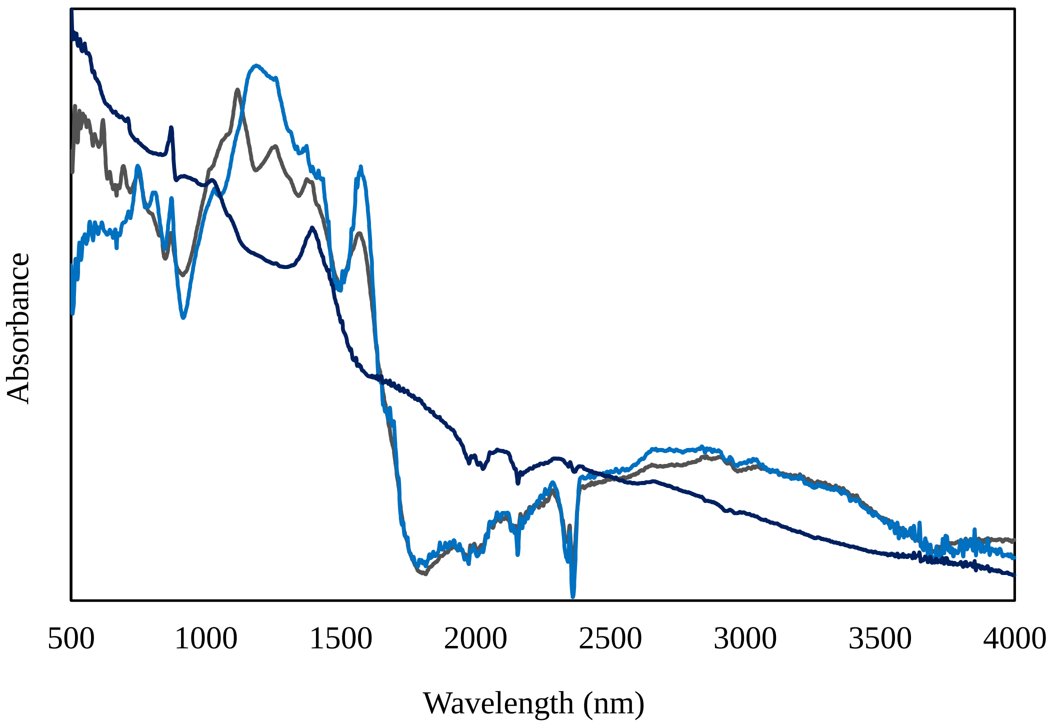

(b)

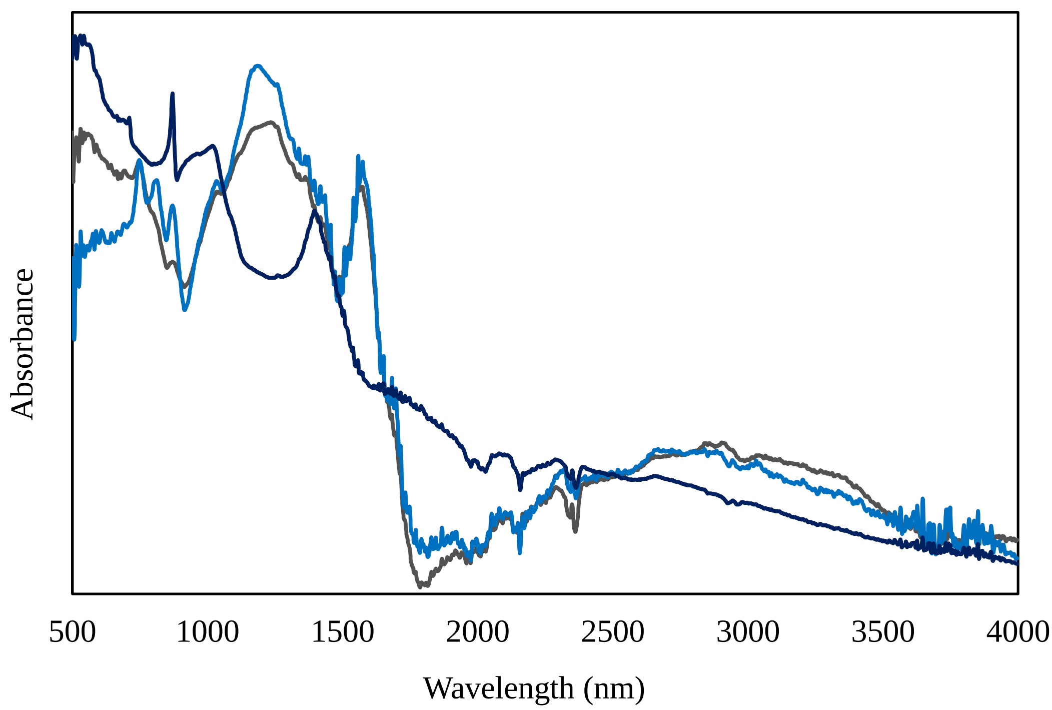

Figure 4.9. The FTIR spectra for (a) GSW, HW and coffee and (b) wetted GSW, HT and coffee chars where the dark blue lines corresponds to GSW, grey to HW and light blue to coffee.

Table 4.3. The FTIR absorbance bands used to interpret the FTIR spectra.

Absorbance Band (cm^{-1})	Chemistry	Ref
500-800	Aromatic C-H wagging	(Chintala *et al.*, 2013; Hossain *et al.*, 2011; Lee *et al.*, 2010; Purevsuren *et al.*, 2003)
874	β-glucosidic linkage C-H bending	(Yao *et al.*, 2011a)
885	Aromatic C-H	(Cantrell *et al.*, 2012; Lee *et al.*, 2010)
950- 1100	P-O stretching	(Cantrell *et al.*, 2012)
1030	Si-O stretching	(Jiang *et al.*, 2015; Yuan *et al.*, 2011)
1030-1100	Polysaccharides e.g. cellulose C-O stretching	(Cantrell *et al.*, 2012; Keiluweit *et al.*, 2010; Lee *et al.*, 2010; Yao *et al.*, 2011a)
1350-1430	Phenolic and hydroxyl O-H or C-O stretching	(Cantrell *et al.*, 2012; Yao *et al.*, 2011a)
1430	Aromatic ring modes	(Lee *et al.*, 2010; Purevsuren *et al.*, 2003)
1440	Phenyl e.g. lignin C=C stretching	(Cantrell *et al.*, 2012; Keiluweit *et al.*, 2010)
1500	Aromatic ring modes	(Brewer *et al.*, 2009; Cantrell *et al.*, 2012; Lee *et al.*, 2010)
1590- 1600	Aromatics (C=C, C=O, C=N) and carboxylate	(Brown *et al.*, 2006; Cantrell *et al.*, 2012; Jiang *et al.*, 2015; Purevsuren *et al.*, 2003; Yuan *et al.*, 2011)
1600- 1640	Aromatic phenolic C=C and C-O stretching	(Lee *et al.*, 2010)
1650	Carbonyl and Amide C=N, C=O and CC=C	(Cantrell *et al.*, 2012)
1700-1740	Carboxyl, Aldehyde and Ketone C=O	(Cantrell *et al.*, 2012)
2300- 2360	C=N stretch	(Chintala *et al.*, 2013)
2860- 3000	Aliphatic C-H	(Brewer *et al.*, 2009; Cantrell *et al.*, 2012; Hossain *et al.*, 2011; Nguyen & Lehmann, 2009; Purevsuren *et al.*, 2003)
3060	Aromatic C-H	(Brewer *et al.*, 2009)
3190- 3600	-OH and NH groups	(Brewer *et al.*, 2009; Cantrell *et al.*, 2012; Hossain *et al.*, 2011; Lee *et al.*, 2010; Nguyen & Lehmann, 2009; Purevsuren *et al.*, 2003; Yu *et al.*, 2016; Yuan *et al.*, 2011)

4.4 DISCUSSION

4.4.1 Sorption Patterns

P sorption did not vary between the chars which is not supported by the data in Chapter 3 or in the literature. A reduction in char hydrophobicity is expected due the prolonged exposure of chars to solutions prior to P addition, through the 'wetting' period. The reduced hydrophobicity facilitates increased interactions between char and P, potentially explaining the increase in P sorption observed in coffee and HW.

Both production regime and feedstock influence char hydrophobicity which can alter nutrient sorption behaviour (Ahmad *et al.*, 2012; Ahmad *et al.*, 2014; Chun *et al.*, 2004; Gray *et al.*, 2014; Kinney *et al.*, 2012; Zornoza *et al.*, 2016). High production temperatures breakdown char functional groups, including hydrophobic groups (Ahmad *et al.*, 2012; Ahmad *et al.*, 2014; Chun *et al.*, 2004; Gray *et al.*, 2014; Kinney *et al.*, 2012; Novais *et al.*, 2018; Zornoza *et al.*, 2016). GSW char, therefore, will likely contain fewer hydrophobic groups than coffee and HW chars, explaining the high P sorption in GSW systems both with and without the 'wetting' period. Time did not influence P sorption in any of the chars presented here (Figure 4.1a-f) which contrasts to the sorption behaviour observed for the GSW char in Chapter 3.

The majority of the literature states that char type influences P sorption (Chintala *et al.*, 2014b; Dari *et al.*, 2016; Jung *et al.*, 2015; Sarkhot *et al.*, 2013; Schneider & Haderlein, 2016; Takaya *et al.*, 2016; Wang *et al.*, 2015; Xu *et al.*, 2014); the data here do not corroborate that assertion (Figure 4.1a- f). The potential variability within each char investigated could cause overlap in P sorption, despite the chars being distinct (Yargicoglu *et al.*, 2015). The use of mixed feedstocks to produce HW and GSW chars (Chapter 2) could result in inconsistent characteristics which, coupled with the small sample (0.1 g) of each char tested, may cause char variability to appear as changes in sorption behaviour. The week-long wetting period, however, is rarely conducted by others conducting biochar-nutrient sorption experiments (Singh *et al.*, 2017) potentially explaining the difference between the data presented here and the literature. The influence of char hydrophobicity on nutrient sorption behaviours suggests wetting periods are required in order to completely understand char-nutrient sorption (Ahmad *et al.*, 2012; Ahmad *et al.*, 2014; Chun *et al.*, 2004; Kinney *et al.*, 2012; Zornoza *et al.*, 2016). This is especially important if char is to be used as a soil amendment since it will be subjected to wetting and drying cycles. Washing techniques have been used in more recent studies to reduce elemental desorption from chars (Schneider & Haderlein, 2016) and will act as a wetting period, however washing does not appear to be common practise. The use of FTIR to explore the presence of hydrophobic functional groups on both 'wetted' and original chars would improve understanding.

4.4.1.1 *P Sorption and Char P Concentration*

All three chars demonstrated a positive correlation between P sorption and P solution concentration for the chars (Lou *et al.*, 2016; Sarkhot *et al.*, 2013; Schneider & Haderlein, 2016; Trazzi *et al.*, 2016) through the formation of a concentration gradient between solution P and available P (Kizito *et al.*, 2017b), as discussed in Chapter 3. The available P within chars is readily released at low P concentrations (Atkinson *et al.*, 2010; Chan *et al.*, 2007; Xu *et al.*, 2014) causing desorption (Figure 4.1a-f) along a concentration gradient. High P availability means a high P concentration is required before the gradient favours P sorption. Coffee had more available P than GSW and HW chars (Chapter 2) explaining the high initial desorption and absence of sorption up to 5 mg L^{-1} P in coffee char systems.

Coffee, HW and GSW chars all have the potential to act as P sorbents when hydrophobicity is accounted for however, addition of a wetting period prior to soil amendment is unlikely to be carried out because of the impracticalities of it on a large scale.

4.4.2 Sorption Isotherm Models

Sorption isotherm models are a useful, predictive tool for sorption potential (Kilpimaa *et al.*, 2014; Wasewar *et al.*, 2008). The ability of isotherm models to describe GSW, HW and coffee sorption data shows sorption within the chars is predictable and allows for discussion of maximal binding, despite the low concentrations of P explored.

4.4.2.1 *GSW Sorption Isotherms*

The outputs from the isotherm models for GSW char are varied (Figure 4.2a; Table 4.2). The maximal binding (N_s) values predicted by Langmuir are similar to GSW sorption observed, suggesting GSW char was close to equilibrium. The L-F N_s values, however, suggest GSW char sorption may have doubled (Table 4.2), which is supported by the high sorption seen in Chapter 3. The L-F considers sorption to a heterogeneous surface meaning it may fit GSW due to the mixed feedstock used in production (Kilpimaa *et al.*, 2014; Wasewar *et al.*, 2008), further suggesting sorption in systems containing GSW would continue to increase.

4.4.2.2 *HW Sorption Isotherms*

The varied fitting of the isotherm models to HW data makes it difficult to infer maximum sorption (Figure 4.2b; Table 4.2). The L-F model suggests HW is close to N_s, where Langmuir suggests elevated sorption levels. The Langmuir model effectively described data from calcareous soils at similar P concentrations to those investigated here (Tunesi *et al.*, 1999), suggesting the high N_s value produced by Langmuir could be realistic. However, the mixed nature of HW feedstock, as for GSW, suggests Freundlich or L-F are best suited (Kilpimaa *et al.*, 2014; Wasewar *et al.*, 2008), making maximal sorption difficult to predict for HW.

4.4.2.3 *Coffee Sorption Isotherms*

Freundlich and L-F models complemented the data for coffee char (Figure 4.2c). The N_s values output from L-F models (Table 4.2) suggest sorption would continue at elevated P concentrations, which contrasts desorption behaviours shown in Chapter 3. No sorption isotherm models effectively described HW or coffee char sorption in Chapter 3 suggesting once hydrophobic parameters have been considered, both HW and coffee chars could act as P sorbents.

The low binding strength (K_l and K_a) presented by most isotherms suggest sorption via outer-sphere complexation or physi-sorption as oppose to inner sphere or precipitation which require stronger bonds (Sparks, 1995). Isotherms, however are not able infer adsorption mechanism meaning further analysis of data is required.

4.4.3 Speciation and Solubility Modelling

The pH of a system will influence any potential Al, Fe, Ca or Mg phosphate precipitates forming, as discussed in Chapters 1 and 3 (Clarkson & Hanson, 1980; Lindsay, 1979; Liu *et al.*, 2018). The pH range presented by the three chars studied here (Figure 4.3) means Al, Mg and Ca speciation were all explored. Fe stability and speciation were omitted as all systems showed 0 mg L^{-1} of Fe.

The production of stability diagrams for Ca, Mg, Sr, Mn and Al, from the WHAM VII speciation data, highlights any precipitates forming within the char systems, as discussed in Chapter 3. Precipitation of phosphate only occurs once maximal adsorption has occurred (Holford & Mattingly, 1975). If precipitation as a mechanism of P sorption is discounted (using elemental stability diagrams) the sorption observed is likely driven by adsorption (Holford & Mattingly, 1975).

4.4.3.1 *Alkali Earth Metal Solubility*

P sorption capacities of chars have previously been linked to concentrations of Ca and Mg in systems due to precipitation reactions (Ngatia *et al.*, 2017; Wang *et al.*, 2015; Xu *et al.*, 2013; Yao *et al.*, 2013) however, there is little exploration of the impacts of Sr on P sorption. The negative correlation of Sr with P concentration (Figure 4.4a) in GSW char, coupled with high char Sr availability of chars (Chapter 2) suggested SrP stability diagrams were a worthwhile investigation.

The under-saturation of chars in relation to Ca, Mg and Sr presented here suggest no precipitation by these elements (Tunesi *et al.*, 1999). Precipitation by Ca, Mg and Sr is therefore not driving the P sorption observed (Figure 4.5; Figure 4.6). The decrease in Ba concentration with increasing P concentration could suggest insoluble complexes are forming, however the small numbers associated with the decrease (Figure 4.4b) suggests P sorption cannot be attributed to Ba precipitation alone. Sorption is therefore driven by adsorption reactions (Chintala *et al.*, 2014b; Hale *et al.*, 2013; Yao *et al.*, 2011a, 2011b) or precipitation of P with alternative elements (Clarkson & Hanson, 1980; Lindsay, 1979; Ngatia *et al.*, 2017; Zhang *et al.*, 2009).

4.4.3.2 *Al and MnP solubility*

P sorption has been linked to Al precipitation within low pH systems (Lindsay, 1979). The under-saturation presented by GSW and HW chars (Figure 4.7a) is therefore expected due to the more basic pH demonstrated (Figure 4.3). The acidic pH in coffee systems (Figure 4.3) suggests AlP precipitates may be causing P sorption. Variscite precipitates observed in coffee systems at concentrations of 0, 1 and 12 mg L^{-1} P could contribute to P sorption. The formation of precipitates at 0 mgL^{-1}, however shows that variscite precipitates are present in the coffee char systems, regardless of P added, suggesting P sorption cannot be attributed to AlP precipitation. The presence of variscite may relate to the high initial concentration of Al in coffee char (Chapter 2).

Manganese interacts with P in soils (Lindsay, 1979) therefore precipitates could potentially form within chars. GSW char was under-saturated with MnP at all P concentrations (Figure 4.7b). MnP precipitates appear to be present within HW and coffee char systems at all P concentrations as the data clusters between or above the two solid phase lines showing solubility products have been exceeded (Figure 4.7b) (Lindsay, 1979). The stability diagram presented however does not take into account system redox potential to which the solubility of MnP precipitates are extremely sensitive (Lindsay, 1979). In order to develop conclusions surrounding MnP precipitation in char further parameters need to be considered when conducing batch sorption.

The $MnPO_4$ speciation data from WHAM VII supports MnP precipitation in HW char but not in coffee (Figure 4.8). The reduction in $MnPO_4$ activity (Figure 4.8), however, does not account for the amount P sorption seen suggesting P sorption (Figure 4.1) is not likely driven by MnP which has been found in relation to other elements (Sarkhot *et al.*, 2013).

The results suggest adsorption, not precipitation, is the driving force behind P sorption, as seen in Chapter 3 and throughout the literature (Chintala *et al.*, 2014b; Hale *et al.*, 2013; Yao *et al.*, 2011a, 2011b; Zhang *et al.*, 2016). Analysis of the char functional groups using FTIR will aid in developing a conclusion on the mechanisms driving P adsorption, particularly as stability diagrams cannot conclusively establish any phosphate mineral (Harrison & Adams, 1987).

4.4.4 FTIR Spectra and P Adsorption

FTIR spectral data allows understanding of the surface functional properties of materials therefore can aid in drawing conclusions surrounding the chemical interactions controlling nutrient adsorption within chars (Chintala *et al.*, 2013; Chun *et al.*, 2004; Ding *et al.*, 2014; Trazzi *et al.*, 2016; Yao *et al.*, 2011b). The functional surface properties of char alter with production as higher production temperatures degrade functional groups causing dehydration (Cantrell *et al.*, 2012; Chun *et al.*, 2004; Ding *et al.*, 2014; Lou *et al.*, 2016; Novais *et al.*, 2018; Trazzi *et al.*, 2016) explaining why GSW char displays less functionality than HW and coffee (Figure 4.9a). FTIR data for GSW, HW and coffee also provide an idea of the hydrophobicity and charge of the chars (Zornoza *et al.*, 2016) and the influence the wetting period had on char functional groups and therefore on adsorption. The presence of cellulose, lignin and β- glucosidase is common within chars from woody or plant feedstock (Cantrell *et al.*, 2012), explaining the presence within all three of the chars presented here (Figure 4.9a &b).

Adsorption can be driven by many mechanisms including physi-sorption, inner sphere and outer sphere complexation and the mechanisms vary depending on both char and nutrient characteristics (Chintala *et al.*, 2014b; Chun *et al.*, 2004; Hale *et al.*, 2013; Lou *et al.*, 2016; Sarkhot *et al.*, 2013; Yao *et al.*, 2011a, 2011b; Zhang *et al.*, 2016). The low binding strength output (K_l and K_a) from isotherm models (Table 4.2), suggests outer-sphere complexation or physi-sorption as inner sphere complexation reactions often produce a higher value for binding strength as discussed in Section 4.4.2.

4.4.4.1 *Physi-sorption*

Adsorption through physi-sorption relates to van der Waals and electrostatic forces which are influenced by BET surface area and surface charge (Sparks, 1995). Chars with larger surface areas show increased P sorption due to physi-sorption (Lou *et al.*, 2016; Mosa *et al.*, 2018; Trazzi *et al.*, 2016). GSW char had the highest BET surface area (Chapter 2) and demonstrates the highest sorption in Chapter 3, implying physi-sorption *via* surface area could act to adsorb P, especially as GSW had low functionality (Figure

4.9 a &b). The difference in BET surface area (42.66 in GSW to 0.1 in coffee and HW chars) however was not mimicked by the P sorption data when a wetting period was added (Figure 4.1a-c) meaning different mechanisms are likely at play in HW and coffee chars.

The surface charge of the chars will influence physi-sorption of P to chars. The chars investigated likely hold a negative surface charge due to the presence of oxygen-containing functional groups (Figure 4.9b), such as carbonyl and phenolic, which form Lewis bases in alkaline conditions creating a negative charge (Lou *et al.*, 2016; Yao *et al.*, 2011a; Zeng *et al.*, 2013). The negative surface charge of chars would limit P adsorption as the surface would repel the negative phosphate ion suggesting surface complexation is the driver of P adsorption in HW and coffee chars where surface area and charge do not appear to be linked. The positive correlation between negative surface charge and pH (Lou *et al.*, 2016; Yao *et al.*, 2011a; Zeng *et al.*, 2013) explains how GSW achieves similar P adsorption levels to HW and coffee, in spite of increased surface area.

4.4.4.2 *Outer Sphere Complexation*

Anion adsorption has been associated with outer sphere complexation (Chintala *et al.*, 2013; Sparks, 1995). Outer sphere complexation would explain the differences in sorption results (Chapters 3 and 4) obtained for HW and coffee chars as the presence of water molecules are required for an outer sphere complex to form. The pre-wetting period adopted within this Chapter exposed the chars to water molecules increasing those on the surface of the char (Sparks, 1995). P sorption to GSW char, however, was observed before the addition of the wetting period (Chapter 3) showing outer sphere complexation is not the adsorption mechanism in GSW char. Furthermore, outer sphere complexes tend to occur on surfaces holding an opposite charge (Sparks, 1995) and the established negative surface of chars coupled with anionic phosphate (Yao *et al.*, 2011a; Zeng *et al.*,

2013) means most conclude that inner sphere complexation is the primary method of P adsorption in chars (Mukherjee *et al.*, 2011; Yao *et al.*, 2011a, 2011b).

4.4.4.3 *Inner Sphere Complexation*

Inner sphere surface complexation is often favoured at more alkaline pH values which are usually the case with chars (Sparks, 1995). Whilst P sorption here did not significantly differ between the chars, the solution pH increase is in the same order (GSW > HW > coffee char), suggesting inner sphere surface complexation may nevertheless contribute to P sorption.

Phosphate adsorption to chars has been linked to ligand exchange mechanisms resulting in an inner sphere complex formation (Chintala *et al.*, 2014a; Hale *et al.*, 2013). Oxygen-containing functional groups, including carboxyl, carbonyl and phenolic groups, which increase after wetting (Figure 4.9a &b), have been associated with anion exchange and P sorption in chars (Sarkhot *et al.*, 2013). The increase in oxygen-containing functional groups after wetting is due to the presence of the partially negative oxygen atom within oxygen-containing functional groups which interacts with water molecules to increase hydrophilicity (Figure 4.9a &b). Anion exchange of OH- (hydroxyl) groups at the biochar surface and P in solution has been proposed as an adsorption mechanism (Chintala *et al.*, 2014b; Sarkhot *et al.*, 2013; Yu *et al.*, 2016). The increased sorption seen in coffee and HW chars after wetting (Figure 4.1a- c) is therefore likely due to the higher presence of hydroxyl groups (Figure 4.9b) facilitating increased anion exchange (Yu *et al.*, 2016). HW char however, had hydroxyl groups prior to wetting and did not show higher P sorption compared to the GSW and coffee chars, suggesting anion exchange with –OH groups is not the lone mechanism for P sorption in HW chars, although likely a key contributor.

Alternative oxygen-containing functional groups, such as carbonyl in HW and coffee chars and phenolic groups in GSW char (Figure 4.9b), seen after the wetting period may also bind to P to increase sorption (Borno *et al.*, 2018; Sarkhot *et al.*, 2013). Trazzi *et al.* (2016) found oxygenated functional groups decreased after P desorption studies suggesting anion exchange may be substituting the functional groups. The low anion exchange capacity (AEC) associated with some chars suggests P does not bind to oxygen-containing functional groups (Hale *et al.*, 2013), therefore quantifying the AEC of the chars would aid in definitively determining the likelihood of P adsorption *via* anion exchange within the three chars explored here.

Metal oxides, such as Ca and Mg oxides, have demonstrated strong sorption *via* inner sphere complexation of negatively charged anions, such as phosphate. For example, MgO (periclase) particles on the surface of chars contribute to P adsorption from solutions (Yao *et al.*, 2011a, 2011b). Calcium carbonate functionalities have also been linked to P adsorption (Zhang *et al.*, 2016), however this is not likely driving the P adsorption observed here (Figure 4.1a-c) due to the lack of carbonate groups within the chars (Figure 4.9b). Potential metal oxides influencing adsorption, including siloxane, are only observed in wetted coffee and GSW chars which show higher adsorption, however the FTIR bands for SiO could also be considered phosphate-containing functional groups (Cantrell *et al.*, 2012). The potential presence of P containing functional groups in wetted chars could support the adsorption of P to oxygen containing functional groups. The formation of the P containing groups may occur as a result of anion exchange of desorbed P from the coffee and GSW chars, which were found to hold a higher water available P content than HW in characterisation studies (Chapter 2).

4.5 CONCLUSIONS AND FUTURE WORK

The general conclusions drawn from this Chapter in relation to the research aims are:

1. Adsorption, not precipitation, is the driving mechanism of P sorption in all three chars analysed here, agreeing with the conclusions from Chapter 3.
2. Each char absorbs P from solution *via* different mechanisms which are influenced by the char's oxygen functionality and surface area. The data presented here suggests the following adsorption mechanisms:
    a. Physi-sorption *via* surface area likely accounts, at least in part, for the adsorption seen within GSW char in both Chapter 3 and here.
    b. The variation in hydrophilic and phobic oxygen-containing functional groups on chars contribute to the varied sorption behaviours observed in Chapter 3 and the addition of the wetting period increases oxygen containing functionality of chars.
    c. Inner sphere surface complexation *via* anion exchange with oxygen containing functional groups contributes to the adsorption seen within the chars. Hydroxyl and phenolic groups contribute to adsorption in HW, coffee and, in part, the GSW chars. Carbonyl groups aid in increasing adsorption in the wetted HW and coffee chars.

To develop more clear conclusions surrounding the impact of char on soil P availability, experiments exploring the practicalities of char amendments in soil are required. The sorption studied here and in Chapter 3 will drive P availability which is essential for plant growth but these mechanisms need to be clearly mapped before char can be recommended as a soil amendment.

The P sorption capacity of the systems is not exceeded where a plateau would be observed within these experiments. Experiments incorporating this and expanding further onto quantifying the sorption mechanisms of the other chars characterised (Chapter 2) would aid in developing P-char understanding. Once P sorption is established and understood in more chars, a model could be devised in which soil parameters can be input and the model provides information on the optimum biochar to improve soil P availability.

5 QUANTIFYING PHOSPHORUS AVAILABLITY OF THREE DIFFERENT SOILS AMENDED WITH GSW, HW AND COFFEE BIOCHARS

5.1 INTRODUCTION

The varied P sorption interactions observed between biochars (Chapters 3 and 4) will influence the P availability within soils (Chintala *et al.*, 2014b; Sarkhot *et al.*, 2013; Schneider & Haderlein, 2016; Wang *et al.*, 2015; Xu *et al.*, 2013; Yao *et al.*, 2011a, 2011b). The diverse physical, chemical and biological nature of soils further results in varied P availability after biochar amendment due to complex reactions between the char and soil (Dari *et al.*, 2016; Laird *et al.*, 2010b; Parvage *et al.*, 2013; Xu *et al.*, 2014). Calcareous soils, for example, are characterised by high calcium (Ca) concentrations and are often P limited due to the precipitation of P into solid phase calcium phosphates (Tunesi *et al.*, 1999; Von Wandruszka, 2006). Acidic soils, below a pH of 5.5, are also often P limited due to precipitation of P by Al and Fe cations or adsorption to Al, Mn and Fe oxides which are more notable in acidic conditions (Xu *et al.*, 2014). Char addition to both acidic and calcareous soils has been linked to increased P availability (Chintala *et al.*, 2014b; Xu *et al.*, 2014). Neutral soils, however, have a pH of around 6.5 at which most precipitation reactions are limited and therefore have been attributed with having the most available P. However, adsorption reactions have been observed within neutral soils which limit P (Noyce *et al.*, 2017; Pierzynski & McDowell, 2005), meaning investigation of biochar as an amendment to soils with a range of pH values is of benefit.

Char contributes P to soils through direct and indirect mechanisms which vary according to char and soil characteristics in which instantaneous or slow release is observed, respectively (Liang *et al.*, 2014; Noyce *et al.*, 2017; Xu *et al.*, 2013). Initial biochar P concentration can directly influence P availability through desorption from char to soils (Chintala *et al.*, 2014b; Liu *et al.*, 2018; Madiba *et al.*, 2016; Qayyum *et al.*, 2015; Xu *et al.*, 2013; Zhang *et al.*, 2016). The addition of P from char to the soil the acts to fill P sorption sites within the soil, leaving more P available within the soils, meaning chars with lower initial P concentrations are less likely to increase soil available P (Borggaard *et al.*, 2004; Madiba *et al.*, 2016; Morales *et al.*, 2013; Sato & Comerford, 2006).

Biochar can also increase a soil's ability to retain P through sorption reactions, both adsorption and precipitation. P adsorption interactions, which occur prior to precipitation, determine P availability in a range of soils (Tunesi *et al.*, 1999; Zhang *et al.*, 2016). Biochars have been characterised as having acidic surface functional groups (Cheng *et al.*, 2006; Cheng *et al.*, 2008b; Liang *et al.*, 2006; Cheng, 2008; Yuan *et al.*, 2011), such as the hydroxides identified in Chapter 4 and Al and Fe oxides, which adsorb P from the soil systems (Jiang *et al.*, 2015; Qayyum *et al.*, 2015). The influence of biochar on soil pH and desorption of elemental cations from chars could also result in P retention through P precipitation reactions (DeLuca *et al.*, 2015; Hong & Lu, 2018; Mosa *et al.*, 2018; Xu *et al.*, 2018). P retention by addition of chars often causes the slow release of P which would hold beneficial effects for biochar as a long term fertiliser and to reduce the loss of P into the environment (Dari *et al.*, 2016; Liang *et al.*, 2014; Nelson *et al.*, 2011).

Soil physical and biological properties, which are influenced by char amendment, also affect the P available from soils. Biological properties, such as the soil microbial population, alter the P availability of soils as microbes hydrolyse P into bioavailable forms (Lehmann *et al.*, 2011; Omil *et al.*, 2013; Sarma *et al.*, 2018; Zhai *et al.*, 2015). Chars support soil microbial biomass therefore are likely to increase the available P within a variety of soils (Hammer *et al.*, 2014; Lehmann *et al.*, 2011; Madiba *et al.*, 2016; Sarma *et al.*, 2018; Zhai *et al.*, 2015). Physical properties, such as the soil texture, influence the soil pore size and alter the number of available sorption sites for nutrients therefore will impact available P concentrations (Horn *et al.*, 1994; Noyce *et al.*, 2017; Yeboah *et al.*, 2009).

The complex chemical, physical and biological mechanisms controlling P availability when biochar is added to soils are not clearly understood due to the many potential interactions involved (Noyce *et al.*, 2017).

The chemistry of P within soils amended with biochar over a range of pH measurements therefore needs to be better understood. **The specific objectives of this chapter were to:**

1. Characterising and quantifying the P availability in three soils with and without biochar amendment using a variety of P extraction techniques.
2. Highlighting and discussing the potential speciation and sorption mechanisms influencing the P availability within soils.

The approach was to conduct a long term soil incubation experiment including GSW, HW and coffee chars. A variety of P extraction techniques were conducted throughout to assess P availability and speciation.

5.2 MATERIALS AND METHODS

5.2.1 Biochar Preparation

The GSW, Coffee and HW biochars used throughout the range finding experiments were produced as detailed in Chapter 2 (Section 2.2.1).

5.2.2 Soil Collection/ Sampling

Calcareous (52.80631 N°, -1.40071 W°), acidic (52.82956 N°, -1.24307 W°) and neutral (52.83514 N°, -1.25095 W°) soils were collected from sites within the East Midlands, UK. The numbers in brackets denote the coordinates, longitude N° and latitude W°, for the sampling points of soils.

5.2.3 Soil Characterisation

The pH, EC and redox potential of the soils were determined by adding 5 g of soil to 12.5 ml Milli-Q water in triplicate in a 50 ml centrifuge tube (Fisher Scientific). pH, redox (HANNA instruments, 209, pH and redox meter), and EC (HANNA, HI9835 Microprocessor Conductivity/TDS meter) readings were taken after placement on an end-over-end shaker for 30 minutes.

Percentage moisture of the soils was calculated using Eq. 2.1 (Chapter 2, Section 2.2.1.1) after oven drying (GenLab Oven) at 105°C for 24 hours. After drying, the % organic matter of the soils was calculated using loss on ignition (LOI). Soils were heated to 550°C in a muffle furnace (Carbolite, AAF 1100 furnace) for 8 hours in triplicate in open crucibles. Organic matter was then calculated using Eq. 5.1.

$$\%\ \text{organic matter} = \left(\frac{\text{weight}_{\text{dry}} - \text{weight}_{\text{LOI}}}{\text{weight}_{\text{dry}}}\right) \times 100$$

Eq. 5.1

Where, $\text{weight}_{\text{dry}}$ is the weight after oven drying (g) and $\text{weight}_{\text{LOI}}$ represents the weight after LOI (g).

Prior to analysis using a C-H-N elemental analyser (Thermo Scientific Flash 2000, Organic Elemental Analyser), a 5-6 mg sample of each dried soil and 2-3 mg of standard were weighed in triplicate as previously described.

5.2.4 Soil Char Incubation Experiment

A 3% amendment of each biochar (<0.5 mm) was added to 300 g of each of the calcareous, acidic and neutral soils in triplicate creating the following treatments:

Table 5.1. The treatments and abbreviations created during the soil incubation experiment.

CAL- Calcareous	NEU- Neutral	ACI- Acidic
CGSW- Calcareous GSW	NGSW- Neutral GSW	AGSW- Acidic GSW
CHW- Calcareous HW	NHW- Neutral HW	AcHW- Acidic HW
CC- Calcareous coffee	NC- Neutral coffee	AC- Acidic coffee

Soil-char treatments were maintained at 15°C and were sampled at 16, 8, 4, 3, 2, 1 and 0 week(s). Soil-char system moisture content was maintained at 30% by dropwise addition of water to achieve the desired weight calculated using Eq 5.2.

$$\text{Weight}_{desired} = \text{Weight}_{original} - \text{Weight}_{sample} \qquad \text{Eq 5.2}$$

Where, $\text{weight}_{desired}$ is the weight to be maintained after sampling (g), $\text{weight}_{original}$ is the weight of the system at 30% moisture content at the time of set up (g) and weight_{sample} is the cumulative sum of the weight of samples removed at each sampling time point (g).

5.2.5 P Extraction

At each time point, the total elemental composition of the soils and soil-char combination was determined by ICP-MS after nitric acid (HNO_3) (Fisher Brand, 70% ACS grade) and hydrogen peroxide (H_2O_2) (Acros Organics, 35% ACS grade) digestion using Aqua Regia. Prior to heating each sample to 95°C for 2 hours, a 0.4g sample was weighed into heat block digestion Digitubes with 8 ml of HNO_3 and 2 ml of H_2O_2. After heating, the digestates were diluted with 10 ml Milli-Q water and transferred into polypropylene Universal tubes using a syringe filter (0.22 µm; BD Discardit II Luer Slip Syringe; Millex Syringe Driven Filter Unit, 33mm, PES membrane). A 1 ml aliquot of each sample was then added to 9 ml milli-Q water to create a 1:10 dilution for ICP-MS analysis.

Ammonium nitrate (NH_4NO_3), water available, Olsen P and Morgan's modified extractions were also conducted on the soil-char combinations at each time point. A 2 g sample of each treatment was weighed into 50ml centrifuge tubes (Fisher Scientific) with 30 ml of NH_4NO_3 (Fisher Chemical, ACS 1M solution), 30 ml DI H_2O, 30 ml, sodium bicarbonate (Fisher Chemical ACS grade, 0.5M) with 0.05% w/v polyacrylamide (Sigma Aldrich) or 10ml ammonium acetate (Fischer Chemical, HPLC grade, 0.5M) with 0.05% w/v polyacrylamide (Sigma Aldrich) adjusted to pH 4.5 using acetic acid glacial (Fisher Chemical, Laboratory grade), respectively. The soil-solution mixtures were placed on end-over-end shaker for 30 minutes then centrifuged (Thermo Scientific Heraeus Megafuge 40) at 2500rpm for 10 minutes. The NH_4NO_3 and H_2O samples were transferred into polypropylene Universal tubes using a syringe filter (0.22µm) and 1:10 dilution of the filtered extracts was made, prior to ICP-MS analysis. The Olsen P and Modified Morgan's extracts were analysed for phosphorus using colorimetric analysis.

5.2.5.1 *Colorimetric Analysis*

Acid molybdate reagent (AMR) required for colorimetric analysis was made up by adding 200ml of sulfuric acid (Fisher Chemical, ACS) to 400 ml of Milli-Q water at 50 ml increments. A 0.435 g sample of antimony potassium tartrate (Sigma Aldrich, HPLC grade) was added to 100 ml of Milli-Q water to create 'solution A' and 19.2 g of ammonium molybdate (Fisher Chemical, ACS) was added to 250 ml Milli-Q water to make 'solution B'. Solution A and B were then combined in a glass beaker and added to the sulfuric acid. AMR was then transferred to polyethylene bottles and stored in the fridge (4°C) until use. On the day of colorimetric analysis, 3.4 g of ascorbic acid (Fisher Scientific, laboratory grade) was dissolved in 200 ml of Milli-Q water.

Prior to measuring char-soil sample absorbance, a calibration absorbance solution range of 0- 50 µg L^{-1} P concentration was developed using 1000 µg L^{-1} stock solution. After experimental extraction, 5-10 ml of biochar-soil solutions were added to 4 ml AMR and 4 ml ascorbic acid and made up to 50 ml using Milli-Q water in a 50 ml centrifuge tube (Fisher Brand). After allowing 20 minutes for colour development, the absorbance of the solution was measured at 880 nm in a 1 cm cuvette (Fisher Brand) using a spectrophotometer (CECIL CE1010, 1000 series) and compared to the calibration curve. Phosphate in solution was calculated using Eq. 5.3:

$$P_{Olsen} = \frac{\mathrm{Slope_{cal.}} \times \left(\frac{P_{char}\ X\ \mathrm{Vol_{sample}}}{\mathrm{Vol_{absorb}}}\right) - \left(\frac{P_{blank}\ X\ \mathrm{Vol_{sample}}}{\mathrm{Vol_{absorb}}}\right)}{\mathrm{Weight_s}}$$

Eq. 5.3

Where P_{oslen} is the available phosphate in solution (mg Kg^{-1}), $Slope_{cal}$ is the slope for the absorbance calibration curve calculated using the slope function in excel. P_{char} and P_{blank} are the measured absorbance of the soil-char samples and blank, respectively. Vol_{sample} is the volume used throughout extraction (ml), vol_{adsorb} is the volume of each 5-10 ml sample used in colorimetry analysis (ml) and $Weight_s$ is the weight of soil-char sample (g).

5.2.6 Speciation Modelling

The Windermere Humic Acid Model VII (WHAM VII) was used to analyse the nutrient speciation therefore solubility in the soil biochar treatments using the water extractable ICP-MS data. The WHAM software considers fulvic acid (colloidal and particulate), humic acid (particulate) and Fe, Mn and Al oxide activities where soils are present.

5.2.6.1 *WHAM Parameters*

Fe, Mn and Al oxide concentrations of soils were found using dithionite- citrate (CBD) extraction methods. Prior to ICP-MS, 2 g of each treatment was dried in the oven at 105°C for 24 hours and then ground to a powder using a mortar and pestle. A 0.25 g sample of each dried, ground soil-char treatment was weighed into 50ml centrifuge tubes (Fisher Scientific) with 20 ml CBD extract (Fischer Chemical, ACS, 1M sodium bicarbonate, 0.3 M sodium citrate and 0.07 M sodium dithionite). Samples were incubated for 24 hours at 20°C in a shaking water bath (Fisher Scientific, DMS360) followed by centrifugation at 2400 rpm for 15 minutes (Thermo Scientific Heraeus Megafuge 40). Samples were prepared for ICP-MS by adding 0.1 ml of syringed-filtered (0.22µm) sample to 9.9 ml of 2% nitric acid.

Colloidal fulvic acid measurements were calculated based on the assumption that 65% of dissolved organic carbon (DOC) found through calcium nitrate ($Ca(NO_3)_2$) extraction equals active fulvic acid and that fulvic acid is 50% C as seen in Eq. 5.4.

$$\mathrm{FA}_{\mathrm{Colloidal}} = 2\ (0.65 \times \mathrm{DOC})$$

Eq. 5.4

Where, $FA_{colloidal}$ refers to the colloidal fulvic acid and DOC refers to dissolved organic carbon measurements. Measurement of TOC (Shimadzu, TOC-V CPH TOC Analyser) was conducted according to the method in Chapter 2 (Section 2.2.3).

Particulate humic acid was calculated using Eq 5.5 on the assumption that active humic acid makes up 50% of soil organic matter found through LOI studies, see Eq. 5.5.

$$\mathrm{HA}_{\mathrm{particulate}} = \frac{\%\ \text{organic matter}}{2}$$

Eq. 5.5

The elemental total, free ion and complex activities of the soil treatments were predicted using WHAM VII with additional input and speciation parameters considering (i) pH, (ii) water and ammonium nitrate extractable Mg, Al, Ca, Mn, Fe, Cu, Zn, Sr and P obtained through ICP-MS analysis, (iii) the concentration of particulate humic acid (iiv) the concentration of Mn, Fe and Al oxides (v) colloidal fulvic acid, (vi) atmospheric partial pressure of CO_2 (set to 400ppm) and (vii) temperature (15°C). The data were run using the modified solute database, as in Chapter 4. Output from WHAM VII included total element concentration (mol L^{-1}), particle-bound element concentration (mol L^{-1}), the activity of different elemental species within char-P solutions (mol L^{-1}) and the fractions of P bound to Mn, Al, Fe oxides, colloidal fulvic acid, particulate humic acid and calcium carbonates ($CaCO_3$).

5.2.6.2 *Phosphate Solubility*

Data output from WHAM VII was used to produce phosphate stability diagrams with double function parameters of P potential vs lime, Mg, Mn, Sr, Fe (II) (Log Fe2+ +2 pH) and Fe (III) (Log Fe3+ +3 pH) potential as in Chapters 3 and 4 based on published solubility products (Table 3.1; Table 4.1; Table 5.2) (Lindsay, 1979; Reddy *et al.*, 1989).

Table 5.2. Iron phosphate mineral reaction equations and Ksp used to draw phosphate solubility diagrams (Lindsay, 1979).

Mineral Formed	Reaction Equation	Log K_{sp}
$FePO_4$	$FePO_4 + 3H^+ \leftarrow\rightarrow Fe^{3+} + H_2PO_4^- + H^+$ $(Fe^{3+}) (H_2PO_4^-) (H^+)/ (H^+)^3 = 10^{-5.37}$ $-5.37 = \log(Fe^{3+}) + \log(H_2PO_4^-) – pH + 3pH$ $\log H_2PO_4^- - pH = -5.37 - (\log Fe^{3+} + 3pH)$	-5.37
$FePO_4.2H_2O$ Strengite	$FePO_4.2H_2O + 3H^+ \leftarrow\rightarrow Fe^{3+} + H_2PO_4^- + H^+ + 2H_2O$ $(Fe^{3+}) (H_2PO_4^-) (H^+)/ (H^+)^3 = 10^{-6.85}$ $-6.85 = \log(Fe^{3+}) + \log(H_2PO_4^-) – pH + 3pH$ $\log H_2PO_4^- - pH = -6.85 - (\log Fe^{3+} + 3pH)$	-6.85
$3Fe^{II(}PO_4)_2.8H_2O$ Vivianite	$Fe_3(PO_4)_2.8H_2O + 8H^+ \leftarrow\rightarrow 3Fe^{2+}+2H_2PO_4 +8H_2O+4H^+$ $(Fe^{2+})^3 (H_2PO_4^-)^2 (H^+)^4 / (H+)^8 =10^{3.11}$ $3.11= 3\log(Fe^{2+}) + 2\log (H_2PO_4^-) - 4pH + 8pH$ $3.11= 3(\log Fe^{2+}+ 2pH) + 2(\log H_2PO_4^- -pH)$ $\log H_2PO_4^- - pH = 1.56 - 1.5 (\log Fe^+ 2pH)$	3.11

5.2.7 Statistical Analysis

The elemental availability at each time point was compared between the soil-char treatments using a one-way ANOVA followed by a post-hoc Tukey's multiple comparisons test using GenStat (19th Edition) which was then repeated on the elemental potentials. A two- way ANOVA was also conducted to account for the potential influence of time.

5.3 RESULTS

5.3.1 Soil Characterisation

The three soils used within the incubation experiment demonstrated different characteristics (Table 5.3 Table 5.4). Calcareous soil held the highest pH, EC, redox, moisture content, N%, C%, and H% (Table 5.3). Organic matter however was highest in acidic soils. pH values were clearly different between the three soils (Table 5.3) (p

<0.001) with calcareous being the most basic followed by neutral and then acidic (Table 5.3). Neutral and acidic EC were much lower than calcareous ($p = 0.007$), whereas calcareous and neutral redox potentials were greater than acidic ($p < 0.001$). Moisture content was lowest in neutral soils and higher in acidic and calcareous (Table 5.3) ($p = 0.044$). Organic matter was the highest in acidic and calcareous soils and much lower in neutral ($p < 0.001$). C%, N% and H% were all highest in calcareous and acidic soils and much lower in neutral (Table 5.3; $p < 0.001$).

Available P was consistently lower in acidic soils, regardless of P extraction used (Table 5.4) ($p < 0.001$). Higher P concentrations were extracted from calcareous soils than neutral when NH_4 was used, whereas values were similar when water extractions were conducted (Table 5.4). Available Ca and Mg were highest in calcareous soils, followed by neutral and acidic for both NH_4 and H_2O extractions (Table 5.4). Water extractable Fe was highest in neutral soils, followed by calcareous and acidic (Table 5.4) ($p<0.001$). NH_4 extractable Fe however was highest in acidic followed by calcareous and then neutral which showed 0 µg kg^{-1}($p<0.001$). Available Sr was highest in neutral and calcareous and lowest in acid for both NH_4 and H_2O extractions (Table 5.4). Water available Al was highest in neutral followed by acidic and calcareous ($p<0.001$), whereas NH_4 extractable Al was highest in acidic soils followed by calcareous and neutral ($p<0.001$). Water available Mn was highest in neutral and calcareous, whereas NH_4 available is highest in acidic (Table 5.4).

Table 5.3. The characteristics of soils used throughout the soil-biochar incubation experiment. Data are means ± SE. Treatments similarly superscripted are not significantly different (Tukey's multiple comparison test). MC denotes moisture content and OM shows organic matter. pH ($p<0.001$), EC ($p= 0.007$), redox ($p<0.001$), MC ($p= 0.044$), OM ($p<0.001$), C% ($p<0.001$), N% ($p<0.001$) and H% ($p=0.004$) all differ between soil type. Significant differences are symbolised by different superscripted lettering.

Soil Type	**pH**	**EC**	**Redox**	**MC (%)**	**OM (%)**	**C (%)**	**N (%)**	**H (%)**
Calcareous	7.51 ± 0.17^{a}	146 ± 23.5^{a}	6.81 ± 0.13^{a}	19.9 ± 3.84^{a}	10.4 ± 0.15^{a}	5.41 ± 0.18^{a}	0.36 ± 0.02^{a}	0.55 ± 0.06^{a}
Neutral	6.81 ± 0.02^{b}	45.8 ± 0.59^{b}	6.51 ± 0.05^{a}	7.29 ± 0.24^{b}	3.85 ± 0.13^{b}	1.37 ± 0.05^{b}	0.12 ± 0.00^{b}	0.21 ± 0.02^{b}
Acidic	3.16 ± 0.04^{c}	41.0 ± 0.87^{b}	5.13 ± 0.07^{b}	15.0 ± 0.20^{ab}	10.9 ± 0.23^{a}	5.04 ± 0.31^{a}	0.33 ± 0.02^{a}	0.55 ± 0.03^{a}

Table 5.4. The elements most likely to interact with P within the soils used throughout the soil-biochar incubation experiment. Data are means ± SE. P ($p<0.001$), Ca (H_2O p= 0.0071; NH_4 $p<0.001$), Fe ($p< 0.001$), Sr (H_2O p=0.001; NH_4 $p<0.001$), Al ($p<0.001$) and Mn (H_2O p=0.001; NH_4 $p<0.001$) all differ between soil type, regardless of extraction technique used. Treatments similarly superscripted are not significantly different (Tukey's multiple comparison test).

Soil Type	**Extraction**	**P (mg kg^{-1})**	**Ca (mg kg^{-1})**	**Mg (mg kg^{-1})**	**Fe (µg kg^{-1})**	**Sr (µg kg^{-1})**	**Al (µg kg^{-1})**	**Mn (µg kg^{-1})**
Calcareous	Ammonium Nitrate	5.38 ± 0.02^a	827 ± 19.82^a	163.3 ± 4.45^b	315 ± 6.76^b	1070 ± 21.5^a	121 ± 63.4^b	63.3 ± 9.91^b
	Water Available	4.32 ± 0.14^b	17.9 ± 1.65^a	8.60 ± 0.58^a	2600 ± 51.7^c	18.6 ± 2.03^a	2410 ± 68.8^b	69.5 ± 0.36^b
Neutral	Ammonium Nitrate	4.26 ± 0.06^b	364 ± 21.96^b	52.9 ± 3.45^c	0.00^c	919 ± 62.9^a	99.9 ±7 .64^b	93.2 ± 2.62^b
	Water Available	4.69 ± 0.26^b	8.91 ± 0.13^b	4.85 ± 0.27^b	9910 ± 9967^b	21.0 ± 0.62^a	11200 ± 456^a	79.4 ± 11. 06^a
Acidic	Ammonium Nitrate	0.63 ± 0.18^c	161.5 ± 8.33^c	35.3 ± 1.71^c	776 ± 25.81^a	539 ± 28.5^b	34600 ±958^a	1100 ± 74.6^a
	Water Available	0.20 ± 0.05^c	1.56 ± 0.07^c	1.22 ± 0.04^c	2580 ± 224^c	6.83 ± 0.25^b	2860 ± 242^b	7.35 ± 1.17^b

5.3.2 Phosphorus Availability

Total P within systems varied according to soil-char treatment ($p<0.001$), however remained constant over time (Figure 5.1a-c) ($p= 0.108$). Total P was highest in calcareous systems followed by neutral and acid, regardless of char added. The addition of coffee char increased the total P of all soils (Figure 5.1 a-c). GSW char increased the total P in neutral soils (Figure 5.1b), however calcareous and acidic total P remained the same. HW did not appear to alter total P in any of the three soils (Figure 5.1).

Ammonium nitrate (NH_4) extractable P varied between systems ($p<0.001$) and remained constant over time (Figure 5.2) ($p=0.983$). GSW and coffee chars increased the NH_4 extractable P in neutral and calcareous systems with GSW contributing the most in neutral and GSW and coffee contributing similar amounts in calcareous systems. HW char did not influence NH_4 extractable P in any of the soil systems (Figure 5.2). Neutral soil treated with GSW char demonstrated the highest NH_4 extractable P and all acidic soil treatments had the lowest concentration of available P (Figure 5.2).

P available through Olsen P increased in the presence of coffee and GSW chars ($p< 0.001$) and was not influenced by time (Figure 5.3) ($p= 0.775$). The increase in Olsen P was highest in neutral systems containing GSW followed by neutral systems containing coffee chars (Figure 5.3). The increase Olsen P availability in calcareous soils containing GSW and coffee chars was apparent, however not as great as observed in neutral systems. HW char did not increase the Olsen P extracted in either calcareous or neutral soils (Figure 5.3).

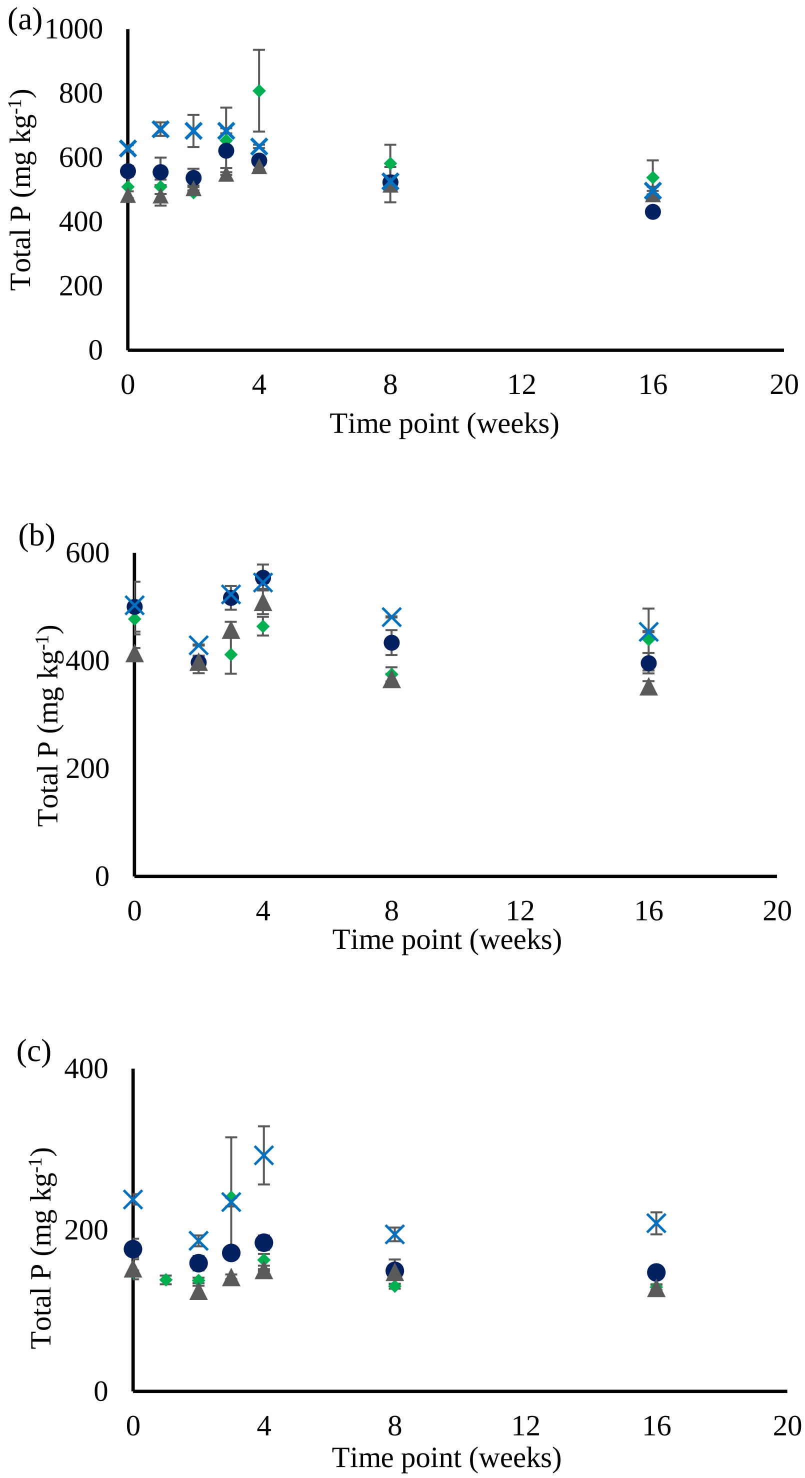

Figure 5.1. Total P within soils (diamonds) with amendments of GSW (circles), HW (triangles) and coffee char (crosses) over time (a) calcareous systems, (b) neutral systems and (c) acidic systems. Data are means ± SE. Total P varied between systems ($p<0.001$) but did not alter over time ($p=0.108$) Note the different scale presented on the y axis.

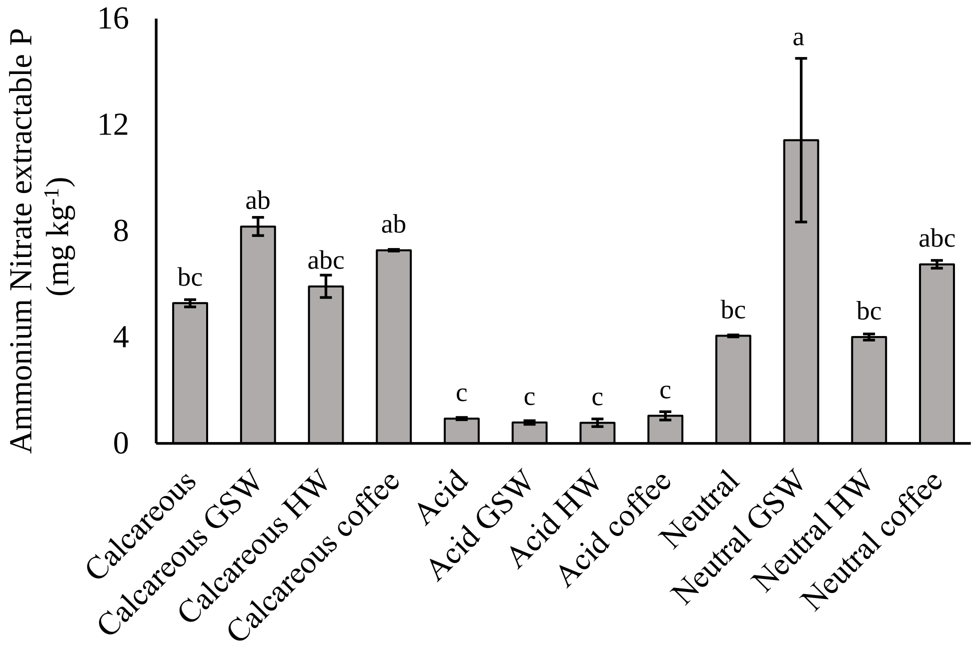

Figure5.2. Ammonium Nitrate extractable P within soils with amendments of GSW, HW and coffee char in calcareous systems, neutral and acidic systems after 4 weeks of incubation. Data are means ± SE. Treatments similarly superscripted are not significantly different (Tukey's multiple comparison test).. The NH_4 extractable P within systems does not change over time ($p=0.983$) therefore only one time point is displayed here for clarity however increase in most treatments.

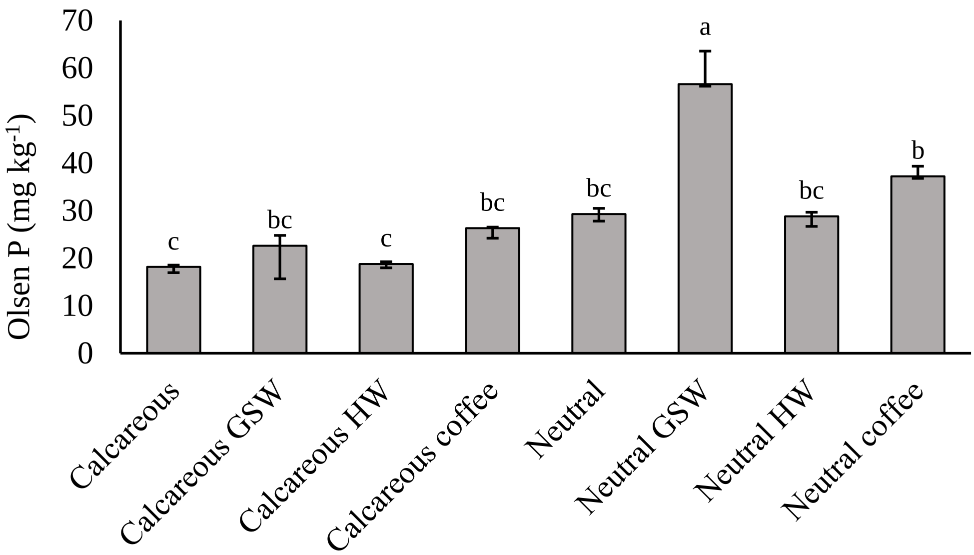

Figure 5.3. Olsen P extractable P within soils with amendments of GSW, HW and coffee char in calcareous and neutral systems after 4 weeks of Treatments similarly superscripted are not significantly different (Tukey's multiple comparison test). similarly superscripted are not significantly different. The Olsen P within systems does not change over time ($p= 0.775$), therefore only one time point is displayed here for clarity. Extractable P *via* Olsen P was higher in most treatments containing char ($p<0.001$) Olsen P does not effectively predict acidic soil P levels, therefore modified Morgan's was also conducted. Different lettering indicates significant difference between treatments.

Olsen P was ineffective on acid soils due to the low available P meaning the stronger extraction method of modified Morgan's was used. The Morgan's extractable P varied between treatment ($p < 0.001$) and increases over time (Figure 5.4 a-c) ($p<0.001$). GSW and coffee char increased the P availability when Morgan's modified extractions were conducted in calcareous and neutral systems at most time points (Figure 5.4 a & b). GSW addition results in the greatest increase in Morgan's modified available P in neutral systems (Figure 5.4b), where coffee char has a greater impact in calcareous systems (Figure 5.4a), with the exception of week 8 and 16. All three chars increased P availability in acidic soils to a similar level (Figure 5.4c).

Water available P varies between treatments ($p < 0.001$) and is not influenced by time in calcareous HW, Neutral HW, acid GSW, acid coffee, neutral soils and calcareous soils (Figure 5.5 a- c). Regardless of time, coffee and GSW char addition increased water extractable P in all soil systems. Coffee char caused the greatest increase in water available P in acidic systems (Figure 5.5 c), whereas GSW addition resulted in the highest available P in neutral systems (Figure 5.5 b). In calcareous systems, GSW and coffee additions resulted in similar amounts of water extractable P which remained higher than systems with HW or no char (Figure 5.5 a). HW char did not increase water available P in any soil system and at some points decreased availability (Figure 5.5 a- c).

Acid soils had lower P availability through all extraction methods, in both the absence and presence of biochar, whereas neutral and calcareous available P increased when GSW and coffee char were added. Neutral soils, with GSW and coffee chars, displayed the highest P availability throughout extractions, in spite of calcareous containing the highest total P (Figure 5.1 a-c).

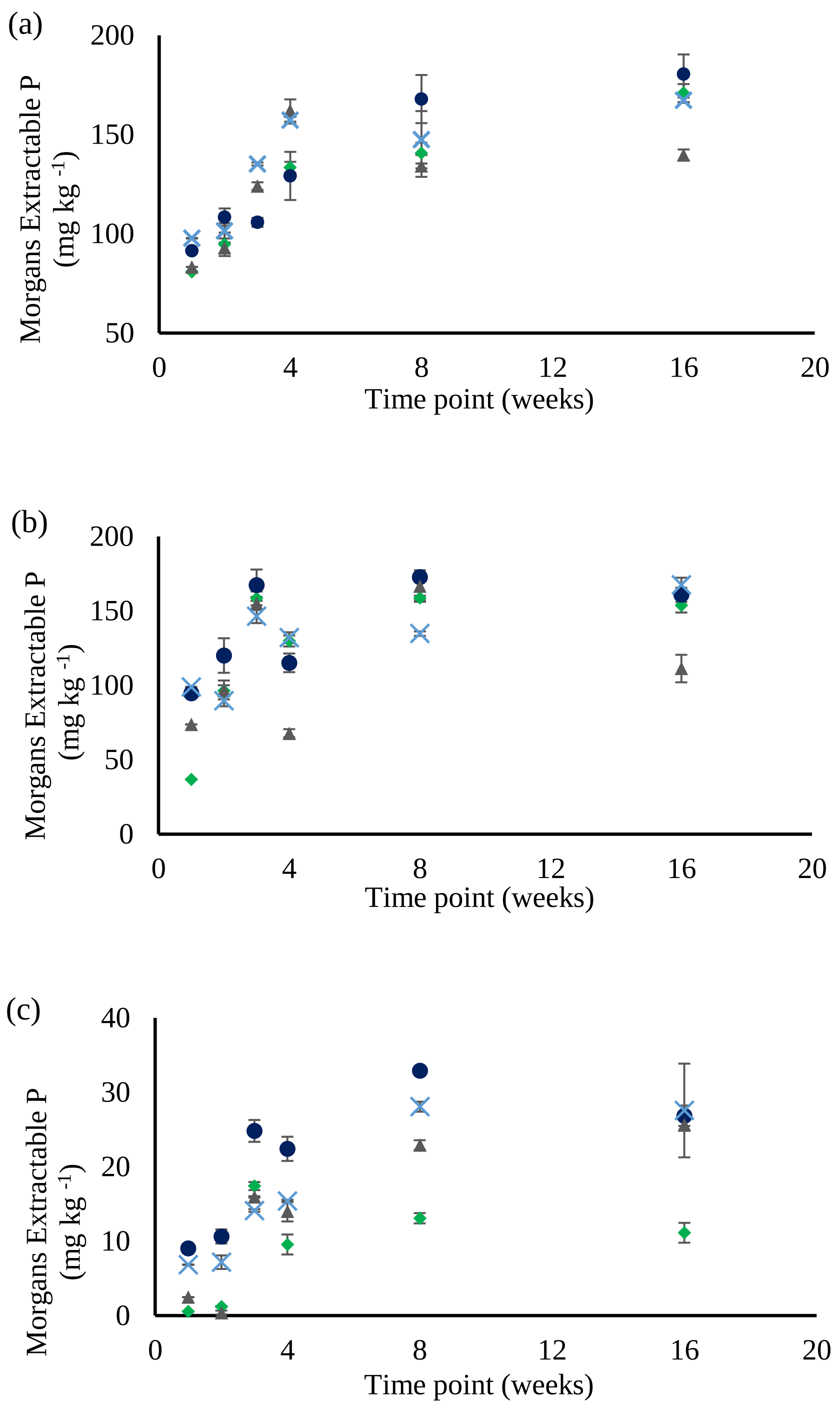

Figure 5.4. Modified Morgan's extractable P within soils (green diamonds) with amendments of GSW (circles), HW (triangles) and coffee char (crosses) over time in (a) calcareous (b) neutral and (c) acidic systems. The modified Morgan's extractable P within systems increases over time ($p<0.001$), and plateaus. Extractable P varies between soil-char systems ($p<0.001$).

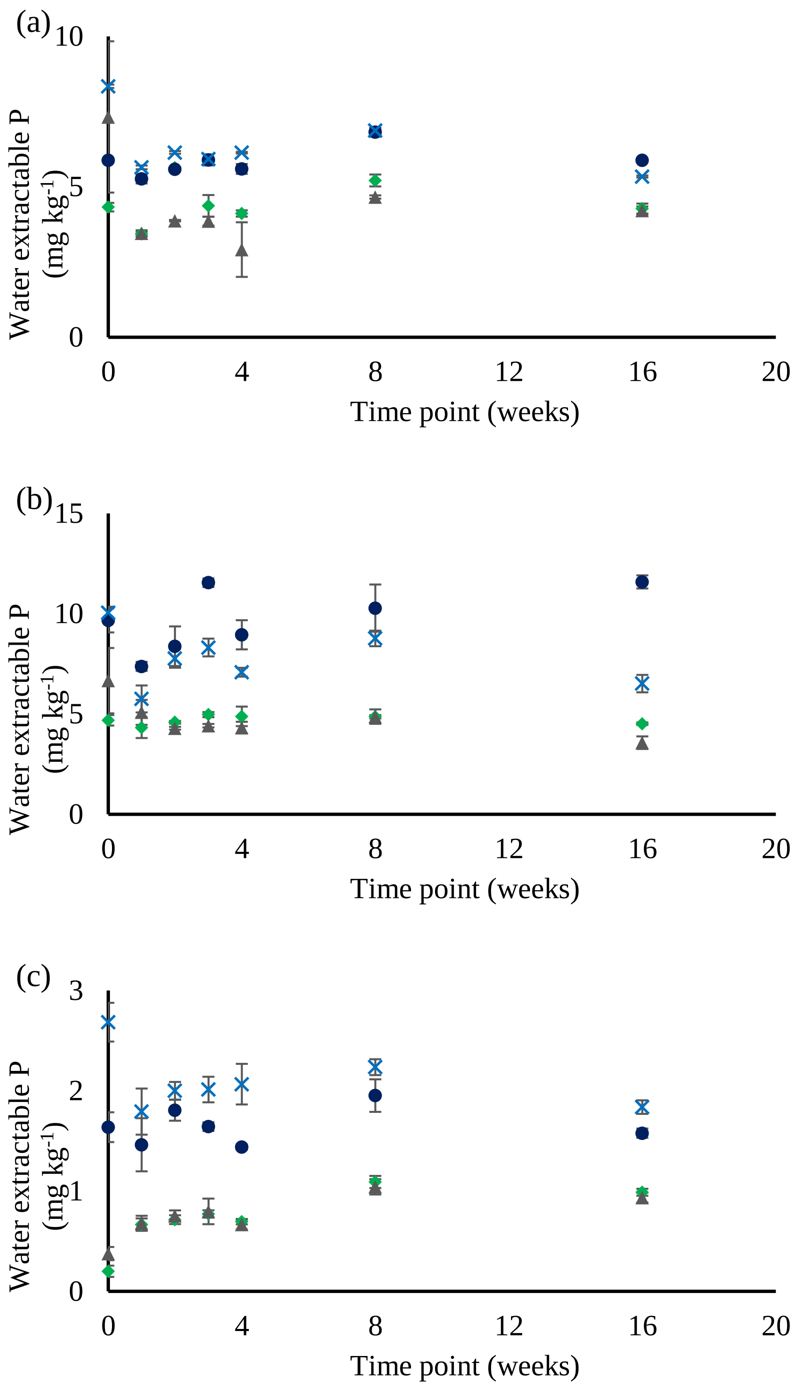

Figure 5.5. Water extractable P within soils (diamond) with amendments of GSW (circles), HW (triangles) and coffee char (crosses) over time (a) calcareous systems (b) neutral systems and (c) acidic systems. The water extractable P changes over time in all systems but calcareous HW, Neutral HW, Acid GSW, Acid coffee, Neutral and calcareous soils. Treatments containing GSW and coffee char have higher water extractable P ($p<0.001$).

5.3.3 Phosphorus Speciation

The pH of a system influences the speciation and precipitates of P that are able to form. Low pH was observed in all acidic soil treatments and higher pH was seen in neutral and calcareous treatments (Table 5.5). The presence of char increased pH in all three soil types (Table 5.5).

Table 5.5. The pH of all soil-char treatments when set up. Char amendment increases system pH ($p < 0.001$). Treatments similarly superscripted are not significantly different (Tukey's multiple comparison test).

Treatment	pH
Calcareous soil	6.53 ± 0.31^{cd}
Calcareous GSW	8.89 ± 0.04^{a}
Calcareous HW	7.81 ± 0.00^{abc}
Calcareous Coffee	8.04 ± 0.11^{abc}
Acid soil	4.63 ± 0.01^{e}
Acid GSW	$6.39.11^{dc}$
Acid HW	5.24 ± 0.51^{de}
Acid Coffee	5.17 ± 0.07^{de}
Neutral soil	6.75 ± 0.14^{bcd}
Neutral GSW	8.96 ± 0.43^{a}
Neutral HW	8.45 ± 0.55^{ab}
Neutral Coffee	8.04 ± 0.05^{abc}

Stability diagrams for MgP, SrP, Fe(II)P and Fe(III)P complexes showed all soil char incubation treatments have different Mg, Sr, Fe(II), Fe (III) and P potential (Figure 5.6 a-d) ($p<0.001$). All treatments within the incubation experiment were under-saturated with respect to MgP, SrP, Fe (II) P and Fe (III) P, regardless of incubation time and char added (Figure 5.6 a-d).

Stability diagrams for possible CaP complexes showed incubation treatment influenced lime and P potential (Figure 5.7 a & b) ($p<0.001$). Lime and P potential were lower at week 0 than any other sampling points suggesting solubility changes over time ($p<0.001$) (Figure 5.7 a). All acidic soil systems remained under-saturated, regardless of char addition and time point. All calcareous systems and neutral systems containing coffee and GSW chars sit above the HA line after 16 weeks of incubation suggesting potential saturation and precipitation occurred (Figure 5.7 b). Neutral soils alone and in the presence of HW char, moved closer to the HA line over time, however do not show saturation (Figure 5.7b).

Stability diagrams for possible MnP complexes also showed incubation treatment influenced Mn and P potential (Figure 5.8) ($p<0.001$). As for lime potential, Mn and P potential were lower at week 0 than any other sampling points ($p<0.001$) (Figure 5.8a). All acidic and calcareous soil systems remained under-saturated, regardless of char addition and time point (Figure 5.8). In all neutral systems chars sit on or above the $MnHPO_4$ line after 16 weeks of incubation suggesting potential saturation (Figure 5.8b).

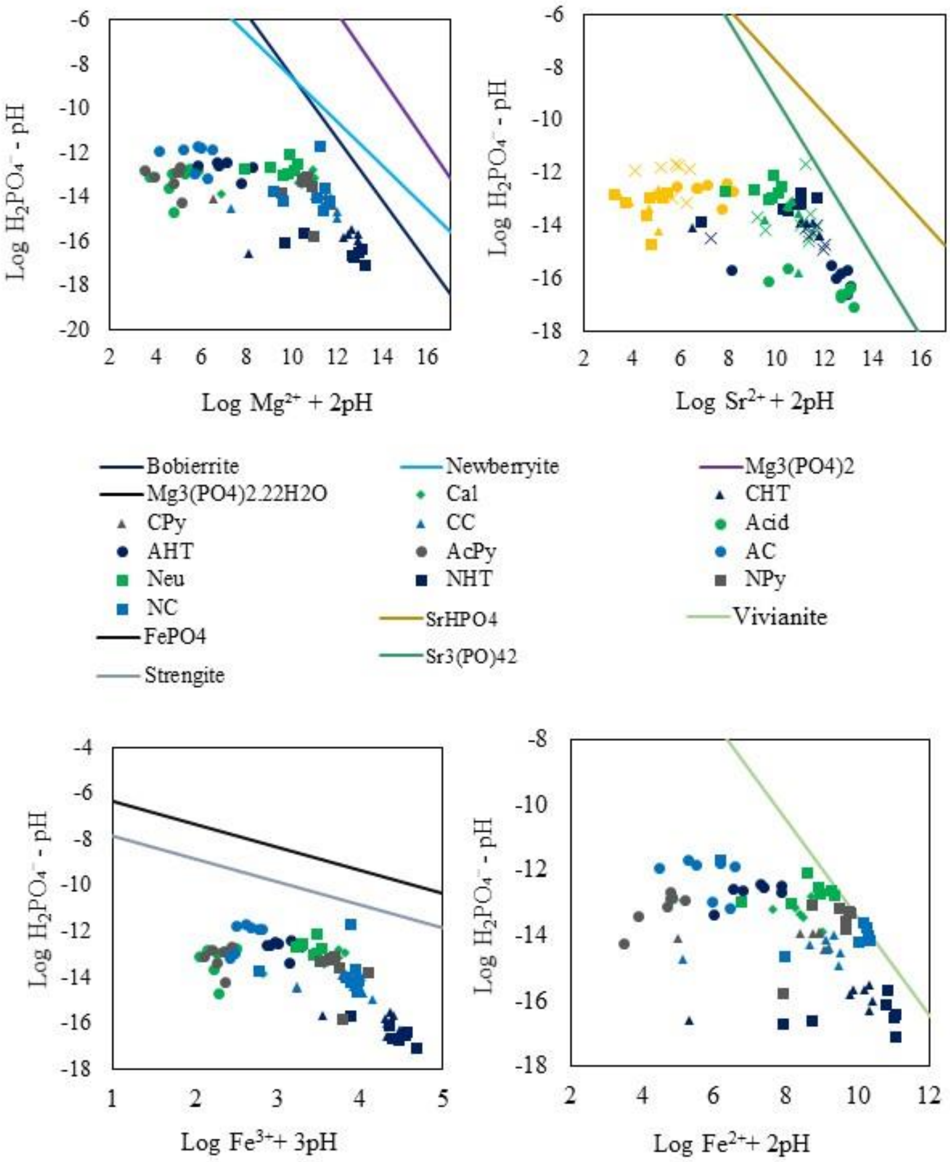

Figure 5.6. Stability diagrams for (a) Mg, (b) Sr, (c) Fe (III) and (d) Fe (II) phosphate complexes using water extractable ICP-MS data at all time points. Cal- calcareous soils, CGSW- calcareous and GSW char, CHW- calcareous and HW char, CC- calcareous and coffee char, Acid- Acidic soil, AGSW- acidic and GSW char, AcHW- Acidic and HW char, AC- acidic and coffee char, Neu- Neutral soil, NGSW- neutral and GSW char, NHW- neutral and HW char and NC- Neutral and coffee char. Data are means and SE is omitted for clarity. The Mg, Sr, Fe(III) and Fe (II) phosphate double function plots showed the solubility of possible P complexes in chars in relation to the crystalline Mg, Sr and Fe-P: bobierrite, newberyite, $Mg_3(PO_4)_2$, $Mg_3(PO_4)_2.22H_2O$, $FePO_4$, strengite, $SrHPO_4$, $Sr_3(PO)_{42}$ and vivianate represented by solid lines. Equilibrium lines for the mineral phases were calculated based on the log K_{sp} values reported by Lindsay (1979) and Reddy et al (1989). The points at which the lines overlap indicate coexistence of the solid phase. All treatments have a different Mg ($p<0.001$), P ($p<0.001$), Sr ($p<0.001$), Fe (II) and (III) potential ($p<0.001$).

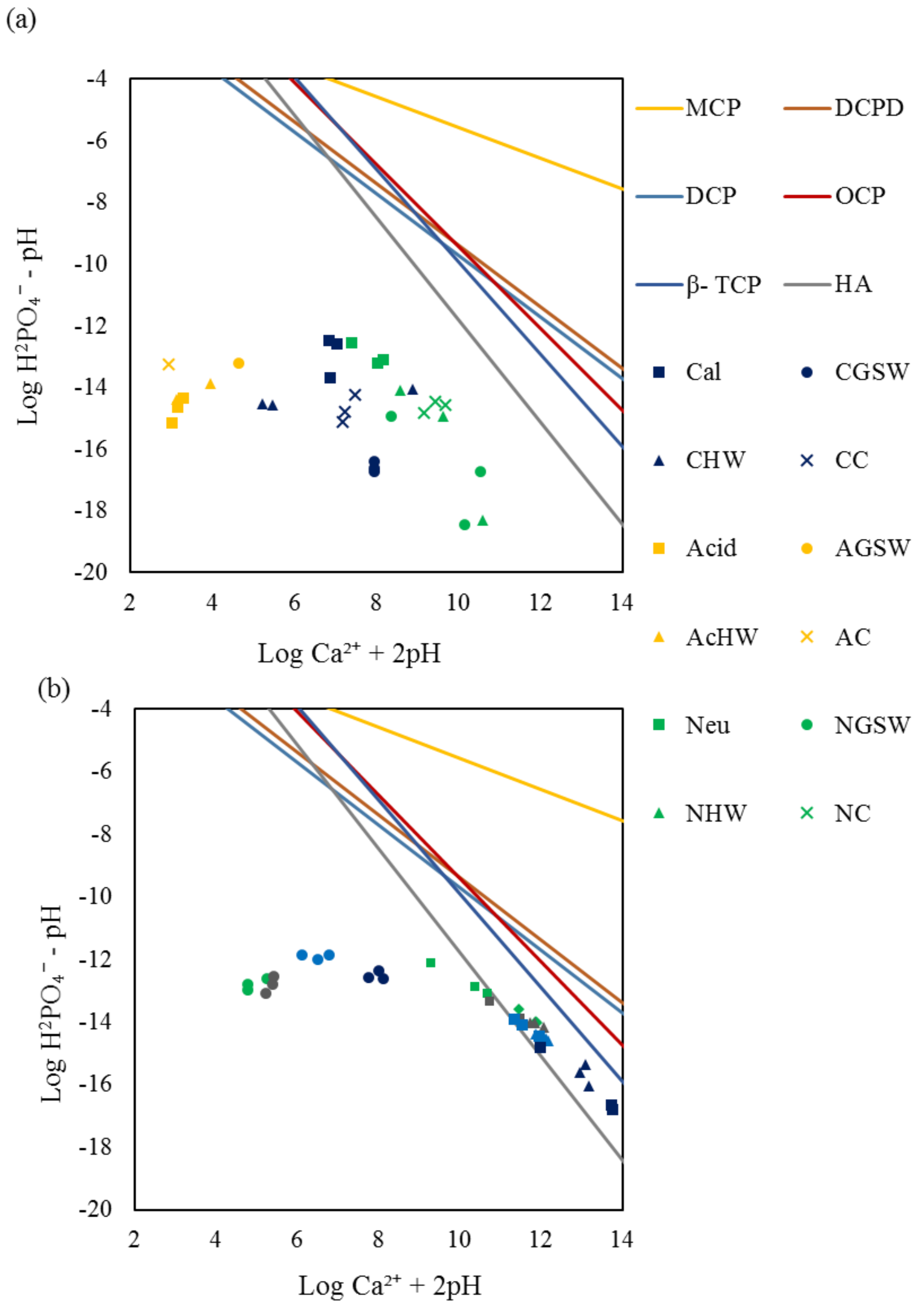

Figure 5.7. Stability diagrams for calcium phosphate complexes using water extractable ICP-MS data after (a) 0 and (b) 16 week(s) of incubation. Cal- calcareous soils, CGSW- calcareous and GSW char, CHW- calcareous and HW char, CC- calcareous and coffee char, Acid- Acidic soil, AGSW- acidic and GSW char, AcHW- Acidic and HW char, AC- acidic and coffee char, Neu- Neutral soil, NGSW- neutral and GSW char, NHW- neutral and HW char and NC- Neutral and coffee char. Data are means and SE is omitted for clarity. The Ca phosphate double function plots showed the solubility of Ca-P complexes in chars in relation to the crystalline Ca-P: monocalcium phosphate (MCP), brushite (DCPD), dicalcium phosphate (DCP), octacalcium phosphate (OCP), β-tricalcium phosphate (TCP) and hydroxyapatite (HA) represented by solid lines. Equilibrium lines for the mineral phases were calculated based on the log K_{sp} values reported by Lindsay (1979). The points at which the lines overlap indicate coexistence of the solid phase. Treatment influences lime ($p<0.001$) and P potential ($p< 0.001$) and lime and potential differs from week 0 and the following sampled time points ($p<0.001$).

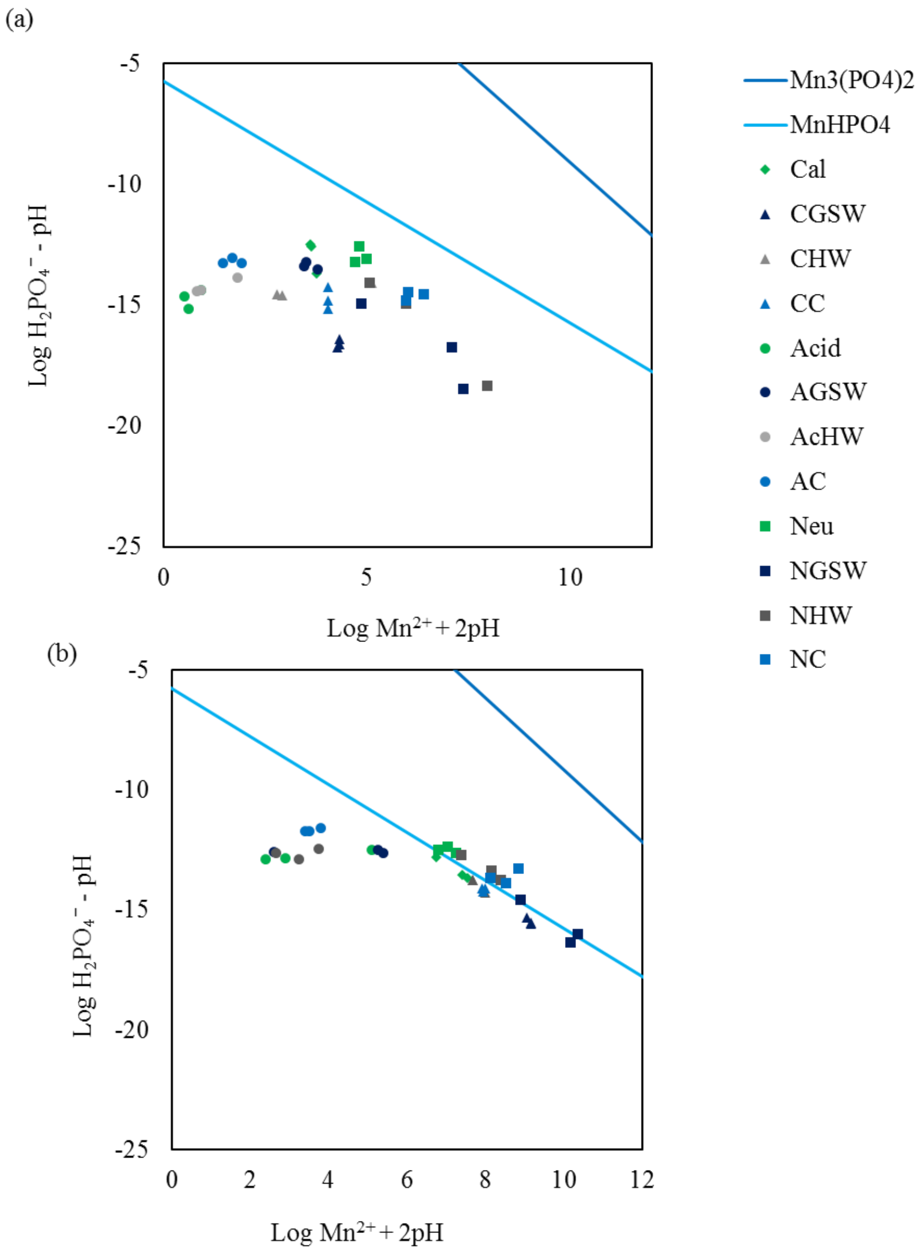

Figure 5.8. Stability diagrams for Mn phosphate complexes using water extractable ICP-MS data after (a) 0 and (b) 16 week(s) of incubation. Cal- calcareous soils, CGSW- calcareous and GSW char, CHW- calcareous and HW char, CC- calcareous and coffee char, Acid- Acidic soil, AGSW- acidic and GSW char, AcHW- Acidic and HW char, AC- acidic and coffee char, Neu- Neutral soil, NGSW- neutral and GSW char, NHW- neutral and HW char and NC- Neutral and coffee char. Data are means and SE is omitted for clarity. The Mn phosphate double function plots show the solubility of Mn-P complexes in chars in relation to the crystalline Mn-P: Mn_3PO_4 and $MnHPO_4$ represented by solid lines. Equilibrium lines for the mineral phases were calculated based on the log K_{sp} values reported by Lindsay (1979). The points at which the lines overlap indicate coexistence of the solid phase. Treatment influences Mn ($p<0.001$) and P potential ($p<0.001$) and lime and potential differs from week 0 and the remaining time points ($P<0.001$).

Table 5.6. The $CaHPO_4$ activity (M ×1014) and MnHPO4 (M × 1016) for neutral and calcareous soil- char treatments using water extractable ICP-MS data. Data are means ± S.E. $CaHPO_4$ ($p< 0.001$) and $MnHPO_4$ ($p< 0.001$) activities increase over time within neutral and calcareous systems. $CaHPO_4$ ($p< 0.001$) and $MnHPO_4$ ($p<0.001$) activities vary according to treatment. Treatments similarly superscripted are not significantly different (Tukey's multiple comparison test).

Treatment	Time	$CaHPO_4$ activity (M $\times 10^{-14}$)	$MnHPO_4$ activity (M$\times 10^{-16}$)
Calcareous	Week 0	5470 ± 2070[a]	1810± 646[cd]
	Week 16	23200000± 206000[a]	1620000± 63600[cd]
CGSW	Week 0	7.42± 1.44[cd]	1.19± 0.25[d]
	Week 16	927000± 3130000[cd]	622000± 73200[d]
CHW	Week 0	6690± 5460[b]	789± 641[d]
	Week 16	20500000± 1820000[b]	1600000± 265000[d]
CC	Week 0	22400± 125[bc]	63.2± 30.1[d]
	Week 16	11400000± 538000[bc]	1220000± 126000[d]
Neutral	Week 0	26700± 4680[bc]	20500± 7550[b]
	Week 16	8890000± 1880000[bc]	6500000± 135000[b]
NGSW	Week 0	948± 466[d]	235± 117[d]
	Week 16	3740000± 476000[d]	1190000± 177000[d]
NHW	Week 0	8300 ± 3520[bc]	1430± 547[cd]
	Week 16	9880000± 1310000[bc]	3250000± 498000[cd]
NC	Week 0	26100 ± 8430[bc]	8400 ± 2830[bc]
	Week 16	8850000± 377000[bc]	3400000± 536000[bc]

The activity of $MnPO_4$ and $CaPO_4$ complexes are influenced by time (Table 5.6) ($p<0.001$) and soil-char treatment ($p<0.001$). Sampling at week 0 showed lower $MnHPO_4$ and $CaHPO_4$ activity concentrations when compared to the remaining time points (Table 5.6) supporting the formation of CaP and MnP precipitates within the incubation treatments. Acid HW treatments showed the lowest activity of both $CaHPO_4$ and $MnHPO_4$, which is expected due to the under-saturation presented by the stability diagrams (Figure 5.7**;** Figure 5.8). Calcareous showed the highest $CaHPO_4$ and neutral the highest $MnHPO_4$ (Table 5.6). $CaHPO_4$ activities (Table 5.6) were higher in treatments which demonstrated a lower P availability (Figure 5.5). $MnHPO_4$ activity did not differ in calcareous soils as expected due to the under-saturation presented (Figure 5.8), whereas differences were noticed between the neutral treatments (Figure 5.8). The differences in $MnHPO_4$ activity, however, did not appear to relate to P availability (Figure 5.5) as NHW treatments which display saturation (Figure 5.8) demonstrate lower $MnHPO_4$ activity than NC (Table 5.6).

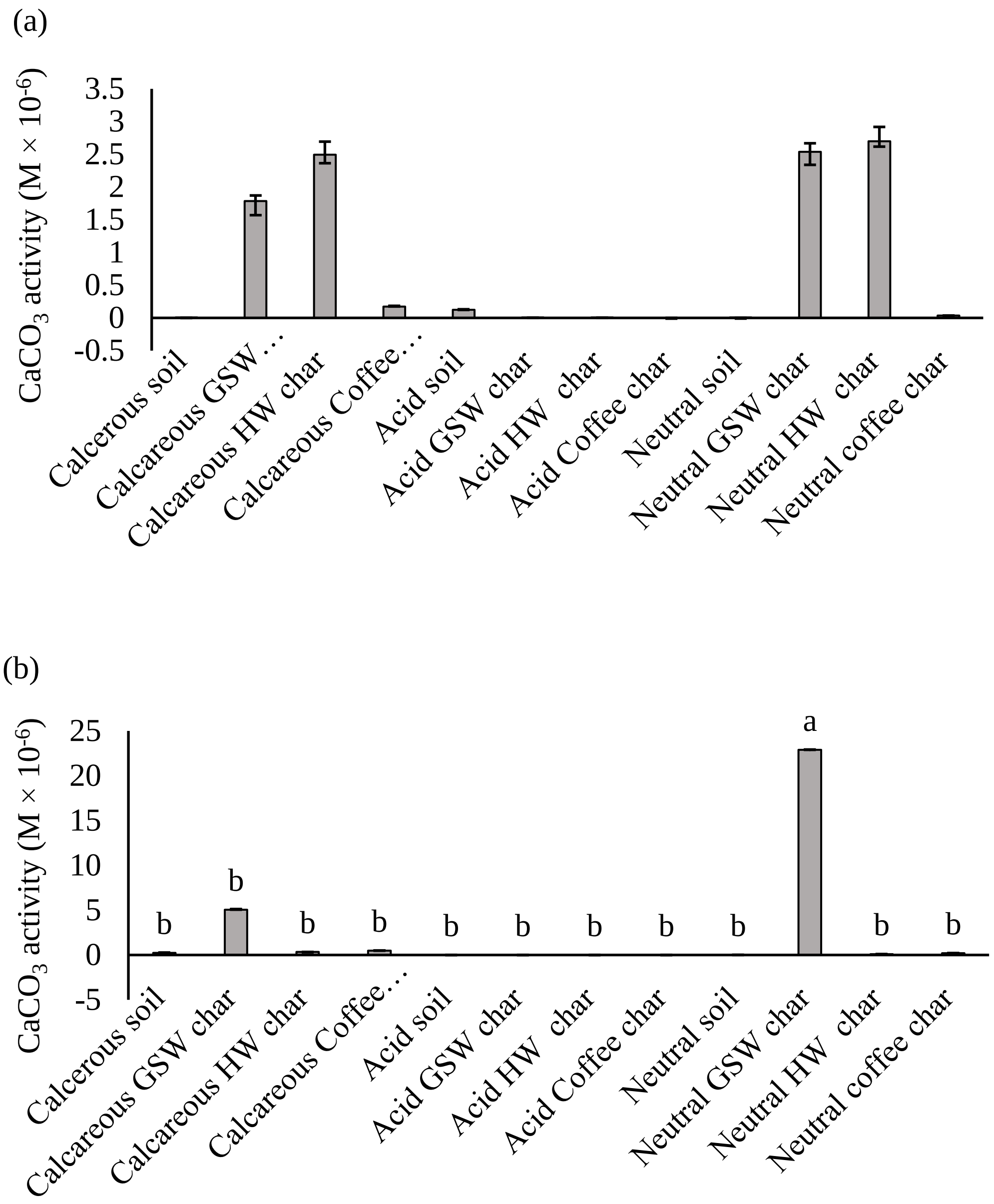

Figure 5.9. $CaCO_3$ activity in each soil treatment at (a) week 0 and (b) week 16. $CaCO_3$ is higher where GSW and HW char is added at week 0 but not significantly. Neutral systems with GSW addition show higher activity at week 16 ($p<0.001$). Data are means ± S.E. Treatments similarly superscripted are not significantly different (Tukey's multiple comparison test).

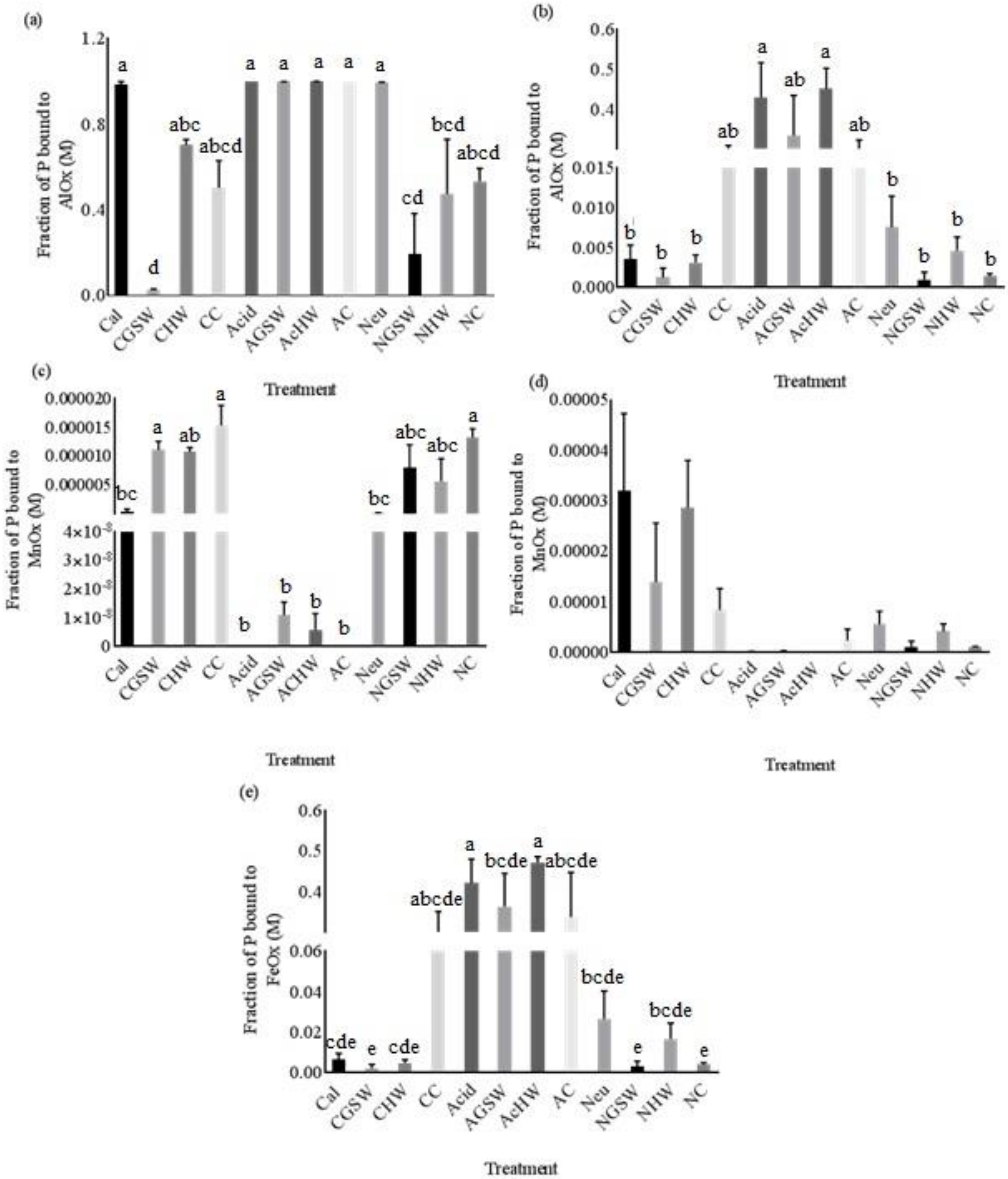

Figure 5.10. The fraction of P bound to Al oxides, (a) week 0 (b) week 16, Mn oxides (c) week 0 (d) week 16 and Fe oxides of (f) week 16 soils with and without char amendment. Fe is only show for week 16 as at week 0, 0 bound P is observed. Data are means ± S.E. Treatments similarly superscripted are not significantly different (Tukey's multiple comparison test). P bound to Fe and Al oxides was influenced by time ($p<0.001$) and treatment ($p<0.001$). P bound to Mn oxides is influenced by time ($p<0.001$) at week 0 a clear difference between P bound to Mn oxides is observed, however this is not the case after 16 weeks of incubation ($p= 0.15$).

5.3.4 Adsorption of P

$CaCO_3$ binds phosphates within soil systems. The $CaCO_3$ activity did not differ between treatments, apart from neutral GSW systems at week 16 (Figure 5.9 (b), $p<0.001$). $CaCO_3$ activities remained low throughout all treatments (Figure 5.9).

The fraction of P bound to Mn, Al and Fe oxides within soils often has a bearing on the P availability within soils. P bound to both Fe and Al oxides differed between the treatments (Figure 5.10 a, b & f) ($p< 0.001$). P bound to Al decreased over time (Figure 5.10 a & b) ($p <0.001$), where Fe oxide binding increased (Figure 5.10 (f) $p< 0.001$). Acidic treatments tended to have the highest amount of Fe and Al oxide bound P (Figure 5.10 a, b & f). After 16 weeks of incubation, Al oxide bound P was much lower in neutral and calcareous than acidic systems, with the exception of calcareous systems containing coffee char (Figure 5.10 a & b). The highest increase in Fe oxide bound P was noticed in all acidic systems and calcareous systems containing coffee char. The remaining systems maintained low P binding abilities. The P bound to Mn oxides increased over time for all calcareous systems, excluding those containing coffee char, remained constant for acidic systems and reduced slightly for neutral systems (Figure 5.10 c & d). The differences observed between treatments at week 16 however are not significant due to high variation (Figure 5.10 c & d).

5.4 DISCUSSION

5.4.1 Soil Characterisation

Characterisation of the three soils allowed understanding of the potential chemical interactions occurring between soils and chars and the bearing of these interactions on the P availabilities of treatments. Higher EC within soils is associated with improved nutrient solubility and availability (Sparks, 1995) meaning the high EC of calcareous soils may be linked to increased amounts of water-soluble Ca and Mg which will influence available P (Table 5.4). A higher redox potential indicates a reduced soil (Vadas & Sims, 1999), therefore less Al, Fe and Mn oxide activities, as seen for calcareous and neutral soils (Figure 5.10) which also display a higher redox potential.

The elemental compositions of the three soils varied (Table 5.4). Calcareous soils are known to hold high calcium concentrations (Hagin & Hadas, 1962; Tunesi *et al.*, 1999) and acidic soils are often associated with high Al and Fe concentrations (Sparks, 1995), as observed for both water and ammonium extractable methods within the soils meaning the characterisation of the soils complements the literature (Table 5.4). Ammonium nitrate extractions are used to measure the mobile and exchangeable elements within systems, not just the water soluble (Schöning & Brümmer, 2008) showing Ca, Mg and Sr are readily exchangeable in all three soils. Exchangeable Fe, Al and Mn are much higher in acidic systems, likely due to the presence of Mn, Fe and Al oxides within acidic soils (Chintala *et al.*, 2014b; Dari *et al.*, 2016; Qayyum *et al.*, 2015; Slavich *et al.*, 2013; Xu *et al.*, 2014). The solubility of elements within water can be influenced by many geochemical processes such as precipitation- dissolution, sorption-desorption and biological solubilisation (Lindsay, 1979) which become more complex when biochar is added to systems.

5.4.2 Biochar and P Availability

The P availability within biochar-soil systems is influenced by char feedstock, production regime and soil properties (Morales *et al.*, 2013; Tan *et al.*, 2018). The variation in total P and extractable P within the systems (Figure 5.1a-c) highlights the importance of char and soils chemistry and their effects on interactions when considering P availability (Schneider & Haderlein, 2016). Total P will not change in systems where plants are not present due to the lack of uptake (Pierzynski & McDowell, 2005) **(**Figure

5.1a-c) however, changes in soil chemistry will impact P availability. For example, the high total P in calcareous soils when compared to extractable P **(**Figure 5.1a) coupled with high extractable Ca concentrations (Table 5.4) suggests CaP precipitation within calcareous systems is rendering the P unavailable (Liang *et al.*, 2014).

5.4.2.1 *Direct P availability*

Chars have been associated with increased P availability within a wide range of soils (Lehmann *et al.*, 2003; Madiba *et al.*, 2016; Parvage *et al.*, 2013; Slavich *et al.*, 2013; Tryon, 1948; Xu *et al.*, 2014; Zhai *et al.*, 2015; Zhang *et al.*, 2016), as seen when GSW and coffee chars are added to neutral and calcareous soils. The increased P availability in soils after char amendment has been associated with the direct release of P (Atkinson *et al.*, 2010; Biederman & Harpole, 2013; DeLuca *et al.*, 2015; Noyce *et al.*, 2017; Parvage *et al.*, 2013). Chars with higher initial P concentrations are, therefore, associated with increased P availability within soils (Chintala *et al.*, 2014; Madiba *et al.*, 2016; Qayyum *et al.*, 2015) and lower total P systems are linked to reduced P availability (Uchimiya & Hiradate, 2014; Zhang *et al.*, 2016). Coffee char, however, often has the highest addition to P in all soil systems, despite a lower total P than GSW (chapter 2) suggesting the chemistry in which P is bound to char influences availability to a greater extent than total P.

The direct release of P from chars into soils often occurs through ion exchange mechanisms, causing desorption, which vary according to char and soil chemistry (Nelson *et al.*, 2011; Sato & Comerford, 2006; Toor & Bahl, 1999; Xu *et al.*, 2014). The chars contributed to water extractable P in soil systems in the same pattern of water soluble P availability within initial char characterisation studies (Figure 5.5a-c; Chapter 2) meaning P is directly released from the char, saturating P sorption sites on the soil and char rendering more available P within systems (Borggaard *et al.*, 2004; Morales *et al.*, 2013; Sato & Comerford, 2006).

5.4.2.1.1 Char Characteristics and Direct P Availability

P concentration of chars alters with production temperature which therefore influences the direct release of P from char, explaining the differences in P availability observed between char amendments (Noyce *et al.*, 2017; Xu *et al.*, 2013). Production temperatures above 700˚C have been linked to lower P availability (Bruun *et al.*, 2017; DeLuca *et al.*, 2015; Zhang *et al.*, 2016) which could explain the higher P availability in coffee amended soils than GSW in some cases (Figure 5.5 a & b). However, GSW total P concentrations found during characterisation are higher than coffee and HW chars (Chapter 2), suggesting loss of P during production is not the cause. Alternatively, the increased surface area of GSW char (Chapter 2, Section 2.3.4) as a result of surface degradation during heating will act to increase P sorption capacities (Hale *et al.*, 2013; Joseph *et al.*, 2010; Keiluweit *et al.*, 2010; Kizito *et al.*, 2017a; Tan *et al.*, 2018; Trazzi *et al.*, 2016), as observed in previous Chapters 2 and 3, which would remove P from the systems making it less available than systems containing coffee char.

A char's ability to increase P availability within soils has also been positively correlated with higher production temperatures. Below a threshold temperature of 700°C, higher production temperatures are associated with higher available P within char amended soils (Morales *et al.*, 2013). The volatilisation of C during production cleaves the bonds binding P to char prior to P volatilisation, allowing increased P desorption within soils (DeLuca *et al.*, 2015). Furthermore the ash content of chars, which increases in line with production temperature and is highest in GSW char (chapter 2), has been linked to high soluble P concentrations (Glaser *et al.*, 2002; Parvage *et al.*, 2013; Zhai *et al.*, 2015) potentially explaining the high P availability in soils amended with GSW chars.

Biochar feedstock also influences P availability within soils (DeLuca *et al.*, 2015). Feedstock has a clear direct impact on available P, shown by the disparities in total and water soluble P within char characterisation studies and the sorption-desorption differences noticed between different feedstocks (chapter 2 and 3) (Kizito *et al.*, 2017a; Kizito *et al.*, 2017b; Morales *et al.*, 2013). Wood-derived biochars contain a large amount of readily available P (Gundale & DeLuca, 2006), which would explain the increase in P availability when GSW chars are added to soils but suggests HW should release more if a direct contribution was being made. Furthermore, the water soluble P concentrations during characterisation (Chapter 2) were higher in the coffee derived chars than the HW or GSW chars made using wood feedstock, suggesting not all wood derived chars release high amounts of P.

The oxidised negative surface charge associated with biochars influences P availability and alters according to surface functional groups within chars (chapter 4) (Cheng *et al.*, 2006; Cheng *et al.*, 2008b; Liang *et al.*, 2006; Cheng, 2008; Novais *et al.*, 2018; Yuan *et al.*, 2011). The negative surface charge of many chars acts to repel negative phosphate anions (Yao *et al.*, 2011a; Zeng *et al.*, 2013). Oxidised functional groups within chars, which often hold negative charges, however have also been associated with P adsorption *via* anion exchange which would decrease P availability within soils (Chintala *et al.*, 2014b; Sarkhot *et al.*, 2013; Yu *et al.*, 2016). The variability of char characteristics through feedstock and production regime clearly influence the impact on direct P availability when added to soils, however the soils chemistry also needs to be considered.

5.4.2.2 *Indirect P availability*

The complexity of soil systems (Pierzynski & McDowell, 2005) coupled with the diversity of chars means some soil- char combinations retain P and slowly release P indirectly through (Chen *et al.*, 2018a; Hagin & Hadas, 1962; Tunesi *et al.*, 1999) precipitation- dissolution and adsorption- desorption (Chintala *et al.*, 2014b; Dari *et al.*, 2016; Lehmann, 2007; Liang *et al.*, 2014; Schneider & Haderlein, 2016; Von Wandruszka, 2006; Xu *et al.*, 2014). Water soluble P from chars is not always directly available within soils due to the ability of soils to sorb P, as well as chars, meaning less P release in biochar amended soils than expected (Xu *et al.*, 2013). Certain soil and char combinations therefore do not increase soil P availability (Slavich *et al.*, 2013) and retain P within soils (Figure 5.5 c; Figure 5.4 c) (Chintala *et al.*, 2014b; Xu *et al.*, 2014; Zhang *et al.*, 2016). For example, calcareous soils amended with chars have been linked to P retention through precipitation (Von Wandruszka, 2006). Considering the adsorption capacities of the three chars, where GSW char is higher than HW char followed by coffee (chapter 2), it is clear that the ability of chars to retain P within soils is hard to predict as GSW displays both a high P sorption capacity in solution and increased P availability within soils.

5.4.2.2.1 Precipitation and Indirect P availability

The presence of solid phase P within soils, formed through precipitation reactions, reduces P availability (Lindsay, 1979; Reddy *et al.*, 1989). Precipitation reactions of P within soils tends include the cations Al, Fe, Ca and Mg which vary in activity depending on system pH (Mackenzie & Amer, 1964; Ngatia *et al.*, 2017; Pierzynski & McDowell, 2005; Qayyum *et al.*, 2015; Sparks, 1995). Chars have been linked to reduced P availability due to the influence on pH and the desorption of cations which cause P precipitation (DeLuca *et al.*, 2015). The previous sorption studies suggest further cations, such as Sr and Mn could contribute to precipitation within the three chars studied (Chapters 3 and 4).

The altered pH of soils after char addition influences the ability of precipitates to form (Xu *et al.*, 2014). McDowell *et al.* (2002) found CaP precipitation within alkaline soils to limit to Olsen P availability to a greater extent than AlP and FeP in acidic soils, disagreeing with the increased P availability in high pH systems presented here (Figure 5.5 a & b; Figure 5.2; Figure 5.4 a & b), suggesting precipitation is not influencing P availability. The link between increased pH with biochar addition to soils means CaP precipitation is often observed in amended soils (Liang *et al.*, 2014; McDowell *et al.*, 2002; Pierzynski & McDowell, 2005; Qian *et al.*, 2013; Tunesi *et al.*, 1999; Von Wandruszka, 2006; Xu *et al.*, 2014) supporting the observed precipitation from neutral and calcareous systems amended with chars (Figure 5.7b). The high initial Ca concentrations within the calcareous soil followed by the neutral soil supports the formation of precipitates as pH increases **(**Table 5.4**)**. Further, CaP activity within calcareous and neutral systems negatively correlates with P availability (Table 5.6) suggesting CaP precipitation contributes to lower P availabilities within treatments, as seen when comparing HW char to GSW and coffee amendments (Figure 5.5 a-c; Figure 5.4 a-c; Figure 5.7)**.** The change in CaP activity (Table 5.6), however, is not great enough to act as the lone mechanism reducing P availability within neutral and calcareous systems where HW is present. The water soluble P observed (Figure 5.5a & b) also remains fairly stable in spite of increased CaP activity suggesting microbes may be acting to solubilise CaP complexes within the soils (Cross & Schlesinger, 1995; Oberson *et al.*, 1996), especially as high pH systems are associated with readily soluble complexes (Pierzynski & McDowell, 2005).

Soils with a pH below 5.8, as observed for the acid systems, have been found to be under-saturated with respect to any Ca-P minerals **(**Figure 5.7**)** and precipitation with the Al and Fe cations is observed (Pierzynski & McDowell, 2005). Precipitation of P into

AlP and FeP solid phases often explains the low P availability observed within acidic soil systems. (McDowell *et al.*, 2002; Zhai *et al.*, 2015). The Al and Fe activities in acidic soil characterisation are high, however the under saturation of all systems with regard to Fe (II) (III) (Figure 5.6c& d) suggests precipitation is not the main mechanism reducing P availability within acidic soils.

Solid phase manganese phosphate precipitation is evident within soils (Boyle & Lindsay, 1986). Some MnP precipitate forms, such as $MnPO_4 \cdot 1.5H_2O$, are more stable than CaP precipitates, including HA in certain soils therefore understanding the role of MnP precipitation within P availability and cycling is important (Boyle & Lindsay, 1986). Precipitation by Mn is heavily linked to a soils redox potential (Lindsay, 1979) and tends to occur within more reduced environments (Scalenghe *et al.*, 2010). The higher redox in calcareous and neutral soils (Table 5.3), increases ability to become reduced supporting MnP precipitation which is apparent in neutral systems only (Figure 5.8b). The P availability, however did not appear linked to MnP precipitate activity (Figure 5.5; Figure 5.8; Figure 5.4) suggesting different mechanisms, such as adsorption potentially coupled with CaP precipitation, are likely influencing P availability within neutral systems.

Soils with a pH of around 6.5 have been associated with the most available P as the environment is not favourable towards Ca, Al or Fe precipitation (Noyce *et al.*, 2017; Pierzynski & McDowell, 2005). The lower P availability within neutral or calcareous soils without GSW and coffee char amendment suggests precipitation is not the mechanism influencing P availability as precipitation would likely increase after char addition due to the increase in alkalinity associated with chars.

5.4.2.2.2 Adsorption and Indirect P Availability

Chars influence P soil adsorption (Chintala *et al.*, 2014b; Jiang *et al.*, 2015; Madiba *et al.*, 2016; Slavich *et al.*, 2013; Xu *et al.*, 2014; Zhang *et al.*, 2016). Phosphates adsorb to Mn, Al and Fe oxide and hydroxide surfaces within soils (Cross & Schlesinger, 1995; Jiang *et al.*, 2015; Pierzynski & McDowell, 2005; Qayyum *et al.*, 2015; Slavich *et al.*, 2013; Tunesi *et al.*, 1999) often through inner sphere surface complexation which occurs prior to precipitation reactions (Tejedor-Tejedor & Anderson, 1990). Coffee and GSW chars may increase P availability within soils through the inhibition of P sorption to Al and Fe oxides by desorbing P and competing for sorption sites, which is associated with soil-char systems (Cui *et al.*, 2011; Jiang *et al.*, 2015; Zhai *et al.*, 2015).

Acidic soils amended with biochar often demonstrate lower available P due to the higher activity of Mn, Fe and Al oxides (Figure 5.10) causing increased sorption, potentially explaining the lack of effect of char throughout the majority of extractions on acidic systems (Chintala *et al.*, 2014b; Dari *et al.*, 2016; Qayyum *et al.*, 2015; Slavich *et al.*, 2013; Xu *et al.*, 2014), particularly as FTIR found the chars to contain oxidised functional groups (chapter 4). Soil P availability is also influenced by the effect of redox on Mn, Fe and Al oxide adsorbents (Pierzynski & McDowell, 2005). The lower redox potential within acidic soils (Table 5.3) presents an oxidised system, which prevents the reductive dissolution of Mn, Al and Fe oxides, increasing the number of P sorption sites (Figure 5.10) making P less available (Pierzynski & McDowell, 2005; Vadas & Sims, 1999). The increased activity of Al and Fe oxidises within acidic systems supports this, however P availability does not appear to be linked (Figure 5.10 a, b & f). The ability of all three chars to adsorb P via anion exchange with oxygen-containing functional groups (Chapter 4) will further reduce P availability within low P environments and may explain the lack of clear link between Al and Fe oxides. The low P availability within acidic soils

(Figure 5.4c; Figure 5.5c; c) means the sorption sites are not saturated within the soil or on the char meaning chars do not release P into the system.

Calcium carbonate activity has also been widely linked to phosphate sorption in soils and therefore availability within soils (Kumari *et al.*, 2014; Noyce *et al.*, 2017). HW char, which consistently appears to have little effect on P availability, may be sorbing P through the $CaCO_3$ activity (Figure 5.9a). Olsen P is a widely used extractant for P and extracts the P loosely adsorbed to Al and Fe oxides and Ca carbonates (Olsen, 1954; Schoenau & Karamanos, 1993) which explains why Olsen P extractable P is much higher than water extractable within neutral and calcareous soils (Figure 5.3). The lack of effect of Olsen P in acidic soils or HW in neutral and calcareous, however, suggests adsorption by $CaCO_3$ or Al and Fe oxides is not reducing P within these systems (Tunesi *et al.*, 1999) which is supported by the low fractions output by WHAM VII (Figure 5.9; Figure 5.10) and the lack of carbonates identified in FTIR analysis of the chars (Chapter 4).

Available P within soils has also been positively correlated with organic matter content as the dissolved organic matter competes for P sorption sites within soils therefore reducing phosphate P sorption (Hunt *et al.*, 2007; Liu *et al.*, 2018; Von Wandruszka, 2006). Char amendments to soils therefore increase P availability within soils through the addition of organic matter creating competitive sorption (Liang *et al.*, 2014; Schneider & Haderlein, 2016; Sun *et al.*, 2018b). The high organic matter of calcareous soils (Table 5.3), which is further increased by char addition, could therefore be reducing P sorption, increasing P availability, however this does not appear to be the case for acidic soils which also hold a high organic matter percentage. Parvage *et al.* (2013), found the adsorption of P to DOM is not likely the main mechanism for P retention in soils amended with biochar (Liang *et al.*, 2014) suggesting different retention mechanisms may hold a larger impact on available P within soils.

Given the discussion above, the chars functionality coupled with the soils sorption sites likely influences the P availability. The lower functionality of GSW char suggests the sorption seen in previous chapters (Chapter 3 and 4) related to surface area, which will be compromised in a soil environment due to competition with other elements. The increased P availability when GSW chars are added to neutral and calcareous is therefore likely through direct desorption into the soil system (Figure 5.4a- c; Figure 5.5 a-c; Figure 5.3; Figure 5.2). Coffee and HW char, however hold a high presence of hydroxyl and phenolic groups (chapter 4) which result in P adsorption via anion exchange (Chintala *et al.*, 2014b; Sarkhot *et al.*, 2013; Yu *et al.*, 2016), however the water available P in coffee (Chapter 2) is the highest of the chars characterised. The high P solubility in coffee chars allows the contribution of P to the neutral and calcareous soil systems through site saturation (Figure 5.4a &b; Figure 5.5 a &b; Figure5.2; Figure 5.3), in spite of the adsorption interactions likely occurring, however this is not the case for HW char which likely adsorbs more P than desorbed.

5.4.3 Soil Characteristics and P Availability

Both biochar and soil properties (Xu *et al.*, 2014) influence the mechanisms, such as precipitation and adsorption, within the P cycle of soils (DeLuca *et al.*, 2015). Soil type influences P availability more than char in many char amended soil systems (Noyce *et al.*, 2017; Yeboah *et al.*, 2009). A char's ability to improve soil P availability therefore varies between soils, as seen for the GSW and coffee chars where GSW contributes most to neutral soils and coffee to calcareous (Figure 5.5 a & b). The variability in char's ability to increase P relates to the soil characteristics, such as a soils microbiological fauna, texture and chemistry (Jin *et al.*, 2016; Noyce *et al.*, 2017; Sarma *et al.*, 2018; Yeboah *et al.*, 2009). The complex nature of soils suggests further characterisation into biological and physical properties is required to understand the P availability and cycling when char amendments are introduced.

5.4.3.1.1 Soil pH and Direct P Availability

The pH of soil positively correlates with P availability (Murphy & Stevens, 2010; Schneider & Haderlein, 2016; Xu *et al.*, 2013). Increased soil pH, as seen after biochar addition, creates a more negative charge within soil systems causing repulsion of phosphate making it directly available (Murphy & Stevens, 2010; Xu *et al.*, 2014; Xue *et al.*, 2009; Zhang *et al.*, 2009). The higher pH in neutral and calcareous systems, further increased with char amendment (Table 5.5), may therefore explain the increase availability when GSW or coffee chars are added (Figure 5.5 a & b; Figure 5.4 a &b). Acidic soils often demonstrate stronger responses to biochar amendments than alkaline, in terms of increased P availability (Noyce *et al.*, 2017; Xu *et al.*, 2014), likely due to increased pH. However, the acidic systems explored here do not display increased P availability in the presence of char presented (Figure 5.5c; Figure 5.4c), potentially due to the adsorption of P to oxidised functional groups which are not saturated due to low initial soil P levels (Table 5.4) (chapter 4). The high P locked into acidic systems, as seen when comparing total to extractable P (Figure 5.1c), is often through Al, Fe and Mn oxide adsorption (Xu *et al.*, 2014) which may be released over time as an indirect increase in availability.

5.4.3.2 *Soil Biology and P*

Biochar supports the soil microbial ecology which influences available P (Hammer *et al.*, 2014; Lehmann *et al.*, 2011; Madiba *et al.*, 2016; Sarma *et al.*, 2018; Zhai *et al.*, 2015). Microbial biomass increases when biochar is added to a system due to the creation of refuge and habitats, which can act as both an indirect sink and a direct source of P depending on the microbial species present which varies according to char and soil type

(Achat *et al.*, 2010; Madiba *et al.*, 2016; Omil *et al.*, 2013; Sarma *et al.*, 2018; Zhai *et al.*, 2015).The increased habitats will encourage P solubilising micro-organisms, which release hydrolysing enzymes, to flourish increasing the P bioavailability within soils (Lehmann *et al.*, 2011; Madiba *et al.*, 2016; Sarma *et al.*, 2018). For example, biochar micropores support mycorrhizal fungi growth within soils and result in an increase the amount of phyto-available P within soils (Hammer *et al.*, 2014; Madiba *et al.*, 2016).

5.4.3.3 ***Soil Texture and P***

Soils hold different textures which are determined by the size and type of particles making up a soil and include the classifications sandy, clayey and silty (Rowell, 2014). The texture holds bearing on the pore size (Rowell, 2014), which in turn influences the availability of sorption sites, (Horn *et al.*, 1994) impacting the P availability meaning soils of different textures demonstrate variable reactions to biochar amendment (Noyce *et al.*, 2017). Soil texture holds a higher bearing on available P availability than char amendment (Noyce *et al.*, 2017) showing the importance of understanding a soils characteristics and the factors limiting P prior to char amendment. Yeboah *et al.* (2009), for example, found a greater yield improvement on sandy loam soils amended with char compared to a silty loam containing the same char, showing development of the understanding of soil-char-P physiochemical interactions is required prior to recommendation as an amendment.

5.5 CONCLUSIONS AND FUTURE WORK

The general conclusions drawn from this Chapter in relation to the research aims are:

1. The ability of biochar to increase soil P availability, either through direct release or through slow release of retained P, varies according to char production and feedstock and soil properties.
   a. Coffee and GSW char amendments increased P availability within calcareous soils, due to increased direct availability saturating char and soil sorption sites.
   b. The addition of GSW char to neutral soils resulted in the greatest increase in P availability, due to increased direct availability saturating char and soil sorption sites.
   c. Acidic soils showed reduced P availability, regardless of char amendment, due to the presence of Al, Mn and Fe oxides in soils and oxygen-containing functional groups on chars resulting in P adsorption, likely *via* anion exchange.
2. The precipitation of P into calcium phosphates was observed in neutral and calcareous soils, however it did not appear to heavily influence P availability.

The complex nature of soil chemical interactions means further analysis is required to definitively understand the mechanisms impacting the P cycle and availability within the different soils studied. Conducting batch sorption phosphate experiments on the char-soil combinations, as seen in Chapters 3 and 4, would better map the potential chemical interactions influencing the fate of P within the soils. The thermodynamic equations used to assess the solubility of potential precipitates throughout the stability diagrams are not always representative of the whole soil system as many assumptions are made

(Pierzynski & McDowell, 2005). Methodologies addressing the solid forms of P, such as NMR, (Lookman *et al.*, 1997) within both the chars and the soils would better determine if P solubility was being controlled by precipitation.

The vast biological and physical complexities associated with soils are also not addressed within this Chapter. Experiments exploring the soil microbial activity, such as fumigation extractions, would provide an understanding of the biological inputs. Further soil characterisation studies, such as soil texture analysis would allow better understanding of how soil pore size links to P availability. Experiments exploring the impact of char on plant growth and phosphate uptake in relation to biochar amendment in different soils would also provide an idea of the potential biochar has to increase yield and P availabilities within soils.

6 SUMMARY, CONCLUSIONS AND FUTURE WORK

6.1 PROJECT OVERVIEW

The concept of biochar as a soil amendment stems from the presence of charcoal in the extremely fertile '*Terra Preta'* soils of the Amazon. The overarching research aims of the project were to assess the feasibility of biochar to improve soil fertility by exploring the interactions of a range of chars with phosphorus, an essential plant nutrient. The interest in biochar as an accessible, environmentally friendly soil amendment has increased in recent years, however the literature and data relating to chars/P interactions are often contradictory. This project addressed the contradictions by quantifying the impact that nine chars had on phosphorus availability within solutions and soils. Characterisation studies of nine different chars were conducted and the ability of the different chars to adsorb and desorb P from solution were outlined. Once the differences in characteristics and P sorption activities of the chars had been established, more detailed sorption experiments to explore the potential mechanisms resulting in phosphorus adsorption and desorption were conducted. Finally, a long-term soil experiment quantifying P availability within three contrasting soil types amended with one of three chars allowed inference of the impact char has on soil P. The conclusions from the experiments conducted are outlined in Table 6.1 and summarised within this section.

Table 6.1. The research aims and conclusions developed throughout the thesis

Chapter	Research Aims	Conclusions
2.0: Characterisation of nine biochars using different feedstocks and production mechanisms	- Quantify the characteristics of nine different biochars. -Relate the characteristics to production mechanism and feedstock.	- Physical and chemical characteristics are unique to each char, however all chars hold an alkali pH. - Both feedstock and production mechanism influence a char's final characteristics and production temperature influences a greater proportion of the char characteristics tested here.
3.0: Exploring phosphorus adsorption-desorption interactions in nine different biochars	- Quantify the ability of nine chars to sorb P. - Identify the potential mechanisms resulting in P sorption.	- The P sorption ability is unique to each char due to distinct characteristics of the chars. Feedstock appears to influence P sorption to a greater extent. - The data presented here suggests adsorption, as oppose to precipitation, is the main mechanism for P sorption.
4.0: Developing and understanding the mechanisms driving phosphorus adsorption- desorption interactions in three biochars	- Establish the mechanisms causing sorption in GSW, HW and Coffee chars.	- Adsorption, not precipitation, is the driving mechanism of P sorption in all three chars analysed. - Each char absorbs P from solution via different mechanisms due to varied char characteristics.
5.0: Quantifying phosphorus availability of three different soils amended with GSW, HW and coffee biochars	- Characterise and quantify the P availability in three soils with and without biochar amendment.	- The ability of biochar to increase soil P availability varies according to char and soil properties. - Acidic soils display reduced P availability, regardless of char amendment. - The precipitation of P into calcium phosphates is observed in neutral and calcareous soils however does not appear to influence P availability.

6.2 BIOCHAR PHOSPHORUS INTERACTIONS

Each char had unique chemical and physical characteristics and initial feedstock and production regime both appeared to influence a chars final properties (Table 6.1; Figure 6.1). All chars, however, demonstrated a basic pH regardless of feedstock and production regime highlighting the potential for char to improve the fertility of acidic soils (Jeffery *et al.*, 2017). Within the chars explored here, production temperature influenced a greater proportion of characteristics including electrical conductivity, total elemental concentrations, surface area, hydrogen and oxygen content. The variation in electrical conductivity, surface area and elemental concentrations will impact the char's interaction with soil nutrients when added as an amendment, reaffirming the importance of quantifying the impact of production temperature on char characteristics. The variation in properties between chars which were produced at the same temperature, highlights the influence of feedstock on final char characteristics. The combination of feedstock and production temperature had the strongest influence on final char properties as the feedstock stability impacts the ability of production temperature to degrade bonds. Both production temperature and feedstock influenced ash, which impacted pH and labile elemental concentrations, as well as carbon contents and total soluble carbon impacting a char's nutrient availability and carbon sequestration potential, both of which relate the potential role of char within soils. The variation in properties observed as a result of production and feedstock explains the contradictory nature of literature surrounding biochar and phosphorus sorption as different properties will facilitate different sorption mechanisms.

Phosphorus interactions in the nine chars characterised were unique to each char, where some showed high amounts of adsorption and other chars desorbed P which is due to the distinct char properties identified in Chapter 2. The varied P sorption behaviours means certain chars would benefit certain soils. For example, the ability of coffee and bamboo char to desorb P is beneficial to soils deficient in P, whereas adsorption of P by cacao, GSW, and LGSW may facilitate the slow release of P over time as a long-term fertiliser or remove soluble P from the system reducing the loss of P to the environment via leaching. Despite the impact of production temperature on char characteristics (Table 6.1), feedstock influenced the P sorption behaviours of chars to a greater extent, shown by the high P sorption in systems containing Cacao which was produced at the same temperature as coffee which showed only desorption. Where sorption was observed within chars, P uptake was driven by adsorption as oppose to precipitation. The diverse P ad and de-sorption behaviours within the chars investigated here occur as a result of the varied chemical and physical properties governing the potential adsorption processes, however one characteristic alone cannot be designated to an increase or decrease P sorption.

Coffee, GSW and HW chars all showed P sorption *via* adsorption not precipitation, however the adsorption occurred via different mechanisms. The adsorption mechanisms observed differed due to varied char properties such as surface area and functionality. The high surface area observed in GSW, seen as a result of high production temperature, resulted in P adsorption. Inner sphere complexation by anion exchange with surface oxygen containing functional groups, which are influenced by feedstock and production temperature, caused P adsorption in HW, coffee and, in part, GSW char. The reduced functionality therefore lowered anion exchange within GSW char occurs as surface groups are degraded at higher production temperatures confirming the impact of production temperature on P sorption mechanism. The clear impact of varied characteristics on P sorption mechanisms in GSW, HW and coffee char suggest the variation in sorption patterns between the nine chars is influenced by the range of production parameters and feedstock employed and the link between production regime and feedstock on char properties.

The postulated mechanisms of phosphorus sorption for GSW, coffee and HW chars allows inference of the impact likely to be observed in soils. For example, the surface area physi-sorption observed in GSW chars may be limited when chars are added to soils due to the blocking of surface pores by soil colloids, increasing available P in soils. Furthermore, the ability of HW and coffee chars and soils to bind phosphorus via anion exchange with functional groups could result in increased P binding sites within soils, reducing P availability in soils. The potential of P precipitation within soils also needs to be considered. Although precipitation does not drive the phosphorus sorption observed in char- solution combinations, the increased presence of precipitating elements, such as Ca, Mg, Al and Fe, within soils has potential to influence the labile P within a system.

6.3 BIOCHAR PHOSPHORUS INTERACTIONS WITHIN SOIL

The impact of chars on available P in soils varies according to char and soil properties. The influence of char production and feedstock on char characteristics coupled with diverse soil characteristics makes quantifying and mapping P availability within soils complex due to the wide variety of potential interactions. The high total P concentrations within GSW and coffee char facilitates an increased P availability within calcareous soils through direct desorption from the chars, resulting in saturation of the soil and char sorption sites. Increased P availability within neutral soils containing GSW char also occurs as a result of direct desorption, however P availability within neutral soils amended with coffee is lower as not all sorption sites with soils and chars are saturated. The influence of production temperature on a char’s total P and the impact of total P on desorption of P to soils shows the interlinked nature of a chars characteristics and the impact observed within soils. The reduced P availability of acidic soils, even when amended with char, occurs due to the high presence of Al, Fe and Mn oxides within soils and oxygen- containing functional groups within chars. The presence of oxides, which is increased with char addition, facilitates P sorption via anion exchange reducing the amount of available P showing how certain soil and char combinations can act to reduce soil fertility. The disparity in available P between the three soils when the same chars are added highlight how both char and soil properties influence P availability meaning it is integral to clearly understand both soil and char characteristics prior to addition to soils.

The use of char is often observed in tropical regions, as oppose to temperate regions where soils are more fertile and less acidic (Jeffery *et al.*, 2017). The basic pH associated with biochar means it often recommended in tropical low nutrient, acidic soils, however when chars were added to acidic soils there was no increase in P availability, meaning a 'one biochar fits all' approach is not applicable. Improved understanding of how production and feedstock influence char characteristics and the knock-on influence on P availability within soils has the potential to facilitate the production of bespoke biochars catering to a soil's requirements. The wide variety of production techniques and feedstocks currently utilised for biochar production allows the development of diverse char characteristics which suits the concept of designer biochar production. The many other benefits associated with biochar, such as climate change mitigation, microbial habitat provision, increased water holding capacity and carbon sequestration are also influenced by soil and char characteristics reiterating the potential of designing biochars for a specific role. The use of biochar as a soil amendment therefore remains worthwhile exploring within both tropical and temperate regions, however fine-tuning of how the characteristics influence the role of chars within soils is required, particularly as char has demonstrated long term stability within soils.

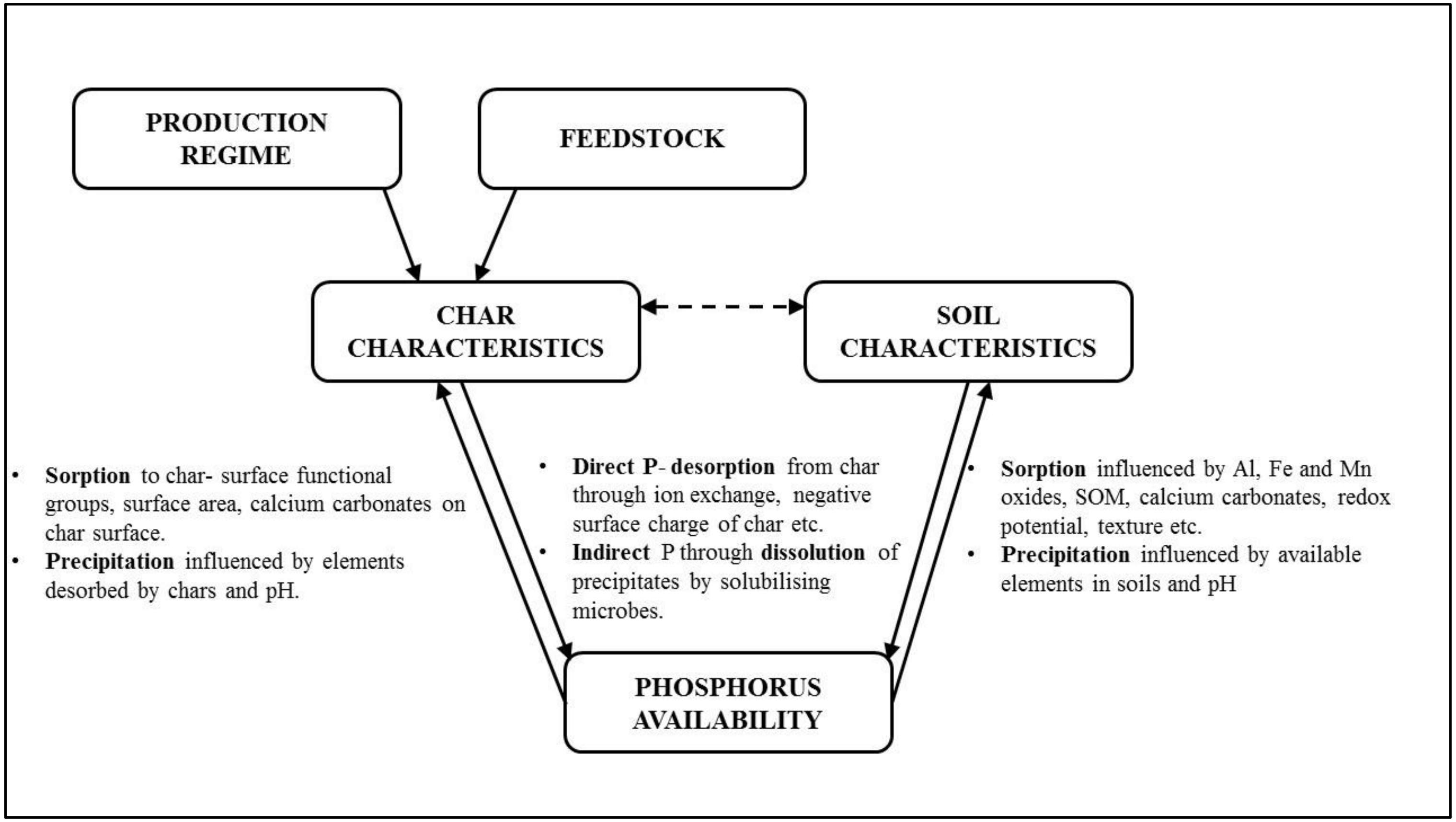

Figure 6.1 Production regime and feedstock influence char characteristics which in turn impact P availability within solution. When char is used as a soil amendment, the soil characteristics also contribute to P solubility showing the complexity of the soil-char system in relation to P availability. The general chemical interactions explored throughout the project are added including: ad- and desorption and precipitation and dissolution, however there are many more contributing reactions relating to phosphorus within soils.

6.4 FUTURE STUDIES

The results and work presented throughout the thesis highlight certain areas in which future work could focus. A study expanding on the chars explored here would conclusively determine the impact of production temperature and feedstock on char characteristics. Creating chars using the same nine initial feedstocks at multiple production temperatures would elucidate the impact of feedstock relative to production temperature on char properties. Quantifying the P sorption abilities and mechanisms of the additional chars would aid in developing the understanding of P char interactions. The varied mechanisms of P adsorption shown by GSW, HW and coffee shows how various chars interact with P differently. Developing the study to a wider variety of chars, produced from common feedstocks but at a variety of temperatures, would aid in elucidating the main characteristics required for P ad- or de-sorption and the production mechanisms and feedstock best suited create a desirable char.

Secondly, developing the understanding of char interactions with soils and the impact on available P is needed. The vast properties of soils impact the ability of chars to increase P availability therefore biological, physical and chemical complexities associated with soils need to be further investigated to definitively understand the mechanisms influencing the P cycle. A study addressing the chemical precipitates present and adsorption for char-P combinations in more detail through the use of NMR and batch sorption studies, respectively, would provide clear information surrounding the potential chemical interactions controlling phosphate availability. Developing the study to consider the presence of microbes and the microbial communities present using fumigation extractions and DNA analysis, respectively, aids in understating the ability of soils, with and without char amendment, to solubilise potential P complexes within the soil. Finally addressing soil characteristics using soil texture analysis techniques would highlight the impact of physical properties on P availability. Such an exhaustive experiment is yet to be conducted within soil char systems and would aid in mapping the influence of char on the soil P cycle.

REFERENCES

Achat, D. L., Morel, C., Bakker, M. R., Augusto, L., Pellerin, S., Gallet-Budynek, A., & Gonzalez, M. (2010). Assessing turnover of microbial biomass phosphorus: Combination of an isotopic dilution method with a mass balance model. *Soil biology and Biochemistry, 42*(12), 2231-2240.

Ahmad, M., Lee, S. S., Dou, X., Mohan, D., Sung, J.-K., Yang, J. E., & Ok, Y. S. 2012). Effects of pyrolysis temperature on soybean stover-and peanut shell-derived biochar properties and tce adsorption in water. *Bioresource Technology, 118*, 536-544.

Ahmad, M., Rajapaksha, A. U., Lim, J. E., Zhang, M., Bolan, N., Mohan, D., Vithanage, M., Lee, S. S., & Ok, Y. S. (2014). Biochar as a sorbent for contaminant management in soil and water: A review. *Chemosphere, 99,* 19-33. doi: 10.1016/j.chemosphere.2013.10.071

Angin, D., Altintig, E., & Kose, T. E. (2013). Influence of process parameters on the surface and chemical properties of activated carbon obtained from biochar by chemical activation. *Bioresource Technology, 148,* 542-549. doi: 10.1016/j.biortech.2013.08.164

Antal, M. J., & Grønli, M. (2003). The art, science, and technology of charcoal production. *Industrial & engineering chemistry research*, *42*(8), 1619-1640.

Atkinson, C. J., Fitzgerald, J. D., & Hipps, N. A. (2010). Potential mechanisms for achieving agricultural benefits from biochar application to temperate soils: A review. *Plant and Soil*, *337*(1-2), 1-18.

Azargohar, R., Nanda, S., Kozinski, J. A., Dalai, A. K., & Sutarto, R. (2014). Effects of temperature on the physicochemical characteristics of fast pyrolysis bio-chars derived from canadian waste biomass. *Fuel, 125,* 90-100.

Basso, A. S., Miguez, F. E., Laird, D. A., Horton, R., & Westgate, M. (2013). Assessing potential of biochar for increasing water - holding capacity of sandy soils. *GCB Bioenergy, 5*(2), 132-143.

Batjes, N. (2011). Global distribution of soil phosphorus retention potential: ISRIC-World Soil Information.

Baulcombe, D., Crute, I., Davies, B., Dunwell, J., Gale, M., Jones, J., Pretty, J., Sutherland, W., & Toulmin, C. (2009). *Reaping the benefits: Science and the sustainable intensification of global agriculture*: The Royal Society.

Biederman, L. A., & Harpole, W. S. (2013). Biochar and its effects on plant productivity and nutrient cycling: A meta - analysis. *GCB Bioenergy, 5*(2), 202-214.

Bird, M. I., Wurster, C. M., de Paula Silva, P. H., Bass, A. M., & De Nys, R. (2011). Algal biochar–production and properties. *Bioresource Technology, 102*(2), 1886-1891.

Biswas, B. K., Inoue, K., Ghimire, K. N., Ohta, S., Harada, H., Ohto, K., & Kawakita, H. (2007). The adsorption of phosphate from an aquatic environment using metal-loaded orange waste. *Journal of Colloid and Interface Science, 312*(2), 214-223.

Borggaard, O. K., Szilas, C., Gimsing, A. L., & Rasmussen, L. H. (2004). Estimation of soil phosphate adsorption capacity by means of a pedotransfer function. *Geoderma, 118*(1-2), 55-61.

Borno, M. L., Muller-Stover, D. S., & Liu, F. L. (2018). Contrasting effects of biochar on phosphorus dynamics and bioavailability in different soil types. *Science of the Total Environment, 627*, 963-974. doi: 10.1016/j.scitotenv.2018.01.283

Boyle, F., & Lindsay, W. (1986). Manganese phosphate equilibrium relationships in soils 1. *Soil Science Society of America Journal, 50*(3), 588-593.

Brewer, C. E., Schmidt - Rohr, K., Satrio, J. A., & Brown, R. C. (2009). Characterization of biochar from fast pyrolysis and gasification systems. *Environmental Progress & Sustainable Energy, 28*(3), 386-396.

Brewer, C. E., Unger, R., Schmidt-Rohr, K., & Brown, R. C. (2011). Criteria to select biochars for field studies based on biochar chemical properties. *Bioenergy Research, 4*(4), 312-323.

Brown, R. A., Kercher, A. K., Nguyen, T. H., Nagle, D. C., & Ball, W. P. (2006). Production and characterization of synthetic wood chars for use as surrogates for natural sorbents. *Organic Geochemistry, 37*(3), 321-333.

Bruun, S., Harmer, S. L., Bekiaris, G., Christel, W., Zuin, L., Hu, Y., Jensen, L. S., & Lombi, E. (2017). The effect of different pyrolysis temperatures on the speciation and availability in soil of p in biochar produced from the solid fraction of manure. *Chemosphere, 169*, 377-386. doi: http://doi.org/10.1016/j.chemosphere.2016.11.058

Buss, W., Kammann, C., & Koyro, H. W. (2012). Biochar reduces copper toxicity in chenopodium quinoa willd. In a sandy soil. *Journal of Environmental Quality, 41*(4), 1157-1165. doi: 10.2134/jeq2011.0022

Cantrell, K. B., Hunt, P. G., Uchimiya, M., Novak, J. M., & Ro, K. S. (2012). Impact of pyrolysis temperature and manure source on physicochemical characteristics of biochar. *Bioresource Technology, 107*, 419-428.

Cao, X., & Harris, W. (2010). Properties of dairy-manure-derived biochar pertinent to its potential use in remediation. *Bioresource Technology, 101*(14), 5222-5228.

Ch'ng, H. Y., Ahmed, O. H., & Majid, N. M. A. (2014). Biochar and compost influence the phosphorus availability, nutrients uptake, and growth of maize (zea mays l.) in tropical acid soil. *Pakistan Journal of Agricultural Sciences, 51*(4), 797-806.

Chan, K. Y., Van Zwieten, L., Meszaros, I., Downie, A., & Joseph, S. (2007). Agronomic values of greenwaste biochar as a soil amendment. *Australian Journal of Soil Research, 45*(8), 629-634. doi: 10.1071/sr07109

Chan, K. Y., & Xu, Z. (2009). Biochar: Nutrient properties and their enhancement. *Biochar for environmental management: Science and technology, 1*, 67-84. .

Cheah, S., Malone, S. C., & Feik, C. J. (2014). Speciation of sulfur in biochar produced from pyrolysis and gasification of oak and corn stover. *Environmental Science & Technology, 48*(15), 8474-8480. doi: 10.1021/es500073r

Chen, H. M., Ma, J. Y., Wei, J. X., Gong, X., Yu, X. C., Guo, H., & Zhao, Y. W. (2018a). Biochar increases plant growth and alters microbial communities via regulating the moisture and temperature of green roof substrates. *Science of the Total Environment, 635*, 333-342. doi: 10.1016/j.scitotenv.2018.04.127

Chen, M., Alim, N., Zhang, Y. T., Xu, N., & Cao, X. D. (2018b). Contrasting effects of biochar nanoparticles on the retention and transport of phosphorus in acidic and alkaline soils. *Environmental Pollution, 239*, 562-570. doi: 10.1016/j.envpol.2018.04.050

Chen, Q. C., Qin, J. L., Cheng, Z. W., Huang, L., Sun, P., Chen, L., & Shen, G. Q. (2018c). Synthesis of a stable magnesium-impregnated biochar and its reduction of phosphorus leaching from soil. *Chemosphere, 199*, 402-408. doi: 10.1016/j.chemosphere.2018.02.058

Chen, X., Chen, G., Chen, L., Chen, Y., Lehmann, J., McBride, M. B., & Hay, A. G. (2011). Adsorption of copper and zinc by biochars produced from pyrolysis of hardwood and corn straw in aqueous solution. *Bioresource Technology, 102*(19), 8877-8884.

Cheng, C.-H., Lehmann, J., Thies, J. E., Burton, S. D., & Engelhard, M. H. (2006). Oxidation of black carbon by biotic and abiotic processes. *Organic Geochemistry, 37*(11), 1477-1488. doi: http://doi.org/10.1016/j.orggeochem.2006.06.022

Cheng, C.-H., Lehmann, J., & Engelhard, M. H. (2008a). Natural oxidation of black carbon in soils: Changes in molecular form and surface charge along a climosequence. *Geochimica et Cosmochimica Acta, 72*(6), 1598-1610.
Cheng, C. H., Lehmann, J., Thies, J. E., & Burton, S. D. (2008b). Stability of black carbon in soils across a climatic gradient. *Journal of Geophysical Research-Biogeosciences, 113*(G2). doi: 10.1029/2007jg000642
Chia, C. H., Downie, A., & Munroe, P. (2015). Characteristics of biochar: Physical and structural properties. *Biochar for Environmental Management: Science and Technology 2nd edn, Earthscan Books Ltd: London*, 89-109.
Chintala, R., Mollinedo, J., Schumacher, T. E., Papiernik, S. K., Malo, D. D., Clay, D. E., Kumar, S., & Gulbrandson, D. W. (2013). Nitrate sorption and desorption in biochars from fast pyrolysis. *Microporous and Mesoporous Materials, 179*, 250-257.
Chintala, R., Mollinedo, J., Schumacher, T. E., Malo, D. D., & Julson, J. L. (2014a). Effect of biochar on chemical properties of acidic soil. *Archives of Agronomy and Soil Science, 60*(3), 393-404.
Chintala, R., Schumacher, T. E., McDonald, L. M., Clay, D. E., Malo, D. D., Papiernik, S. K., Clay, S. A., & Julson, J. L. (2014b). Phosphorus sorption and availability from biochars and soil/biochar mixtures. *Clean-Soil Air Water, 42*(5), 626-634. doi: 10.1002/clen.201300089
Chun, Y., Sheng, G., Chiou, C. T., & Xing, B. (2004). Compositions and sorptive properties of crop residue-derived chars. *Environmental Science & Technology, 38*(17), 4649-4655.
Clarkson, D. T., & Hanson, J. B. (1980). The mineral nutrition of higher plants. *Annual review of plant physiology, 31*(1), 239-298.
Cordell, D., Drangert, J.-O., & White, S. (2009). The story of phosphorus: Global food security and food for thought. *Global environmental change, 19*(2), 292-305.
Cordell, D., Rosemarin, A., Schröder, J. J., & Smit, A. (2011). Towards global phosphorus security: A systems framework for phosphorus recovery and reuse options. *Chemosphere, 84*(6), 747-758.
Crini, G., & Badot, P.-M. (2010). *Sorption processes and pollution: Conventional and non-conventional sorbents for pollutant removal from wastewaters*: Presses Univ. Franche-Comté.
Cross, A., & Sohi, S. P. (2013). A method for screening the relative long‐term stability of biochar. *GCB Bioenergy, 5*(2), 215-220.
Cross, A. F., & Schlesinger, W. H. (1995). A literature review and evaluation of the. Hedley fractionation: Applications to the biogeochemical cycle of soil phosphorus in natural ecosystems. *Geoderma, 64*(3-4), 197-214.
Cui, H. J., Wang, M. K., Fu, M. L., & Ci, E. (2011). Enhancing phosphorus availability in phosphorus-fertilized zones by reducing phosphate adsorbed on ferrihydrite using rice straw-derived biochar. *Journal of Soils and Sediments, 11*(7), 1135-1141. doi: 10.1007/s11368-011-0405-9
Dari, B., Nair, V. D., Harris, W. G., Nair, P., Sollenberger, L., & Mylavarapu, R. (2016). Relative influence of soil-vs. Biochar properties on soil phosphorus retention. *Geoderma, 280*, 82-87.
Deenik, J. L., McClellan, A., & Uehara, G. (2009). *Biochar volatile matter content effects on plant growth and nitrogen transformations in a tropical soil.* Paper presented at the Western Nutrient Management Conference.
Deenik, J. L., McClellan, T., Uehara, G., Antal, M. J., & Campbell, S. (2010). Charcoal volatile matter content influences plant growth and soil nitrogen transformations. *Soil Science Society of America Journal, 74*(4), 1259-1270.

DeLuca, T. H., Gundale, M. J., MacKenzie, M. D., & Jones, D. L. (2015). Biochar effects on soil nutrient transformations. *Biochar for environmental management: science, technology and implementation, 2*, 421-454.
Ding, W. C., Dong, X. L., Ime, I. M., Gao, B., & Ma, L. Q. (2014). Pyrolytic temperatures impact lead sorption mechanisms by bagasse biochars. *Chemosphere, 105*, 68-74. doi: 10.1016/j.chemosphere.2013.12.042
Downie, A., Crosky, A., & Munroe, P. (2009). Physical properties of biochar. *Biochar for environmental management: Science and technology*, 13-32.
EBC. (2012, 19th June 2015,). 'European biochar certificate - guidelines for a sustainable production of
biochar.'. Version 6.1 from http://www.europeanbiochar.org/en/download.
Eberhardt, T. L., Min, S.-H., & Han, J. S. (2006). Phosphate removal by refined aspen wood fiber treated with carboxymethyl cellulose and ferrous chloride. *Bioresource Technology, 97*(18), 2371-2376.
Enders, A., Hanley, K., Whitman, T., Joseph, S., & Lehmann, J. (2012). Characterization of biochars to evaluate recalcitrance and agronomic performance. *Bioresource Technology, 114*, 644-653.
Findlay, S., McDowell, W. H., Fischer, D., Pace, M. L., Caraco, N., Kaushal, S. S., & Weathers, K. C. (2010). Total carbon analysis may overestimate organic carbon content of fresh waters in the presence of high dissolved inorganic carbon. *Limnology and Oceanography: Methods, 8*(5), 196-201.
Fristak, V., Pipiska, M., & Soja, G. (2018). Pyrolysis treatment of sewage sludge: A promising way to produce phosphorus fertilizer. *Journal of Cleaner Production, 172*, 1772-1778. doi: 10.1016/j.jclepro.2017.12.015
Gao, Y., Chen, N., Hu, W., Feng, C., Zhang, B., Ning, Q., & Xu, B. (2013). Phosphate removal from aqueous solution by an effective clay composite material. *Journal of Solution Chemistry, 42*(4), 691-704.
Gaskin, J. W., Steiner, C., Harris, K., Das, K. C., & Bibens, B. (2008). Effect of low-temperature pyrolysis conditions on biochar for agricultural use. *Transactions of the Asabe, 51*(6), 2061-2069.
Glaser, B., Haumaier, L., Guggenberger, G., & Zech, W. (2001). The 'terra preta' phenomenon: A model for sustainable agriculture in the humid tropics. *Naturwissenschaften, 88*(1), 37-41. doi: 10.1007/s001140000193
Glaser, B., Lehmann, J., & Zech, W. (2002). Ameliorating physical and chemical properties of highly weathered soils in the tropics with charcoal - a review. *Biology and Fertility of Soils, 35*(4), 219-230. doi: 10.1007/s00374-002-0466-4
Godfray, H. C. J., Beddington, J. R., Crute, I. R., Haddad, L., Lawrence, D., Muir, J. F., Pretty, J., Robinson, S., Thomas, S. M., & Toulmin, C. (2010). Food security: The challenge of feeding 9 billion people. *Science*, 1185383.
Gray, M., Johnson, M. G., Dragila, M. I., & Kleber, M. (2014). Water uptake in biochars: The roles of porosity and hydrophobicity. *Biomass and bioenergy, 61*, 196-205.
Gul, S., Whalen, J. K., Thomas, B. W., Sachdeva, V., & Deng, H. Y. (2015). Physico-chemical properties and microbial responses in biochar-amended soils: Mechanisms and future directions. *Agriculture Ecosystems & Environment, 206*, 46-59. doi: 10.1016/j.agee.2015.03.015
Gundale, M. J., & DeLuca, T. H. (2006). Temperature and source material influence ecological attributes of ponderosa pine and douglas-fir charcoal. *Forest ecology and management, 231*(1-3), 86-93.
Hagin, J., & Hadas, A. (1962). Solubility of calcium phosphate in calcareous soils. *Nature, 193*, 1211. doi: 10.1038/1931211a0

Hale, S., Alling, V., Martinsen, V., Mulder, J., Breedveld, G., & Cornelissen, G. (2013). The sorption and desorption of phosphate-p, ammonium-n and nitrate-n in cacao shell and corn cob biochars. *Chemosphere, 91*(11), 1612-1619.
Hammer, E. C., Balogh-Brunstad, Z., Jakobsen, I., Olsson, P. A., Stipp, S. L. S., & Rillig, M. C. (2014). A mycorrhizal fungus grows on biochar and captures phosphorus from its surfaces. *Soil Biology & Biochemistry, 77,* 252-260. doi: 10.1016/j.soilbio.2014.06.012
Harrison, R. B., & Adams, F. (1987). Solubility characteristics of residual phosphate in a fertilized and limed ultisol 1. *Soil Science Society of America Journal, 51*(4), 963-969.
Hartemink, A. E. (2007). Soil science, population growth and food production: Some historical developments *Advances in integrated soil fertility management in sub-saharan africa: Challenges and opportunities* (pp. 85-97): Springer.
He, H., Qian, T. T., Liu, W. J., Jiang, H., & Yu, H. Q. (2014). Biological and chemical phosphorus solubilization from pyrolytical biochar in aqueous solution. *Chemosphere, 113,* 175-181. doi: 10.1016/j.chemosphere.2014.05.039
Holford, I., & Mattingly, G. (1975). Phosphate sorption by jurassic oolitic limestones. *Geoderma, 13*(3), 257-264.
Hollister, C. C., Bisogni, J. J., & Lehmann, J. (2013). Ammonium, nitrate, and phosphate sorption to and solute leaching from biochars prepared from corn stover (l.) and oak wood (spp.). *Journal of Environmental Quality, 42*(1), 137-144.
Hong, C., & Lu, S. G. (2018). Does biochar affect the availability and chemical fractionation of phosphate in soils? *Environmental Science and Pollution Research, 25*(9), 8725-8734. doi: 10.1007/s11356-018-1219-8
Horn, R., Taubner, H., Wuttke, M., & Baumgartl, T. (1994). Soil physical properties related to soil structure. *Soil and Tillage Research, 30*(2-4), 187-216.
Hossain, M. K., Strezov, V., Chan, K. Y., Ziolkowski, A., & Nelson, P. F. (2011). Influence of pyrolysis temperature on production and nutrient properties of wastewater sludge biochar. *Journal of Environmental Management, 92*(1), 223-228. doi: 10.1016/j.jenvman.2010.09.008
Hunt, J. F., Ohno, T., He, Z., Honeycutt, C. W., & Dail, D. B. (2007). Inhibition of phosphorus sorption to goethite, gibbsite, and kaolin by fresh and decomposed organic matter. *Biology and Fertility of Soils, 44*(2), 277-288.
IBI. (2012). The international biochar imitative standardized product definition and product testing guidelines for biochar that is used in soil. Final Version Retrieved 15 May 2012, from http://www.biochar-international.org/sites/default/files/Guidelines_for_Biochar_That_Is_Used_in_Soil_Final.pdf.
Jeffery, S., Abalos, D., Prodana, M., Bastos, A. C., Van Groenigen, J. W., Hungate, B. A., & Verheijen, F. (2017). Biochar boosts tropical but not temperate crop yields. *Environmental Research Letters, 12*(5), 053001.
Jeppu, G. P., & Clement, T. P. (2012). A modified langmuir-freundlich isotherm model for simulating ph-dependent adsorption effects. *Journal of contaminant hydrology, 129,* 46-53.
Jiang, J., Yuan, M., Xu, R., & Bish, D. L. (2015). Mobilization of phosphate in variable-charge soils amended with biochars derived from crop straws. *Soil and Tillage Research, 146, Part B,* 139-147. doi: http://doi.org/10.1016/j.still.2014.10.009
Jin, Y., Liang, X., He, M., Liu, Y., Tian, G., & Shi, J. (2016). Manure biochar influence upon soil properties, phosphorus distribution and phosphatase activities: A microcosm incubation study. *Chemosphere, 142,* 128-135.

Jones, D. L., Edwards-Jones, G., & Murphy, D. V. (2011). Biochar mediated alterations in herbicide breakdown and leaching in soil. *Soil Biology & Biochemistry, 43*(4), 804-813. doi: 10.1016/j.soilbio.2010.12.015

Joseph, S., Camps-Arbestain, M., Lin, Y., Munroe, P., Chia, C., Hook, J., Van Zwieten, L., Kimber, S., Cowie, A., & Singh, B. (2010). An investigation into the reactions of biochar in soil. *Soil Research, 48*(7), 501-515.

Joseph, S., Kammann, C. I., Shepherd, J. G., Conte, P., Schmidt, H. P., Hagemann, N., Rich, A. M., Marjo, C. E., Allen, J., Munroe, P., Mitchell, D. R. G., Donne, S., Spokas, K., & Graber, E. R. (2018). Microstructural and associated chemical changes during the composting of a high temperature biochar: Mechanisms for nitrate, phosphate and other nutrient retention and release. *Science of the Total Environment, 618*, 1210-1223. doi: 10.1016/j.scitotenv.2017.09.200

Jung, K.-W., Hwang, M.-J., Ahn, K.-H., & Ok, Y.-S. (2015). Kinetic study on phosphate removal from aqueous solution by biochar derived from peanut shell as renewable adsorptive media. *International journal of environmental science and technology, 12*(10), 3363-3372.

Kasozi, G. N., Zimmerman, A. R., Nkedi-Kizza, P., & Gao, B. (2010). Catechol and humic acid sorption onto a range of laboratory-produced black carbons (biochars). *Environmental Science & Technology, 44*(16), 6189-6195.

Keiluweit, M., Nico, P. S., Johnson, M. G., & Kleber, M. (2010). Dynamic molecular structure of plant biomass-derived black carbon (biochar). *Environmental Science & Technology, 44*(4), 1247-1253.

Khan, S., Reid, B. J., Li, G., & Zhu, Y. G. (2014). Application of biochar to soil reduces cancer risk via rice consumption: A case study in miaoqian village, longyan, china. *Environment International, 68*, 154-161. doi: 10.1016/j.envint.2014.03.017

Kilpimaa, S., Runtti, H., Kangas, T., Lassi, U., & Kuokkanen, T. (2014). Removal of phosphate and nitrate over a modified carbon residue from biomass gasification. *Chemical Engineering Research and Design, 92*(10), 1923-1933.

Kinney, T., Masiello, C., Dugan, B., Hockaday, W., Dean, M., Zygourakis, K., & Barnes, R. (2012). Hydrologic properties of biochars produced at different temperatures. *Biomass and bioenergy, 41*, 34-43.

Kizito, S., Wu, S. B., Kirui, W. K., Lei, M., Lu, Q. M., Bah, H., & Dong, R. J. (2015). Evaluation of slow pyrolyzed wood and rice husks biochar for adsorption of ammonium nitrogen from piggery manure anaerobic digestate slurry. *Science of the Total Environment, 505*, 102-112. doi: 10.1016/j.scitotenv.2014.09.096

Kizito, S., Luo, H., Wu, S., Ajmal, Z., Lv, T., & Dong, R. (2017a). Phosphate recovery from liquid fraction of anaerobic digestate using four slow pyrolyzed biochars: Dynamics of adsorption, desorption and regeneration. *Journal of Environmental Management, 201*, 260-267.

Kizito, S., Lv, T., Wu, S., Ajmal, Z., Luo, H., & Dong, R. (2017b). Treatment of anaerobic digested effluent in biochar-packed vertical flow constructed wetland columns: Role of media and tidal operation. *Science of the Total Environment, 592*, 197-205.

Knicker, H. (2007). How does fire affect the nature and stability of soil organic nitrogen and carbon? A review. *Biogeochemistry, 85*(1), 91-118.

Kookana, R. S., Sarmah, A. K., Van Zwieten, L., Krull, E., & Singh, B. (2011). Biochar application to soil: Agronomic and environmental benefits and unintended consequences. In D. L. Sparks (Ed.), *Advances in agronomy, vol 112* (Vol. 112, pp. 103-143). San Diego: Elsevier Academic Press Inc.

Kumari, K., Moldrup, P., Paradelo, M., Elsgaard, L., Hauggaard-Nielsen, H., & de Jonge, L. W. (2014). Effects of biochar on air and water permeability and colloid and

phosphorus leaching in soils from a natural calcium carbonate gradient. *Journal of Environmental Quality, 43*(2), 647-657.
Laird, D., Fleming, P., Wang, B., Horton, R., & Karlen, D. (2010a). Biochar impact on nutrient leaching from a midwestern agricultural soil. *Geoderma, 158*(3), 436-442.
Laird, D. A., Fleming, P., Davis, D. D., Horton, R., Wang, B. Q., & Karlen, D. L. (2010b). Impact of biochar amendments on the quality of a typical midwestern agricultural soil. *Geoderma, 158*(3-4), 443-449. doi: 10.1016/j.geoderma.2010.05.013
Lee, J. W., Kidder, M., Evans, B. R., Paik, S., Buchanan, A. C., Garten, C. T., & Brown, R. C. (2010). Characterization of biochars produced from cornstovers for soil amendment. *Environmental Science & Technology, 44*(20), 7970-7974. doi: 10.1021/es101337x
Lee, Y., Ryu, C., Park, Y.-K., Jung, J.-H., & Hyun, S. (2013). Characteristics of biochar produced from slow pyrolysis of geodae-uksae 1. *Bioresource Technology, 130*, 345-350.
Lehmann, J., da Silva, J. P., Steiner, C., Nehls, T., Zech, W., & Glaser, B. (2003). Nutrient availability and leaching in an archaeological anthrosol and a ferralsol of the central amazon basin: Fertilizer, manure and charcoal amendments. *Plant and Soil, 249*(2), 343-357. doi: 10.1023/a:1022833116184
Lehmann, J., Gaunt, J., & Rondon, M. (2006). Bio-char sequestration in terrestrial ecosystems–a review. *Mitigation and adaptation strategies for global change, 11*(2), 395-419.
Lehmann, J., & Rondon, M. (2006). Bio-char soil management on highly weathered soils in the humid tropics. *Biological approaches to sustainable soil systems. CRC Press, Boca Raton, FL*, 517-530.
Lehmann, J. (2007). Bio-energy in the black. *Frontiers in Ecology and the Environment, 5*(7), 381-387. doi: 10.1890/1540-9295(2007)5[381:bitb]2.0.co;2
Lehmann, J., Rillig, M. C., Thies, J., Masiello, C. A., Hockaday, W. C., & Crowley, D. (2011). Biochar effects on soil biota - a review. *Soil Biology & Biochemistry, 43*(9), 1812-1836. doi: 10.1016/j.soilbio.2011.04.022
Liang, B., Lehmann, J., Solomon, D., Kinyangi, J., Grossman, J., O'neill, B., Skjemstad, J., Thies, J., Luizao, F., & Petersen, J. (2006). Black carbon increases cation exchange capacity in soils. *Soil Science Society of America Journal, 70*(5), 1719-1730.
Liang, Y., Cao, X. D., Zhao, L., Xu, X. Y., & Harris, W. (2014). Phosphorus release from dairy manure, the manure-derived biochar, and their amended soil: Effects of phosphorus nature and soil property. *Journal of Environmental Quality, 43*(4), 1504-1509. doi: 10.2134/jeq2014.01.0021
Lindsay, W. L. (1979). *Chemical equilibria in soils*: John Wiley and Sons Ltd.
Liu, Y., Zhu, Z. Q., He, X. S., Yang, C., Du, Y. Q., Huang, Y. D., Su, P., Wang, S., Zheng, X. X., & Xue, Y. J. (2018). Mechanisms of rice straw biochar effects on phosphorus sorption characteristics of acid upland red soils. *Chemosphere, 207*, 267-277. doi: 10.1016/j.chemosphere.2018.05.086
Lookman, R., Grobet, P., Merckx, R., & Van Riemsdijk, W. H. (1997). Application of 31p and 27al mas nmr for phosphate speciation studies in soil and aluminium hydroxides: Promises and constraints. *Geoderma, 80*(3-4), 369-388.
Lorenz, K., & Lal, R. (2014). Biochar application to soil for climate change mitigation by soil organic carbon sequestration. *Journal of Plant Nutrition and Soil Science, 177*(5), 651-670. doi: 10.1002/jpln.201400058
Lou, K. Y., Rajapaksha, A. U., Ok, Y. S., & Chang, S. X. (2016). Pyrolysis temperature and steam activation effects on sorption of phosphate on pine sawdust biochars in

aqueous solutions. *Chemical Speciation and Bioavailability, 28*(1-4), 42-50. doi: 10.1080/09542299.2016.1165080
Lozano-Castelló, D., Cazorla-Amoros, D., & Linares-Solano, A. (2004). Usefulness of co2 adsorption at 273 k for the characterization of porous carbons. *Carbon, 42*(7), 1233-1242.
Lucchini, P., Quilliam, R. S., DeLuca, T. H., Vamerali, T., & Jones, D. L. (2014). Does biochar application alter heavy metal dynamics in agricultural soil? *Agriculture Ecosystems & Environment, 184*, 149-157. doi: 10.1016/j.agee.2013.11.018
Mackenzie, A., & Amer, S. (1964). Reactions of iron, aluminum and calcium phosphates in six ontario soils. *Plant and Soil, 21*(1), 17-25.
Madiba, O. F., Solaiman, Z. M., Carson, J. K., & Murphy, D. V. (2016). Biochar increases availability and uptake of phosphorus to wheat under leaching conditions. *Biology and Fertility of Soils, 52*(4), 439-446.
Manya, J. J. (2012). Pyrolysis for biochar purposes: A review to establish current knowledge gaps and research needs. *Environmental Science & Technology, 46*(15), 7939-7954. doi: 10.1021/es301029g
Marshall, J. A., Morton, B. J., Muhlack, R., Chittleborough, D., & Kwong, C. W. (2017). Recovery of phosphate from calcium-containing aqueous solution resulting from biochar-induced calcium phosphate precipitation. *Journal of Cleaner Production, 165*, 27-35. doi: 10.1016/j.jclepro.2017.07.042
McDowell, R., Brookes, P., Mahieu, N., Poulton, P., Johnston, A., & Sharpley, A. (2002). The effect of soil acidity on potentially mobile phosphorus in a grassland soil. *The Journal of Agricultural Science, 139*(1), 27-36.
Mohan, D., & Chander, S. (2006). Single, binary, and multicomponent sorption of iron and manganese on lignite. *Journal of Colloid and Interface Science, 299*(1), 76-87.
Mohan, D., Pittman, C. U., & Steele, P. H. (2006). Pyrolysis of wood/biomass for bio-oil: A critical review. *Energy & Fuels, 20*(3), 848-889.
Mohanty, P., Nanda, S., Pant, K. K., Naik, S., Kozinski, J. A., & Dalai, A. K. (2013). Evaluation of the physiochemical development of biochars obtained from pyrolysis of wheat straw, timothy grass and pinewood: Effects of heating rate. *Journal of Analytical and Applied Pyrolysis, 104*, 485-493.
Morales, M., Comerford, N., Guerrini, I. A., Falcão, N., & Reeves, J. (2013). Sorption and desorption of phosphate on biochar and biochar–soil mixtures. *Soil Use and Management, 29*(3), 306-314.
Mosa, A., El-Ghamry, A., & Tolba, M. (2018). Functionalized biochar derived from heavy metal rich feedstock: Phosphate recovery and reusing the exhausted biochar as an enriched soil amendment. *Chemosphere, 198*, 351-363. doi: 10.1016/j.chemosphere.2018.01.113
Mukherjee, A., Zimmerman, A., & Harris, W. (2011). Surface chemistry variations among a series of laboratory-produced biochars. *Geoderma, 163*(3), 247-255.
Mukome, F. N., Zhang, X., Silva, L. C., Six, J., & Parikh, S. J. (2013). Use of chemical and physical characteristics to investigate trends in biochar feedstocks. *Journal of Agricultural and Food Chemistry, 61*(9), 2196-2204.
Murphy, P. N., & Stevens, R. (2010). Lime and gypsum as source measures to decrease phosphorus loss from soils to water. *Water, Air, & Soil Pollution, 212*(1-4), 101-111.
Nellemann, C. (2009). *The environmental food crisis: The environment's role in averting future food crises: A unep rapid response assessment*: UNEP/Earthprint.
Nelson, N. O., Agudelo, S. C., Yuan, W., & Gan, J. (2011). Nitrogen and phosphorus availability in biochar-amended soils. *Soil Science, 176*(5), 218-226.

Ngatia, L., Hsieh, Y., Nemours, D., Fu, R., & Taylor, R. (2017). Potential phosphorus eutrophication mitigation strategy: Biochar carbon composition, thermal stability and ph influence phosphorus sorption. *Chemosphere, 180*, 201-211.

Nguyen, B. T., & Lehmann, J. (2009). Black carbon decomposition under varying water regimes. *Organic Geochemistry, 40*(8), 846-853.

Novais, S. V., Zenero, M. D. O., Tronto, J., Conz, R. F., & Cerri, C. E. P. (2018). Poultry manure and sugarcane straw biochars modified with mgcl2 for phosphorus adsorption. *Journal of Environmental Management, 214*, 36-44. doi: 10.1016/j.jenvman.2018.02.088

Novak, J. M., Lima, I., Xing, B., Gaskin, J. W., Steiner, C., Das, K., Ahmedna, M., Rehrah, D., Watts, D. W., & Busscher, W. J. (2009). Characterization of designer biochar produced at different temperatures and their effects on a loamy sand. *Ann. Environ. Sci, 3*(2), 195-206.

Noyce, G. L., Jones, T., Fulthorpe, R., & Basiliko, N. (2017). Phosphorus uptake and availability and short-term seedling growth in three ontario soils amended with ash and biochar. *Canadian Journal of Soil Science, 97*(4), 678-691. doi: 10.1139/cjss-2017-0007

Oberson, A., Besson, J., Maire, N., & Sticher, H. (1996). Microbiological processes in soil organic phosphorus transformations in conventional and biological cropping systems. *Biology and Fertility of Soils, 21*(3), 138-148.

Olsen, S. R. (1954). *Estimation of available phosphorus in soils by extraction with sodium bicarbonate*: United States Department Of Agriculture; Washington.

Omil, B., Piñeiro, V., & Merino, A. (2013). Soil and tree responses to the application of wood ash containing charcoal in two soils with contrasting properties. *Forest ecology and management, 295*, 199-212.

Parvage, M. M., Ulén, B., Eriksson, J., Strock, J., & Kirchmann, H. (2013). Phosphorus availability in soils amended with wheat residue char. *Biology and Fertility of Soils, 49*(2), 245-250.

Peng, X., Ye, L. L., Wang, C. H., Zhou, H., & Sun, B. (2011). Temperature- and duration-dependent rice straw-derived biochar: Characteristics and its effects on soil properties of an ultisol in southern china. *Soil & Tillage Research, 112*(2), 159-166. doi: 10.1016/j.still.2011.01.002

Peterson, S. C., & Jackson, M. A. (2014). Simplifying pyrolysis: Using gasification to produce corn stover and wheat straw biochar for sorptive and horticultural media. *Industrial Crops and Products, 53*, 228-235. doi: 10.1016/j.indcrop.2013.12.028

Pierzynski, G. M., & McDowell, R. W. (2005). Chemistry, cycling, and potential movement of inorganic phosphorus in soils. *Phosphorus: agriculture and the environment*(phosphorusagric), 53-86.

Pietikainen, J., Kiikkila, O., & Fritze, H. (2000). Charcoal as a habitat for microbes and its effect on the microbial community of the underlying humus. *Oikos, 89*(2), 231-242. doi: 10.1034/j.1600-0706.2000.890203.x

Pituello, C., Francioso, O., Simonetti, G., Pisi, A., Torreggiani, A., Berti, A., & Morari, F. (2015). Characterization of chemical-physical, structural and morphological properties of biochars from biowastes produced at different temperatures. *Journal of Soils and Sediments, 15*(4), 792-804. doi: 10.1007/s11368-014-0964-7

Purevsuren, B., Avid, B., Tesche, B., & Davaajav, Y. (2003). A biochar from casein and its properties. *Journal of Materials Science, 38*(11), 2347-2351.

Qayyum, M. F., Ashraf, I., Abid, M., & Steffens, D. (2015). Effect of biochar, lime, and compost application on phosphorus adsorption in a ferralsol. *Journal of Plant Nutrition and Soil Science, 178*(4), 576-581. doi: 10.1002/jpln.201400552

Qian, K. Z., Kumar, A., Bellmer, D., Yuan, W. Q., Wang, D. H., & Eastman, M. A. (2015). Physical properties and reactivity of char obtained from downdraft gasification of sorghum and eastern red cedar. *Fuel, 143*, 383-389. doi: 10.1016/j.fuel.2014.11.054

Qian, T., Zhang, X., Hu, J., & Jiang, H. (2013). Effects of environmental conditions on the release of phosphorus from biochar. *Chemosphere, 93*(9), 2069-2075.

Rapagna, S., Jand, N., Kiennemann, A., & Foscolo, P. (2000). Steam-gasification of biomass in a fluidised-bed of olivine particles. *Biomass and bioenergy, 19*(3), 187-197.

Reddy, K., Drever, J., Essington, M., & Lindsay, W. (1989). Selection of standard free energies of formation for use in soil chemistry.

Rillig, M. C., & Thies, J. E. (2012). Characteristics of biochar: Biological properties *Biochar for environmental management* (pp. 117-138): Routledge.

Rittmann, B. E., Mayer, B., Westerhoff, P., & Edwards, M. (2011). Capturing the lost phosphorus. *Chemosphere, 84*(6), 846-853.

Robinson, J. S., Baumann, K., Hu, Y. F., Hagemann, P., Kebelmann, L., & Leinweber, P. (2018). Phosphorus transformations in plant-based and bio-waste materials induced by pyrolysis. *Ambio, 47*, 73-82. doi: 10.1007/s13280-017-0990-y

Ronsse, F., Van Hecke, S., Dickinson, D., & Prins, W. (2013). Production and characterization of slow pyrolysis biochar: Influence of feedstock type and pyrolysis conditions. *GCB Bioenergy, 5*(2), 104-115.

Rowell, D. L. (2014). *Soil science: Methods & applications*: Routledge.

Sarkhot, D., Ghezzehei, T., & Berhe, A. (2013). Effectiveness of biochar for sorption of ammonium and phosphate from dairy effluent. *Journal of Environmental Quality, 42*(5), 1545-1554.

Sarma, B., Gogoi, N., Bharali, M., & Mali, P. (2018). Field evaluation of soil and wheat responses to combined application of hardwood biochar and inorganic fertilizers in acidic sandy loam soil. *Experimental Agriculture, 54*(4), 507-519. doi: 10.1017/s0014479717000205

Sato, S., & Comerford, N. B. (2006). Organic anions and phosphorus desorption and bioavailability in a humid brazilian ultisol. *Soil Science, 171*(9), 695-705.

Scalenghe, R., Edwards, A., Barberis, E., & Ajmone Marsan, F. (2010). The influence of pulsed redox conditions on soil phosphorus. *Biogeosciences Discussions*(6), 9009-9037.

Schneider, F., & Haderlein, S. B. (2016). Potential effects of biochar on the availability of phosphorus—mechanistic insights. *Geoderma, 277*, 83-90.

Schoenau, J., & Karamanos, R. (1993). Sodium bicarbonate extractable p, k, and n. *Soil sampling and methods of analysis*, 51-58.

Schöning, A., & Brümmer, G. W. (2008). Extraction of mobile element fractions in forest soils using ammonium nitrate and ammonium chloride. *Journal of Plant Nutrition and Soil Science, 171*(3), 392-398.

Shenbagavalli, S., & Mahimairaja, S. (2012). Production and characterization of biochar from different biological wastes. *International journal of plant, animal and environmental sciences, 2*(1), 197-201.

Singh, B., Camps-Arbestain, M., & Lehmann, J. (2017). *Biochar: A guide to analytical methods*: Csiro Publishing.

Slavich, P., Sinclair, K., Morris, S., Kimber, S., Downie, A., & Van Zwieten, L. (2013). Contrasting effects of manure and green waste biochars on the properties of an acidic ferralsol and productivity of a subtropical pasture. *Plant and Soil, 366*(1-2), 213-227.

Sohi, S., Lopez-Capel, E., Krull, E., & Bol, R. (2009). *Biochar, climate change and soil: A review to guide future research*: CSIRO Glen Osmond, Australia.

Sorrenti, G., Masiello, C. A., Dugan, B., & Toselli, M. (2016). Biochar physico-chemical properties as affected by environmental exposure. *Science of the Total Environment, 563*, 237-246.
Sparks, D. L. (1995). *Environmental soil chemistry*: Academic Press, Book Marketing Department.
Sposito, G. (2008). *The chemistry of soils*: Oxford university press.
Srinivasan, P., & Sarmah, A. K. (2015). Characterisation of agricultural waste-derived biochars and their sorption potential for sulfamethoxazole in pasture soil: A spectroscopic investigation. *Science of the Total Environment, 502*, 471-480. doi: 10.1016/j.scitotenv.2014.09.048
Stutter, M. I. (2015). The composition, leaching, and sorption behavior of some alternative sources of phosphorus for soils. *Ambio, 44*, S207-S216. doi: 10.1007/s13280-014-0615-7
Suliman, W., Harsh, J. B., Abu-Lail, N. I., Fortuna, A.-M., Dallmeyer, I., & Garcia-Perez, M. (2016). Influence of feedstock source and pyrolysis temperature on biochar bulk and surface properties. *Biomass and bioenergy, 84*, 37-48.
Sun, D. Q., Hale, L., Kar, G., Soolanayakanahally, R., & Adl, S. (2018a). Phosphorus recovery and reuse by pyrolysis: Applications for agriculture and environment. *Chemosphere, 194*, 682-691. doi: 10.1016/j.chemosphere.2017.12.035
Sun, K., Qiu, M. Y., Han, L. F., Jin, J., Wang, Z. Y., Pan, Z. Z., & Xing, B. S. (2018b). Speciation of phosphorus in plant- and manure-derived biochars and its dissolution under various aqueous conditions. *Science of the Total Environment, 634*, 1300-1307. doi: 10.1016/j.scitotenv.2018.04.099
Takaya, C., Fletcher, L., Singh, S., Okwuosa, U., & Ross, A. (2016). Recovery of phosphate with chemically modified biochars. *Journal of Environmental Chemical Engineering*.
Tan, Z. X., Zou, J. H., Zhang, L. M., & Huang, Q. Y. (2018). Morphology, pore size distribution, and nutrient characteristics in biochars under different pyrolysis temperatures and atmospheres. *Journal of Material Cycles and Waste Management, 20*(2), 1036-1049. doi: 10.1007/s10163-017-0666-5
Tang, J. C., Zhu, W. Y., Kookana, R., & Katayama, A. (2013). Characteristics of biochar and its application in remediation of contaminated soil. *Journal of Bioscience and Bioengineering, 116*(6), 653-659. doi: 10.1016/j.jbiosc.2013.05.035
Tejedor-Tejedor, M. I., & Anderson, M. A. (1990). The protonation of phosphate on the surface of goethite as studied by cir-ftir and electrophoretic mobility. *Langmuir, 6*(3), 602-611.
Toor, G., & Bahl, G. (1999). Kinetics of phosphate desorption from different soils as influenced by application of poultry manure and fertilizer phosphorus and its uptake by soybean. *Bioresource Technology, 69*(2), 117-121.
Trazzi, P., Leahy, J., Hayes, M., & Kwapinski, W. (2016). Adsorption and desorption of phosphate on biochars. *Journal of Environmental Chemical Engineering, 4*(1), 37-46.
Tryon, E. H. (1948). Effect of charcoal on certain physical, chemical, and biological properties of forest soils. *Ecological Monographs, 18*(1), 81-115. doi: 10.2307/1948629
Tunesi, S., Poggi, V., & Gessa, C. (1999). Phosphate adsorption and precipitation in calcareous soils: The role of calcium ions in solution and carbonate minerals. *Nutrient Cycling in Agroecosystems, 53*(3), 219-227.
Uchimiya, M., Lima, I. M., Thomas Klasson, K., Chang, S., Wartelle, L. H., & Rodgers, J. E. (2010a). Immobilization of heavy metal ions (cuii, cdii, niii, and pbii) by broiler litter-derived biochars in water and soil. *Journal of Agricultural and Food Chemistry, 58*(9), 5538-5544.

Uchimiya, M., Wartelle, L. H., Lima, I. M., & Klasson, K. T. (2010b). Sorption of deisopropylatrazine on broiler litter biochars. *Journal of Agricultural and Food Chemistry, 58*(23), 12350-12356. doi: 10.1021/jf102152q
Uchimiya, M., Bannon, D. I., Wartelle, L. H., Lima, I. M., & Klasson, K. T. (2012). Lead retention by broiler litter biochars in small arms range soil: Impact of pyrolysis temperature. *Journal of Agricultural and Food Chemistry, 60*(20), 5035-5044.
Uchimiya, M., & Hiradate, S. (2014). Pyrolysis temperature-dependent changes in dissolved phosphorus speciation of plant and manure biochars. *Journal of Agricultural and Food Chemistry, 62*(8), 1802-1809.
UN. (2008). World population prospects: The 2008 revision population database. Retrieved 24.07, 2018, from http://www.un.org/esa/population/publications/wpp2008/wpp2008_highlights.pdf
USDA. (2015). Soil electrical conductivity. Retrieved 09/07/2018, from https://www.nrcs.usda.gov/Internet/FSE_DOCUMENTS/nrcs142p2_053280.pdf
Vadas, P., & Sims, J. T. (1999). Phosphorus sorption in manured atlantic coastal plain soils under flooded and drained conditions. *Journal of Environmental Quality, 28*(6), 1870-1877.
Von Wandruszka, R. (2006). Phosphorus retention in calcareous soils and the effect of organic matter on its mobility. *Geochemical transactions, 7*(1), 6.
Wang, S. D., Kong, L. J., Long, J. Y., Su, M. H., Diao, Z. H., Chang, X. Y., Chen, D. Y., Song, G., & Shih, K. M. (2018). Adsorption of phosphorus by calcium-flour biochar: Isotherm, kinetic and transformation studies. *Chemosphere, 195*, 666-672. doi: 10.1016/j.chemosphere.2017.12.101
Wang, Y., Hu, Y. T., Zhao, X., Wang, S. Q., & Xing, G. X. (2013). Comparisons of biochar properties from wood material and crop residues at different temperatures and residence times. *Energy & Fuels, 27*(10), 5890-5899. doi: 10.1021/ef400972z
Wang, Z., Guo, H., Shen, F., Yang, G., Zhang, Y., Zeng, Y., Wang, L., Xiao, H., & Deng, S. (2015). Biochar produced from oak sawdust by lanthanum (la)-involved pyrolysis for adsorption of ammonium (nh 4+), nitrate (no 3−), and phosphate (po 4 3−). *Chemosphere, 119*, 646-653.
Wasewar, K. L., Atif, M., Prasad, B., & Mishra, I. M. (2008). Adsorption of zinc using tea factory waste: Kinetics, equilibrium and thermodynamics. *CLEAN–Soil, Air, Water, 36*(3), 320-329.
Xu, G., Wei, L., Sun, J., Shao, H., & Chang, S. (2013). What is more important for enhancing nutrient bioavailability with biochar application into a sandy soil: Direct or indirect mechanism? *Ecological Engineering, 52*, 119-124.
Xu, G., Sun, J., Shao, H., & Chang, S. X. (2014). Biochar had effects on phosphorus sorption and desorption in three soils with differing acidity. *Ecological Engineering, 62*, 54-60.
Xu, K. N., Lin, F. Y., Dou, X. M., Zheng, M., Tan, W., & Wang, C. W. (2018). Recovery of ammonium and phosphate from urine as value-added fertilizer using wood waste biochar loaded with magnesium oxides. *Journal of Cleaner Production, 187*, 205-214. doi: 10.1016/j.jclepro.2018.03.206
Xue, Y., Hou, H., & Zhu, S. (2009). Characteristics and mechanisms of phosphate adsorption onto basic oxygen furnace slag. *Journal of Hazardous Materials, 162*(2), 973-980.
Yao, Y., Gao, B., Inyang, M., Zimmerman, A. R., Cao, X., Pullammanappallil, P., & Yang, L. (2011a). Biochar derived from anaerobically digested sugar beet tailings: Characterization and phosphate removal potential. *Bioresource Technology, 102*(10), 6273-6278.

Yao, Y., Gao, B., Inyang, M., Zimmerman, A. R., Cao, X., Pullammanappallil, P., & Yang, L. (2011b). Removal of phosphate from aqueous solution by biochar derived from anaerobically digested sugar beet tailings. *Journal of Hazardous Materials, 190*(1), 501-507.

Yao, Y., Gao, B., Zhang, M., Inyang, M., & Zimmerman, A. R. (2012). Effect of biochar amendment on sorption and leaching of nitrate, ammonium, and phosphate in a sandy soil. *Chemosphere, 89*(11), 1467-1471.

Yao, Y., Gao, B., Chen, J., & Yang, L. (2013). Engineered biochar reclaiming phosphate from aqueous solutions: Mechanisms and potential application as a slow-release fertilizer. *Environmental Science & Technology, 47*(15), 8700-8708. doi: 10.1021/es4012977

Yargicoglu, E. N., Sadasivam, B. Y., Reddy, K. R., & Spokas, K. (2015). Physical and chemical characterization of waste wood derived biochars. *Waste Management, 36*, 256-268.

Yeboah, E., Ofori, P., Quansah, G., Dugan, E., & Sohi, S. (2009). Improving soil productivity through biochar amendments to soils. *African Journal of Environmental Science and Technology, 3*(2), 34-41.

Yin, Q. Q., Zhang, B. D., Wang, R. K., & Zhao, Z. H. (2018). Phosphate and ammonium adsorption of sesame straw biochars produced at different pyrolysis temperatures. *Environmental Science and Pollution Research, 25*(5), 4320-4329. doi: 10.1007/s11356-017-0778-4

Yu, P., Xue, Y., Gao, F., Liu, Z., Cheng, X., & Yang, K. (2016). Phosphorus removal from aqueous solution by pre- or post-modified biochars derived from agricultural residues. *Water, Air, & Soil Pollution, 227*(10), 370. doi: 10.1007/s11270-016-3066-x

Yuan, J.-H., Xu, R.-K., & Zhang, H. (2011). The forms of alkalis in the biochar produced from crop residues at different temperatures. *Bioresource Technology, 102*(3), 3488-3497.

Zabaniotou, A., Stavropoulos, G., & Skoulou, V. (2008). Activated carbon from olive kernels in a two-stage process: Industrial improvement. *Bioresource Technology, 99*(2), 320-326.

Zeng, Z., Li, T.-q., Zhao, F.-l., He, Z.-l., Zhao, H.-p., Yang, X.-e., Wang, H.-l., Zhao, J., & Rafiq, M. T. (2013). Sorption of ammonium and phosphate from aqueous solution by biochar derived from phytoremediation plants. *Journal of Zhejiang University Science B, 14*(12), 1152-1161.

Zhai, L. M., Caiji, Z. M., Liu, J., Wang, H. Y., Ren, T. Z., Gai, X. P., Xi, B., & Liu, H. B. (2015). Short-term effects of maize residue biochar on phosphorus availability in two soils with different phosphorus sorption capacities. *Biology and Fertility of Soils, 51*(1), 113-122. doi: 10.1007/s00374-014-0954-3

Zhang, G., Liu, H., Liu, R., & Qu, J. (2009). Removal of phosphate from water by a fe–mn binary oxide adsorbent. *Journal of Colloid and Interface Science, 335*(2), 168-174.

Zhang, H., Chen, C., Gray, E. M., Boyd, S. E., Yang, H., & Zhang, D. (2016). Roles of biochar in improving phosphorus availability in soils: A phosphate adsorbent and a source of available phosphorus. *Geoderma, 276*, 1-6.

Zhao, L., Cao, X., Mašek, O., & Zimmerman, A. (2013). Heterogeneity of biochar properties as a function of feedstock sources and production temperatures. *Journal of Hazardous Materials, 256*, 1-9.

Zornoza, R., Moreno-Barriga, F., Acosta, J., Muñoz, M., & Faz, A. (2016). Stability, nutrient availability and hydrophobicity of biochars derived from manure, crop residues, and municipal solid waste for their use as soil amendments. *Chemosphere, 144*, 122-130.